Chiral Lanthanide complexes as probes for bioactive species

Alessandra Badari

CHIRAL LANTHANIDE COMPLEXES AS PROBES FOR BIOACTIVE SPECIES

Alessandra Badari

A thesis submitted for the degree of Doctor of Philosophy

Department of Chemistry
University of Durham

2005

To Mum and Dad

And what is it to work with love?

It is to weave the cloth with threads drawn from your heart,
as if your beloved were to wear that cloth.

It is to build a house with affection,
as if your beloved were to dwell in that house.

It is to sow seeds with tenderness and reap the harvest with joy,
as if your beloved were to eat the fruit.

It is to charge all things you fashion with a breath of your own spirit...

E che cosa significa lavorare con amore?

Significa tessera un abito con fili tratti dal vostro cuore,
come se dovesse indossarlo il vostro amato.

Significa costruire una casa con dedizione,
come se dovesse abitarla il vostro amato.

Significa impregnare tutte le cose che fate con un respiro vestito di gioia,
come se dovesse consumarne il frutto il vostro amato.

Significa impregnare tutte le cose che fate del soffio del vostro spirito...

Kahlil Gibran - "The Prophet"

Acknowledgements

Sincere thanks to:

Dr. Rachel Dickins, for her constant, patient, and precious help, whilst positively guiding me through my research, and for being an excellent supervisor and a very special friend;

Professor David Parker for his co-supervision on my project;

Dr Alan Kenwright, Ian McKeag and Catherine Heffernan for running VT and 2D NMR spectra;

Dr Mike Jones and Lara Turner for their assistance with the mass spectrometry measurements;

The current and past members of the DP group: the postdocs (Yann Bretonniere, Juan C. Frias, David Fulton, Stephane Gaillard, Horst Puschmann, Kanthi Senanayake, Jun Hua Yu) and the PhD students (Paul Atkinson, Gabriella Bobba, Aileen Congreve, Elisa Elemento, Robert Pal, Filip Kielar, Robert Poole, Nicola Thompson, Simon Welsh) for helping me with the chemistry and for their friendship;

All the friends I have met in Durham, for making me feel at home in a foreign country, and my Italian friends, for staying close to me and for waiting for me to come back;

A special thanks to Andrea, for sharing with me both the good and the hard time of these three years, for making me believe in myself, and for his love;

A deep thanks to my Mum and Dad, for bringing me up with much love and dedication and for always being a landmark in my life.

Declaration

The research described in this thesis was undertaken at the Department of Chemistry of the University of Durham between January 2002 and November 2004. All of the work is my own; no part of it has previously been submitted for a degree at this or any other university.

Statement of Copyright

Abstract

In vivo detection of lactate by ^{1}H MRS is of prime importance in the diagnosis, grading and therapeutic monitoring of pathological states such as cancer, stroke and heart disease. However, the detection of this metabolite is affected by the limits of the MRS technique, such as the low sensitivity, and the overlapping resonances of lactate with other biological species. A solution to the problem is to envisage the use of a paramagnetic metal chelate system, acting as a shift and relaxation agent, in order to affect spectral resolution and also to allow rapid acquisition times to be implemented, giving increased signal intensity. For an effective shift reagent the binding to lactate should be reversible and in fast exchange on the NMR timescale. A single isomer in solution is preferred, in order to simplify the interpretation of the spectra, and a large lanthanide induced shift is necessary to avoid any overlapping of biological background signals with the resonances of interest. Moreover, water soluble, kinetically stable complexes are required for use *in vivo*.

With these features in mind, several enantiopure heptadentate lanthanide complexes have been designed, and their ability to bind selectively and reversibly to lactate has been investigated. In order to achieve the fast exchange conditions required, the binding affinity and selectivity for lactate have been modulated by varying the Ln^{3+} ion and the ligand structure, in particular the peripheral electrostatic charge of the complex (i.e. anionic vs. neutral) and the local charge and steric demand at the metal centre.

The binding of lactate to these novel chiral, heptadentate lanthanide complexes has been effectively signalled by ^{1}H NMR (Yb^{3+}), emission spectroscopy (Eu^{3+}), hydration state studies (Tb^{3+}) and circular dichroism (Yb^{3+}). These spectroscopic and chiroptical techniques have also been employed to investigate the binding of such complexes to several biological anions in aqueous media, with the aim of assessing the potential of such systems as effective NMR, luminescent and chiroptical probes for a wider range of bioactive species.

Contents

Abbreviations

Compounds

ADP	adenosine diphosphate
ATP	adenosine triphosphate
AMP	adenosine monophosphate
APP	aminopropylphosphonate
Cho	choline
Cr	creatine
DMF	N, N-dimethylformamide
DMSO	dimethylsulphoxide
DCM	dichloromethane
DOTA	1,4,7,10-tetraazacyclododecane-1,4,7,10-tetraacetic acid
EDTA	ethylenediamine-N, N, N', N'-tetraacetic acid
DOTP	1,4,7,10-tetraazacyclododecane-N, N', N'',N'''-tetra(methylene phosphonate)
Glucose-6-P	glucose-6-phosphate
GPC	glycerophosphocholine
GPE	glycerophosphoethanolamine
Ins	inositol
Lac	lactate
MOPS	3-[N-morpholino]propanesulfonic acid
12N4	1,4,7,10-tetraazacyclododecane (cyclen)
NAA	N-acetylaspartate
NTP	nucleoside triphosphates
PC	phosphocholine
PCr	phosphocreatine
PDE	phosphodiesters
PE	phosphoethanolamine
P_i	inorganic phosphate
PME	phosphomonoesters

Ph		phenyl
Bn		benzyl
Cbz		benzyloxycarbonyl
Ar		aromatic
Tos		tosyl
TFA		trifluoroacetic acid
OTf		triflate

Techniques and Spectroscopy

CD		circular dichroism
IR		infra-red spectroscopy
	br	broad
	m	medium
	s	strong
	w	weak
m.p.		melting point
MS		mass spectroscopy
	ESMS	electrospray mass spectrometry
	ES^+	electrospray ionisation using positive ion detection mode
	ES^-	electrospray ionisation using negative ion detection mode
	M	molecular ion
MRI		magnetic resonance imaging
MRS		magnetic resonance spectroscopy
NMR		nuclear magnetic resonance
	COSY	correlation spectroscopy
	NOESY	nuclear overhauser enhancement spectroscopy
	br	broad
	d	doublet
	m	multiplet
	s	singlet
	t	triplet

	o	ortho
	m	meta
	p	para
TLC		thin layer chromatography
u.v.		ultraviolet

Miscellaneous

Ln	generic symbol for a lanthanide ion
M	mol l^{-1}
h	hours
eq	equivalents

Amino acids

AA	amino acid
Ala	alanine
Gly	glycine
Glu	glutamic acid
Lys	lysine
Met	methionine
Phe	phenylalanine
Ser	serine
Thr	threonine
Tyr	tyrosine
OP-Serine	phosphoserine
OP-Tyrosine	phosphotyrosine
OP-Threonine	phosphothreonine

CHAPTER 1

Introduction

1.1 Magnetic Resonance Spectroscopy

1.1.1 Introduction to MRS

Treating diseased states such as cancer requires knowledge of what is happening inside the human body. Many medical techniques address this problem, but none is entirely satisfactory, as most carry a penalty. Methods involving X-rays or injection of radioactive chemicals expose the patient to ionising radiation and thus to a slight risk of developing cancer. Therefore an increasing interest has been shown towards the development of non invasive methods based on Magnetic Resonance Imaging (MRI) and Magnetic Resonance Spectroscopy (MRS), which do not involve ionising radiation.

The two techniques are performed by placing the patient in a hospital scanner operating at 1.5 T (slightly modified for MRS) where electromagnetic waves are used to make the atomic nuclei resonate. MRI is performed by exciting the nuclei of the hydrogen atoms in water molecules and by introducing a gradient magnetic field that makes the nuclei in different parts of the body resonate at different frequencies. These frequency-encoded signals are then decoded by a computer programme to produce a map of the water distribution in the body. Thus MRI is recognised as the best method for imaging the anatomy of many parts of the body and many diseases. Although incredibly detailed images may be obtained, no actual biochemical information is available.

In MRS the nuclei of different atoms in a chemical compound resonate at slightly different frequencies and in this case the frequency-encoding gives us a spectrum. Signals are plotted as peaks on a normalized frequency scale and the area under each peak is proportional to the concentration of the atoms that gave rise to it. This means that MRS, yielding both qualitative and quantitative information, offers a means of analyzing the chemical content of living tissue and may be used as a non invasive alternative to biopsy.[1]

MRS can detect changes in the chemistry of the body thus assessing the state of normal and pathological tissues. *In vivo* clinical MRS has found widespread application in the investigation of a variety of pathological conditions including hereditary metabolic disorders,[2] stroke,[3] dementia,[4] multiple sclerosis,[5] epilepsy,[6] schizophrenia,[7] and neoplasms.[8] Some key metabolites studied in clinical MRS include N-acetylaspartate (NAA), choline (Cho), lactate (Lac) and inositol (Ins). NAA is regarded as a marker of neuronal integrity. The decrease in its concentration is observed in virtually all focal brain lesions and in regional brain lesion, such as Alzheimer's disease[9] and multiple sclerosis. Lactate is the product of anaerobic glycolysis and it is a non specific sign of disease. It can be elevated in hypoxia, stroke, haemorrhage, neoplasm and infection. Choline is considered to be an indicator of membrane activity and the major components of the Cho peak are the phosphorylated choline precursors, which are released during degradation of cell membrane and myelin. Cho is seen in high concentration in rapidly proliferating tissue such as the neonatal brain and in brain neoplasm, while a decrease of its concentration has been found in infarction and hepatic encephalopathy. The concentration of Cho is typically assessed by reference to the height of the creatine peak, which is the total peak from Cr and phosphocreatine. Creatine (Cr) is a supplier of phosphate, converting adenosine diphosphate (ADP) to adenosine triphosphate (ATP) and it is relatively constant throughout the brain. Cr levels tend not to change significantly in disease processes, however there is evidence that they can change in malignant tumours. Inositol is a sugar alcohol which is thought to be a product of myelin breakdown and its concentration is often higher in conditions such as Alzeheimer's disease and malignant tumours.[10]

The weakness of MRS is its low sensitivity: currently the minimum size of a tumour that can be studied is $1cm^3$. Furthermore, long acquisition times are required for a good signal-to-noise intensity ratio and resonances of interest are often masked by overlapping lipid and protein signals. MRS is therefore widely applied *in vitro* and over the past decade many improvements in instrumentation and methodology have been addressed to enhance its routine clinical role.[11]

1.1.2 Nuclei of Interest in MRS

Much clinical research has been targeted towards cancer and MRS provides a powerful tool for studying tumour biochemistry[12] and physiology.[13] Biochemical information obtained by MRS can be related to tumour metabolism and can indicate ways in which the diseased tissue differs from that of normal tissue. Spectral characteristics may give diagnostic information on the grade and the state of differentiation of a tumour. MRS can also be used to monitor the response of a tumour to therapy[14] and to follow the pharmacokinetics of some chemotherapeutic agents.[15] MRS is concerned with signals from ^{1}H or ^{31}P atoms in endogenous metabolites or ^{19}F signals from drugs. In the laboratory, ^{13}C is also used to look at exogenously administered substances.

^{31}P MRS

The nucleus most commonly observed in MRS studies of tumours is ^{31}P. Metabolically significant phosphorus-containing compounds occur in living systems at high enough concentrations to be detected by ^{31}P (> 0.2 mM),[15] thus providing an ideal means of monitoring tumour energetics, phospholipid metabolism and intracellular pH.[16]

A typical ^{31}P spectrum from a normal brain (Figure 1.1) demonstrates seven resolved peaks from nucleotide triphosphates (NTP, α, β, γ resonances, predominantly ATP), phosphocreatine (PCr), phosphodiesters (PDE), inorganic phosphate (P_i) and phosphomonoesters (PME).[17] PDE signals are primarly due to glycerophosphocholine (GPC) and glycerophoshoethanolamine (GPE), which are produced by membrane catabolism, while PME signals primarily arise from phospholipid precursors such as phosphocholine (PC) and phosphoethanolamine (PE),[18] which are membrane synthesis substrates. The large PDE and PME resonances are related to cell membrane turnover, thus changes in the PME/PDE ratio may correspond to high rates of membrane synthesis within rapidly proliferating tissue, or membrane decomposition within necrotic regions.[19] A number of studies performed *in vitro* demonstrated that significant increases in the PE/PC

and PC/GPC ratio, with respect to normal tissue, may be considered as an indicator of the status of cell growth and proliferation.[20] General findings were that human cancer cells typically have a pH that is neutral to slightly alkaline, low PCr level, high PME and PDE levels.[21]

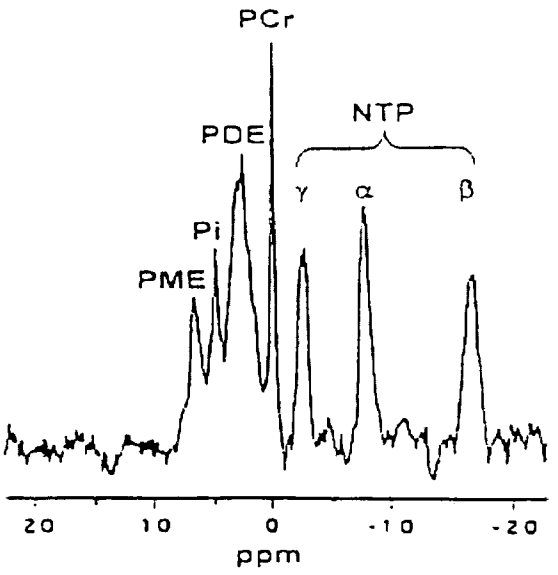

Figure 1.1 Typical ^{31}P spectrum from normal human brain.[17]

Intracellular tumour pH can be derived from the chemical shift of P_i signals[22] and it has been found that tumour pH is not acidic, as it had been thought for many years, but neutral or slightly alkaline.[23] The acidic tumour pH previously measured by microelectrodes is actually extracellular and probably arises from lactic acid production from glycolysis, a classical feature of tumours.[24] Presumably tumour cells maintain neutrality by pumping acid into the extracellular compartment and therefore the pH gradient across the tumour cell membrane is reversed ($pH_i > pH_e$), in contrast to normal cells, which are more acidic than their extracellular environment. This has now been confirmed by ^{31}P MRS, using the extracellular pH probe 3-aminopropylphosphonate (3-APP).[25] Reversal of the pH gradient results in redistribution of many other ionic species and may explain the increase in accumulation of intracellular Ca^{2+} and the calcification associated with many tumours[26] (Figure 1.2).

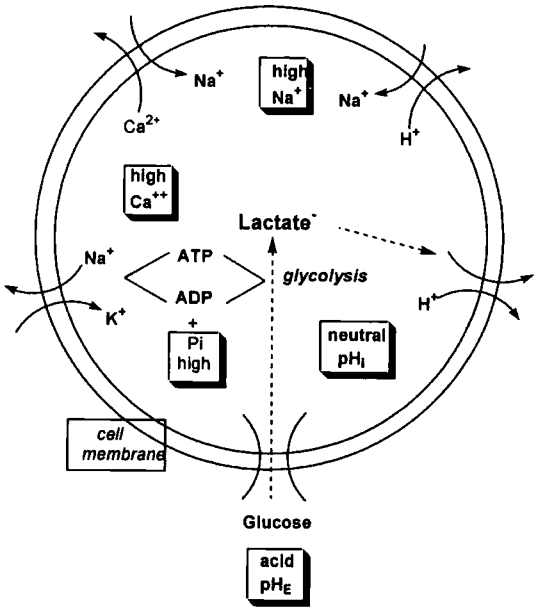

Figure 1.2 Ion balances across the tumour cell measured in part by MRS techniques. Compared to normal cells, the cancer cell has high calcium, sodium, lactate, ADP, P_i, low ATP and acid extracellular pH. The removal of protons, produced intracellularly from high lactic acid production, and a low ATP, leads to an influx of Na^+ ions into the cell. This decreases the energy of the Na^+ gradient, which leads to an accumulation of intracellular Ca^{2+}, which may precipitate with P_i to form insoluble calcium phosphate.[13]

^{31}P MRS has been used to study changes in the energy and phospholipid metabolism of tumours during therapy,[27] in particular breast cancer,[28] and to observed tumour response to a range of chemotherapeutic agents such as 5-fluorouracil (5-FU), cyclophosphamide and 1,3-bis(2-chloroethyl)-1-nitrosourea.[29] The decrease in PME signal intensity or in PME/PDE ratio have been found to be good predictors of the eventual response to either radio or chemotherapy.[20]

^1H MRS

Pre-clinical studies of tumours by ^1H MRS *in vivo* are few, even though the proton occurs naturally, is the most sensitive nucleus and is present in nearly every compound in living tissue. However, ^1H MRS allows observation of several metabolites that are not detected by MRS using other nuclei. The major obstacles to

overcome are the high concentrations of tissue water and lipids, which produce intense background signals that must be suppressed to observe the metabolites of interest. Although adequate water suppression can now be achieved, most of the clinical studies have been limited to intracranial (brain) tumour models which have very little motion and less intense lipid signals.[30]

A typical ^{1}H MRS spectrum of a normal human brain shows resonances for N-acetylaspartate (NAA), creatine (Cr), choline compounds (Cho), glutamate (Glu), inositol (Ins), lactate (Lac) and mobile lipids (Figure 1.3).

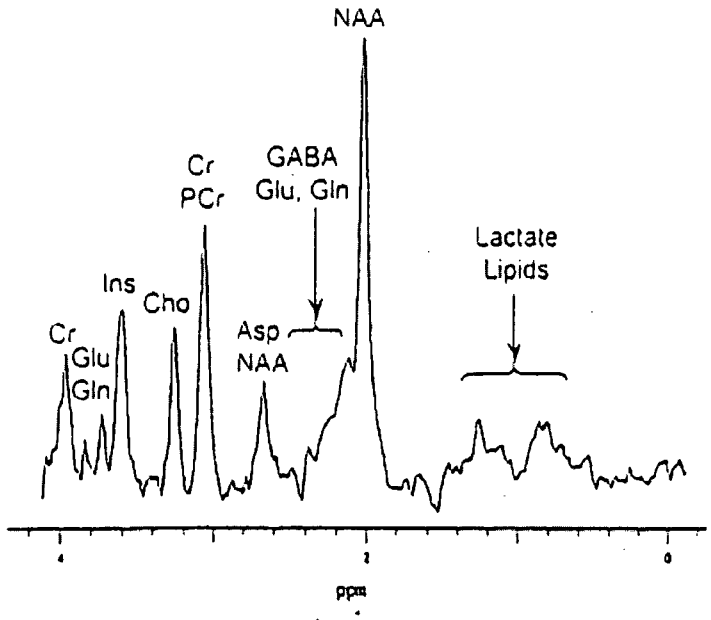

Figure 1.3 A water-suppressed ^{1}H spectrum of a normal human brain.[17]

A number of studies have shown that ^{1}H NMR spectra of human brain tumours differ significantly from those of healthy brain tissue, suggesting the use of this technique in the diagnosis of the type and grade of tumour. The most consistent findings of ^{1}H NMR studies of intracranial neoplasms are increased levels of choline, inositol, lactate and lipids and decreased levels of NAA and Cr.[31] Metabolite ratio maps comparing Cho to Cr or NAA are useful in the evaluation of focal brain lesions suspected of being neoplastic.[32]

^{1}H MRS measurement of citrate and other metabolites has demonstrated high specificity in discriminating prostate cancer from surrounding regions of normal peripheral zone and it is now well established that prostate cancer is characterized by a decrease in citrate levels.[33,34]

The increased capability for glycolytic metabolism is a well known characteristic of neoplastic cells. Because lactic acid is the end product of the anaerobic respiration, *in vivo* MRS measurements of its concentration may provide valuable information about tumour metabolism, which will aid the development, clinical diagnosis and treatment of tumours.[35] Lactate is typically maintained at very low levels in the normal brain and is not detected. However, a doublet resonance from the methyl protons can be observed at 1.35 ppm in certain pathological conditions such as some, but not all, metastases and glial brain tumours.[36] Lactate concentration can be correlated with grade or type of tumour, though its absolute level is dependent on the balance between production rate and clearance.

^{19}F MRS

Another nucleus utilized for clinical *in vivo* MRS studies of cancer is ^{19}F. Several advantages include the high sensitivity of the nucleus, being nearly equal to that of the ^{1}H, a wide chemical shift range and the absence of interfering background signals, due to the lack of endogenous fluorine. ^{19}F MRS is useful in pre-clinical and clinical oncology for monitoring pharmacokinetics and for assessing tumour biochemistry by using probe molecules. Of the chemotherapeutic agents, the fluoropyrimidines have been the most widely studied, particularly the prodrug 5-Fluorouracil (5-FU),[37] and ^{19}F MRS has been used to detect its uptake and metabolism. Compounds containing ^{19}F have also been utilized as probes for intracellular and extracellular pH.[38]

^{13}C MRS

^{13}C MRS has been used to study cancer, despite the poor sensitivity and low natural abundance of this nucleus. Currently, the major application of *in vivo* ^{13}C MRS for studying cancer is to monitor glycolysis and other metabolic pathways, and the flux

of metabolites in tumours relative to normal tissue. The presence (or the absence) of glucose, lactate, citrate and alanine, can be detected, along with their concentration, mobility and relaxation characteristics. The pharmacokinetics of ^{13}C-labelled chemotherapeutic agents,[3] can also be assessed by ^{13}C MRS. However, detection of a drug *in vivo* is limited due to the poor sensitivity of the nucleus.

1.2 Paramagnetism of Lanthanide(III) Ions

1.2.1 Introduction

The electronic configurations $[Xe]4f^n$ (where n = 0-14) of the lanthanide(III) ions dictate their magnetic properties. La(III) and Lu(III) are diamagnetic due to the lack of unpaired electrons while the other ions in this series, having 1 to 7 unpaired 4f electrons, are paramagnetic. The 4f valence electrons are shielded by the 5s and 5p electrons therefore they are not readily available for covalent interactions with ligand. Interactions are largely electrostatic and consequently the geometry of lanthanide(III) complexes is usually determined by steric factors rather than by electronic ones.[39] Lanthanide(III) ions can be classified as hard Lewis acids and the affinity for donor sites of the ligand follows the order of electronegativity (i.e. $F^- > OH^- > NO_3^- > Cl^-$). Due to the shielding of the 4f electrons, the lanthanide(III) ions are chemically very similar. Commonly, the various lanthanide(III) complexes of a particular ligand are almost isostructural. Each of the lanthanide(III) ions, however, exhibits its own characteristic effect on the NMR parameters of nuclei in its proximity.[40] When a Lewis base interacts with a lanthanide cation, any NMR active nucleus within that base molecule 'feels' the presence of the unpaired f electrons. This leads to paramagnetic relaxation, broadening and, in some cases, a shifting of that resonance.[41]

1.2.2 Lanthanide Induced Shift

The lanthanide induced shift (LIS) for a nucleus of a ligand coordinated to a lanthanide(III) cation (Δ) can be expressed as the sum of three terms: the diamagnetic

(Δ_d), the contact (Δ_c) and the pseudo-contact (Δ_p) shift (equation 1.1). Each of these, but particularly the contact and pseudocontact shifts, contain useful information regarding the structure of the concerning lanthanide(III) complex.[42]

$$\Delta = \Delta_d + \Delta_c + \Delta_p \qquad \textbf{(1.1)}$$

Diamagnetic Shift

The diamagnetic or complexation shift (Δ_d) is usually small and is often neglected. It originates from effects such as conformational changes, inductive effects and direct electrical field effects which are usually insignificant, with exception for the nuclei directly coordinated to the lanthanide cation.[43]

Contact Shift

Scalar interactions result in Fermi or contact shifts which involve a through-bond transmission of unpaired electron-spin density from the lanthanide f orbital to the nucleus of interest. The contact shift (Δ_c) is given by equation 1.2:

$$\Delta_c = \langle S_Z \rangle F = \langle S_Z \rangle \frac{\beta}{3kT\gamma_I} \cdot \frac{A}{\hbar} \cdot 10^6 \qquad \textbf{(1.2)}$$

$$\langle S_Z \rangle = [J(J+1)g(g-1)]$$

$$g = [3J(J+1) - L(L+1) + S(S+1)]/2J(J+1)$$

where $\langle S_Z \rangle$ is the reduced value of the average spin polarization, β is the Bohr magneton, k is the Boltzmann constant, γ is the gyromagnetic ratio of the nucleus in question, T is the absolute temperature, A/ħ is the hyperfine coupling constant (in rad s^{-1}), g is the Landé factor, L and S are the quantum numbers for the orbital angular moment and the electron spin, respectively. Δ_c is expressed in ppm.

Values for $\langle S_Z \rangle$ have been tabulated[44] (Table 1.1) for each of the lanthanides and have been found to be linearly related to measured ^{17}O shifts for the aquo lanthanides[45] and to the ^{15}N shifts for the lanthanide–pyridine complexes.[46] This

suggests that the LIS for a donor atom is predominantly of contact origin and that the hyperfine coupling constant does not vary significantly along the lanthanide series. The contact shift, in general, rapidly decreases in magnitude upon increasing the number of bonds between the lanthanide(III) ion and the nucleus under study,[43] with the largest contact shifts being observed for the directly Ln(III) bonded donor sites. The donor sites in a ligand can therefore be easily identified by observation of their relatively large contact shifts.[47]

Pseudo-contact Shifts

A pseudo-contact or dipolar shift (Δ_p) arises from the local magnetic field induced in the nucleus under study by the magnetic moment of the lanthanide ion. It is the result of a through-space interaction between the unpaired electrons of the lanthanide(III) ion and the nuclear magnetic dipoles. This is the type of interaction that predominates with lanthanide shift reagents. A prime reason for this is that the unpaired electrons reside in the 4 f orbitals and these orbitals are well shielded from the valence orbitals involved in bonding between the metal and the ligand. Thus, the unpaired electron spin density remains largely on the lanthanide cation and the NMR shift is most commonly a result of through-space interaction. For this dipole-dipole interaction to occur, the unpaired electron density must be anisotropically distributed with respect to the magnetic field. Gd^{3+} has 7 unpaired electrons, but these are isotropically distributed so there is no pseudo-contact contribution. However, Gd^{3+} induces a contact shift and so can be used to separate out the contributions of each effect.

Bleaney has calculated the pseudocontact shifts with the assumption that the ligand field splittings for the lowest J states in the lanthanide complexes are small compared to kT.[48] A general expression for the pseudo-contact shift is given by equation 1.3.

$$\Delta_p = C_j G = C_j \frac{\beta^2}{60k^2T^2} \cdot \frac{\langle r^2 \rangle A_2^0 \left(3\cos^2\theta - 1\right) + \langle r^2 \rangle A_2^2 \left(\sin^2\theta \cdot \cos 2\varphi\right)}{r^3} \qquad \textbf{(1.3)}$$

where $C_j = g^2 J\,(J+1)\,(2J-1)\,(2J+3) \langle J|a|Jc \rangle$

C_j is Bleaney's constant, characteristic of the Ln(III) ion, $\langle r^2 \rangle A_2^0$ and $\langle r^2 \rangle A_2^2$ second order crystal field coefficients, r, θ, φ are the polar coordinates of the observed ligand nucleus with respect to the principal magnetic axis (as the z-axis) of the complex with the lanthanide(III) ion at the origin, g is the Landé factor, $\langle J|a|J \rangle$ is a numerical coefficient and L and S are the quantum numbers for the orbital angular moment and the electron spin, respectively. The theoretical pseudocontact (C_j)[48] and contact $(\langle S_Z \rangle)$[44] constants, the quantum numbers and the Landé g factor of the ground electronic states of the paramagnetic lanthanide(III) ions, are reported in Table 1.1.

Ln(III)	$4f^n$	$^{2S+1}L_j$	S	L	J	g	C_j[48]	$\langle S_Z \rangle$[44]
Ce	f^1	$^2F_{5/2}$	1/2	3	5/2	6/7	-6.3	-0.98
Pr	f^2	$^3H_4$	1	5	4	4/5	-11.0	-2.97
Nd	f^3	$^4I_{9/2}$	3/2	6	9/2	8/11	-4.2	-4.49
Pm	f^4	$^5I_4$	2	6	4	3/5	2.0	4.01
Sm	f^5	$^6H_{5/2}$	5/2	5	5/2	2/7	-0.7	0.06
Eu	f^6	$^7F_0$	3	3	0	0	4.0	10.68
Gd	f^7	$^8S_{7/2}$	7/2	0	7/2	2	0.0	31.50
Tb	f^8	$^7F_6$	3	3	6	3/2	-86	31.82
Dy	f^9	$^6H_{15/2}$	5/2	5	15/2	4/3	-100	28.55
Ho	f^{10}	$^5I_8$	2	6	8	5/4	-39	22.63
Er	f^{11}	$^4I_{15/2}$	3/2	6	15/2	6/5	33	15.37
Tm	f^{12}	$^3H_6$	1	5	6	7/6	53	8.21
Yb	f^{13}	$^2F_{7/2}$	1/2	3	7/2	8/7	22	2.59

Table 1.1 Parameters affecting the contact and the pseudocontact contribution to the LIS.

With isostructural complexes (i.e. r, θ, φ independent of the lanthanide), it is assumed that the ligand field coefficients $\langle r^2 \rangle A_2^0$ and $\langle r^2 \rangle A_2^2$ do not vary along the lanthanide series. Thus they may be combined with Bleaney's constant to give a simplified equation 1.4:

$$\Delta_p = \frac{D_1\left(3\cos^2\theta - 1\right) + D_2\left(\sin^2\theta\cos 2\varphi\right)}{r^3} \qquad \textbf{(1.4)}$$

In the case of axially symmetric systems, the second term in equation 1.4 is equal to zero and the measured pseudo-contact shift is expressed in equation 1.5, which is frequently used to calculate LIS in structural analysis even if the complex has no axial symmetry.[49]

$$\Delta_p = \frac{D_1\left(3\cos^2\theta - 1\right)}{r^3} \qquad \textbf{(1.5)}$$

The pseudocontact contribution usually predominates for the lanthanides as the electron spin density largely resides on the lanthanide(III) ion. The pseudocontact shift depends on the orientation of the resonating nucleus with respect to the lanthanide(III) ion (Figure 1.4) and provides useful angular and distance information which has found widespread application from the determination of solution structures of lanthanide chelates to gaining structural information on proteins, nucleotides and amino acids.[40]

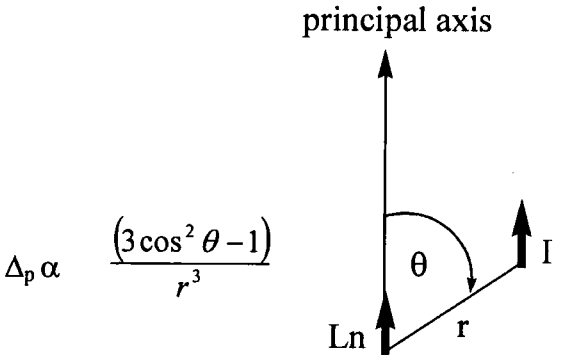

Figure 1.4 Dependence of the dipolar shift on the geometrical factors.

1.2.3 Separation of Shift Contributions

Since only the dipolar term contains the geometric information of interest, any quantitative structural analysis requires a reliable separation of the observed shift into the contact and dipolar terms. The diamagnetic shifts are usually small and can be determined directly or by interpolation from shifts induced by the diamagnetic La^{3+} and Lu^{3+} ions. Subtraction of the diamagnetic contributions gives the paramagnetic shift Δ', expressed in equation 1.6.

$$\Delta' = \Delta_c + \Delta_p = \langle S_Z \rangle F + C_j G \qquad \textbf{(1.6)}$$

The terms $\langle S_Z \rangle$ and C_j are characteristic of the lanthanide(III) ion but independent of the ligand, whereas F and G are characteristic of the ligand nucleus under study. Assuming that the lanthanide complexes studied are isostructural and of axial symmetry, using theoretical calculated values for $\langle S_Z \rangle$ and C_j tabulated in the literature, F and G may be determined by linear regression according to equation 1.7 and 1.8, if the Δ' values of a ligand are known for two or more lanthanide(III) ions.[50]

$$\frac{\Delta'}{\langle S_Z \rangle} = F + \frac{C_j G}{\langle S_Z \rangle} \qquad \textbf{(1.7)}$$

$$\frac{\Delta'}{C_j} = \frac{\langle S_Z \rangle F}{C_j} + G \qquad \textbf{(1.8)}$$

Equation 1.7 should be used when Δ' is dominated by dipolar shifts and equation 1.8 used when the contact contribution dominates Δ'. Since the ionic radii of the lanthanide(III) ions decrease across the series from 1.36 to 1.17 Å (lanthanide ion contraction), slight changes in the orientation of the ligands around the lanthanide(III) often occur, which is reflected in small changes only of G. These changes in G are thus magnified by using equation 1.7, because C_j values for the first part of the series (Ce → Eu) (0.7-11) are much smaller than those of the second part (Tb → Yb) (22-100) and breaks are often observed in the plots according to this

equation. However, the F values are not affected by these slight structural changes, and plots according to equation 1.8 show no breaks in these cases. Non linearity of both types of plots indicates that either a significant structural change occurs (i.e., a change of coordination mode of a ligand) or that the crystal field coefficients vary across the lanthanide series.[51]

1.3 Shift Reagents

1.3.1 Introduction

The peculiar magnetic properties of lanthanide(III) ions have been exploited in NMR spectroscopy for many years. Each lanthanide(III) has its own characteristic shift and relaxation properties which can affect NMR parameters of proximate nuclei. A chiral shift reagent is a paramagnetic metal chelate that forms a weak complex, in fast exchange on the NMR timescale, with a species of interest, thereby causing a lanthanide induced shift. The chiral ligand of the shift reagent provides a chiral environment for the substrates with which they form adducts, thus enantiotopic nuclei become diastereotopic and are, in principle, distinguishable by NMR. An effective shift reagent requires a paramagnetic metal ion in a non-S ground state electronic configuration, with a high magnetic moment and a short value of the electronic relaxation time (10^{-13}s), in order to cause a minimal degree of line broadening. The most efficient shift reagents are chiral complexes of paramagnetic lanthanide ions, whose induced pseudocontact shift depends on the position of the donor along the symmetry axis (LIS α $(3\cos^2\theta - 1)/r^3$). Paramagnetic lanthanide(III) chelates endowed with shift reagent capabilities, have been used as NMR probes for biomedical applications, including the separation of NMR resonances of species present in the inner and outer cellular compartment and the measurement of pH and temperature in a given organ or tissue.[52] Since the first report by Hinckley[53] of the use of lanthanide complexes to simplify unresolved proton resonances in low field NMR spectra, the lanthanide induced shift (LIS) method has also been applied to a variety of NMR problems. These have ranged from qualitative spectral simplification

and proof of molecular stereochemistry to the quantitative analysis of dynamic solution structures[54] and the resolution of enantiomers.[40,51]

1.3.2 Choice of the Metal

In selecting the appropriate lanthanide(III) ion for use as a shift reagent, the shifting ability and the degree of line broadening should be considered. The chemical shift of the most shifted resonance of three chelators in the presence of lanthanide(III) complexes of tris(dipivaloylmethanato), $Ln(dpm)_3$ have been reported[55] (Figure 1.5).

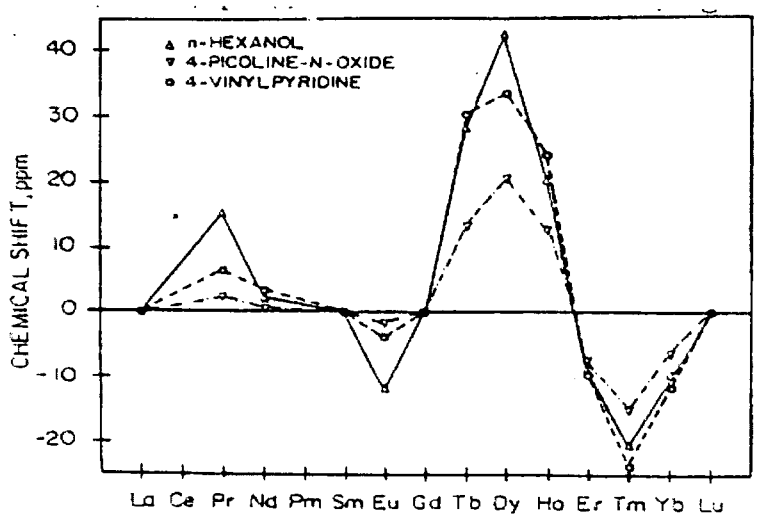

Figure 1.5 Isotropic shifts for the most shifted resonances of the three chelators in the presence of Ln (dipivaloylmethanato)$_3$.[55]

Of interest are the low frequency isotropic shifts produced by Pr^{3+}, Nd^{3+}, Tb^{3+}, Dy^{3+}, Ho^{3+} and the high frequency shifts induced by Eu^{3+}, Er^{3+}, Tm^{3+}, and Yb^{3+}. The lanthanides(III) exhibiting negative Bleaney constant give rise to low frequency shifts whereas those with positive C_j values shift to higher frequency, providing further evidence in favour of the largely dipolar origin of the LIS.

The degree of line broadening experienced by the nuclei in the presence of each lanthanide(III) is shown in Table 1.2.

Ln^{3+}	Ce	Pr	Nd	Pm	Sm	Eu	Gd	Tb	Dy	Ho	Er	Tm	Yb
$\Delta\nu_{1/2}$[55]	-	5.6	4.0	-	4.4	5.0	-	96	200	50	50	65	12

Table 1.2 Half peak height line width resonance of the methyl of 2-picoline, in the presence of the tris(dipivaloylmethane) complexes of the Ln(III) ion, values in Hz.[55]

The shifts in response to Pr^{3+} and Eu^{3+} both occur with negligible line broadening. Dy^{3+}, Ho^{3+} and Tb^{3+} all induce huge shifts with severe line broadening and, of course, the diamagnetic La^{3+} and Lu^{3+} produce no shift at all. Gd^{3+} is not a shift agent and has $\Delta_p = 0$, due to the isotropic distribution of the 7 unpaired f electrons. Yb^{3+} has an NMR shift which is essentially dipolar in nature and it induces such a large spectral range that despite broadening effects being severe, the signals appear sharp and well-defined.[56] Usually the best LIS for ^{1}H and ^{13}C NMR are obtained with Yb^{3+}, Eu^{3+} and Pr^{3+} (which shifts signals in the opposite sense to Yb^{3+} and Eu^{3+}).

1.3.3 Choice of the Ligand Structure

The 'free' lanthanide ions are known to be toxic as they can replace Ca^{2+} in the body, thus water soluble complexes of high kinetic and thermodynamic stability, with respect to the metal ion dissociation, are required for use *in vivo*.[57]

The coordination number exhibited by Ln^{3+} ions has been found to range from 3 to 12 in a variety of solid compounds. The strongly ionic nature of the bonding results in coordination geometries that reflect a balance of electrostatic and steric demand. It can be assumed that the range of coordination numbers for lanthanides in aqueous solution resembles that in solids, although 8 and 9 are most frequently observed.[40]

The lanthanides behave as hard acids, interacting preferentially with hard donor atoms such as O and N. Amine nitrogens are preferred to ether oxygens, due to their

more polarisable lone pair, and carboxamides are good stabilizing binding groups, owing to the large ground state dipole moments. The lanthanide-ligand coordination is mainly electrostatic in nature, thus negative charge on the donor atoms (i.e. carboxylic and phosphonic acids) increases the complex stability.

Water is a strong ligand for lanthanides and affects the complex stability in aqueous media, particularly when the ligand is monodentate and uncharged. Complex stabilities can be improved by the incorporation of donor atoms into chelating rings.[58] For the lanthanide ions, the larger bite angle of a 5-membered chelate ring (72°) is favoured over a 6-membered chelate (60°) (the chelate effect).[59] Additional complex stability can be gained by incorporating the donor atoms into macrocycles, due to enthalpic and entropic factors which vary according to the macrocycle and the metal ion.[60]

Macrocycles based on 1,4,7,10-tetraazacyclododecane with functionalised pendent arms are suitable ligands to bind lanthanides. Among the pendent arms, the carboxylate group has been shown to be sterically very efficient. Unusual stabilities can be achieved due to the ability of the carboxylate to occupy little space close to the lanthanide ion, allowing for more efficient coordination of other donor groups present (i.e. amine) (Figure 1.6).

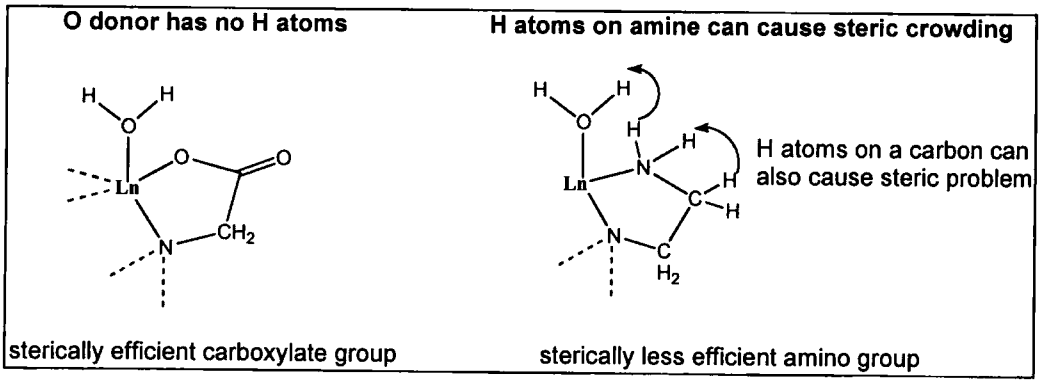

Figure 1.6 Schematic representation of the potential coordination of carboxylate and amine pendent arms to the Ln^{3+} ion.[59]

High stability constants (logK ≥ 25) for lanthanide complexes based on the DOTA (1,4,7,10-tetraazacyclododecane-N,N',N'',N'''-tetraacetic acid) ligand (Figure 1.7 a) have been reported.[61]

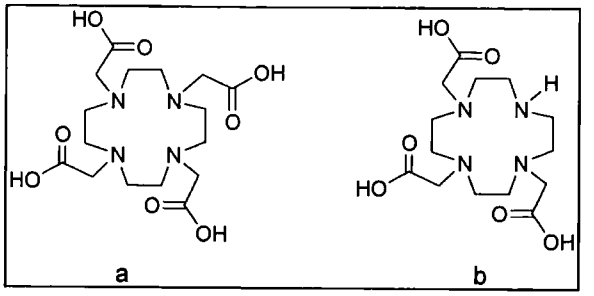

Figure 1.7 DOTA (a) and DO3A (b) ligands.

Such ligands provide eight coordination sites for the Ln^{3+} ion and a water molecule completes the coordination sphere. Complexes of heptadentate ligands based on DO3A (Figure 1.7 b) are typically diaqua systems and are of lower overall stability with respect to lanthanide ion dissociation. However, the two water molecules may be displaced by a variety of monodentate and chelating anions, providing a potential probe for anion binding.

1.3.4 Stereoisomerism

In lanthanide complexes of DOTA or its carboxamide derivatives, there are two elements of chirality: the conformation of the macrocyclic ring (δ or λ), associated with the NCCN torsion angle (Figure 1.8) and the orientation of the pendent arms (Δ or Λ), associated with the NCCO torsion angle (Figure 1.9).[62]

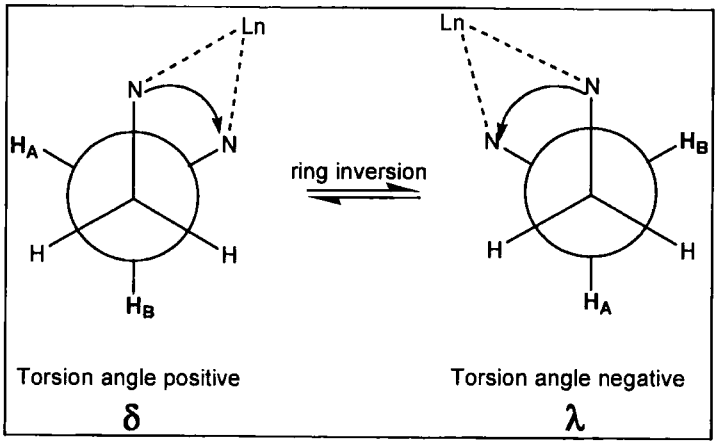

Figure 1.8 Newman Projection of the NCCN bond showing torsion angles.

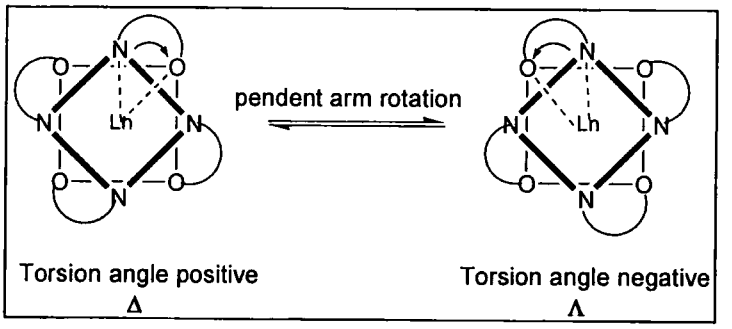

Figure 1.9 Possible orientations of the pendent arms around the NCCO bond.

The ring may adopt two enantiomeric conformations in the complex (λλλλ or δδδδ in each five-ring chelate following Corey and Bailar's original classification[63]) and two in the pendent arms, which may be arranged in either a clockwise (Δ) or anticlockwise (Λ) fashion. Thus in such lanthanide complexes there are two enantiomeric pairs of diastereoisomers in solution, which may interconvert via pendent arm rotation (Δ ↔ Λ) or ring inversion (λλλλ ↔ δδδδ) (Figure 1.10).[64]

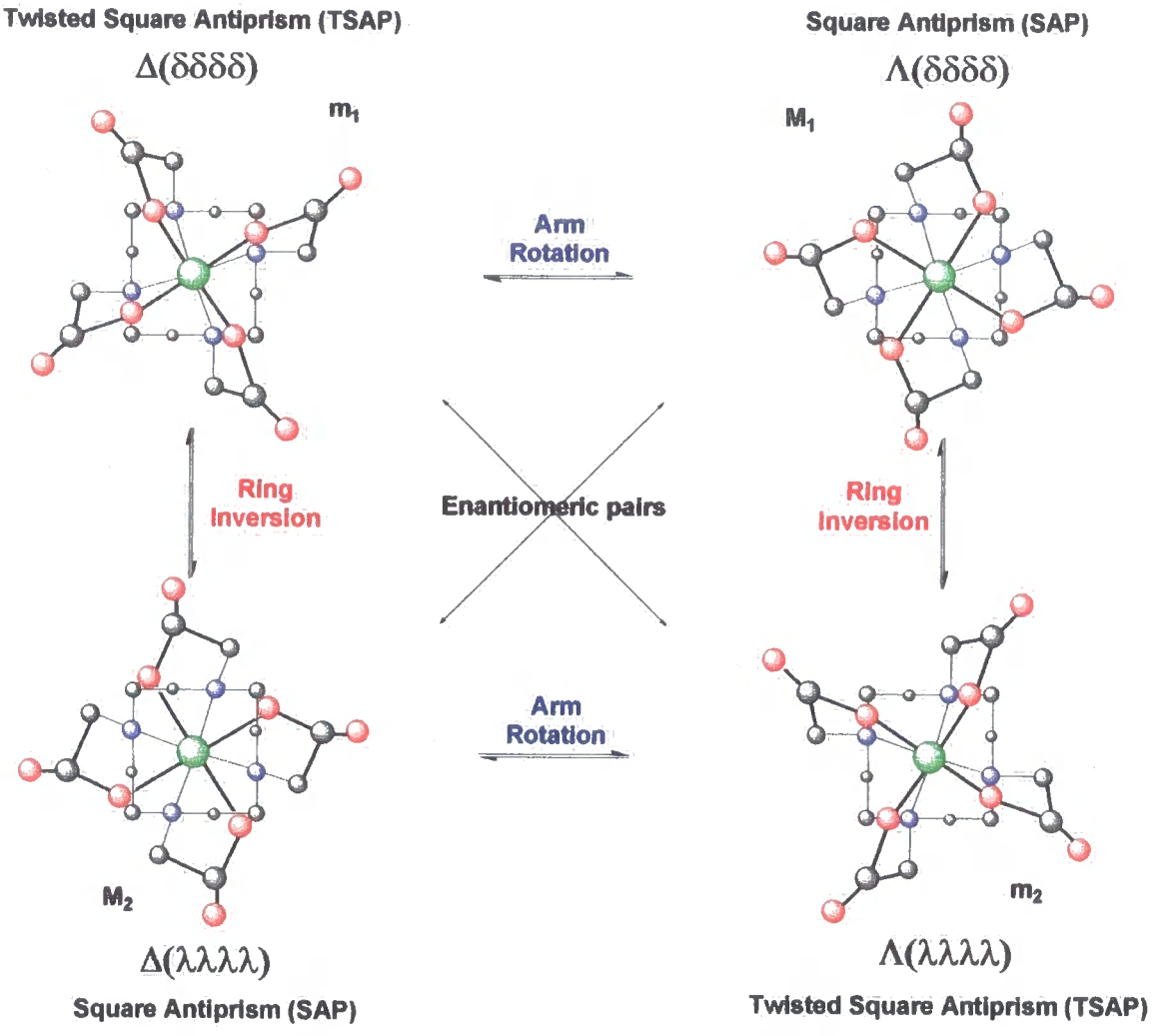

Figure 1.10 Schematic representation of the stereoisomers of Ln(DOTA)$^-$ complexes, showing the possible exchange mechanisms.

The major stereoisomer found in solution (M_1 or M_2) possesses a regular square–antiprism structure (twist angle ca. 40° between the N_4 and O_4 planes), whereas the minor isomer (m_1 or m_2) adopts a twisted square-antiprism structure (twist angle ca. 29°). Ring inversion or arm rotation alone results in exchange between these two geometries, while the combination of both processes results in exchange between the enantiomeric pairs.

The introduction of a chiral centre α to the ring nitrogen in DOTA systems and α or β to the ring nitrogen in tetraamide Ln(III) complexes imparts extra-rigidity, inhibiting arm rotation in particular.[65] The introduction of a chiral centre δ to the ring nitrogen also imparts considerable conformational rigidity to the complex and leads to the formation of an enantiopure complex. The configuration of this remote stereogenic carbon centre has been reported to determine the macrocyclic ring conformation and the helicity of the pendent arms (i.e., R and S at the carbon favours the square antiprism geometries Λ (δδδδ) and Δ (λλλλ) respectively).[66] The incorporation of substituents into the macrocyclic ring also rigidifies the macrocycle, preventing ring inversion. The simultaneous use of α substituents, in the pendent arm, with substituents on the ring, leads to a single isomer in solution, since ring inversion and arm rotation are frozen out.[67]

1.3.5 Chiral Shift Reagents for Aqueous Solutions

Chiral resolution by lanthanide shift reagents is a topic of high relevance in several fields of chemistry, including catalysis and biochemistry. It has found widespread application in the analysis of enantiomeric mixtures, especially in organic solvent,[68] while only a few studies have been reported in aqueous media.[69]

Since the first pioneering work in the field of chiral aqueous shift reagents, performed by Reuben,[70] who showed that 1:1 Ln (III) complexes of chiral α-hydroxycarboxylates can be employed to resolve enantiomer signals in NMR, further studies have been performed on this topic. Kabuto and Sasaki have introduced Ln (III) complexes of a chiral methyl substituted EDTA derivative, (R)-propylenediamine tetraacetate (PDTA, Ln = Eu) (Figure 1.11 a), which resolve enantiotopic signals of a range of amino acids and hydroxycarboxylates.[71,72] The magnitude of the shift difference between enantiomers (ΔΔδ) is small (0.1 ppm) but sufficient to determine enantiomeric purity. The chemical shift differences between the enantiomeric nuclei were shown to be strongly dependent on the pH, for example the separation of lactic acid was optimal at pH 4 and that of amino acids was observed at high pH (12). Improved results have been reported for the Eu(III)

complex of (S,S)-ethylenediamine-N,N-disuccinate (EDDS)[73] (Figure 1.11 b) which is a useful chiral shift reagent for aqueous work, as long as the solution pH is maintained between 9 and 11.

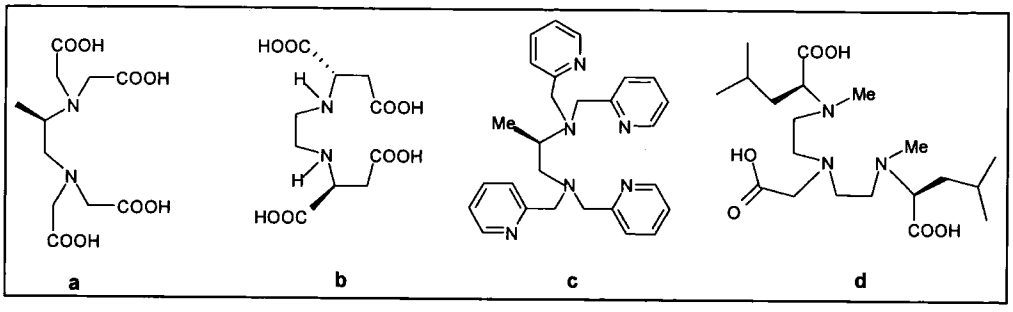

Figure 1.11 Structure of the ligands (R)-PDTA (a), (S,S)-EDDS (b), TPPN (c) and TRENBMTA (d).

A new chiral lanthanide shift reagent,[74] the Eu(III)-N, N, N', N,'-tetrakis(2-pyridinylmethyl)-(R)-propylenediamine (TPPN) (Figure 1.11 c) complex, was shown to resolve the enantiomer signals of α-amino acids in neutral, aqueous solution (typical $\Delta\Delta\delta$ values are in the range of 0.03 ppm and 0.41 ppm). This property is advantageous as it avoids any possible undesired change in the substrate under the alkaline conditions usually employed with other shift reagents. These aqueous chiral lanthanide shift agents are 6 coordinate, form weak addition complexes in fast exchange on the NMR timescale and have $\Delta\Delta\delta$ values of typically < 1 ppm.

Several new water soluble chiral lanthanide shift reagents have been developed in recent years.[75] Europium complexes with the ligands N,N'-ethylenebis(L-amino acid) in which the amino acid is either S-histidine methyl ester or S-aspartic acid dimethylester,[76] and N,N-bis[2-{N-methyl((1S)-1-carboxy-3-methyl)butylamino}ethyl]glycine[77] (TRENBMTA) (Figure 1.11 d) were shown to be useful chiral shift reagents for some unprotected natural α–amino acids in neutral aqueous solution. Such complexes do not exhibit any significant signal broadening however, the $\Delta\Delta\delta$ values are again very small.

1.3.6 Shift Reagents for Metal Cations in Biological Systems

NMR active metal cations of clinical importance such as $^{7}Li^{+}$, $^{23}Na^{+}$ and $^{39}K^{+}$ are normally found in biological systems in both the intra- and extracellular compartments and, in routine high resolution NMR spectra, are characterized by a single resonance.[52] The application of metal NMR spectroscopy to biomedical studies implies obtaining distinct signals from the two compartments that may then be simultaneously monitored and individually analyzed. This is made possible by the use of aqueous shift reagents such as water soluble paramagnetic chelates which only distribute in the extracellular space and thus are able to remove the signal degeneracy by selectively affecting the extracellular resonance. Negatively charged groups need to be present on the surface of the coordination cage (i.e. carboxylic, phosphonic, etc.) in order to give rise to strong electrostatic interactions with the metal cations and to favour the distribution of the complex in the extracellular space. With the aim of increasing the magnitude of the shift, axially symmetric complexes having the cation binding site along the symmetry axis are favoured (LIS $\alpha\ (3\cos^2\theta - 1)/r^3$).

Examples of effective shift reagents are the Dy^{3+} and Tm^{3+} complexes of 1,4,7,10-tetraazacyclododecane-N, N', N'',N'''-tetra(methylene phosphonate) $DOTP^{8-}$ (Figure 1.12).[78] They have been reported to be extremely resistant to dissociation processes over a wide range of pH and they present interaction sites for cations very close to their axis of symmetry, thus ensuring a maximum shifting efficiency.

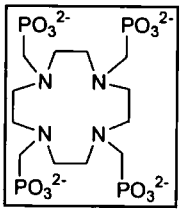

Figure 1.12 Structure of $DOTP^{8-}$ ligand.

1.4 Luminescence Properties of Lanthanide(III) Ions

1.4.1 Lanthanide Luminescence

Luminescence is defined as emission of electromagnetic radiation from a molecule or atom in an electronically excited state. This radiative process involves electrons which, having absorbed energy to enter an excited state, revert back to their ground states, losing energy by emitting light. The radiative pathway which occurs between two levels of the same spin multiplicity ($\Delta S = 0$) is called fluorescence and lasts 10^{-9}-10^{-6} s. When the radiative transition involves a change in spin multiplicity ($\Delta S \neq 0$), due to a process named intersystem crossing, phosphorescence takes place, which is forbidden and therefore is longer lived (10^{-4}- 10^{2} s).

The trivalent lanthanide ions and their complexes are known to luminesce and give rise to narrow bands corresponding to transitions within the f orbitals. Since the 4f orbitals are shielded from the environment by the outer shell of 5s and 5p orbitals, they are only minimally involved in bonding. The consequent small interaction between the ligand and the f orbitals results in very small ligand field splittings, therefore the emission bands do not broaden and shift upon complexation.[79]

The ions Sm^{3+}, Eu^{3+}, Tb^{3+}, Dy^{3+}, Yb^{3+} and Gd^{3+}exhibit strong luminescence due to their relatively large energy gap between the lowest excited state and the highest ground state levels, which makes competing non radiative deactivation processes less likely to occur. Whereas weak luminescence is shown by Pr^{3+}, Nd^{3+}, Ho^{3+}, Er^{3+}, and Tm^{3+}, whose relatively small energy gap allows efficient non radiative decay processes to compete.

1.4.2 Eu(III) and Tb(III) Luminescence

Eu^{3+} and Tb^{3+} emit in the visible region of the spectrum upon excitation at 580 and 485 nm respectively (Figure 1.13).

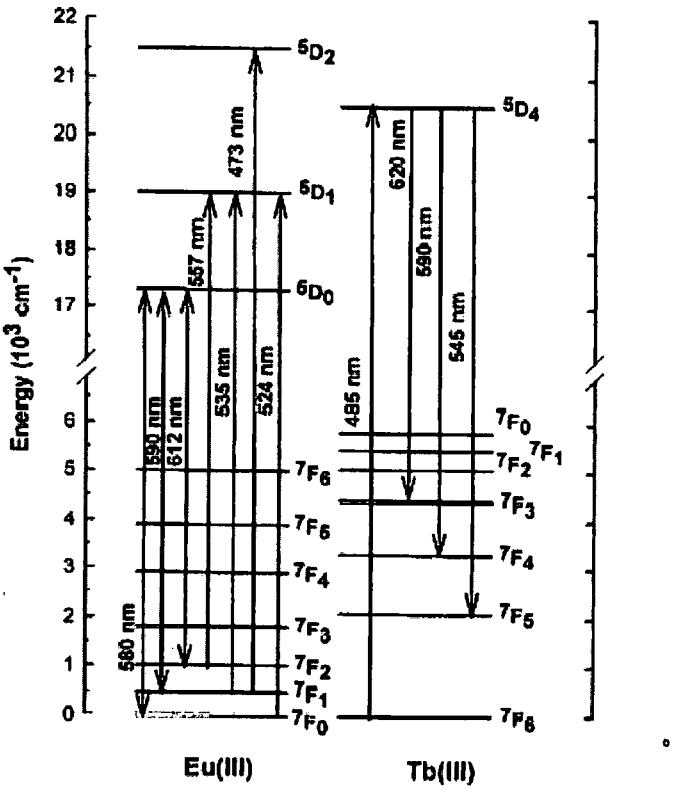

Figure 1.13 Energy levels for Eu^{3+} and Tb^{3+} showing their excitation wavelengths and their most intense emissive transitions.

For Eu^{3+} complexes, the strongest emission generally arises from $^5D_0 \rightarrow {}^7F_{1,2}$ transitions at 590 and 612 nm respectively. The $^5D_0 \rightarrow {}^7F_1$ transition ($\Delta J = 1$) is magnetic dipole in character and largely independent of the coordination sphere but very sensitive to the symmetry of the complex. Two bands are observed if the complex possesses a C_3 or a C_4 axis and three in complexes of lower symmetry. The electric dipole $^5D_0 \rightarrow {}^7F_2$ ($\Delta J = 2$) transition is extremely sensitive to the symmetry of the coordination sphere; its intensity being enhanced by distortion of the symmetry around the ion. The $^5D_0 \rightarrow {}^7F_4$ transition is also relatively intense and sensitive to the ligand field, being predominantly electric dipole in character. The remaining $^5D_0 \rightarrow {}^7F_j$ transitions are generally weak. The $^5D_0 \rightarrow {}^7F_0$ transition at 580 nm is sensitive to

the ligand environment and it can be used to determine the number of different species in solution.

For Tb^{3+} all emissions arise from the $^5D_4$ level (Figure 1.13). The $^5D_4 \rightarrow {}^7F_5$ emission at 545 nm is the most intense and hypersensitive while the $^5D_4 \rightarrow {}^7F_{0,1}$ are always very weak. The $^5D_4 \rightarrow {}^7F_{5,3}$ transitions are magnetic dipole in character but, owing to the degeneracy of the $^5D_4$ level, they do not provide information about the local symmetry of the metal ion.

1.4.3 Sensitised Emission

The lanthanide absorbance transitions within the 4f shell are forbidden by the parity (Laporte) selection rule and give rise to low molar absorption coefficients ($\varepsilon < 1$ M^{-1} cm^{-1}). Thus the absorbance bands are very weak and the excited states are not readily populated with conventional light sources. This limitation can be overcome by directly exciting the lanthanide with a powerful laser source or by sensitised emission, which involves the indirect excitation of the lanthanide by energy transfer from a neighbouring chromophore, which may be incorporated into the ligand.[80] This so called *antenna* must absorb strongly at a suitable wavelength and transfer its excitation energy to the metal, which becomes excited to the emissive state (Figure 1.14). The energy transfer is favoured by a short distance between the sensitiser and the lanthanide ion and the efficiency is dependent on the energy difference between the higher lying triplet state of the sensitiser and the emissive state of the lanthanide. This energy difference should be $\geq$ 1500 cm^{-1} to prevent the occurrence of the thermally activated back energy transfer process,[81] which would result in a reduction of the emission intensity and lifetime of luminescence. Back energy transfer is more likely to be a problem for Tb^{3+}, whose emissive state ($^5D_4$ Tb^{3+} = 20 400 cm^{-1}) is quite high in energy while for Eu^{3+} ($^5D_0$ Eu^{3+} = 17 240 cm^{-1}), a photoinduced electron transfer from the chromophore to the metal can occur, due to the ease of reduction of Eu^{3+} to Eu^{2+}. This process often deactivates the singlet excited state of the antenna in a non-radiative way, thus reducing its efficiency as a sensitiser.

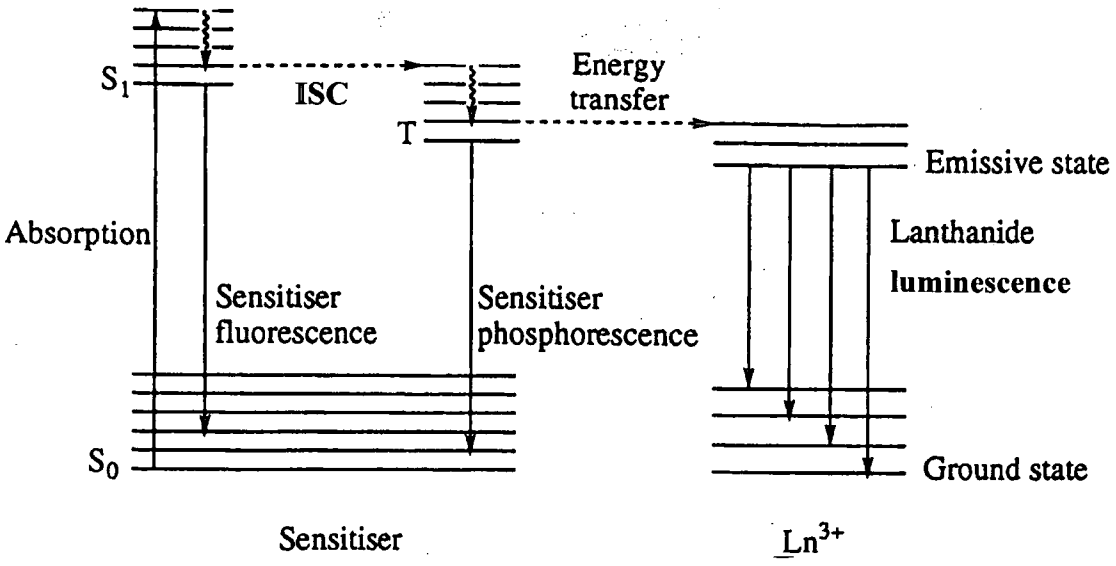

Figure 1.14 Jablonski diagram for sensitised emission.

1.4.4 Hydration State

Deactivation of the luminescence from an excited Ln^{3+} in solution can occur by means of a vibrational energy transfer process, which involves high-energy vibrations of solvent molecules or the bound ligand.[82] O-H stretching vibrations of coordinated or closely diffusing water molecules are the most effective quenchers of the metal emissive state, due to their high vibrational stretching frequency (> 3000 cm^{-1}) which is close to the energy level of the Ln^{3+} emissive state.[83] The extent of luminescence quenching by water molecules has been reported to be inversely proportional to the energy gap between the emitting state and the ground state manifold,[83] therefore Eu^{3+} (ΔE = 12 400 cm^{-1}) is more susceptible than Tb^{3+} (ΔE = 14 800 cm^{-1}). Other oscillators are less efficient but evidence for the quenching effects of N-H, C-H, C=O has also been provided[84] with each oscillator quenching the excited state independently.[85] The corresponding O-D, N-D and C-D oscillators possess lower stretching frequencies and any energy matching is only possible with higher vibrational states, thus the resulting luminescence of Ln^{3+} complexes is more intense in D_2O than in H_2O. The rate constant for depopulation of the lanthanide excited state in water, may be partitioned as the sum of the different quenching contributions (equation 1.9):

$$k_{H2O} = k_{nat} + \sum k_{nr} + \sum k_{XH} + \sum k_{C=O} \quad \textbf{(1.9)}$$

where k_{H2O} is the observed luminescence decay constant in water, k_{nat} is the natural radiative rate constant, $\sum k_{nr}$ is the sum of the rate constants for non radiative processes and $\sum k_{XH}$/ $\sum k_{C=O}$ are the sums of the rate constants for energy transfer to proximate matched X-H and C=O oscillators. Assuming that in D_2O all exchangeable X-H do not contribute, then the rate equation simplifies (equation 1.10).

$$k_{D2O} = k_{nat} + \sum k_{nr} + \sum k_{C=O} \quad \textbf{(1.10)}$$

As a consequence, the difference in measured rate constants for depopulation of the lanthanide excited state in H_2O and D_2O is proportional to the quenching effect of exchangeable X-H oscillators (O-H and N-H) (equation 1.11).

$$\Delta k = k_{H2O} - k_{D2O} = \sum k_{XH} \quad \textbf{(1.11)}$$

The energy transfer process is distance dependent thus, assuming the contribution of the O-H oscillators of coordinated water molecules to be dominant ($\sum k_{XH} = k_{OH}$), an equation (1.12) was derived to estimate q, the number of water molecules coordinated to the lanthanide ion (inner sphere).[86]

$$q = A_{Ln} (k_{H2O} - k_{D2O}) = A_{Ln} \Delta k \quad \textbf{(1.12)}$$

where A_{Ln} is a proportionality constant specific to the lanthanide ion, reflecting its sensitivity to vibronic quenching (A_{Eu} = 1.05 ms and A_{Tb} = 4.2 ms).

A revised method[82] for assessing the q value for luminescent complexes, has led to the modified equation (equation 1.13) which accounts for correction factors in Δk for outer sphere water molecules (-0.25 ms^{-1} for Eu^{3+} and -0.06 ms^{-1} for Tb^{3+}) and,

where appropriate, amine or amide N-H oscillators (0.075 ms^{-1} for Eu^{3+}). A revised value of A_{Ln} has also been reported (A_{Eu} = 1.2 ms and A_{Tb} = 5 ms).

$$q = A'_{Ln} (\Delta k_{corr}) \qquad \textbf{(1.13)}$$

$$q_{Eu} = 1.2 (k_{H2O} - k_{D2O} - 0.25 - n \times 0.075)$$

$$q_{Tb} = 5 (k_{H2O} - k_{D2O} - 0.06)$$

1.4.5 Lanthanide Complexes as Luminescent Probes

Under favourable conditions, many of the Ln^{3+} ions are able to exhibit long-lived luminescence following excitation into higher electronic states. This phenomenon is often observed in the solid state and it has been exploited in phosphors for television screens and in ubiquitous YAG lasers.[80]

The long lived emission from Ln^{3+} compounds in solution can be observed under ambient conditions and has been utilized extensively in biological systems. Most applications envisaged for responsive luminescent Ln^{3+} complexes involve their use in aqueous solution as fluorescent labels. Therefore water soluble complexes are required which have high kinetic and thermodynamic stability with respect to metal ion dissociation, over a wide pH range. Suitable lanthanide chelates should contain a highly absorbing chromophore (to ensure good excitation) and a high yield of energy transfer from the ligand to the Ln^{3+} ion. Thus they should be effectively shielded from the non radiative deactivating effects of the X-H oscillators (i.e. O-H and N-H vibrations), suggesting the use of octa or nonadentate ligands.[87] The long luminescence lifetimes of Ln^{3+} ions, which fall in the range of μs (i.e. Yb^{3+}, Nd^{3+}) to ms (i.e. Eu^{3+} and Tb^{3+}), allows a time-resolved detection procedure to be employed, in order to minimise the interference of background luminescence in biological media. A delay is set between the excitation pulse and the measurement of the lanthanide luminescence, during which time the short-lived (ns to μs) background fluorescence and scattered light decay to negligible levels.[88] Moreover Ln^{3+} emission spectra show bands which are very narrow and remarkably insensitive to

environmental changes and the use of sensitized emission results in a large Stoke shift ($\lambda_{em} > \lambda_{ex}$ of 200 nm), which eliminates problems of concentration-dependent self absorption of emitted light.[80]

In the last 20 years, Ln^{3+} chelates have been developed as fluorescence labels for time resolved fluoroimmunoassay (TR-FIA), the DNA hybridization assay, fluorescence imaging microscopy, the detection of cellular function *in vivo* as well as for the elucidation of structure and function of enzymes and proteins.[89] Ln^{3+}(i.e. Eu^{3+}, Tb^{3+}) chelates have been successfully used as labels of antigens and antibodies for fluoroimmunological analysis (i.e. the commercially available DELFIA[90]), which provides a safer and equally sensitive alternative to radioimmunoassay, avoiding the problems associated with the handling and disposal of radiolabelled substances. The technique is based on the binding of an antigen (analyte) with an appropriate antibody, thus forming an immunological complex. The immunoassay can be carried out on a solid support (i.e. plastic surface, electrophoretic gel, etc.) to which the antibody is covalently linked. In order to measure the amount of analyte in the solid phase, the emissive label is attached to one of the reactants of the immunological reaction.[91] The complexes should possess functional groups capable of covalent binding with the immunologically active compounds, such as antigens or antibodies.

The application of luminescent Ln^{3+} compounds has been extended to the investigation of other targeting molecules such as small peptides[92], nucleic acid strand[93] or cyclodextrins[94] and to the monitoring of the fate of molecules or ions within the cell. The use of a luminescent label may provide further advantages over radioisotopes as the binding of the analyte may cause a direct effect on the luminescence, which can be observed as a quenching or enhancement of the emission or a shift in the excitation or emission wavelength maxima.

1.5 Circular Dichroism

Electromagnetic radiation is composed of an electric and magnetic field which oscillate perpendicularly to one another. Also associated with this radiation are left and right handed circularly polarized components. These have electric field vectors which have constant magnitude in time but trace out a helix in the direction of propagation. If a medium is chiral then the two right and left handed components interact differently with the chiral substrate resulting in unequal absorption. The transmitted beam is now elliptically polarized, giving rise to circular dichroism (CD). Circular dichroism can be defined as the difference in absorption, A, of left and right circularly polarised light (equation 1.14).

$$CD = A_L - A_R \qquad \textbf{(1.14)}$$

In a chiral molecule, rearrangement of electrons occurs in a helical fashion. Different electronic transitions result in electron redistribution of different handedness and so any one molecule may give rise to both positive and negative CD signals.[95] The measurement of circular dichroism is based on instrumentation where linearly polarised light is passed through a quarter wave plate, a material that produces a 90° phase difference between left or right circularly polarised components. This modulates the linearly polarised light alternately into left or right circularly polarised light which is detected by a photomultiplier tube, the output of which is converted into two signals. One signal is the result of the differential absorption of one component over the other and is proportional to the circular dichroism, while the other one is averaged and related to the mean light absorption.

Spectropolarimeters produce a CD spectrum in units of ellipticity, θ, which is the angle whose tangent is the ratio of the minor and major axes of the ellipse, in millidegrees versus wavelength λ. CD probes the chirality of molecular ground states giving rise to structural information and is often used to probe changes in conformation and interactions of biological molecules such as DNA and proteins.[95]

Chiral lanthanide complexes are amenable to study by CD. Circular dichroism associated with f-f transitions in lanthanides in a chiral environment is rather weak and difficult to observe. However, near IR-CD from Yb^{3+}, centered around 980 nm associated with the magnetic dipole-allowed $^2F_{7/2} \rightarrow {}^2F_{5/2}$ transition has been reported recently.[96] Spectral analysis is not straightforward owing to the large number of transitions possible between the different J states, therefore full exploitation of structural studies awaits further spectral-structure correlation. However, near IR-CD has been used effectively to signal anion binding at coordinatively unsaturated lanthanide complexes and the form of the CD is remarkably sensitive to the nature of the axial donor.[97,98]

References

1. M. Stubbs, and J. R. Griffiths, *Br. J. Cancer,* 1999, **80**, 86.
2. R. Kreis, *Eur. J. Pedriatr.*, 2000, **159**, S126.
3. Y. J. Liu, C. Y. Chen, H. W. Chung, I. J. Huang, C. S. Lee, S. C. Chin, and M. Liou, *Radiology*, 2003, **229**, 366.
4. M. C. Martinez-Bisbal, E. Arana, L. Marti-Bonmati, E. Molla, and B. Celda, *Eur. J. Neurol.*, 2004, **11**, 187.
5. K. T. M. Fernando, M. A. McLean, D. T. Chard, D. G. MacManus, C. M. Dalton, K. A. Miszkiel, R. M. Gordon, G. T. Plant, A. J. Thompson, and D. H. Miller, *Brain,* 2004, **127**, 1361.
6. A. A. Cohen-Gadol, J. W. Pan, J. H. Kim, D. D. Spencer, and H. H. Hetherington, *J. Neurosurg.*, 2004, **101**, 613.
7. J. Theberge, Y. Al-Semaan, D. J. Drost, A. K. Malla, R. W. Neufeld, R. Bartha, R. Manchad-Menon, M. Densmore, B. Schaefer, P. C. Williamson, *Psychiatry Res.*, 2004, **131**, 107.
8. C. E. Mountford, S. Dorean, C. L. Lean, and P. Russel, *Chem. Rev.*, 2004, **104**, 3677.
9. A. D. Waldman, and G. S. Rai, *Neuroradiology,* 2003, **45**, 507.
10. D. W. McRobbie, E. A. Moore, M. J. Graves, and M. R. Prince, 'MRI from Picture to Proton', University Press, Cambridge, 2003, Chapter 15.
11. M. O. Leach, *Anticancer Res.*, 1996, **16**, 1503.
12. J. L. Evelhoch, R. J. Gillies, G. S. Karczmar, J. A. Koutcher, R. J. Maxwell, O. Nalcioglu, N. Raghunand, S. M. Ronen, B. D. Ross, and H. M. Swartz, *Neoplasia*, 2000, **2**, 152.
13. M. Stubbs, *Acta Oncol.*, 1999, **38**, 845.
14. M. O. Leach, *Phys. Medica*, 2001, **17**, 50.
15. S. P. Robinson, S. J. Barton, P. M. J. Mc Sheehy, and J. R. Griffiths, *Br. J. Radiol.*, 1997, **70**, S 60.
16. V. L. Doyle, S. J. Barton, and J. R. Griffiths, *Curr. Science*, 1999, **76**, 772.
17. E. E. Kim, and E. F. Jackson, 'Molecular Imaging in Oncology', Springer, New York, 1999, Chapter 4.
18. S. J. Vaidya, G. S. Payne, M. O. Leach, and C. R. Pinkerton, *Eur. J. Cancer*, 2003, **39**, 728.
19. P. F. Daly, R. C. Lyon, P. J. Faustino, and J. S. Cohen, *J. Biol. Chem.*, 1987, **262**, 14875.
20. F. Podo, *NMR Biomed.*, 1999, **12**, 413.
21. W. Negendank, *NMR Biomed.*, 1992, **5**, 303.
22. R. B. Moon, and J. H. Richards, *J. Biol. Chem.,* 1973, **248**, 7276.
23. J. R. Griffiths, A. N. Stevens, R. A. Iles, R. E. Gordon, and D. Shaw, *Biosci. Rep.*,1981, **1**, 319.
24. J. R. Griffiths, *Br. J. Cancer,* 1991, **64**, 425.
25. R. J. Gillies, Z. Liu, and Z. M. Bhujwalla, *Am. J. Physiol.*, 1994, **267**, C 195.
26. M. Stubb, L. M. Rodrigues, F. A. Howe, J. Wang, K. S. Jeong, and R. L. Veech, *Cancer Res.*, 1994, **54**, 4011.
27. S. S. Rajan, J. P. Wehrle, S. L. Li, R. G. Steen, and J. D. Glickson, *NMR Biomed.*, 1989, **2**, 165.

28. M. O. Leach, M. Verrill, J. Glaholm, T. A. D. Smith, D. J. Collins, G. S. Payne, J. C. Sharp, S. M. Ronen, V.R. McCready, T. J. Powles, and I. E. Smith, *NMR Biomed.*, 1998, **11**, 314.
29. S. J. Li, J. P. Wehrle, J. D. Glickson, N. Kumar, and P.G. Braunschweiger, *Magn. Reson. Med.*, 1991, **22**, 47.
30. C. Majos, J. Alonso, C. Aguilera, M. Serralonga, J. Perez-Martin, J. J. Acebes, C. Arus, and J. Gili, *Eur. Radiol.*, 2003, **13**, 582.
31. E. E. Kim, and E. F. Jackson, 'Molecular Imaging in Oncology', Springer, New York, 1999, Chapter 14.
32. Z. Tong, T. Yamaki, K. Harada, K. Houkin, *Magn. Reson. Imaging,* 2004, **22**, 1017.
33. L. C. Costello, R. B. Franklin, and P. Narayan, *Prostate*, 1999, **38**, 237.
34. R. Kumar, M. Kumar, N. R. Jagannathan, N. P. Gupta, A. K. Hemal, *Urol. Res.*, 2004, **32**, 36.
35. M. Terpstra, W. B. High, Y. Luo, R. A. deGraaf , H. Merkle, and M. Garwood, *NMR Biomed.*, 1996, **9**, 185.
36. H. Bruhn, J. Frahm, M. L. Gyngell, K. D. Merboldt, W. Hanicke, R. Sauter, and C. Hamburger, *Radiology,*1989, **172**, 541.
37. J. R. Griffiths, and J. D. Glickson, *Adv. Drug Deliv. Rev.*, 2000, **41**, 75.
38. V. D. Mehta, P. Kulkarni, R. P. Mason, A. Constantinescu, S. Aravind, N. Goomer and P. P. Antich, *FEBS Lett.*, 1994, **349**, 234.
39. A. D. Sherry, and C. F. G. Geraldes, 'Lanthanide Probes in Life, Chemical and Earth Science', Eds. J. G. Bunzli and G. R. Choppin, Elsevier, Amsterdam, 1989, Chapter 1.
40. J. A. Peters, J. Husken, and D. J. Raber, *Prog. Nucl. Magn. Reson. Spectrosc.*, 1996, **28**, 283.
41. A. D. Sherry and C. F. G. Geraldes, 'Lanthanide Probes in Life, Chemical and Earth Science', Eds. J. G. Bunzli and G. R. Choppin, Elsevier, Amsterdam, 1989, Chapter 4.
42. J. P. Jesson, 'NMR of Paramagentic Molecules: Principles and Applications', Eds. G. N. LaMar, W. DeW. Horrocks, Jr., and R. H. Holm, Academic Press, London, 1973, Chapter 12.
43. J. A. Peters, M. S. Nieuwenhuizen, and D. J. Raber, *J. Magn. Reson.*, 1985, **65**, 417.
44. R. M. Golding, and M. P. Halton, *Aust. J. Chem.*, 1972, **25**, 2577.
45. J. Reuben, and D. Fiat, *J. Chem. Phys.*, 1969, **51**, 4909.
46. J. Ajisaka, and M. Kainosho, *J. Am. Chem. Soc.*, 1975, **97**, 330.
47. A. E. Merbach, and E. Toth, 'The Chemistry of Contrast Agents in Medical Magnetic Resonance Imaging', Wiley, New York, 2001, Chapter 8.
48. B. J. Bleaney, *J. Magn. Reson.*, 1972, **8**, 91.
49. J. M. Briggs, G. P. Moss, E. W. Randall, and K. D. Sales, *J. Chem. Soc., Chem. Commun.*, 1972, 1180.
50. R. S. Dickins, D. Parker, H. Pushmann, C. Crossland and J. A. K. Howard, *Chem. Rev.*, 2002, **102**, 1977.
51. C. F. G. C. Geraldes, and C. Luchinat, 'Metal Ions in Biological Systems: The Lanthanides and their Interrelations with Biosystems', Eds. H. Sigel and A. Sigel, Marcel Dekker, New York, 2003, Chapter 14.

52. S. Aime, M. Botta, M. Fasano, and E. Terreno, *Chem. Soc. Rev.*,1998, **27**, 19.
53. C. C. Hinckley, *J. Am. Chem. Soc.*, 1969, **91**, 5160.
54. C. F. G. C. Geraldes, 'NMR in Supramolecular Chemistry', Ed. M. Pans, Kluwer, Netherlands, 1999, pp. 133-154.
55. W. DeW. Horrocks, Jr., and J. P. Sipe, *J. Am. Chem. Soc.*, 1971, **93**, 6800.
56. J. Reuben, *Prog. Nucl. Magn. Reson. Spectrosc.*, 1973, **9**,1.
57. C. H. Evans, 'Biochemistry of Lanthanides', Plenum Press, New York, 1990, Chapter 3.
58. G. Schwarzenbach, *Helv. Chim. Acta,* 1952, **35**, 2344.
59. R. D. Hancock, and A. E. Martell, *Chem. Rev.*, 1989, **89**, 1875.
60. D. K. Cabbiness, and D. W. Margerum, *J. Am. Chem. Soc.*, 1969, **91**, 6540.
61. W. P. Cacheris, S. K. Nickle, and A. D. Sherry, *Inorg. Chem.*, 1987, **26**, 958.
62. R. S. Dickins, J. A. K. Howard, C. L. Maupin, J. M. Moloney, D. Parker, R. D. Peacock, J. P. Riehl, and G. Siligardi, *New J. Chem.*, 1998, **22**, 891.
63. E. J. Corey, and J. C. Bailar, *J. Am. Chem. Soc.*,1959, **81**, 2620.
64. S. Aime, M. Botta, and G. Ermondi, *Inorg. Chem.*, 1992, **31**, 4291.
65. S. Aime, A. S. Basanov, M. Botta, R. S. Dickins, S. Faulkner, C. E. Foster, A. Harrison, J. A. K. Howard, J. M. Moloney, T. J. Norman, D. Parker, L. Royle, and J. A. G. Williams, *J. Chem. Soc., Dalton Trans.*, 1997, 3623.
66. R. S. Dickins, J. A. Howard, C. L. Maupin, J. M. Moloney, D. Parker, J. P. Riehl, G. Siligardi, and J. A.G. Williams, *Chem. Eur. J.*, 1999, **5**, 1095.
67. R. S. Ranganathan, N. Raju, H. Fan, X. Zhang, M. F. Tweedle, J. F. Desreux, and V. Jacques, *Inorg. Chem.*, 2002, **41**, 6856.
68. D. Parker, *Chem. Rev.*, 1991, **91,** 1441.
69. K. Kabuto, and Y. Sasaki, *J. Chem. Soc., Chem. Commun.*, 1984, 316.
70. J. Reuben, *J. Chem. Soc., Chem. Commun.*, 1979, 68.
71. K. Kabuto, and Y. Sasaki, *J. Chem. Soc., Chem. Commun.*, 1984, 316.
72. K. Kabuto, and Y. Sasaki, *Chem. Lett.*, 1989, 385.
73. J. Kido, Y. Okamoto, and H. G. Brittain, *J. Org. Chem.*, 1991, **56**, 1412.
74. R. Hazama, K. Umakoshi, C. Kabuto, and Y. Sasaki, *Chem. Commun.*, 1996, 15.
75. T. J. Wenzel, and J. D. Wilcox, *Chirality*, 2003, **15**, 256.
76. M. Takemura, K. Yamato, M. Doe, M. Watanabe, H. Miyake, T. Kikunaga, N. Yanagihara, and Y. Kojima, *Bull. Chem. Soc. Jpn.*, 2001, **74**, 707.
77. M. Watanabe, T. Hasegawa, H. Miyake, and Y. Koijma, *Chem. Lett.*, 2001, 4.
78. V. Seshan, M. J. Germann, P. Preisig, C. R. Malloy, A. D. Sherry, and N. Bansal, *Magn. Reson. Med.*, 1995, **34**, 25.
79. J. I. Bruce, M. P. Lowe, and D. Parker, 'The Chemistry of Contrast Agents', Eds. A. Merbach and E. Toth, Wiley, New York, 2001, Chapter 11.
80. D. Parker, and J. A.G. Williams, *J. Chem. Soc., Dalton Trans.*, 1996, **3**, 3613.
81. A. Beeby, D. Parker, and J. A. G. Williams, *J. Chem. Soc., Perkin Trans. 2,* 1996, 1565.
82. A. Beeby, I. M. Clarkson, R. S. Dickins, S. Faulkner, D. Parker, L. Royle, A. S. de Sousa, J. A. G. Williams, and M. Woods, *J. Chem. Soc., Perkin Trans. 2,* 1999, 493.
83. J. L. Kropp, and M. W. Windsor, *J. Chem. Phys.*, 1963, **39**, 2769.
84. J. L. Kropp, and M. W. Windsor, *J. Chem. Phys.*, 1965, **42**, 1599.

85. G. Stein, and E. Wurzberg, *J. Chem. Phys.*, 1975, **62**, 208.
86. W. DeW. Horrocks, and D. R. Sudnick, *J. Am. Chem. Soc.*, 1979, **101**, 334.
87. D. Parker, *Coord. Chem. Rev.*, 2000, **205**, 109.
88. D. Parker, and J. A. G. Williams, 'Metal Ions in Biological Systems: The Lanthanides and their Interrelations with Biosystems', Eds. H. Sigel and A. Sigel, Marcel Dekker, New York, 2003, Chapter 7.
89. K. Matsumoto, and J. Yuan, 'Metal Ions in Biological Systems: The Lanthanides and their Interrelations with Biosystems', Eds. H. Sigel and A. Sigel, Marcel Dekker, New York, 2003, Chapter 6.
90. H. Harma, P. Aronkyto, and T. Lovgren, *Anal. Chim. Acta.*, 2000, **410**, 85.
91. C. Turro, P. K. L. Fu, and P. M. Bradley, 'Metal Ions in Biological Systems: The Lanthanides and their Interrelations with Biosystems', Eds. H. Sigel and A. Sigel, Marcel Dekker, New York, 2003, Chapter 9.
92. P. Gottlieb, E. Hazum, E. Tzehoval, M. Feldman, S. Segal, and M. Fridkin, *Biochem. Biophys. Res. Commun.*, 1984, **119**, 203.
93. J. Coates, P. G. Sammes, G. Yahioglu, R. M. West, and A. J. Garman, *J. Chem. Soc., Chem. Commun.*, 1994, 2311.
94. D. M. Gravett, and J. E. Guillet, *J. Am. Chem. Soc.*,1993, **115**, 5970.
95. K. Nakanishi, N. Berova, and R. W. Woody, 'Circular Dichroism: Principles and Applications', Wiley-VCH, New York, 2000.
96. L. Di Bari, G. Pintacuda, P. Salvadori, R. S. Dickins, and D. Parker, *J. Am. Chem. Soc.*, 2000, **122**, 9257.
97. J. I. Bruce, R. S. Dickins, L. J. Govenlock, T. Gunnlaugsson, S. Lopinski, M. P. Lowe, D. Parker, R. D. Peacock, J. J. B. Perry, S. Aime, and M. Botta, *J. Am. Chem. Soc.*, 2000, **122**, 9674-9684.
98. R. S. Dickins, A. S. Basanov, D. Parker, H. Puschmann, S. Salamano, and J. A. K. Howard, *Dalton Trans.*, 2004, **1**, 70.

CHAPTER 2

Chiral Lanthanide Complexes as Shift and Relaxation Agents for MRS

2.1 Synthesis of Shift and Relaxation Agents for S-Lactate

2.1.1 Introduction

In vivo detection of lactate by ^{1}H MRS is of prime importance in the diagnosis, grading and therapeutic monitoring of pathological conditions such as cancer, stroke and heart disease. However, the limitations of the MRS technique, as previously discussed (1.1.1), severely affect the investigation of the metabolite (1.1.2). A possible solution to the problem is to envisage the use of a *paramagnetic metal chelate* system, which may act as a *shift and relaxation agent*, in order to affect spectral resolution. The short longitudinal relaxation time of the paramagnetic centre will also allow rapid acquisition times to be implemented, giving enhanced signal intensity.

Cationic lanthanide complexes based on the heptadentate ligand (RRR)-DO3Ph (Figure 2.1) have two coordinated water molecules which may be readily displaced by a variety of monodentate and chelating anions.[1,2]

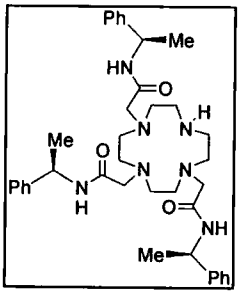

Figure 2.1 (RRR)-DO3Ph.

Such complexes have been reported to show high affinity for oxy-anions, in particular lactate.[1] Lactate binds in a bidentate manner, forming a favourable 5-ring chelate, with the hydroxyl group occupying the axial position and a carboxylate oxygen binding equatorially, completing the O_4 plane (Figure 2.2). The lactate CH and CH_3 were shown to experience large lanthanide induced shifts upon chelation to (RRR)-[Yb.DO3Ph]$^{3+}$; the CH resonating at +58 ppm and the CH_3 at +20 ppm, for (S)-lactate (c.f. +4.2 and +1.3 ppm respectively in the free form).

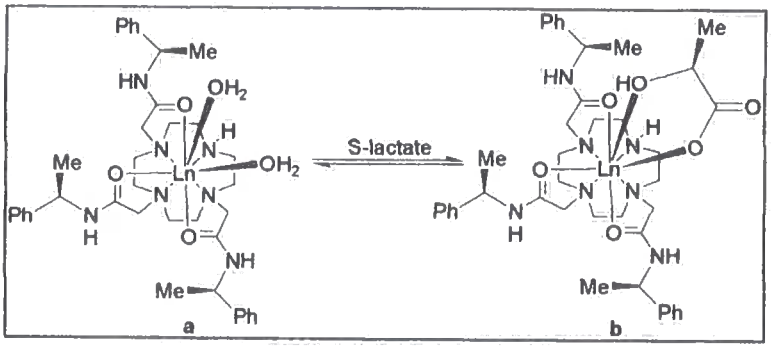

Figure 2.2 Structure of (RRR)-[Ln.DO3Ph]$^{3+}$ as diaqua species (a) and as S-lactate adduct with the hydroxyl group occupying the axial position and a carboxylate oxygen binding equatorially.

The observed lanthanide induced shifts, which for Yb^{3+} are largely dipolar in origin and can be approximated to having a $3\cos^2\theta - 1/r^3$ dependance, suggest the lactate CH lies closer to the principal axis of the complex than the CH_3 group, consistent with reported X-ray data[3] (CH: θ = 25.62°, r = 3.93 Å; CH_3: θ = 22.64°, r = 4.87 Å) (Figure 2.3).

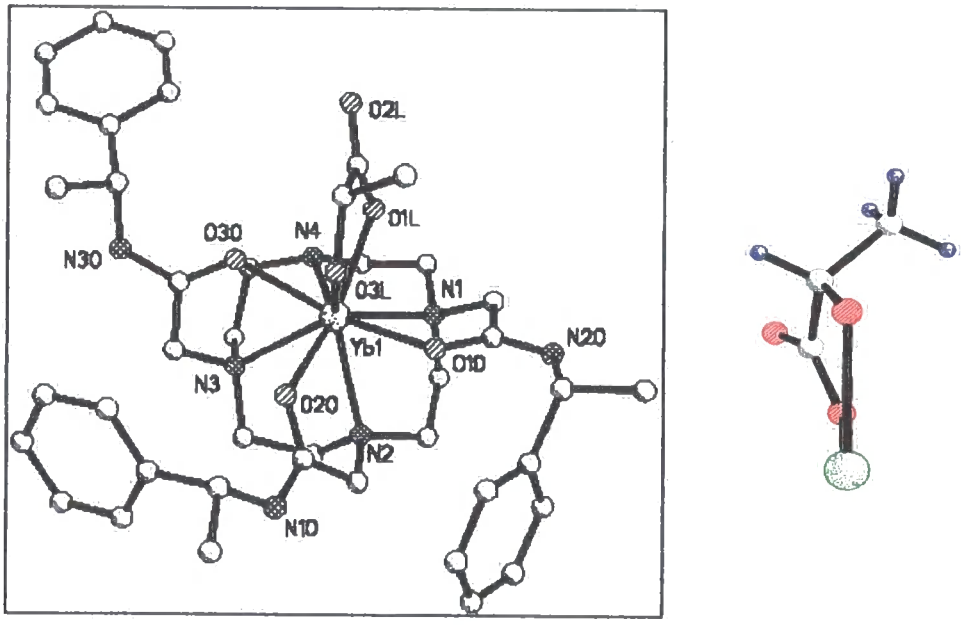

Figure 2.3 Crystal structure of (RRR)-[Yb.DO3Ph]$^{3+}$ ($\Lambda(\delta\delta\delta\delta)$) with S-lactate and representation of the lactate chelation clearly demonstrating that the lactate CH lies closer to the principal axis than the hydrogens of the methyl group.[3]

However, the binding of such complexes to lactate was found to be in slow exchange on the NMR timescale, the complexes behaving as chiral derivatising agents rather than shift reagents.

For an effective shift reagent the binding to lactate should be reversible and in fast exchange on the NMR timescale. A single isomer in solution is preferred, in order to simplify the interpretation of the spectra, and a large LIS is necessary to avoid any overlapping of lipid and protein signals for example, with the lactate resonances of interest. Water soluble, kinetically stable complexes are also required for use *in vivo*.

With these features in mind, shift and relaxation agents for MRS based on heptadentate ligands depicted in Figure 2.4, with the potential to bind to lactate in a selective and reversible manner have been designed.

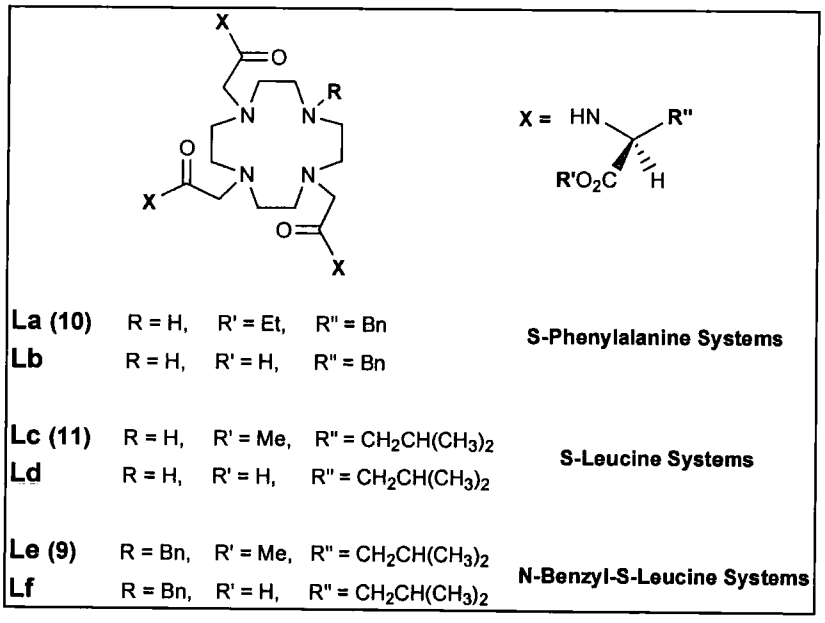

Figure 2.4 Structures of the chiral ligands discussed in this chapter.

In order to achieve the fast exchange conditions required, the binding affinity and selectivity for lactate have been modulated by varying the Ln^{3+} ion (i.e. the less

charge dense Pr^{3+}, Eu^{3+} versus the high charge density of Tm^{3+}, Yb^{3+}) and the ligand structure, in particular the peripheral electrostatic charge of the complex (i.e. anionic vs. neutral) and the local charge and the steric demand at the metal centre. The binding has been investigated through ^1H NMR, emission spectroscopy and circular dichroism.

2.1.2 Synthesis of the Ligands

The first step of the ligand synthesis was the formation of the chiral chloroamide, achieved by reacting the appropriate chiral amine with chloroacetylchloride in the presence of triethylamine in dry diethyl ether, at -20°C, under argon (Scheme 2.1).

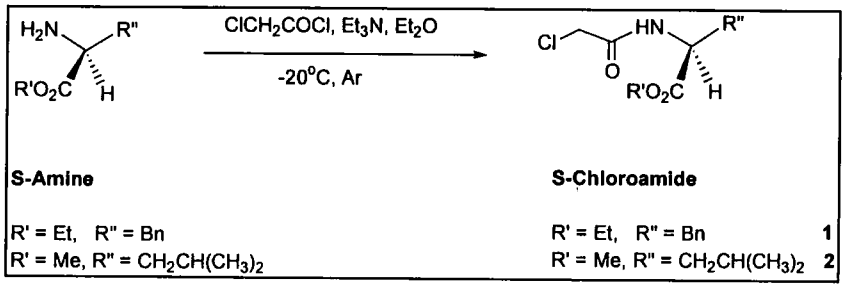

Scheme 2.1

Trialkylation of tetraazacyclododecane (cyclen, 12N4), to obtain ligand La (Figure 2.4) was attempted through three different routes.

Route 1

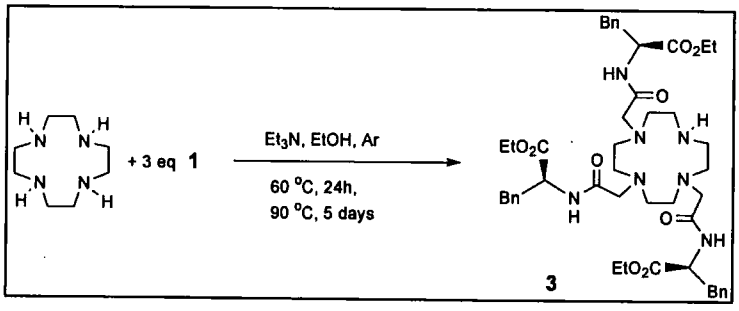

Scheme 2.2

Trialkylation was achieved by reacting cyclen with three equivalents of the chiral chloroamide **1**, added over 6 hours, in the presence of triethylamine in ethanol. The

reaction mixture was stirred at 60°C for 24 h and then at 90°C for 5 days (Scheme 2.2). Positive ion ESMS revealed the presence of tri, di and monoalkylated products. A quick washing of the organic layer with water removed traces of the more soluble mono- and dialkylated products. The trialkylated product, **3**, was obtained via exhaustive washing of the organic phase with purite water (7x30 ml). This single step reaction to the trialkylated cyclen has generally worked for several systems. However, due to the lack of reproducibility and the poor yield of the product obtained (41 %), alternative methods were sought. Routes involving the selective protection of one of the ring nitrogens followed by trialkylation and subsequent deprotection were employed.

Route 2

Following the procedure used to synthesize selectively functionalised tetraazacycloalkanes,[4] a bisaminal derivative of cyclen, **4**, was obtained by reacting 12N4 in acetonitrile with a solution of pyruvic aldehyde in purite water (Scheme 2.3).

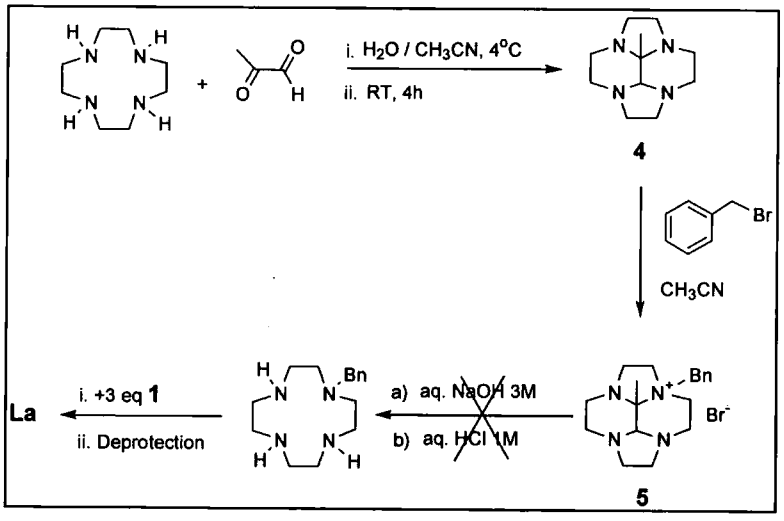

Scheme 2.3

The addition of benzylbromide in acetonitrile to **4**, yielded the monobenzylated bisaminal protected 12N4 as a quaternary salt **5**. The removal of the bisaminal bridge was attempted by both base (a) and acid (b) catalysed hydrolysis. However, the deprotection conditions used did not yield the expected monobenzylated 1,4,7,10-

tetraazacyclododecane product. Inconclusive ES^+, ^1H and ^{13}C NMR spectra were obtained, thus the route was abandoned.

Route 3

A successful method for the synthesis of the trialkylated ligands is outlined in Scheme 2.4.

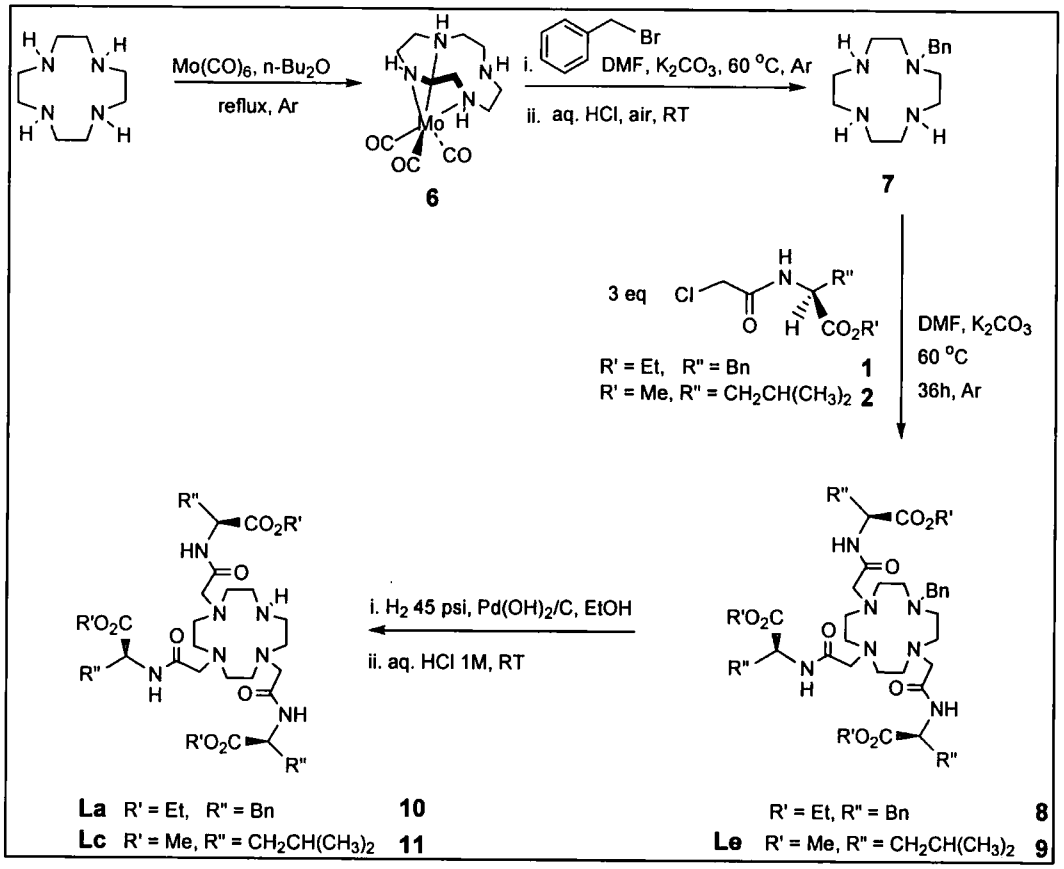

Scheme 2.4

The selective monoalkylation of cyclen was achieved by protecting three nitrogen atoms of the ring by reaction with molybdenum hexacarbonyl in dibutyl ether, under argon.[5] This quantitative reaction resulted in the formation of an octahedral molybdenum tricarbonyl complex **6,** where three of the four nitrogen atoms are coordinated to the molybdenum and the fourth is left available for reaction. Reaction of the molybdenum complex in dry DMF with benzyl bromide, in the presence of potassium carbonate at 60°C, followed by decomplexation of the molybdenum

moiety in aqueous acid, yielded the monoalkylated macrocycle **7**. The protected triamide ligand (**8**, **9**) was synthesized by reacting N-benzyl-1,4,7,10-tetraazacyclododecane **7** with three equivalent of the appropriate S-chloroamide (**1**, **2**) in dry DMF, under an argon atmosphere at 60°C and in the presence of potassium carbonate. The reductive deprotection of the N-benzyl group was achieved by treating the compound, in ethanol, with hydrogen (45 psi) at room temperature for 48 hours, in the presence of hydrochloric acid solution (1 M, few drops) and a catalytic amount of palladium hydroxide on carbon, yielding La and Lc (compounds **10** and **11** respectively).

2.1.3 Synthesis of the Complexes

The cationic lanthanide complexes were prepared by refluxing the macrocyclic ligands in anhydrous acetonitrile, with the appropriate trifluoromethanesulphonate salt, under an argon atmosphere for 18 h (Scheme 2.5). Purification by precipitation onto diethyl ether yielded the enantiopure (SSS) complexes.

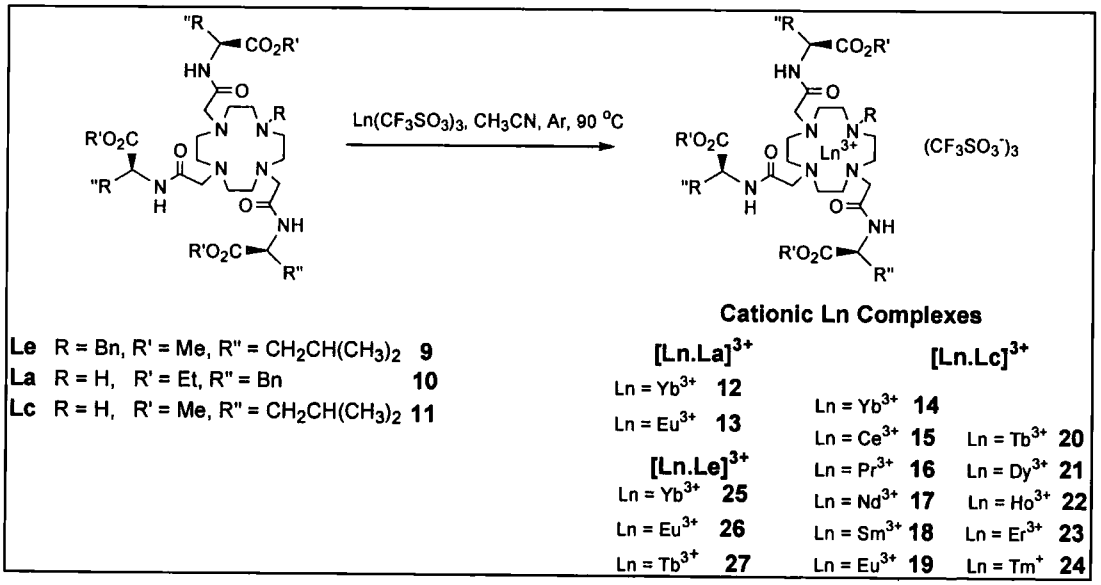

Scheme 2.5

Neutral lanthanide complexes were synthesized by hydrolysis of the corresponding cationic complexes in an aqueous solution of sodium hydroxide (0.02 M). The

products were obtained after purification by cation exchange (Dowex, 50 WH^+), eluting with water and aqueous ammonia (6 %) (Scheme 2.6).

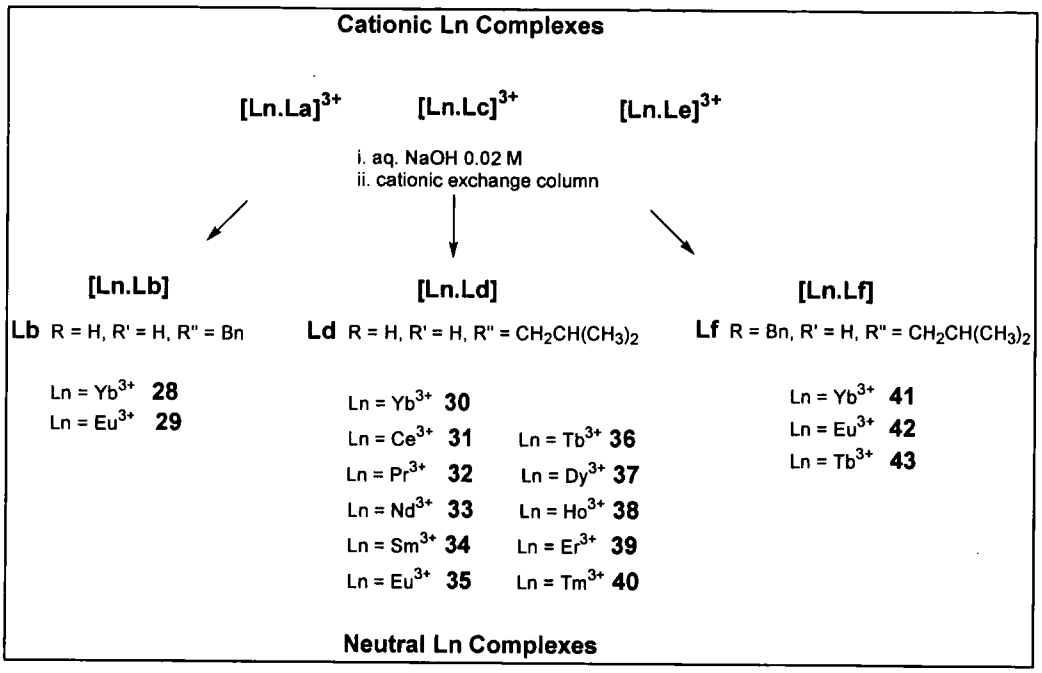

Scheme 2.6

2.2 Solution ^{1}H NMR Investigation of Ligand Variation

Nuclear magnetic resonance (NMR) spectroscopy is one of the most valuable techniques for the study of molecular structures. However, the use of NMR is sometimes restricted due to the insufficient sensitivity of proton chemical shifts to changes in the chemical and stereochemical environment. Lanthanide shift reagents are effective in removing the chemical shift equivalence of certain nuclei through transmission of electron spin density from the lanthanide ion to the nuclei of interest. This can occur through bonds (contact shift) or through space (pseudocontact shift) and gives rise to a lanthanide induced shift (1.2.2) and a separation of the resonances. The fast electronic relaxation times of certain lanthanides (e.g. Yb^{3+}, Eu^{3+}, Pr^{3+}) gives rise to a small degree of line broadening and improved sensitivity, since many scans may be taken in a short time.

The potential use of the Ln^{3+} complexes described above to act as shift reagents for lactate was monitored through ^1H NMR studies. Each of the heptadentate complexes has two free sites on the metal available for bidentate coordination to lactate. Upon binding, the resonant signals of lactate protons should experience a lanthanide induced shift, from their unbound positions at 4.1 ppm (CH) and 1.3 ppm (CH_3), resulting in separation of the lactate resonances from any potential overlapping background signals. A change in the appearance of the paramagnetically shifted proton resonances of the complex should also occur, as the ligand field at the Ln^{3+} centre is changing. Initially, Yb^{3+} complexes were assessed as they are highly suited to NMR analysis, owing to their large LIS combined with minimal line broadening.

2.2.1 Phenylalanine Systems

In devising enantiopure complexes, conformationally rigid on the NMR timescale and in fast exchange with S-lactate, (SSS) Ln^{3+} complexes based on ligands La and Lb have been synthesized (Figure 2.4). The three pendent amide arms are based on the amino acid S-phenylalanine. Amino acids were primarily chosen as they afford simple routes to both cationic (as ester) and neutral complexes (as acid, via subsequent hydrolysis of the corresponding ester). The remote chiral centre δ to the ring should favour the formation of one rigid diastereomer. Phenylalanine was initially chosen as it contains a chromophore which can be exploited as an *antenna* in sensitized emission (1.4.3). Furthermore, due to its steric encumbrance, it may also contribute to freezing out conformational motion within the macrocycle.

Cationic Complex

^1H NMR investigations were performed on the cationic $[Yb.La]^{3+}$complex, **12**, (Figure 2.5).

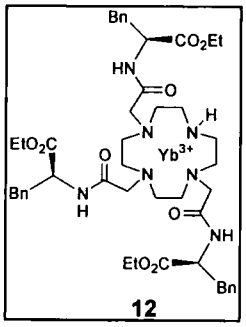

12

Figure 2.5 Structure of the chiral $[Yb.La]^{3+}$ complex **12**, whose three pendent arms are based on the ethyl ester of the amino acid S-phenylalanine (Phe).

The spectrum of the free ligand, **10**, (Figure 2.6) exhibited resonances from +7.60 ppm → +1.12 ppm. After complexation with Yb^{3+}, the spectral range extended to +100 ppm → -65 ppm and the ^1H NMR spectrum of the complex **12** (Figure 2.7) revealed the presence of two sets of paramagnetically shifted resonances, which were attributed to the presence of two isomers in solution.

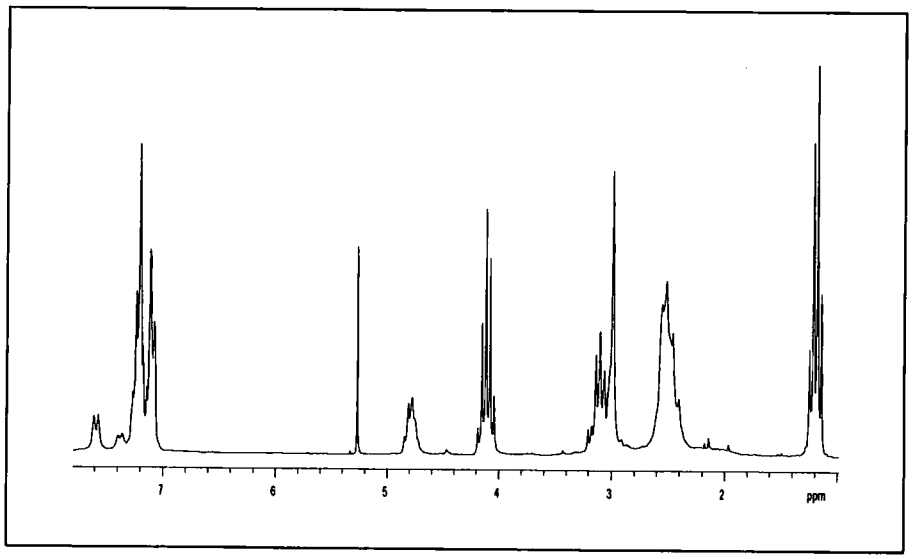

Figure 2.6 ^1H NMR spectrum of **10** (200 MHz, CD_3Cl, 295 K).

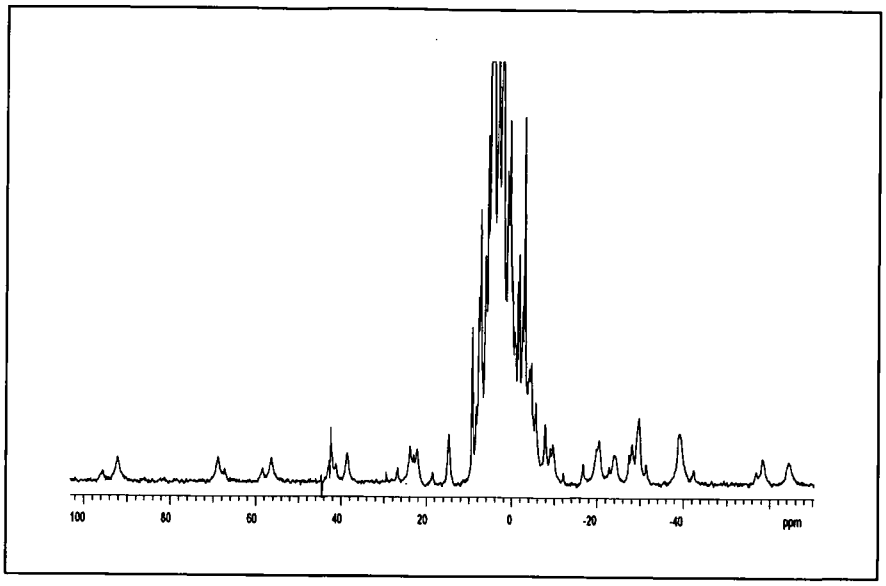

Figure 2.7 ^{1}H NMR spectrum of $[Yb.La]^{3+}$ (200 MHz, D_2O/CD_3OD, 295 K).

In lanthanide complexes of DOTA and its achiral carboxamide derivatives, there are two enantiomeric pairs of diastereoisomers in solution which may interconvert via pendent arm rotation or ring inversion (1.3.4). The major stereoisomer found in solution, M_1 [Λ (δδδδ)] or M_2 [Δ (λλλλ)], possesses a regular square-antiprismatic structure, whereas the minor isomer, m_1 [Δ(δδδδ)] or m_2 [Λ(λλλλ)], adopts a twisted square-antiprismatic structure.[6] In the chiral Yb^{3+} complex **12**, the four isomers are all diastereomeric due to the presence of the δ-chiral centre on the pendent arms of the ligand (Figure 2.8).

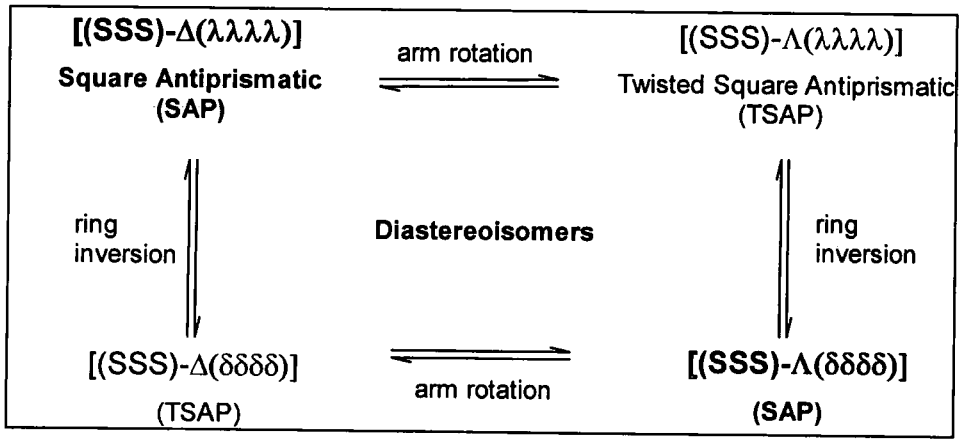

Figure 2.8 General schematic representation of the exchange mechanisms of the four possible diastereoisomers.

However, only two of the four possible diastereoisomers were observed (in ratio 3:1) in solution. The chemical shifts of the two isomers are indicative of square antiprismatic structures, by comparison with the observed ^{1}H NMR shifts of the most shifted axial ring proton (Table 2.1)[7] in Yb^{3+} complexes based on DOTA and some of its tetramide derivatives (Figure 2.9). Twisted square antiprisms usually exhibit much smaller δ values to those observed for the complex.

Complex	Solvent	Most Shifted δH_{ax} (ppm) **SAP** (major isomer)	Most Shifted δH_{ax} (ppm) **TSAP** (minor isomer)
[Yb.DOTA]$^-$	D_2O	+126	+74
	CD_3CN	+113	+77
[Yb.DOTAMPh]$^{3+}$	D_2O	+102	-
[Yb.DOTTA]$^{3+}$	D_2O	+120	-
	CD_3CN	+140	+85

Table 2.1

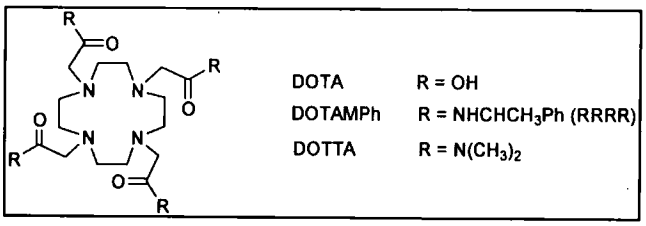

Figure 2.9 Structure of the octadentate ligands forming the Yb^{3+} complexes mentioned in Table 2.1.

The major isomer is suggested to be the Δ(λλλλ) form, because an S configuration at the chiral carbon centre usually determines a Δ helicity of the pendent arms.[8] The minor isomer is therefore likely to be of Λ(δδδδ) configuration. Each isomer has a set of eight broadened singlet resonances to high frequency, corresponding to the four most shifted axial and equatorial ring protons (Figure 2.10).

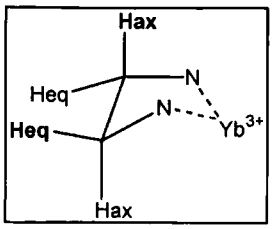

Figure 2.10 Partial structure of 12N4, showing in bold the most shifted axial and equatorial protons of the ring.

The lack of rotational symmetry in the complex means that each ring proton is in a different chemical environment and so will resonate at a different frequency. The occurence of shifting of the resonances to both high and low frequency is due to the dependence of the pseudocontact shift on the orientation of the resonating nucleus (i.e. proton) with respect to the Ln^{3+} (i.e. Yb^{3+}) (1.2.2, equation 1.5). Thus a cone is defined, inside of which the protons are shifted to higher frequencies while, if they lie outside, they are shifted to lower frequency (Figure 2.11).[9]

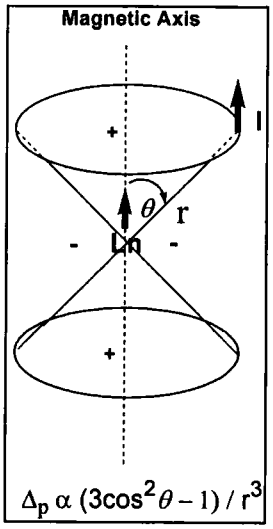

Figure 2.11 Schematic representation of the cone described by the paramagnetic shift dependence of the polar coordinates.

Lactate titration

0.01 ml aliquots of a solution of S-lactate sodium salt (in D_2O, 175 mM, complex to lactate ratio ranging from 4:1 to 1:2) were added successively to a solution of $[Yb.La]^{3+}$ (0.70 ml, 10 mM) and the ^1H spectrum was run for each increment. The effect of the incremental addition of S-lactate (Figure 2.12) caused a decrease in the overall magnitude of the paramagnetic shift from +97 ppm → -66 ppm (162 ppm) to +90 → -56 ppm (146 ppm). On the addition of 0.25 equivalents of S-lactate, for both the major and the minor isomer, an additional set of axial and equatorial ring resonances appeared. These may be attributed to the lactate bound species, which is in slow exchange on the NMR timescale with the free form. Subsequent incremental additions of lactate resulted in an increase in the bound to free ratio and, after addition of 1.0 equivalent, only the bound form was observed.

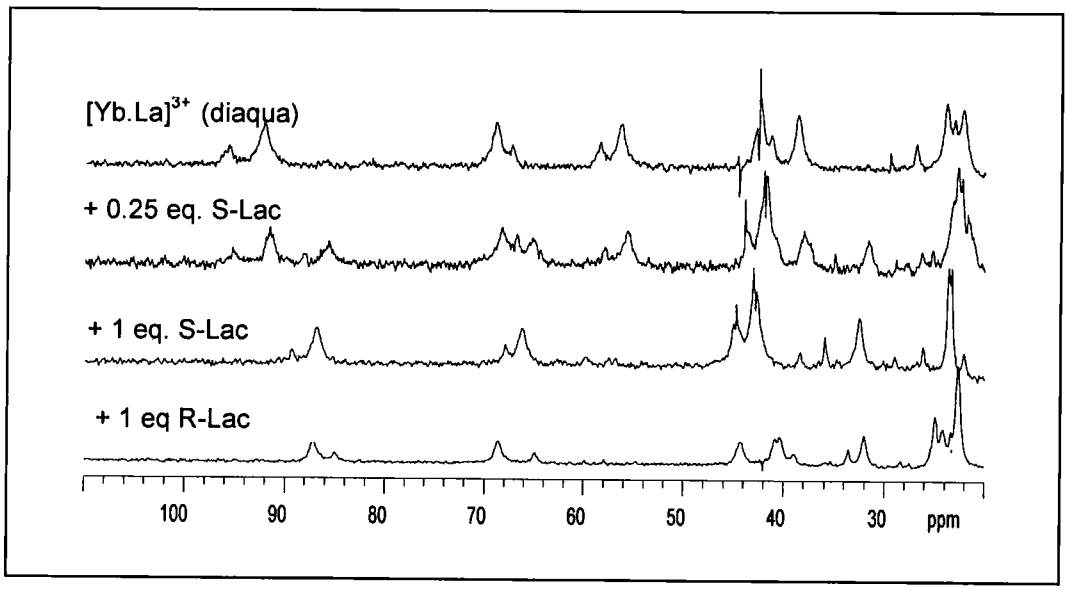

Figure 2.12 Partial ^1H NMR spectrum of $[Yb.La]^{3+}$ (upper) in the presence of S-lactate (0.25, 1 equivalents respectively) and in the presence of 1 equivalent of R-lactate (lower) (200 MHz, D_2O/CD_3OD, 295 K).

Observation of the integrals of the peaks in the high frequency range (>20 ppm) in the fully bound spectrum, showed additional resonances corresponding to four protons which were attributed to the lactate bound CH and CH_3. The exact frequency

of the lactate bound CH resonance could not be assigned by 2D COSY experiments. Such 2D experiments often fail with Yb^{3+} complexes as the degree of the line broadening is greater than the expected coupling constant, hence cross peaks cannot be observed. However, the lactate CH was suggested to resonate in the region between 30-45 ppm. A signal integrating to three protons was apparent around +20 ppm (not shown) which may correspond to the proton resonance of the bound lactate methyl group. These observations are consistent with the chemical shifts reported for the lactate bound CH and CH_3 resonances of the chiral (RRR)-$[Yb.DO3Ph]^{3+}$ analogue (δ_{CH} = +58 ppm, δ_{CH3} = +20ppm for S-lactate, and δ_{CH} = +48 ppm, δ_{CH3} = +30 ppm for R-lactate).[3]

The bidentate chelation of lactate can occur via two different binding modes (Figure 2.13).

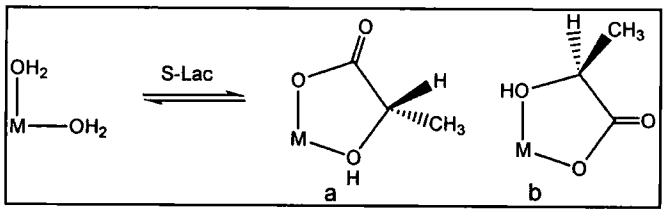

Figure 2.13 Two possible conformations, resulting from the bidentate chelation of S-lactate with the carboxylate in an axial position (a), and in an equatorial position (b).

Due to the $3\cos^2\theta$-$1/r^3$ dependence to the LIS, the maximum shift will be observed if the lactate protons lie close to the principal axis (conformation b). Hence, considering the large induced shift experienced by the lactate protons upon chelation to $[Yb.La]^{3+}$ **12**, and by comparison to the crystal structure of the (RRR)-$[Ln.DO3Ph\text{-}lactate]^{2+}$ adduct (Figure 2.3), the lactate is suggested to bind in a bidentate manner with the hydroxyl group occupying the axial position (Figure 2.14).

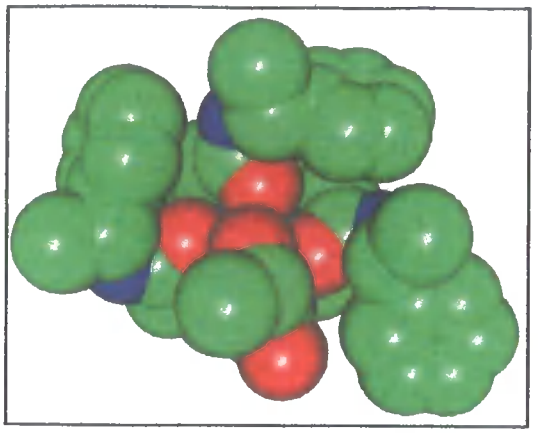

Figure 2.14 Top view of a space filling representation of (RRR)-[Yb.DO3Ph-lactate]$^{2+}$ showing the lactate OH occupying the axial position.

Similar observations were made upon the incremental addition of R-lactate to **12**. The signal of the bound methyl resonance of lactate occurred at +23 ppm whereas the exact position of the lactate bound CH resonance could not be assigned, due to the inconclusive 2D COSY spectra.

A racemic lactate mixture (2.5 equivalents of S and R-lactate) was added to [Yb.La]$^{3+}$ in order to determine if there is any enantioselectivity in the binding. However, due to the broad proton resonances, the diastereomeric peaks for the R and S lactate complexes overlapped and it was not possible to assess the degree of enantioselectivity associated with the binding.

Neutral Complex

Modulation of the affinity of a complex towards an anion can be achieved by varying the overall charge on the complex. In order to try to reduce the affinity and gain fast exchange between the bound and unbound forms of the complex to lactate, the neutral heptadentate complex [Yb.Lb] **28** (Figure 2.15) was synthesized. The cationic core (Ln^{3+}) allows the lactate to bind efficiently but the CO_2^- periphery renders the complex neutral overall.

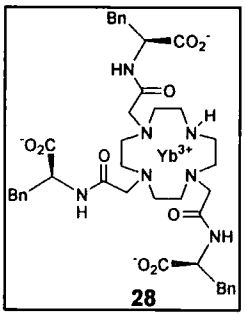

28

Figure 2.15 Structure of the zwitterionic chiral [Yb.Lb] complex **28**.

In the high frequency region of the ^{1}H NMR spectrum of **28** (Figure 2.16) each of the shifted proton signals of the ring appeared to be exchange broadened, suggesting the presence of two species in solution (probably the two SAP forms), which are in fast exchange on the NMR timescale.

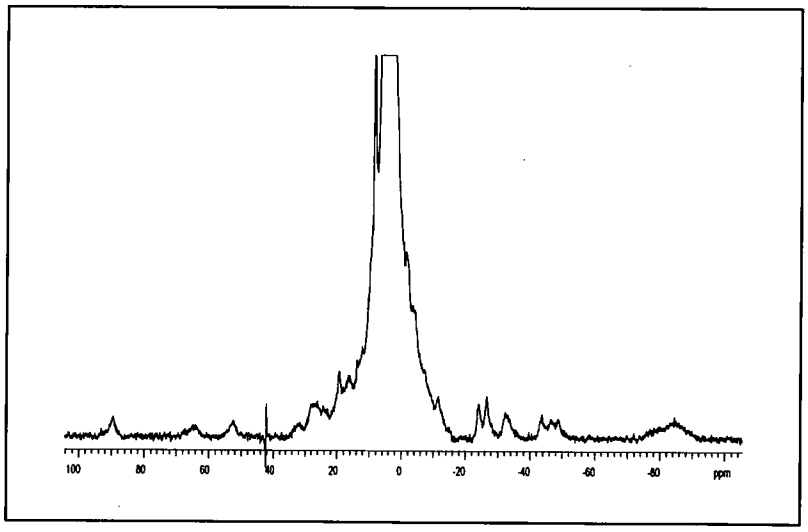

Figure 2.16 ^{1}H NMR spectrum of the zwitterionic [Yb.Lb] complex **28** (200 MHz, D_2O/CD_3OD, 295 K).

Lactate titration

Upon addition of 0.25 equivalents of S-lactate to [Yb.Lb] an additional set of ring resonances was observed, corresponding to the lactate-bound species, which was in slow exchange with the free form on the NMR timescale. Following the addition of 1

equivalent of the appropriate lactate sodium salt, only the peaks of the fully bound adduct were observed. Two isomers were apparent in a ratio of 2:1, the chemical shifts being consistent with the square antiprismatic conformations $\Delta(\lambda\lambda\lambda\lambda)$ and Λ $(\delta\delta\delta\delta)$ respectively. The peaks appeared much sharper than the diaqua complex resonances; the binding of the lactate prevents exchange between the two SAP isomers, occurring within the NMR timescale. An additional resonance integrating to three protons was attributed to the lactate methyl group, experiencing a large paramagnetic shift to around +26 ppm for S-lactate and between +24 and +28 ppm for R-lactate. Again, the lactate CH resonance could not be accurately assigned due to inconclusive COSY analysis. Following the addition of 2.0 equivalents of racemic lactate to the complex, broad and overlapping proton resonances were observed in the ^{1}H NMR spectrum preventing the identification of any diastereomeric peaks for the R and S lactate adducts and hence the degree of enantioselectivity in the binding could not be assessed.

Europium Complexes

Eu^{3+} complexes are also suitable for analysis by NMR, as they experience relatively large shifts with minimal line broadening. However, the ^{1}H NMR spectra obtained for the cationic $[Eu.La]^{3+}$ **13** and the neutral [Eu.Lb] **29** complexes showed signals in the usual range (+30 → -20 ppm) but were too broad to be of any interest.

Conclusions

The two chiral heptadentate Yb^{3+} complexes **12** and **28** appeared to bind to lactate in a bidentate manner via displacement of the two bound water molecules. This binding was signalled by ^{1}H NMR and was in slow exchange on the NMR timescale. The presence of a major and a minor species in solution complicated the interpretation of the spectra and hence the enantioselectivity in the binding of R and S lactate could not be assessed. Furthermore, the hydrophobic phenyl groups on the pendent arms of the ligand resulted in a poor water solubility of the complexes, which is undesirable for use *in vivo*.

2.2.2 Leucine Systems

In the search for water soluble, enantiopure complexes, conformationally rigid on the NMR timescale and in fast exchange with S-lactate, Ln^{3+} complexes based on ligands Lc and Ld (Figure 2.4) have been synthesized. The remote S-chiral centre δ to the ring is expected to lead to the preferential formation of one rigid diastereoisomer out of the four possibilities (Figure 2.8). The three pendent amide arms are based on the amino acid S-leucine. The isopropyl groups are expected to enhance the steric encumbrance thus possibly contributing to the freezing out of any conformational motion of the arms and possibly the ring, leading to the generation of a single isomer in solution. Furthermore, such complexes should be soluble in water. N-benzyl derivatives (based on ligands Le and Lf, Figure 2.4) were also synthesized to assess the effect of N-alkylation on the affinity and selectivity towards anions.

Cationic Complex

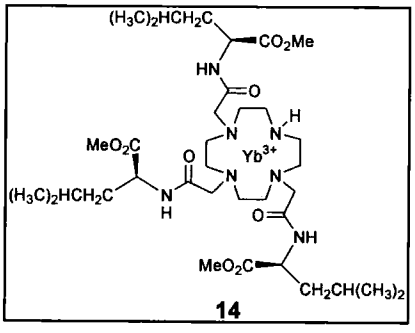

14

Figure 2.17 Structure of $[Yb.Lc]^{3+}$ **14**.

Analysis of $[Yb.Lc]^{3+}$ **14** (Figure 2.17) by ^{1}H NMR spectroscopy showed the presence of only one isomer in solution (Figure 2.18 a), which was suggested to adopt a square antiprismatic conformation [(SSS)Δ(λλλ λ)] (2.2.1). The eight broadened singlet resonances in the high frequency region correspond to the four most shifted axial and equatorial ring protons.

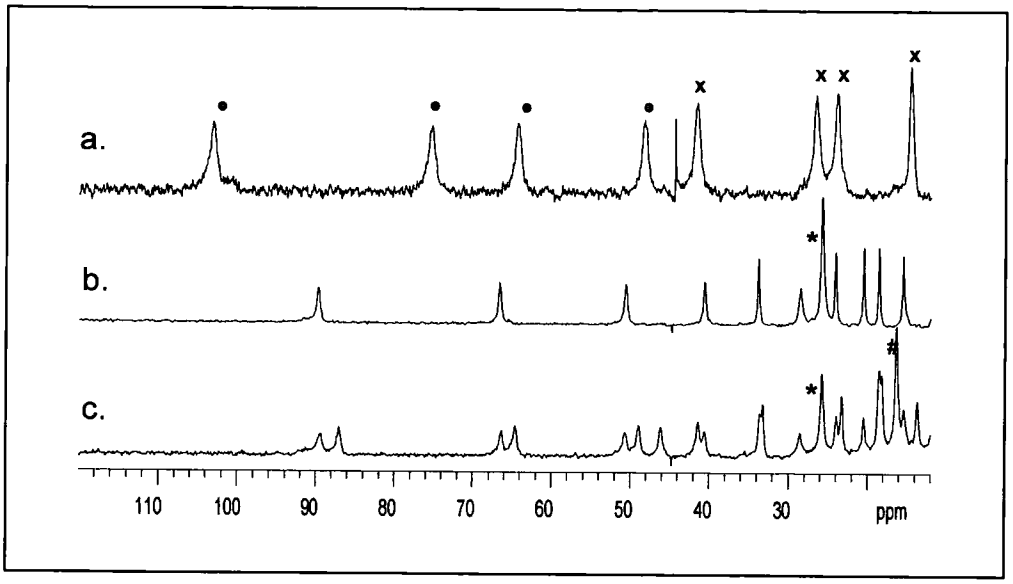

Figure 2.18 Partial ^{1}H NMR of (a) $[Yb.Lc]^{3+}$ **14** (diaqua species showing four axial (•) and four equatorial (x) ring protons), (b) in the presence of 1 equivalent of (S)-Lac [(*) (S)-Lac CH_3], and (c) 2 equivalents of racemic Lac [(#) (R)-Lac CH_3] (200 MHz, D_2O/CD_3OD, 295 K).

Lactate Titration

On addition of 0.25 equivalents of S-lactate sodium salt to **14**, the appearance of an additional set of axial and equatorial ring resonances were evident, corresponding to the lactate bound species in slow exchange on the NMR time scale with the free form. After addition of 1 equivalent of S-lactate, only the bound form was observed (Figure 2.18 b) and an additional singlet resonance at +25 ppm was evident, integrating to three protons, which was subsequently attributed to the methyl resonance of the bound S-lactate. The expected methyl doublet was not resolved due to the broadening effect of the paramagnetic ion. The exact position of the lactate CH resonance could not be defined due to the inconclusive two dimensional spectrum obtained for this system, although an extra singlet resonance observed in the high frequency region of the spectrum, could be accounted for.

A lack of enantioselectivity in adduct formation was apparent following addition of 2 equivalents of racemic lactate to $[Yb.Lc]^{3+}$ and a 1:1 mixture of diastereomeric

complexes was observed by ^{1}H NMR (Figure 2.18 c). The methyl lactate resonance was clearly resolved for the S (+25 ppm) and R (+16 ppm) diastereoisomers ($\Delta\Delta\delta \sim 9$ ppm) and experienced a large lanthanide induced shift (+1.3 ppm in the free form). This is indicative of the bidentate chelation of lactate where the carboxylate and the hydroxyl groups are in an equatorial and axial position respectively.

N-Bn Cationic Complex

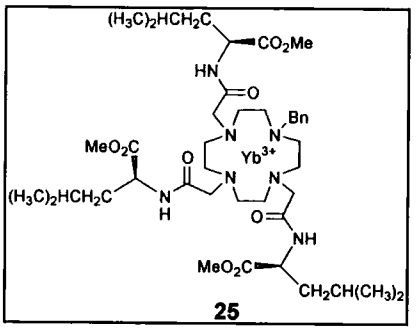

25

Figure 2.19 Structure of $[Yb.Le]^{3+}$ **25.**

The solution ^{1}H NMR investigation of $[Yb.Le]^{3+}$ **25** (Figure 2.19) performed in CD_3OD showed the presence of mainly one isomer (square antiprism) in solution with traces of a minor species (< 8%) to lower frequency, with shifts indicative of a twisted square antiprism conformation (Figure 2.20). However, solely one isomer was observed in a mixture of D_2O and CD_3OD.

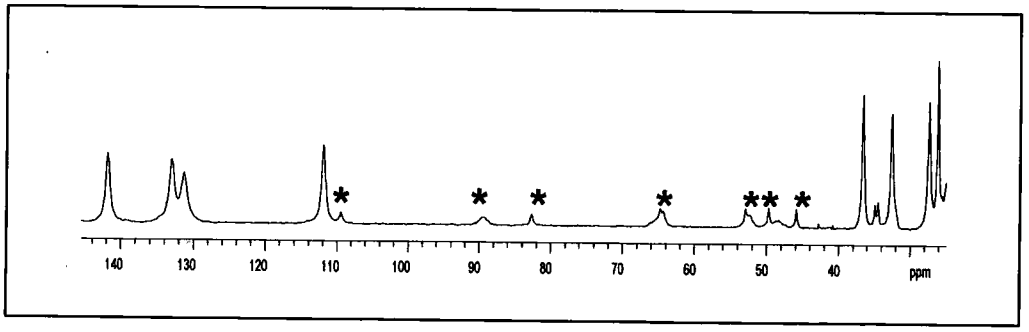

Figure 2.20 Partial ^{1}H NMR spectra of $[Yb.Le]^{3+}$ showing the traces of the minor TSAP species (*) (200 MHz, CD_3OD, 295 K).

Lactate Titration

The ^{1}H NMR investigation of lactate binding showed the occurrence of slow exchange between the free and lactate bound form of the complex. The overall chemical shift range of the spectra increased for both the free complex (212 ppm) and in the presence of lactate (for S-lactate 213 ppm) in comparison to the N-H analogue $[Yb.Lc]^{3+}$ (diaqua: 177 ppm, with S-lactate: 142 ppm) (Table 2.2).

The addition of 2 equivalents of racemic lactate to $[Yb.Le]^{3+}$ revealed a preferential binding for S-lactate (1.4:1, S:R), compared to the lack of enantioselectivity reported for $[Yb.Lc]^{3+}$. The substitution of the free ring N-H with the sterically demanding benzyl group gives rise to a conformation of the complex that favours binding to S-lactate over R-lactate, probably resulting in a low energy chelation form for the S-anion with respect to the R.

	Most Shifted δH_{ax} (ppm)	Range (ppm)	Lactate δCH_3 (ppm)
$[Yb.Le]^{3+}$ (25) = N-Bn	+130	+130 → -82	-
$[Yb.Lc]^{3+}$ (14) = N-H	+103	+103 → -73	-
N-Bn + S-Lac	+129	+129 → -84	+16
N-H + S-Lac	+90	+90 → -48	+25
N-Bn + R-Lac	+127	+127 → -87	+22
N-H + R-Lac	+87	+87 → -61	+16
N-Bn S:R	1.4:1	**N-H S:R**	1:1

Table 2.2 Summary of ^{1}H NMR investigation performed on $[Yb.Lc]^{3+}$ **14** and $[Yb.Le]^{3+}$ **25** (200 MHz, D_2O/CD_3OD, 295 K).

Neutral Complex

^{1}H NMR investigation of a 10 mM solution of the water soluble [Yb.Ld] **30** (Figure 2.21) revealed the presence of many broadened peaks. Upon dilution to 1 mM some of the peaks disappeared and the presence of only one species in solution was observed, characterized in the high frequency range by the eight singlet resonances of the four most shifted axial and equatorial ring protons (Figure 2.22).

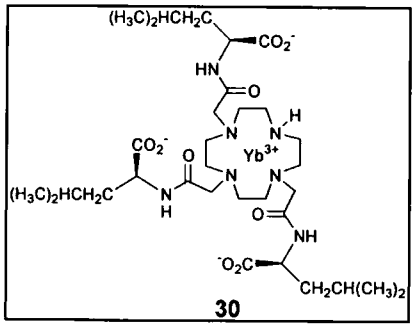

30

Figure 2.21 Structure of [Yb.Ld] **30**.

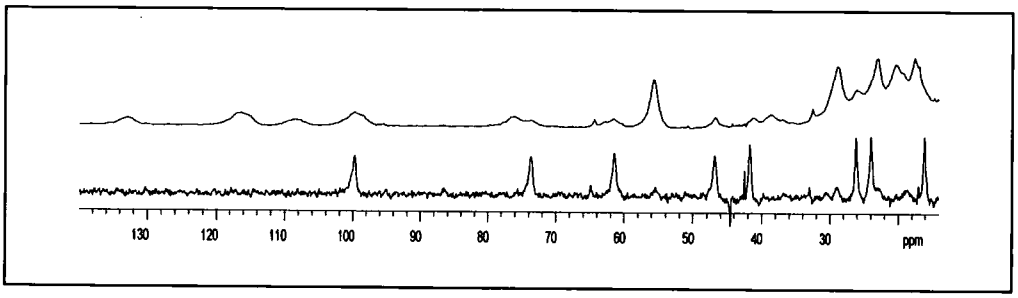

Figure 2.22 Partial ^{1}H NMR spectra of [Yb.Ld] **30**, showing the presence of dimers in a 10 mM solution of the complex (upper) and only one species in 1 mM solution (lower) (200 MHz, D_2O, 295 K).

These observations are consistent with the formation of dimeric structures at higher concentration, the electrostatic interactions in which become much weaker in the diluted solution. This hypothesis was also confirmed by the observation of dimer peaks in the ES^+ spectrum [1735 (10%, M_2Na^+)], and by their subsequent disappearance upon dilution.

Lactate Titration

On addition of 0.25 equivalents of S-lactate to a 10 mM solution of **30**, the dimers disappeared and the characteristic spectrum corresponding to the free and lactate bound forms, in slow exchange, was observed. After addition of 1 equivalent of S-lactate only the bound form was observed (Figure 2.23 b). The evidence of an additional singlet resonance at +30 ppm, integrating to three protons, was attributed

to the methyl resonance of the bound S-lactate. An additional singlet resonance, of intensity one in the high frequency range, was also apparent due to the bound lactate CH. However, its position could not be accurately assigned due to inconclusive 2D-NMR experiments.

A lack of enantioselectivity in binding was apparent following the addition of 2 equivalents of racemic lactate to [Yb.Ld], and a 1:1 mixture of diastereomeric complexes was observed by ^{1}H NMR (Figure 2.23 c). The methyl lactate resonance was clearly resolved for the S (+30 ppm) and R (+20 ppm) diastereoisomers ($\Delta\Delta\delta \sim 10$ ppm). The large lanthanide induced shifts experienced by the lactate methyl bound group compared to the free form, suggested the occurrence of bidentate chelation with the carboxylate equatorially disposed.

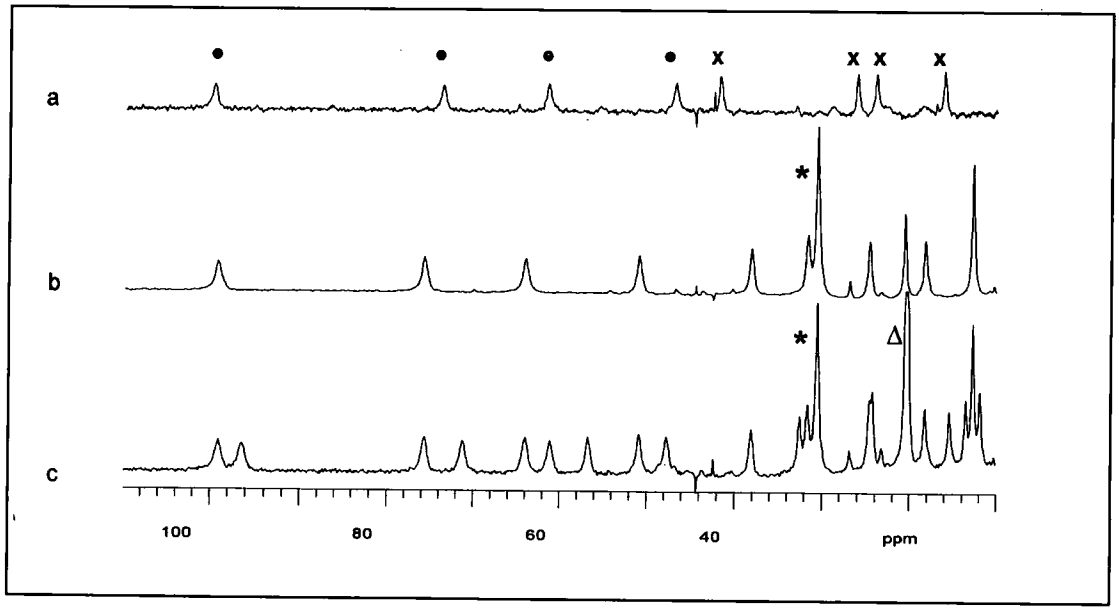

Figure 2.23 Partial ^{1}H NMR of (a) [Yb.Ld] **30** (1 mM) (diaqua species showing four axial (•) and four equatorial (x) ring protons), (b) in the presence of 1 equivalent of (S)-Lac [(*) (S)-Lac CH_3], and (c) 2 equivalents of racemic Lac [(Δ) (R)-Lac CH_3] (200 MHz, D_2O, 295 K).

N-Bn Neutral Complex

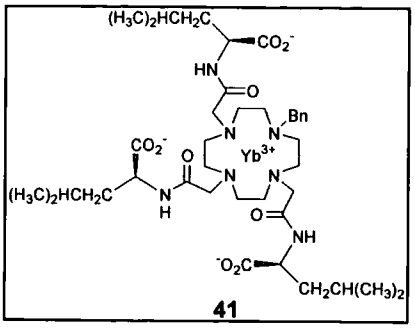

41

Figure 2.24 Structure of [Yb.Lf] **41**.

The ^{1}H NMR spectrum of this water soluble system (Figure 2.24) showed the presence of two isomers in solution, in slow exchange on the NMR timescale. Interestingly, the major species occurred with shifts indicative of a twisted square antiprismatic (TSAP) conformation while the minor species appeared to adopt a square antiprismatic (SAP) geometry (3:1, TSAP: SAP) (Figure 2.25). This was confirmed by observation of a change in the isomer ratio in a range of solvents, with polar aprotic solvents favouring purely the twisted form. The steric nature of the benzyl group coupled with the anionic periphery of the complex must be stabilizing the TSAP form preferentially. No dimers were observed for this system.

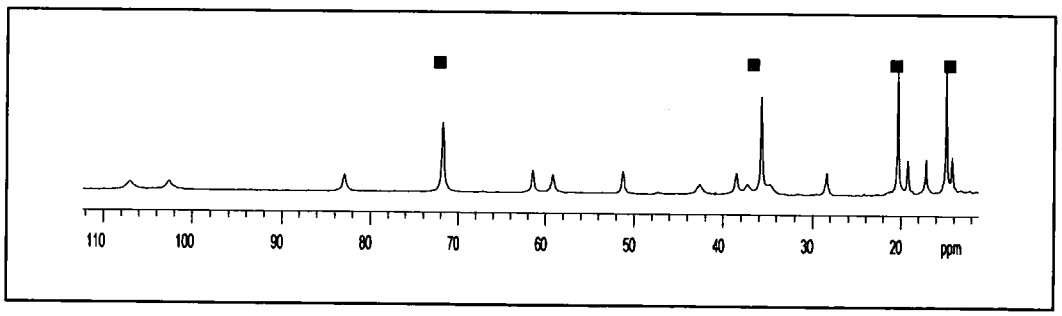

Figure 2.25 Partial ^{1}H NMR spectra of [Yb.Lf] **41** showing the presence of two isomers in solution, the SAP and TSAP (■) forms (200 MHz, D_2O/CD_3OD, 295 K).

Lactate Titration

The addition of 0.25 equivalents of S-lactate to a 10 mM solution of [Yb.Lf] **41** revealed the occurrence of three sets of resonances corresponding to the free and the lactate bound SAP form of the complex, in slow exchange, and the unbound TSAP

isomer. The neutral system appeared to exhibit a lower affinity for the anion compared to the N-H analogue [Yb.Ld] **30**. In fact, in the presence of an excess of lactate (2 equivalents), traces of the unbound complex were still apparent (TSAP + SAP). This may be due to the sterically demanding benzyl group which produces a synergic effect with the overall neutral charge of the system, thus disfavouring the chelation of the negatively charged lactate. Upon addition of 5 equivalents of S-lactate two species were observed in solution, attributed to the fully bound lactate SAP form and to the unbound TSAP species (2:1, respectively). No additional resonances were apparent for the lactate-bound TSAP adduct therefore the TSAP does not favour lactate binding. However, as the TSAP form is in slow exchange with the SAP form, upon addition of excess lactate the relative ratio of the TSAP form was found to decrease as the equilibrium is favoured towards the formation of the SAP-lactate adduct.

The addition of an excess of racemic lactate to [Yb.Lf], revealed preferential binding for S-Lac (2:1, S:R), compared to the lack of enantioselectivity reported for the N-H analogue [Yb.Ld] (Table 2.3). The sterically demanding benzyl group must adopt a conformation in which the binding to S-lactate is favoured.

	Most shifted δH_{ax} (ppm)	**Range** (ppm)	**Lactate δCH_3** (ppm)
[Yb.Ld] 30 = N-H	+100	+100 → -120	-
[Yb.Lf] 41 = N-Bn	+110 (SAP)	+110 → -131 (SAP)	-
	+70 (TSAP)	+70 → -8 (TSAP)	-
N-H + S Lac	+99	+99 → -56	+30
N-Bn + S-Lac	+140 (SAP)	+140 → -77	+20
	+70 (TSAP)	+70 → -8 (unbound TSAP)	
N-H + R Lac	+97	+97 → -64	+20
N-Bn + R-Lac	+137 (SAP)	+137 → -79	+22
	+70 (TSAP)	+70 → -8 (unbound TSAP)	
N-H S:R	1:1	**N-Bn S:R**	2:1

Table 2.3 Summary of ^{1}H NMR investigation performed on [Yb.Ld] **30** and [Yb.Lf] **41** (200 MHz, D_2O, 295 K).

Conclusions

The ^1H NMR spectra of the Yb^{3+} leucine cationic and neutral systems showed the presence of only one isomer in solution. Moreover, an improved and total water solubility have been reported for $[Yb.Lc]^{3+}$ and [Yb.Ld], respectively. Lactate binding occurs in slow exchange on the NMR timescale, hence the complexes are not suitable for use as shift reagents. The lactate CH_3 resonances are clearly resolved for the R and S diastereoisomers ($\Delta\Delta\delta \cong 10$ ppm) and exhibit large lanthanide induced shifts (Table 2.2 and 2.3) in comparison to the much smaller $\Delta\Delta\delta$ values reported for shift reagents ($\Delta\Delta\delta < 0.1$ ppm) in the literature. The apparent lack of kinetic resolution augurs well for the development of such complexes as NMR chiral derivatising agents (Chapter 3).

The N-Bn leucine systems exist as two isomers in solution, with the cationic complex existing in mainly the SAP geometry (>10:1 in CD_3OD, 100% in D_2O/CD_3OD) whereas the neutral system prefers to adopt the TSAP conformation (3:1). The presence of the sterically demanding benzyl group also resulted in a preferential binding for S-lactate ($[Yb.Le]^{3+}$ 1.4:1, S:R; [Yb.Lf] 2:1, S:R) and, for the neutral complex [Yb.Lf], a dramatic decrease in the affinity for lactate (weak binding).

2.2.3 α, β Chiral Systems

The introduction of a chiral centre α or β to the ring N of cyclen in DOTA-like Ln^{3+} complexes has been reported to impart extra rigidity, inhibiting arm rotation in particular.[10] With the aim of obtaining new, enantiopure heptadentate complexes, which appear as a single isomer in solution, the synthesis of systems based on ligands bearing both an α and β chiral centre (Figure 2.26) was attempted. Threonine was chosen as the starting compound due to the presence of two chiral centres (2S, 3R), which may be attached to the macrocyclic ring, generating α and β chiral centres, by conversion of the hydroxyl side group into a good leaving group.

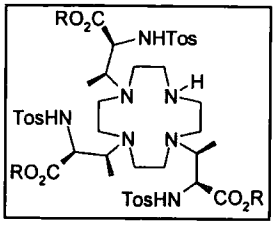

Figure 2.26 General structure of the ligand (Lg) bearing α and β (SS) chiral centres.

α, β (SS) Chiral Centres via Triflate

The first route attempted to obtain an enantiopure complex of known chirality, involved the use of reactive compounds, such as triflate derivatives, which are known to react with a nucleophile with complete inversion of configuration (stereoselective S_N2). The triflation of the N-Boc protected (2S, 3R)-threonine methyl ester was attempted, following a variety of literature procedures.[11,12,13] A range of reaction conditions were employed varying temperature, reaction time, relative quantities of the starting materials and purification procedures. However, the required product was not isolated. The triflate derivative proved to be too unstable, readily undergoing competing elimination reactions to form double bond products and the formation of an aziridine ring (Scheme 2.7). This route was abandoned.

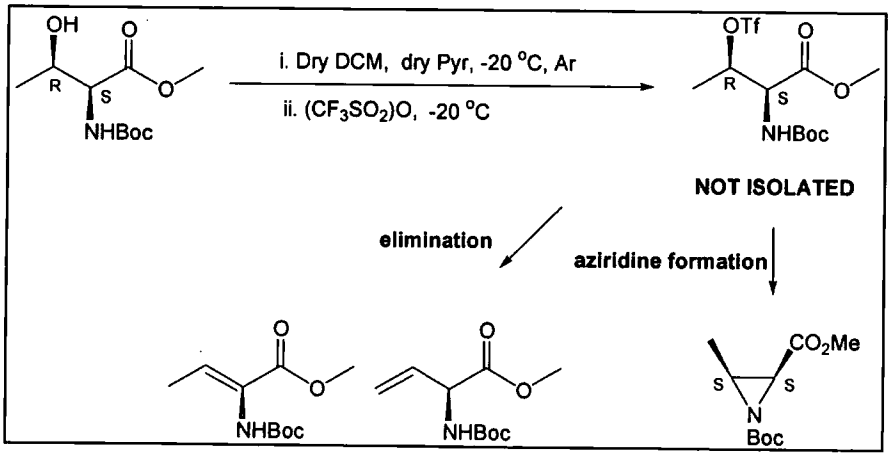

Scheme 2.7

α, β (SS) Chiral Centres via Aziridine

Aziridine-2-carboxylates and their derivatives have found widespread use as intermediates for the synthesis of a number of amine-containing molecules by stereospecific ring opening reactions with various nucleophiles.[14] It has been reported that Lewis acid (i.e. BF_3) mediated nucleophilic ring opening reactions of *cis*-3-alkylaziridine-2-carboxylates occur with concomitant breakage of the bond between N-1 and C-3 of the aziridine ring and with retention of configuration at the α and β positions.[15] Thus, these relevant stereochemical results were considered as a route to our enantiopure ligand Lg (Figure 2.26).

The synthesis of enantiopure (2S,3S) aziridines was undertaken (Scheme 2.8) following a literature procedures, reported for a similar system.[16]

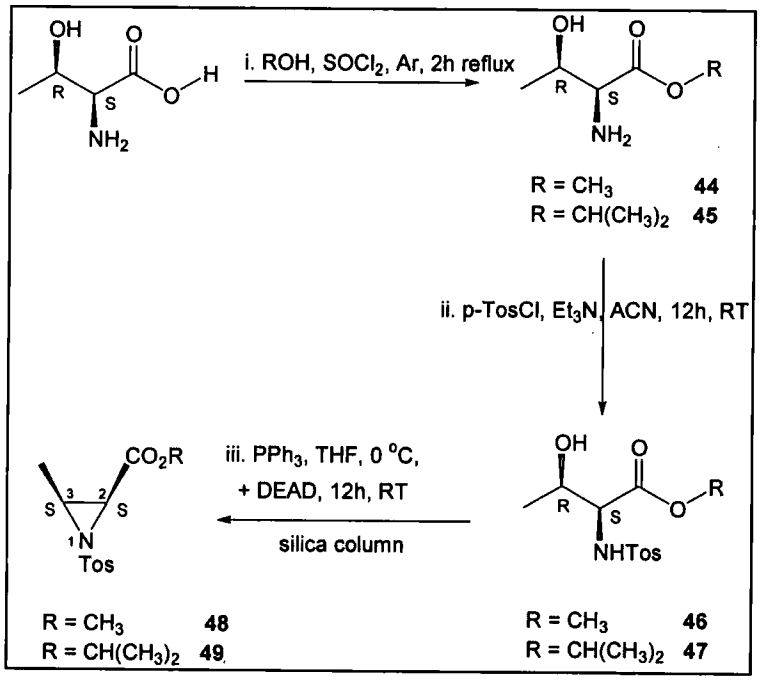

Scheme 2.8

The first step in the synthesis of the chiral aziridine (**48**, **49**) was the esterification, with the appropriate alcohol (methanol or isopropanol), of the enantiomerically pure amino acid, (2S,3R)-threonine. The primary amine of the resulting product (**44**, **45**)

was then protected by reaction with p-toluenesulfonyl chloride in acetonitrile, in the presence of triethylamine, to yield the tosylated compound (**46** and **47**). The ring closure, which takes place with inversion of configuration (S_N2) at C-3, was performed by adding diethyl azodicarboxylate (DEAD) dropwise to a cold (0 °C) mixture of **46** or **47,** in the presence of triphenylphosphine (PPh_3), in tetrahydrofuran (THF). After 12 h stirring at room temperature, the crude product was purified by silica chromatography, yielding the enantiopure (2S, 3S) tosyl aziridine **48** or **49**. Two dimensional NMR spectra (NOESY) of the products confirmed the *cis* configuration at C-2 and C-3.

The trialkylation of cyclen with **48** or **49** was performed in refluxing acetonitrile in the presence of a catalytic amount of the Lewis acid, BF_3OEt_2, in order to gain a selective ring opening by breakage of the N-1 and C-3 bond (Scheme 2.9). The reaction, which was followed by ES^+, did not yield the desired trisubstituted cyclen but two products: the dialkylated product, which subsequently underwent an intramolecular lactam formation via attack of a free ring N-H onto the ester carbonyl group, to give the monoalkylated intralactam side product (Lh).

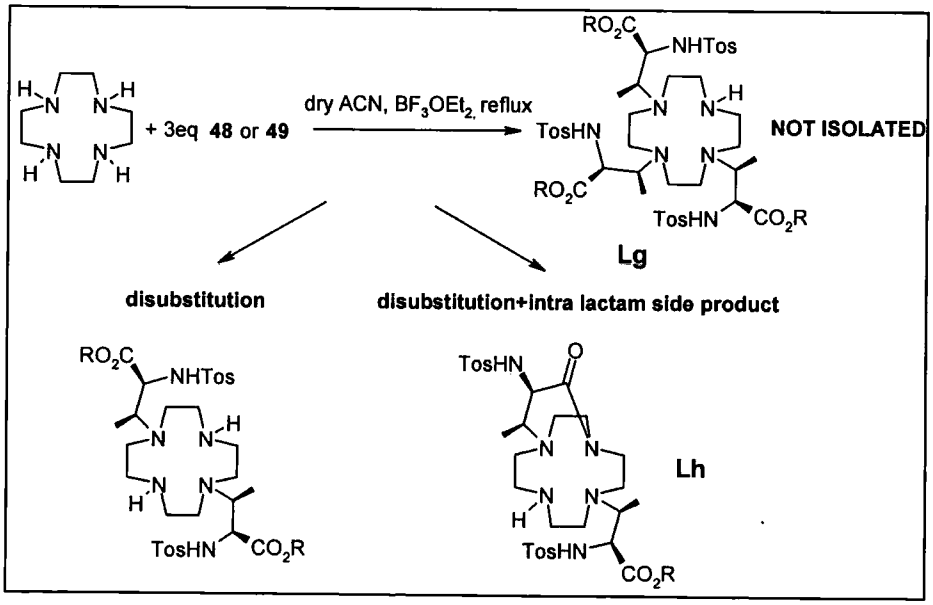

Scheme 2.9

In an attempt to prevent the lactam formation product, the aziridine **49** with the more sterically demanding isopropyl group was prepared (Scheme 2.8). Although the formation of the intralactam product in the subsequent trialkylation step was slower and less efficient than in the methyl ester case, it still formed in appreciable amounts. Thus, the synthesis of an N-protected aziridine, bearing the bulkier tert-butyl ester, was attempted. However, the synthesis of the N-tosyl protected tert-butyl ester of (2S,3R)-threonine proved to be problematic. Hence the N-Cbz protected analogue was synthesised[17] but the following aziridination step did not yield the expected N-Cbz (2S, 3S) aziridine. Instead, a double bond-containing side product was obtained. Due to lack of time, this synthetic procedure was abandoned but it could be a key route for future synthetic approaches.

2.3 Solution NMR Investigation of Lanthanide(III) Variation

The use of the [Pr.DO3A] chelate (Figure 2.27) as a shift agent for differentiating between intra and extracellular S-lactate resonances by ^{1}H NMR spectra ($\Delta\Delta\delta \approx 0.2$ ppm) has recently been reported.[18] Hence, an approach for the modulation of the anion affinity and the control of the size and the direction of the paramagnetic shift, may be envisaged by varying both the Ln ion and the overall charge (+3, 0) on the chelate.

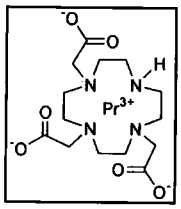

Figure 2.27 [Pr.DO3A].

Thus, the synthesis of a variety of Ln^{3+} complexes based on the leucine ligands Lc and Ld (Figure 2.28) has been undertaken and ^{1}H NMR solution studies have been performed in the absence and presence of S-lactate.

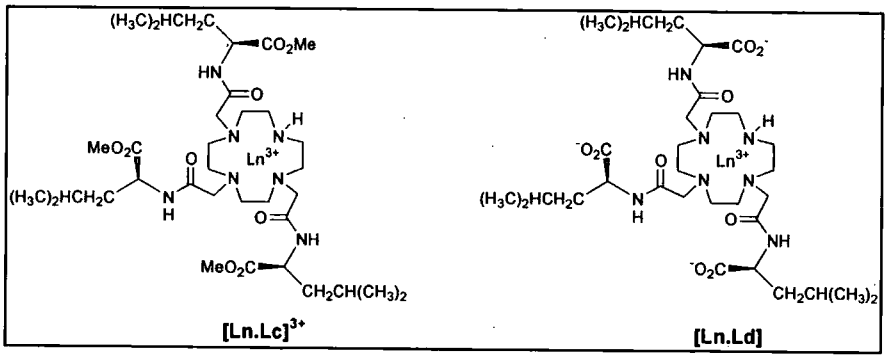

Figure 2.28 General structures of the complexes under investigation.

2.3.1 Diaqua Complexes

The observed lanthanide induced shift (LIS) has a Fermi contact (Δ_c) and a pseudocontact (Δ_p) contribution which, in axially symmetric complexes, can be expressed by equation 2.1.

$$\Delta = \Delta_C + \Delta_P = F\langle S_z\rangle + D\langle r^2\rangle A_2^0 G = \tag{2.1}$$

$$= F\langle S_z\rangle + C_j \frac{\beta^2}{60k^2T^2} \cdot \frac{\langle r^2\rangle A_2^0 (3\cos^2\theta - 1)}{r^3}$$

The contact contribution is the product of F, which is proportional to the hyperfine coupling constant, A, and the spin expectation value, $\langle S_Z\rangle$, for the paramagnetic Ln^{3+} ion. The dipolar shift is a function of the magnetic anisotropy constant D (proportional to the Bleaney's constant C_j and to the anisotropy of the magnetic susceptibility tensor of the complex along the z axis), the ligand field coefficient of the Ln^{3+} complex $\langle r^2\rangle A_2^0$ and the geometric factor G, $(3\cos^2\theta - 1)/r^3$ (1.2.2). Theoretical $\langle S_Z\rangle$ and D (C_j) values are reported in the literature for each Ln^{3+} ion.[19,20] The pseudocontact contribution predominates with the lanthanides due to the fact that the unpaired electrons reside in the 4 f orbitals and these orbitals are well shielded from the valence orbitals involved in bonding between the metal and the ligand. Thus, the unpaired electron spin density remains largely on the lanthanide cation and the NMR shift is most commonly a result of a through-space interaction. The magnitude and sign of the LIS is dependant on both the nature of the Ln^{3+} ion and the location of the nucleus relative to the metal centre.[21]

A ^{1}H NMR investigation performed on the diaqua $[Ln.Lc]^{3+}$ and [Ln.Ld] complexes (Table 2.4 and 2.5 respectively) showed the presence of only one species in solution for each of the lanthanides. The ^{1}H NMR spectra of complexes of the lighter Ln^{3+} ions (i.e. Ce^{3+}- Eu^{3+}, **15- 19** and **31-35**), appeared to be characterized by relatively small paramagnetic shifts, compared to complexes of the heavier Ln^{3+} ions (i.e. Tb^{3+}-Yb^{3+}, **20-24**, **14** and **36-40**, **30**). Moreover, considering the sign of the observed shifts, it is possible to divide the Ln^{3+} complexes into two groups, according to which Ce^{3+}, Pr^{3+}, Nd^{3+}, Sm^{3+}, Tb^{3+}, Dy^{3+}, and Ho^{3+} complexes have one sign of magnetic anisotropy and Eu^{3+}, Er^{3+}, Tm^{3+} and Yb^{3+} complexes have the opposite sign. This is due to the Bleaney constant (C_j) which is characteristic of each lanthanide and determines both the direction and the size of the paramagnetic shift. The maximal magnitude of the Bleaney constant is observed for Tb^{3+}, Dy^{3+} and Tm^{3+} (C_j = -86, -100, +53 respectively), complexes of which experience the largest paramagnetic shifts. [Note, Tb^{3+} and Dy^{3+} shift the most shifted axial ring proton to lower frequencies (-319, -379 ppm respectively) whereas Tm^{3+} shifts to higher frequency (+293 ppm)].

$[Ln.Lc]^{3+}$ diaqua	C_j[19]	δH_{ax} (ppm)	Range (ppm)	$\langle S_Z \rangle$[20]	$\nu_{1/2}$ (Hz)
15. $[Ce.Lc]^{3+}$	-6.3	-12	+15→ -12	-0.98	223
16. $[Pr.Lc]^{3+}$	-11.0	-30	+25→ -30	-2.97	187
17. $[Nd.Lc]^{3+}$	-4.2	-16	+16→ -16	-4.49	273
18. $[Sm.Lc]^{3+}$	-0.7	-	+7→ 0.0	+0.06	-
19. $[Eu.Lc]^{3+}$	+4.0	+25	+25→ -19	+10.68	205
20. $[Tb.Lc]^{3+}$ *	-86	-320	+81→-320	+31.82	418
21. $[Dy.Lc]^{3+}$ *	-100	-379	+300→-379	+28.55	365
22. $[Ho.Lc]^{3+}$	-39	-125	+191→ -125	+22.63	596
23. $[Er.Lc]^{3+}$	+33	+118	+118→ -75	+15.37	425
24. $[Tm.Lc]^{3+}$ *	+53	+293	+293→-254	+8.21	480
14. $[Yb.Lc]^{3+}$	+22	+120	+120→ -91	+2.59	209

Table 2.4 ^{1}H NMR investigation of the diaqua cationic complexes of ligand Lc, reporting the chemical shift of the most shifted axial proton of the ring and its half peak height line width, the spectral range and the tabulated values of the pseudocontact (C_j)[19] and contact ($\langle S_Z \rangle$)[20] constants (200 MHz or 65 MHz*, CD_3OD, 295 K).

For example, among the cationic $[Ln.Lc]^{3+}$ systems (Table 2.4), $[Nd.Lc]^{3+}$**17** and $[Eu.c]^{3+}$ **19** (with C_j = -4.2 and +4.0, respectively) exhibit a much narrower spectral range (+16→ -16 and +25→ -19 respectively) compared to $[Tb.Lc]^{3+}$ **20** (C_j = -86) and $[Tm.Lc]^{3+}$ **24** (C_j = +53) (+81→-320 and +293→-254 respectively) (Figure 2.29).

[Ln.Ld] diaqua	δH_{ax} (ppm)	Range (ppm)	$\nu_{1/2}$ (Hz)
31. [Ce.Ld]	-15	+19 → -15	101
32. [Pr.Ld]	-33	+34 → -33	92
33. [Nd.Ld]	-17	+17 → -17	75
34. [Sm.Ld]	-	+11 → -1.0	-
35. [Eu.Ld]	+26	+26 → -15	53
36. [Tb.Ld] *	-333	+250 → -333	722
37. [Dy.Ld] *	-381	+250 → -381	301
38. [Ho.Ld]	-195	+142 → -195	876
39. [Er.Ld]	+123	+123 → -65	370
40. [Tm.Ld] *	+290	+290 →-389	704
30. [Yb.Ld]	+106	+106 →-121	330

Table 2.5 ^{1}H NMR investigation of the diaqua neutral complexes of ligand Ld, reporting the chemical shift of the most shifted axial proton of the ring, the half peak height line width and the spectral range (200 MHz or 65 MHz*, CD_3OD, 295 K).

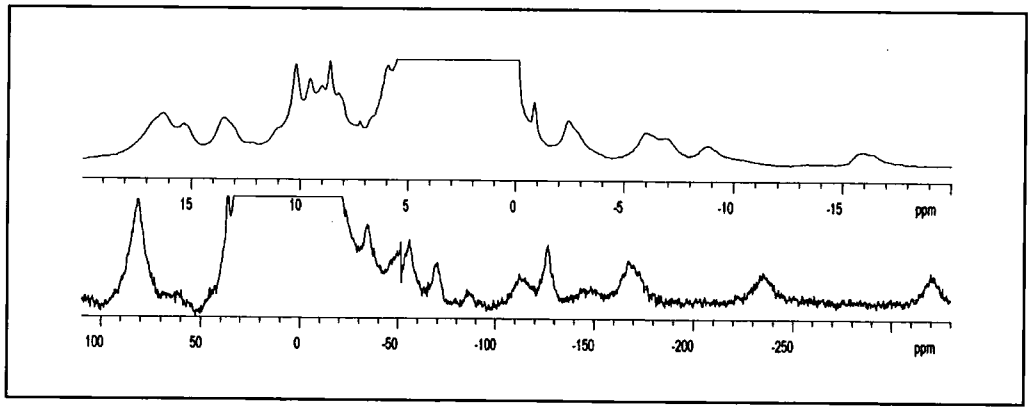

Figure 2.29 ^{1}H NMR spectra of (upper) $[Nd.Lc]^{3+}$ **17** (200 MHz, CD_3OD, 295 K) and (lower) $[Tb.Lc]^{3+}$ **20** (65 MHz, CD_3OD, 295 K), highlighting the large difference in the chemical shift range exhibited by the two complexes.

In order to assess the relative magnitude of the dipolar broadening of the nuclear resonances, the half peak height line width ($\nu_{1/2}$) has been measured for the most shifted axial proton of the ring in each of the cationic and neutral complexes. The results, reported in Table 2.4 ($[Ln.Lc]^{3+}$) and in Table 2.5 ([Ln.Ld]) show that the complexes of the Ln^{3+} ions belonging to the second part of the series (from Tb^{3+} to Tm^{3+}), though better shifters, are also more efficient dipolar broadeners than the complexes of the early Ln^{3+} (i.e. Pr^{3+}, Eu^{3+}) (Figure 2.30).

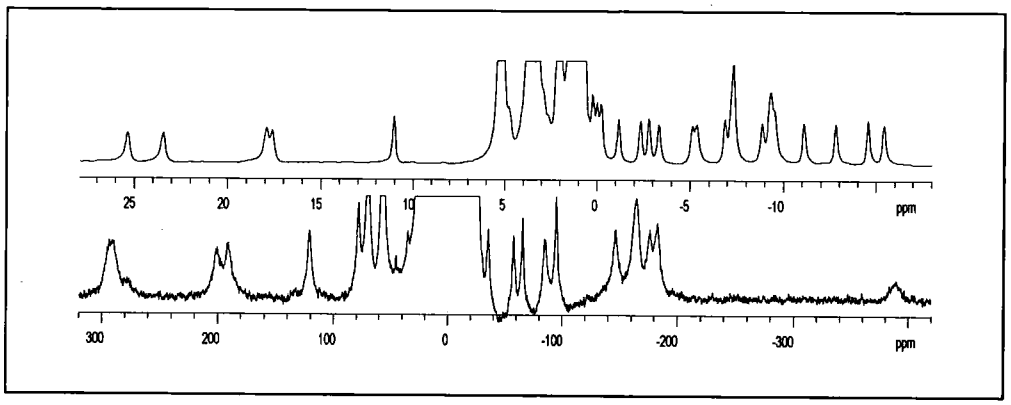

Figure 2.30 ^{1}H NMR spectra of [Eu.Ld] **35** (200 MHz, CD_3OD, 295 K) (upper) and [Tm.Ld] **40** (65 MHz, CD_3OD, 295 K) (lower), highlighting the greater shifting and broadening ability of the Tm^{3+} ion compared to the Eu^{3+} ion.

The best compromise between line broadening and amplitude of the shifts is exhibited by the Yb^{3+} complexes **14** and **30**, although such complexes have been reported to be unsuitable as shift reagents for lactate (2.2.2) as the binding occurs in slow exchange on the NMR timescale.

The charge density of the Ln^{3+} ions increases along the series, causing the well known lanthanide contraction. Complexes of Yb^{3+}, which is the most charge dense ion, are expected to have a higher affinity towards anions than complexes of early Ln^{3+} ions such as Pr^{3+}, Nd^{3+}, Eu^{3+}, which are less charge dense. Therefore a systematic study was undertaken to assess whether fast exchange conditions could be achieved by variation of the Ln^{3+} ion.

2.3.2 Lactate Adducts

0.01 ml aliquots of a solution of S-lactate sodium salt (in D_2O, 175 mM, complex to lactate ratio ranging from 4:1 to 1:2) were added successively to a solution of $[Ln.Lc]^{3+}$ and [Ln.Ld] (0.70 ml, 10 mM) and the ^1H spectrum of the complexes was run for each increment. The results of the ^1H NMR studies performed for the cationic $[Ln.Lc]^{3+}$ and the neutral [Ln.Ld] complexes in the presence of lactate are reported in Table 2.6 and 2.7 respectively.

$[Ln.Lc]^{3+}$ + S-Lac or racemic Lac	Most shifted S δH_{ax} (ppm)	Most shifted R δH_{ax} (ppm)	Range (S-Lac adduct) (ppm)	S:R
15. $[Ce.Lc]^{3+}$	-	-	+20 → -12	-
16. $[Pr.Lc]^{3+}$	-25	-	+23 → -25	-
17. $[Nd.Lc]^{3+}$	-	-	+16 → -12	-
18. $[Sm.Lc]^{3+}$	-	-	+6 → -1.0	-
19. $[Eu.Lc]^{3+}$	+25	+23	+25 → -14	1:1
20. $[Tb.Lc]^{3+}$ *	-311	-	+199 → -311	-
21. $[Dy.Lc]^{3+}$*	-328	-	+270 → -328	-
22. $[Ho.Lc]^{3+}$	-159	-	+100 → -159	-
23. $[Er.Lc]^{3+}$	+115 S δCH_3=30	-	+115 → -74	-
24. $[Tm.Lc]^{3+}$ *	+255	+248	+255 → -185	1:1
14. $[Yb.Lc]^{3+}$	+90 S δCH_3=25	+87 R δCH_3=16	+90 → -48	1:1

Table 2.6 ^1H NMR investigation performed on the $[Ln.Lc]^{3+}$ complexes in the presence of S-lactate and racemic lactate. The resonance of the most shifted axial proton of the ring, in the S-Lac and in the R-Lac adducts are reported along with the spectral range of the complexes with S-Lac (200 MHz or 65 MHz*, D_2O/CD_3OD, 295 K).

[Ln.Ld] + S-Lac or racemic Lac	Most Shifted S δH_{ax} (ppm)	Most Shifted R δH_{ax} (ppm)	Range (S-Lac adduct) (ppm)	S:R
31. [Ce.Ld]	-	-	+17 → -13	-
32. [Pr.Ld]	-16	-	+27 → -16	-
33. [Nd.Ld]	-	-	+16 → -16	-
34. [Sm.Ld]	-	-	+6 → -1.0	-
35. [Eu.Ld]	+25 S δCH_3=+6		+25 → -14	-
36.[Tb.Ld] *	-345	-335	+233 → -345	1:1
37.[Dy.Ld]*	-351	-301	+238 → -351	1:1
38.[Ho.Ld]	-172 S δCH_3=-57	-167 R δCH_3=-42	+117 → -172	1:1
39. [Er.Ld]	+133 S δCH_3=+39	+127	+133 → -72	1:1
40.[Tm.Ld] *	+297	+283	+297 → -213	1:1
30.[Yb.Ld]	+99 S δCH_3=+30	+97 R δCH_3=+20	+99 → -55.7	1:1

Table 2.7 ^{1}H NMR investigation performed on the [Ln.Ld] complexes in the presence of S-lactate and of racemic lactate. The resonance of the most shifted axial proton of the ring, in the S-Lac and in the R-Lac adducts are reported along with the spectral range of the complexes with S-Lac (200 MHz or 65 MHz*, D_2O, 295 K).

Upon addition of 0.25 equivalents of S-lactate, slow exchange on the NMR time scale was observed between the lactate-bound and the free form for most of the cationic and neutral complexes. The lactate CH_3 experienced a large LIS, the size and direction of which is highly dependant on the Ln^{3+} ion (i.e. -42 ppm for [Ho.Ld]; +20 ppm for [Yb.Ld]). Following the addition of 2.0 equivalents of racemic lactate, the ^{1}H NMR spectrum of the cationic $[Eu.Lc]^{3+}$ **19**, $[Tm.Lc]^{3+}$ **24**, $[Yb.Lc]^{3+}$ **14** and of the neutral [Tb.Ld] **36**, [Dy.Ld] **37**, [Ho.Ld] **38**, [Er.Ld] **39**, [Tm.Ld] **40**, and [Yb.Ld] **30** complexes, showed a 1:1 mixture of the diastereomeric R and S adducts. Broad and overlapping proton resonances for the remaining Ln complexes prevented the identification of any diastereomeric peaks for the R and S lactate complexes.

On lactate addition, the ^{1}H NMR spectra of $[Ce.Lc]^{3+}$ **15** and $[Sm.Lc]^{3+}$ **18** complexes varied slightly but as they experienced severe broadening over the narrow spectral range, the results were inconclusive. Similar results were obtained for the neutral analogues [Ce.Ld] **31** and [Sm.Ld] **34**. The ^{1}H NMR spectra of the Pr^{3+} complexes **16** and **32,** were difficult to interpret and additional experiments were undertaken.

The ^{1}H NMR spectrum of the cationic $[Pr.Lc]^{3+}$ complex showed a change upon the addition of lactate but, as the spectrum experienced severe broadening, the condition of fast or slow exchange could not be defined. In order to gain further information, 0.1 equivalents of $[Pr.Lc]^{3+}$ **16** were added to a 10 mM solution of S-lactate, in D_2O, and the ^{1}H NMR spectrum was run (Figure 2.31).

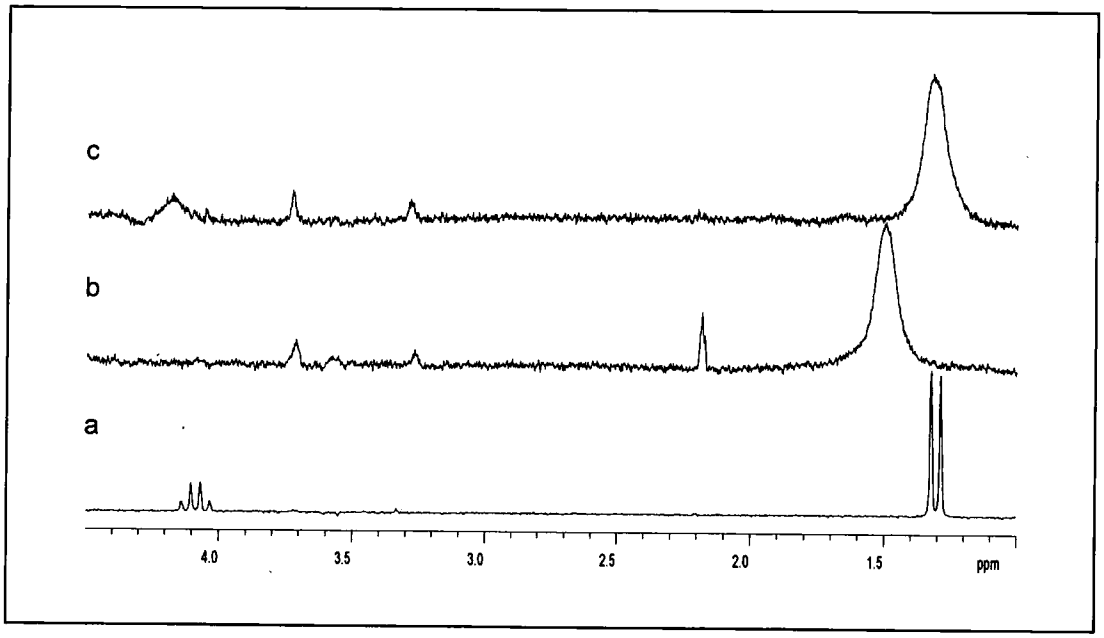

Figure 2.31 ^{1}H NMR spectra of a) S-lactate solution (10 mM), b) S-lactate solution +0.1 equivalents of $[Pr.Lc]^{3+}$, c) S-lactate solution +0.1 equivalents of $[Nd.Lc]^{3+}$ (200 MHz, D_2O, 295 K).

The disappearance of the S-lactate CH resonance (+4.1 in the free form) in the presence of the paramagnetic species was observed, suggesting either a severe

broadening of this resonance or the occurrence of fast exchange on the NMR timescale between the free and bound forms. The lactate CH_3 resonance experienced a slight shift (+0.2 ppm) and broadened significantly. The same ^1H NMR investigation was undertaken with some of the other complexes. Although a severe broadening of both the S-lactate CH and CH_3 resonances was observed, for all the cationic $[Ln.Lc]^{3+}$ and neutral [Ln.Ld] complexes, for example $[Nd.Lc]^{3+}$ (Figure 2.31 c), slow exchange conditions were observed and no significant shift and disappearance of the lactate peaks were apparent. Therefore, fast exchange conditions may possibly have been achieved for the $[Pr.Lc]^{3+}$ complex. However, due to the severe line broadening exhibited by the complex, coupled with the small spectral range, the actual shifted lactate CH peak could not be assigned. The $[Pr.Lc]^{3+}$ complex is therefore not a useful shift reagent for lactate.

The ^1H NMR spectrum of the neutral [Pr.Ld] **32** complex, in the presence of 0.25 equivalents of S-lactate, was very broad and no relevant changes in its appearance were observed. On addition of 0.1 equivalents of [Pr.Ld] to S-lactate the CH and CH_3 resonances broadened but did not shift. It appears that the neutral charge of the system coupled with the low charge density of the Pr^{3+} ion decreases the affinity towards the anion sufficiently, and no significant binding to S-lactate is observed.

2.3.3 Phosphorylated Adducts

^{31}P MRS provides an ideal means of monitoring tumour energetics, phospholipid metabolism and intracellular pH by detecting the concentration of phosphorylated metabolites. Key metabolites are phosphocholine (PC) and phosphoethanolamine (PE), which are membrane synthesis substrates and phosphodiesters (i.e glycerophosphoethanolamine and glycerophosphocholine), which are membrane breakdown products (1.1.2). Thus, changes in the PME/PDE ratio may correspond to high rates of membrane synthesis within rapidly proliferating tissue, or membrane decomposition within necrotic regions.[22]

Phosphate has been shown to bind to heptadentate Ln complexes via monodentate chelation.[1] The potential use of shift reagents for phosphorylated compounds would

result in the separation of overlapping ^{31}P resonances (discussed in 1.1.2) and in the implementation of rapid acquisition times. Thus a ^{1}H and ^{31}P NMR study was performed on $[Ln.Lc]^{3+}$ and [Ln.Ld] (Ln^{3+} = Pr^{3+}, Eu^{3+}, Ho^{3+} and Yb^{3+}) in the presence of PE and PC.

The ^{1}H NMR spectrum of a 10 mM solution of the cationic $[Ln.Lc]^{3+}$ or the neutral [Ln.Ld] system, in the presence of 0.5 equivalents of PC or PE (pH 7.5) showed an additional set of ring resonances corresponding to the phosphorylated-bound species, which was in slow exchange on the NMR timescale with the free form. The ^{31}P NMR spectrum run on the same solution of the neutral [Pr.Ld] **32**, [Eu.Ld] **35**, [Ho.Ld] **38**, [Yb.Ld] **30** complexes, revealed the presence of two signals, attributed to the free and the phosphorylated-bound species, thus indicating a relatively poor binding affinity of the neutral systems for these anions. The increased electrostatic interaction exhibited with the cationic complexes, however, gave rise to the observation of only the fully bound phosphorylated species. Upon addition of an excess of PE or PC (10 equivalents) to a 10 mM solution of the complexes, the ^{1}H NMR spectrum showed only the signals of the phospho-bound species (Table 2.8).

complex	DIAQUA		PC		PE	
	δH_{ax} (ppm)	range (ppm)	δH_{ax} (ppm)	range (ppm)	δH_{ax} (ppm)	range (ppm)
14. [Yb.Lc]$^{3+}$	+103	+103 → -73	+120	+120 → -81	+119	+119 → - 80
19. [Eu.Lc]$^{3+}$	+23	+23 → -18	+24	+24 → -16	+23	+23 → -15
22. [Ho.Lc]$^{3+}$	-178	+122 → -178	-176	+141 → -176	-174	+139 → -174
16. [Pr.Lc]$^{3+}$	-25	+24 → -25	-36	+31 → -36	-34	+29 → -34
30. [Yb.Ld]	+100	+100 → -120	+120	+120 → -86	+115	+115 → -85
35. [Eu.Ld]	+25	+25 → -17	+26	+26 → -15	+25	+25 → -15
38. [Ho.Ld]	-196	+134 → -196	-186	+136 → -186	-185	+135 → -185
32. [Pr.Ld]	-30	+28 → -30	-38	+57 → -38	-38	+56 → -38

Table 2.8 ^{1}H NMR investigation performed on $[Ln.Lc]^{3+}$ and [Ln.Ld] (10 mM, D_2O/CD_3OD and D_2O respectively), in the presence of 10 equivalents of PC or PE (200 MHz, 295 K).

The ^{31}P NMR spectrum of the same solution of the complexes showed two signals, attributed to the free phosphorylated compound and the phosphorylated-bound species, which were thus confirmed to be in slow exchange on the NMR timescale. Despite fast exchange conditions not being observed, a huge LIS was revealed by ^{31}P NMR for the phosphorylated-bound species (c.f. free form +4.9 ppm, pH 7.5), at higher frequency (+) for Pr^{3+} and Eu^{3+} complexes, and at lower frequency (-) for Yb^{3+} and Ho^{3+} complexes (Table 2.9).

	Sign of the shift	+ PE ΔΔδ (ppm)	+ PC ΔΔδ (ppm)
16. [Pr.Lc]$^{3+}$	+	131	129
19. [Eu.Lc]$^{3+}$	+	164	172
22. [Ho.Lc]$^{3+}$	-	57	65
14. [Yb.Lc]$^{3+}$	-	74	80
32. [Pr.Ld]	+	130	131
35. [Eu.Ld]	+	161	159
38. [Ho.Ld]	-	74	74
30. [Yb.Ld]	-	60	68

Table 2.9 ^{31}P absolute ΔΔδ of [Ln.Lc]$^{3+}$ and [Ln.Ld] (10 mM, D_2O/CD_3OD and D_2O respectively) in the presence of 10 equivalents of PE or PC (200 MHz, 295 K, pD ≅ 8).

2.3.4 Future Studies: +2 and +1 Systems

Following the ^{1}H and ^{31}P NMR investigation, both the cationic [Ln.Lc]$^{3+}$ and the neutral [Ln.Ld] systems were reported to be unsuitable as shift reagents for lactate and phosphorylated compounds, due to either a high affinity, resulting in slow exchange or a weak affinity resulting in poor binding for the anions. However, the bound anions experienced huge lanthanide induced shifts to regions where background signals would not interfere.

The design of +1 and +2 systems coupled with the systematic modulation of the Ln^{3+} ion, may lead to complexes which are able to undergo fast exchange on the NMR

timescale with anions. For this purpose, the synthesis of the enantiopure heptadentate chelates based on ligand Li and Lj (Figure 2.32) have been designed.

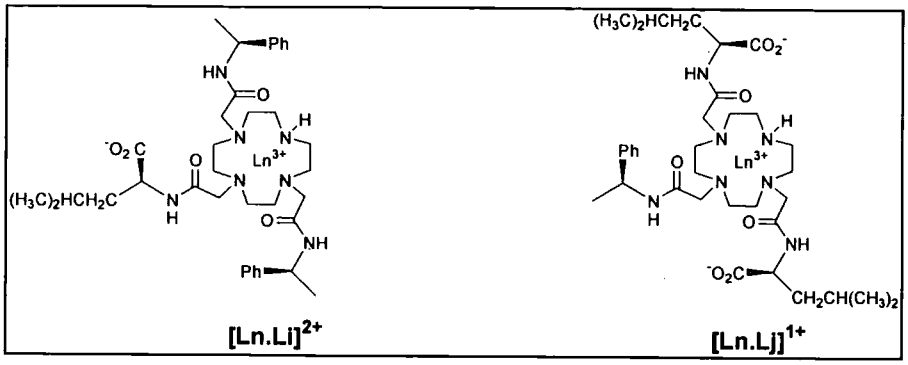

Figure 2.32 Structures of the chiral heptadentate $[Ln.Li]^{2+}$ and $[Ln.Ll]^{1+}$ complexes.

A possible common route for compound $[Ln.Li]^{2+}$ and $[Ln.Lj]^{1+}$ involves a protection-functionalization-deprotection methodology (Scheme 2.10) and the use of two different S-chiral chloroamides for the alkylating steps **2** and **4.**

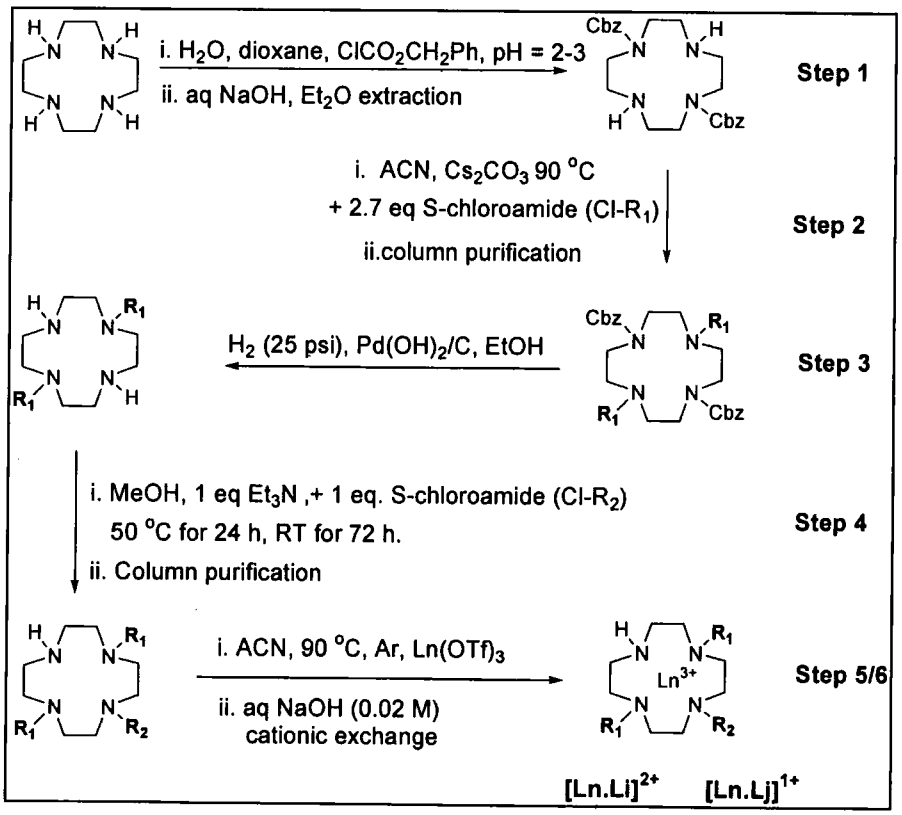

Scheme 2.10

This route has been attempted for the synthesis of $[Ln.Li]^{2+}$ (Appendix 1). The selective trans protection of the ring nitrogens in position 1 and 7 of cyclen, has been carried out by reacting 12N4 with benzoyl chloroformate, maintaining the pH between 2 and 3.[23] In this pH range, two of the ring nitrogens are protonated, and the remain two are free to react, giving the trans Cbz-diprotected product (step 1). The following alkylation and purification (step 2) led to a tetrasubstituted cyclen, which yielded the trans dialkylated product by reductive deprotection (step 3). The following monoalkylation (step 4) was performed at room temperature in methanol, following the addition of 1 equivalent of the second S-chloroamide ($Cl\text{-}R_2$) over 4 hours to the trans disubstituted cyclen, in the presence of 1 equivalent of triethylamine. The reaction was stirred at 50 °C for 24 h, then at RT for 72h, and followed by ES^+ which showed the presence of a mixture of starting material, tri-, and tetra-alkylated products. The purification of the cyclen derivative was difficult and, due to lack of time, the pure product was not separated successfully. Further studies need to be performed in order to gain suitable chromatographic conditions for such systems.

2.4 Luminescence Investigation of Lactate Binding

Lactate binding was also investigated through excited state lifetime measurements and emission studies using Tb^{3+} and Eu^{3+} complexes of ligands La, Lb, Lc, Ld, Le, Lf (Figure 2.2). The deactivation of the excited state of the Ln^{3+} ions can occur via energy transfer to the vibrational modes of C-H, N-H, and O-H oscillators within the bound ligand or solvent (1.4.4). The displacement of bound water molecules by anions leads to an enhancement of the metal based emission intensity and to an increase in the excited state lifetime ($\tau = 1/k$ ms). The efficiency of the direct excitation of the lanthanide is low but the presence of the phenyl group on the pendent arms of some these complexes enables sensitised emission (1.4.3) to be utilised.

2.4.1 Phenylalanine Systems

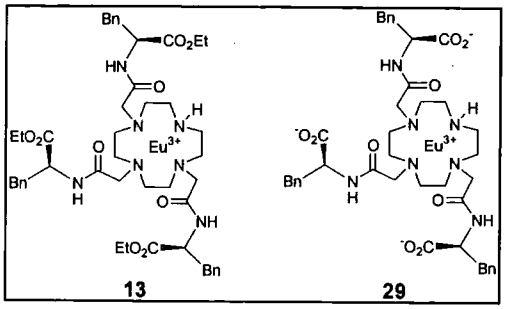

Figure 2.33 Structure of $[Eu.La]^{3+}$ **13** and [Eu.Lb] **29**.

Hydration State

The hydration states of the complexes **13** and **29** (Figure 2.33) were determined by measuring the rates of decay of the emissive state in H_2O/CH_3OH and D_2O/CD_3OD, before and after addition of a ten-fold excess lactate. Unfortunately, due to the presence of the two species in solution, the decay curves could not be fitted accurately and lifetime values were not obtained.

Emission Spectra

Owing to the large J values associated with the terbium energy levels, Tb^{3+} emission bands normally consist of a large number of transitions which are rarely fully resolved. By contrast, the absence of degeneracy of the emissive ^5D_o state of Eu^{3+} leads to relatively simple spectra which can be readily analysed. Thus, the emission spectrum for each Eu^{3+}complex was recorded in 0.1M MOPS buffer (0.25 mM complex, pH 7.4, 295 K) following excitation at 254 nm, in the absence and in the presence of a ten fold excess of added R or S lactate.

The emission spectrum of $[Eu.La]^{3+}$ **13** (Figure 2.34) exhibits the typical $\Delta J = 0$ to $\Delta J = 4$ transitions ($^5D_o \rightarrow {}^7F_j$). The $\Delta J = 0$ transition is unique for a given chemical environment, since both the initial (^7F_o) and the final states (^5D_o) are non degenerate.[24] The number of components observed for this transition is therefore related to the number of chemically distinct environments of the Eu^{3+} ion, thus this transition can be used to determine the number of different species in solution.

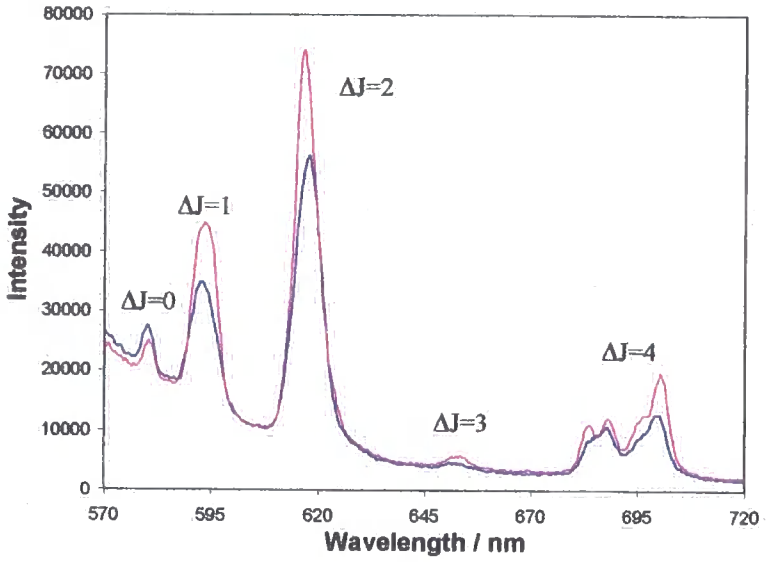

Figure 2.34 Emission spectra of $[Eu.La]^{3+}$ **13** (blue) and in presence of a 10 fold excess of added S-lactate (pink) (λ_{ex}= 254 nm, 0.25 mM, pH 7.4, 0.1 M MOPS, 295 K).

The ^{1}H NMR spectrum of $[Yb.La]^{3+}$ **12** showed the presence of a minor and a major species in solution. However, due to a lack of resolution, the $\Delta J = 0$ transition of **13** was not resolved into the expected two components. The $\Delta J = 1$ band is magnetic dipole allowed and is little affected by changes in the coordination environment. The complex does not possess axial symmetry thus three components should be present for this transition. However, a broad band at 595 nm was observed. The hypersensitive $\Delta J = 2$ transition, whose intensity is highly sensitive to the nature and the polarisability of the axial donor, also appeared as a broad band at 618 nm. The $\Delta J = 3$ was very weak and the $\Delta J = 4$, which as $\Delta J = 2$ is predominantly electric dipole in character thus highly sensitive to the ligand environment,[25] exhibited some fine structure at 689 nm and 701 nm respectively. Due to the presence of the two species in solution, much structural information was lost due to a broadening of the emission peaks and subsequent loss of resolution and fine structure.

Upon addition of a ten-fold excess of S-lactate to $[Eu.a]^{3+}$ **13**, an increase in the intensity and significant changes in the emission were observed (Figure 2.34 pink)

indicative of lactate binding. The diastereomeric R and S lactate bound complexes exhibited identical emission spectra.

Similar emission characteristics were observed for [Eu.Lb] **29** and the lactate adduct.

2.4.2 Leucine Systems

Hydration State of Tb^{3+} Complexes

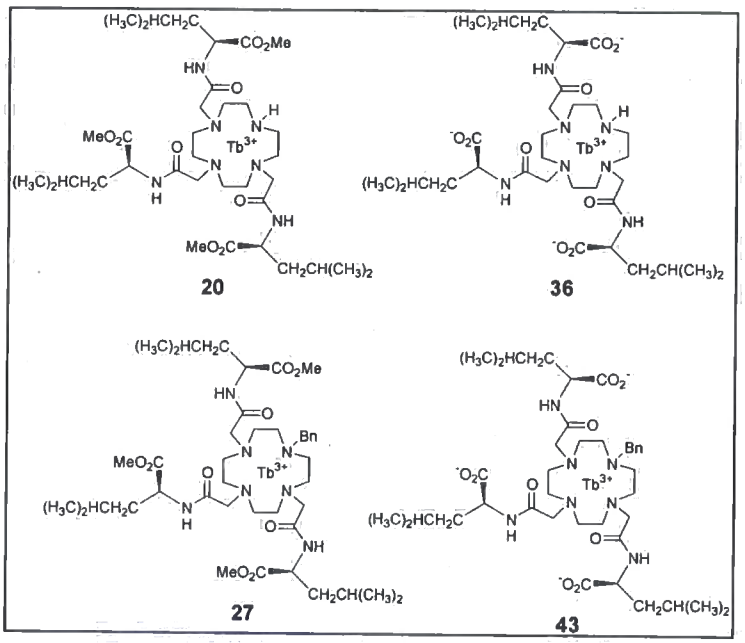

Figure 2.35 Structure of [Tb.Lc]$^{3+}$ **20**, [Tb.Ld] **36**, [Tb.Le]$^{3+}$ **27** and [Tb.Lf] **43**.

Following direct (**20**, **36**) or indirect (**27**, **43**) excitation, the luminescence emission decay rates of the Tb^{3+} complexes (Figure 2.35) were measured in H_2O and D_2O in the absence and presence of a ten-fold excess of S-lactate, by observing the intensity of luminescence after a range of delay times. These measurements allowed the estimation of q, the number of coordinated water molecules, according to equation 2.2:

$$q = A' (\Delta k_{corr}) \qquad \textbf{(2.2)}$$

$$q_{Tb} = 5 (k_{H2O} - k_{D2O} - 0.06)$$

where A' = 5 for Tb^{3+} and a correction to Δk has been made to account for the quenching effect of closely diffusing O-H (-0.06 ms^{-1}) oscillators (second sphere water molecules).[26] The lifetimes and the rate constants of decay for the excited state of the Tb^{3+}complexes **20**, **36**, **27**, **43** together with the estimated q values are reported in Table 2.10. The diastereomeric R-lactate Tb^{3+} complexes exhibited identical behaviour.

Complex/anion	τ_{H2O} ms	τ_{D2O} ms	k_{H2O} $(ms)^{-1}$	k_{D2O} $(ms)^{-1}$	q
20. [Tb.Lc]$^{3+}$	1.14	2.27	0.88	0.44	1.9
[Tb.Lc]$^{3+}$ + S-Lac	1.49	1.96	0.67	0.50	0.55
36. [Tb.Ld]	1.16	2.38	0.86	0.42	1.9
[Tb.Ld] + S-Lac	1.69	2.27	0.59	0.44	0.45
27. [Tb.Le]$^{3+}$	1.49	1.96	0.67	0.51	0.50
[Tb.Le]$^{3+}$ + S-Lac	2.00	2.32	0.50	0.43	0.30
43. [Tb.Lf]	1.51	2.38	0.66	0.42	0.90
[Tb.Lf] + S-Lac	1.85	2.5	0.54	0.40	0.40

Table 2.10 Effect of 10 fold added S-lactate on the lifetime and on the rate constant for depopulation of the excited state of Tb^{3+} complexes and derived hydration numbers, q, (λ_{ex} = 355 nm, 2.5 mM, 295 K, for [Tb.Lc]$^{3+}$, [Tb.Ld]; λ_{ex} = 254 nm, 0.25 mM, 295 K, for [Tb.Le]$^{3+}$, [Tb.Lf]).

The rates of luminescence emission decay were slower in D_2O than in H_2O due to the replacement of the O-H oscillators of the bound water by O-D oscillators, which are less effective quenchers, due to the poor Franck-Condon overlap. The rates of decay were also slower in the presence of lactate, indicative of displacement of the bound water molecules.

The [Tb.Lc]$^{3+}$ **20** and [Tb.Ld] **36** complexes were shown to possess two bound water molecules (q = 1.9). On addition of S-lactate, a hydration state of q = 0.55 and 0.45 was observed respectively, indicative of bidentate chelation of lactate (Figure 2.36) via displacement of the two bound water molecules.

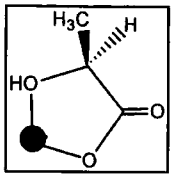

Figure 2.36 Structure of the ternary S-lactate complex.

The partial q values obtained for the complexes are due to the presence of the O-H oscillator of lactate which is close to the Ln^{3+} ion, and therefore will independently quench the excited state with approximately half the efficiency of a coordinated water molecule.[1]

Complexes $[Tb.Le]^{3+}$ **27** and [Tb.Lf] **43** are likely to be 8 coordinate, monoaqua systems (q value of 0.5 and 0.9 respectively) and this may be due to the hydrophobic and sterically demanding nature of the benzyl pendent arm, which prevents coordination of a second water molecule to the Ln^{3+} ion. Upon lactate addition, an increase in lifetime of the excited state of Tb^{3+} and a decrease of hydration state of the complexes (q = 0.3 and 0.4 respectively) were observed, thus confirming bidentate lactate binding, with displacement of the coordinated water molecule.

Emission Spectra

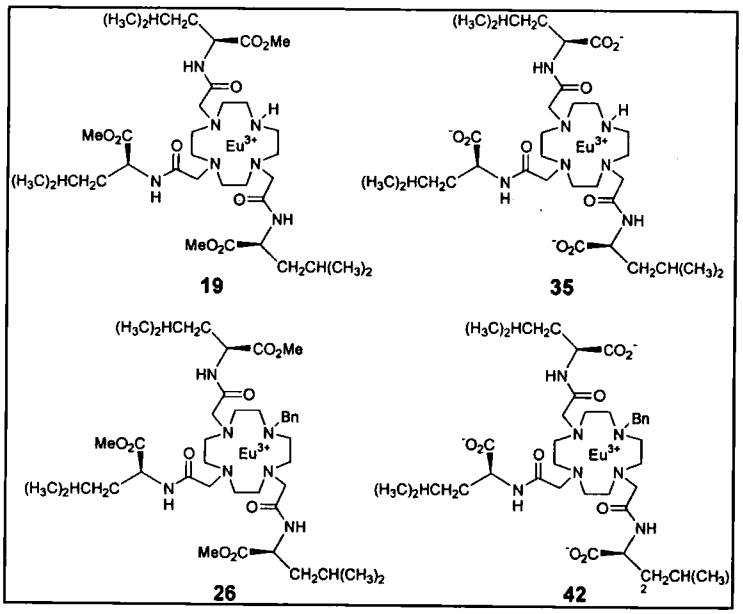

Figure 2.37 Structure of $[Eu.Lc]^{3+}$ **19**, [Eu.Ld] **35**, $[Eu.Le]^{3+}$ **26**, [Eu.Lf] **42**.

The Eu^{3+} emission spectra for complexes **19** and **35** (Figure 2.37) were recorded in 0.1 M MOPS buffer (2.5 mM complex, pH 7.4, 295 K) following direct excitation at λ_{ex} = 397 nm, in the absence and in the presence of excess added lactate (S or R) while indirect excitation (λ_{ex} = 254 nm) was employed for **26**, **42** (0.25 mM complex).

The emission spectra of the zwitterionic [Eu.Ld] **35** complex (Figure 2.38) showed a single band for the $\Delta J = 0$ (582 nm), consistent with the presence of a single diastereoisomer in solution and the $\Delta J = 3$ transition at 650 nm was always very weak.[27] Three components were observed in the $\Delta J = 1$ band, at 590, 592 and 595 nm, consistent with the absence of axial symmetry. The $\Delta J = 4$ manifold revealed some fine structure at 688, 695 and 698 nm and the hypersensitive $\Delta J = 2$ transition appeared as a single broad band at 614 nm.

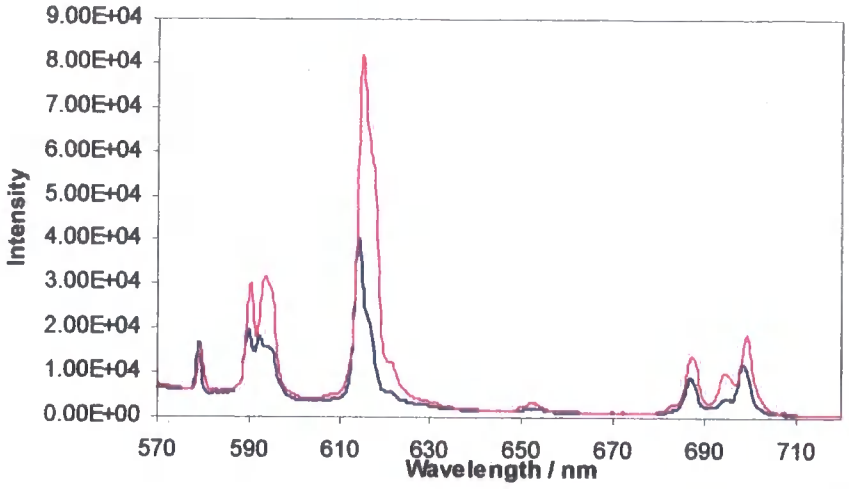

Figure 2.38 Emission spectra of the zwitterionic [Eu.Ld] **35** (blue) and in the presence of a 10 fold excess of S-lactate (pink) (λ_{ex}= 397 nm, 2.5 mM, pH 7.4, 0.1 M MOPS, 295 K).

On addition of S-lactate, an increase in the intensity of the metal based emission spectra was observed, consistent with the total displacement of the coordinated water molecules and the binding of the anion to the Eu^{3+} centre. The ratio of the $\Delta J = 2/\Delta J$

= 1 band intensities increased from 1.5 to 2.2 and the ΔJ = 1 band displayed a larger splitting, indicative of the nature of the more polarisable OH donor of lactate.[1,7] The emission spectrum of the diastereomeric R and the S lactate bound complexes exhibited identical characteristics.

Similar observations were made for $[Eu.Lc]^{3+}$ **19** which, on lactate addition, showed a significant increase in the emission spectral intensity and an increase in the intensity ratio of the ΔJ = 2/ΔJ = 1 from 1.64 to 2.25, consistent with the change in polarisability of the axial donor upon lactate chelation.

On addition of lactate to $[Eu.Le]^{3+}$ **26** a slight decrease in the emission intensity was actually observed. This may be due to the hydrophobic nature of the benzyl group leading to a longer bond between the coordinated water molecule and the Eu^{3+} centre, thus it is less effective at quenching the excited state. Indeed, the hydration state measurements (Table 2.10) of the diaqua Tb^{3+} complex were also consistent with a partial q value (0.5). Upon the addition of the anion, the long range water molecule is replaced with the OH of lactate, which must bind more closely to the Eu^{3+} centre in the formation of the 5-ring chelate thereby efficiently deactivating the excited state and giving rise to a slight decrease in the emission intensity of the complex.

On addition of S-lactate to [Eu.Lf] **42**, although an increase in emission intensity was observed, this increase was less than that exhibited by the N-H [Eu.Ld] derivative, consistent with the replacement of only one water molecule, compared to two with the latter.

Apparent Affinity Constant for S-Lactate Binding

The relative binding affinities of $[Eu.Lc]^{3+}$ **19**, [Eu.Ld] **35**, and [Eu.Lf] **42**, for S-lactate were measured by plotting the changes of intensity of the ΔJ = 2 transition (614 nm) as a function of the added anion concentration (1 mM complex (**19**, **35**) or 0.25 mM (**26**, **42**), in 0.1 M MOPS buffer, pH 7.4, 295 K). The resulting binding

isotherms (Figure 2.39, i.e. for **19**; spreadsheet of binding data in Appendix 2) were fitted to a 1:1 binding model by least-squares iterative analysis,[1] and binding affinities are reported in Table 2.11.

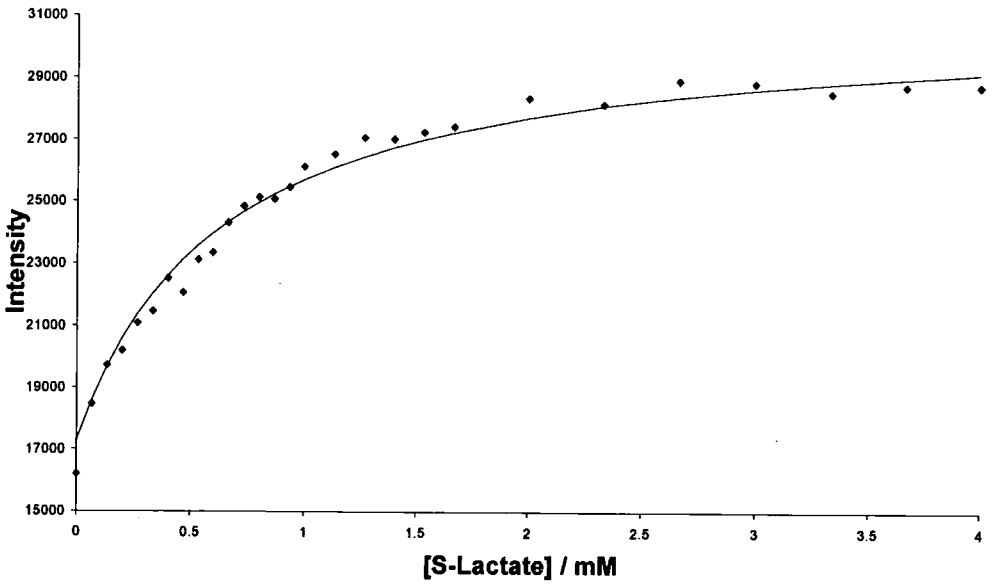

Figure 2.39 Variation of Eu^{3+} emission intensity (614 nm) for $[Eu.Lc]^{3+}$ **19** as a function of added S-lactate (1 mM complex, pH 7.4, 0.1 M MOPS, 295 K), showing the fit to the experimental data points.

Complex	Log K	K (mM^{-1})
19. $[Eu.Lc]^{3+}$	3.20	1.59
35. [Eu.Ld]	2.58	0.38
42. [Eu.Lf]	4.24	17.4

Table 2.11 Apparent S-lactate binding affinities for 1:1 complex formation (1 mM complex, pH 7.4, 0.1 M MOPS, 295 K).

The reduced affinity for S-lactate observed for the neutral complex **35** compared to the cationic complex **19** is consistent with the reduced coulombic attraction due to the electrostatic repulsion between the anion and the carboxylate of the pendent arms.

The N-alkylated [Eu.Lf] **42** system reported a higher apparent binding constant for S-lactate (log K = 4.24) than the N-H derivative [Eu.Ld] **35** (Table 2.11), which reflects the lesser degree of hydration around the anion binding site for the former and hence the greater overall free energy change accompanying the anion binding. The apparent lack of consistency with the results obtained by ^{1}H NMR investigation of the analogous [Yb.Lf] **41** complex (2.2.2), which appeared to exhibit a weaker affinity for lactate than the N-H derivative [Yb.Ld] **30**, can be explained by the different geometries adopted by the complexes in solution. The [Yb.Lf] **41** complex exists as two species in solution. The major TSAP isomer (3:1 TSAP: SAP) did not bind lactate, whereas the minor SAP species, in equilibrium with the TSAP, exhibited lactate binding. The ^{1}H NMR spectrum of the [Eu.Lf] **42** complex showed the presence of a single isomer in solution, whose shifts are indicative of a SAP conformation.[28] The SAP form appears to favour lactate binding, thus explaining the increase in affinity towards the anion observed in the Eu^{3+} binding experiment.

Conclusions

The displacement of up to two metal bound water molecules at the Ln^{3+} centre of the heptadentate complexes upon lactate addition, was signalled by an increase in the luminescence intensity (Eu^{3+}) or lifetime of the emissive state (Tb^{3+}). Upon lactate binding a change in the coordination environment of the complexes results, giving rise to a modulation in the form and intensity of the emission spectra and hydration states. An important probe of lactate binding is the relative intensity ratio of the $\Delta J = 2/\Delta J = 1$ transitions, being highly sensitive to the coordination environment and in particular, indicative of the nature of the axial donor.

2.5 Lactate Chelation Probed by Circular Dichroism

Circular dichroism associated with f-f transitions of lanthanide ions in a chiral environment is usually weak and therefore difficult to observe. However, the electronic properties of the unfilled f-shell of Yb^{3+} can be exploited because the

unique f-f transitions between the $^2F_{7/2} \rightarrow {}^2F_{5/2}$ states are magnetically-dipole allowed ($\Delta J = 1$) and are defined as "most CD sensitive".[29] The transitions between the $^2F_{7/2} \rightarrow {}^2F_{5/2}$ states are split by the crystal field into 4 and 3 doubly degenerate sublevels respectively. A temperature dependent Boltzmann distribution of the populations of the four states of the $^2F_{7/2}$ is expected, due to the small energy separation between the states of the lower term (of the order of 100 cm^{-1}). Thus, up to 12 transitions may be observed, centred around 980 nm (near IR-CD).[30] Circular dichroism associated with the chiral metal centres of $[Yb.Lc]^{3+}$ **14** and [Yb.Ld] **30** is sensitive to changes in the first coordination sphere and is therefore potentially responsive to lactate binding.[2]

The CD spectra of $[Yb.Lc]^{3+}$ **14** and [Yb.Ld] **30** (Figure 2.40) were recorded before and after the addition of a ten-fold excess of S-lactate (10 mM and 20 mM complex respectively, 0.1 M MOPS, pH 7.4, 295 K).

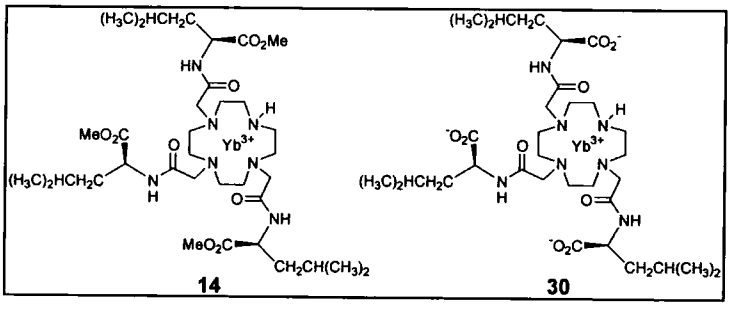

Figure 2.40 Structure of $[Yb.Lc]^{3+}$ **14**, [Yb.Ld] **30**.

The CD spectrum of the diaqua [Yb.Ld] exhibited three peaks at 966 nm, 978 nm and 989 nm respectively (Figure 2.41). On addition of a ten-fold excess of S-lactate the peak at 966 nm was shifted to longer wavelength (973 nm) and displayed a 35% decrease in intensity, the peak at 978 nm disappeared and the one at 989 nm shifted to 987 nm and increased in intensity by 52%. The observed modifications in the CD spectrum are due to the changing nature of the donor atom, going from a neutral water molecule to the charged lactate carboxylate, which affects the electronic properties of the Ln^{3+} ion by modulation of the crystal field splitting.

Similar observations were recorded for the cationic analogue $[Yb.Lc]^{3+}$.

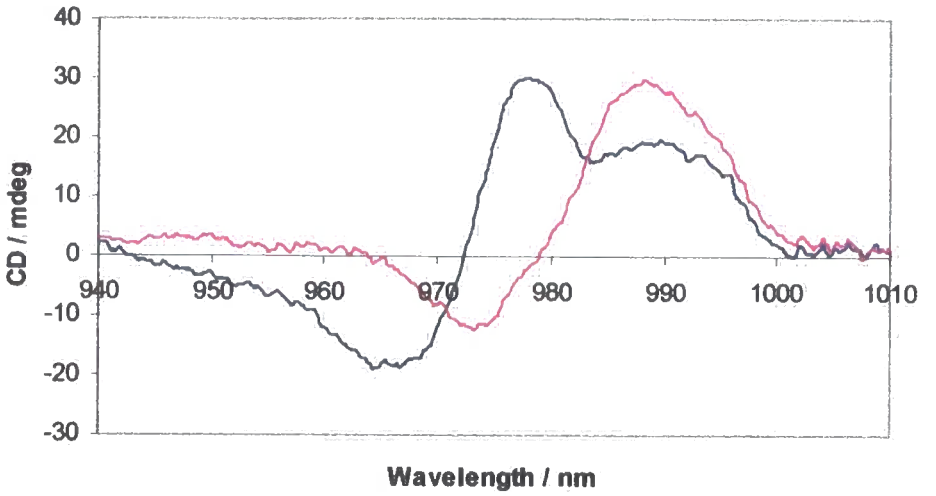

Figure 2.41 Near-IR CD spectra of [Yb.Ld] (blue) and in the presence of 10 equivalents of S-lactate (pink) (20 mM complex, 0.1 M MOPS, pH 7.4, 295 K).

Conclusions

The local coordination environment about the lanthanide centre may be probed by NIR-CD of the Yb^{3+} complexes. Changes in the shape, shifts and intensity of the peaks were observed for both complexes upon the addition of a ten-fold excess of S–lactate. These spectral modifications are consistent with changes in the primary coordination sphere of the Yb^{3+} ion and are indicative of the bidentate binding of lactate to the metal centre.

2.6 Overall Conclusions

In the search for potential NMR shift reagents for lactate, a variety of heptadentate Ln^{3+} complexes have been synthesised and assessed. In order to achieve the required conditions of fast exchange on the NMR timescale, the binding affinity and selectivity for lactate has been modulated by variation of the Ln^{3+} ion and the ligand structure, in particular the peripheral electrostatic charge of the complex and local charge and steric demand at the metal centre. The binding has been effectively

signalled by ^{1}H NMR, emission, hydration states studies and circular dichroism. Only in the $[Pr.Lc]^{3+}$ complex fast exchange conditions with lactate were observed. However, due to the small spectral range and severe line broadening experienced, such complex is unsuitable as shift reagent.

The leucine cationic $[Ln.Lc]^{3+}$ and neutral [Ln.Ld] complexes existed as one species in aqueous solution. The Yb^{3+} complexes exhibited the best compromise between a large lanthanide induced shift and relatively small degree of line broadening. The bound lactate resonances were well resolved and exhibited large lanthanide induced shifts to regions in the spectrum where background resonances would not interfere. Although such complexes are not suitable as shift and relaxation agents for MRS (slow exchange on the NMR timescale), they show great promise as effective NMR, luminescent and chiroptical probes for lactate and for a number of other bioactive species, as reported in chapter 3.

References

1. J. I. Bruce, R. S. Dickins, L. J. Govenlock, T. Gunnlaugsson, S. Lopinski, M. P. Lowe, D. Parker, R. D. Peacock, J. J. B. Perry, S. Aime, and M. Botta, *J. Am. Chem. Soc.*, 2000, **122**, 9674-9684.
2. R. S. Dickins, S. Aime, A. S. Batsanov, A. Beeby, M. Botta, J. I. Bruce, J. A. K. Howard, C. S. Love, D. Parker, R. D. Peacock, and H. Puschmann, *J. Am. Chem. Soc.*, 2002, **124**, 12697.
3. R. S.Dickins, C. S. Love, H. Puschmann, *Chem. Commun.* 2001, **22**, 2308.
4. F. Boschetti, F. Denat, E. Espinosa, and R. Guilard, *Chem. Commun.*, 2002, **4**, 312.
5. K. P. Pulukkody, T. J. Norman, D. Parker, L. Royle, C. J. Broan, *J. Chem. Soc., Perkin Trans. 2,* 1993, 605.
6. S. Aime, M. Botta, and G. Ermondi, *Inorg. Chem.*, 1992, **31**, 4291.
7. R. S. Dickins, D. Parker, J. I. Bruce, and D. J. Tozer, *Dalton Trans.*, 2003, **7**, 1264.
8. R. S. Dickins, J. A. K. Howard, C. L. Maupin, J. M. Moloney, D. Parker, J. P. Riehl, G. Siligardi, and J. A. G. Williams, *Chem. Eur. J.*, 1999, **5**, 1095.
9. J. A. Peters, J. Husken, and D. J. Raber, *Prog. Nucl. Magn. Reson. Spectrosc.*, 1996, **28**, 283.
10. S. Aime, A. S. Basanov, M. Botta, R. S. Dickins, S. Faulkner, C. E. Foster, A. Harrison, J. A. K. Howard, J. M. Moloney, T. J. Norman, D. Parker, L. Royle, and J. A. G. Williams, *J. Chem. Soc., Dalton Trans.*, 1997, 3623.
11. S. I. Hang, R. S. Ranganathan, J. E. Emswiler, K. Kumar, J. Z. Gougoutas, M. F. Malley, and M. F. Tweedle, *Inorg. Chem.*, 1993, **32**, 2912.
12. G. Lowe, and T. Vilaivan, *J. Chem. Soc., Perkin Trans. 1,* 1997, 539.
13. L. Flore-Santos, E. Martin, M. Dieguez, A. M. Masdeu-Bulto, and C. Claver, *Tetrahedron: Asymmetry,* 2001, **12**, 3029.
14. D. Tanner, *Angew. Chem., Int. Ed. Engl.*, 1994, **33**, 599.
15. K-D. Lee, J-M. Suh, J-H. Park, H-J. Ha, H. G. Choi, C. S. Park, J. W. Chang, W. K. Lee, Y. Dong, and H. Yun, *Tetrahedron*, 2001, **57**, 8267.
16. D. A. Alonso, and P. G. Andersson, *J. Org. Chem.*,1998, **63**, 9455.
17. I. Wilson, and R. F. W. Jackson, *J. Chem. Soc., Perkin Trans. 1,* 2002, 2845.
18. S. Aime, M. Botta, V. Mainero, and E. Terreno, *Magn. Reson. Med.*, 2002, **47**, 10.
19. B. J. Bleaney, *J. Magn. Reson.*, 1972, **8**, 91.
20. R. M. Golding, and M. P. Halton, *Aust. J. Chem.*, 1972, **25**, 2577.
21. C. F. G. C. Geraldes, S. Zhanrong, and A. D. Sherry, *Inorg. Chim. Acta,* 2004, **357**, 381.
22. P. F. Daly, R. C. Lyon, P. J. Faustino, and J. S. Cohen, *J. Biol. Chem.*, 1987, **262**, 14875.
23. Z. Kovacs, and A. D. Sherry, *Synthesis*, 1997, 759.
24. D. Parker, and J. A. G. Williams, *J. Chem. Soc., Dalton Trans.*,1996, 3613.
25. M. F. Reid, and F. S. Richardson, *J. Phys. Chem.*, 1984, **88**, 3579.
26. A. Beeby, I. M. Clarkson, R. S. Dickins, S. Faulkner, D. Parker, L. Royle, A. S. de Sousa, J. A. G. Williams, and M. Woods, *J. Chem. Soc., Perkin Trans. 2,* 1999, 493.

27. F. S. Richardson, *Chem. Rev.*, 1982, **82**, 541.
28. M. P. M. Marques, C. F. G. C. Geraldes, A. D. Sherry, A. E. Merbach, H. Powell, D. Pubanz, S. Aime, and M. Botta, *J. Alloys Compd.*, 1995, **225**, 303.
29. F. S. Richardson, *Inorg. Chem.*, 1980, **19**, 2806.
30. L. Di Bari, G. Pintacuda, P. Salvadori, R. S. Dickins, and D. Parker, *J. Am. Chem. Soc.*, 2000, **122**, 9257.

CHAPTER 3

Signalling Anion Binding with Chiral Lanthanide Complexes

3.1 Anion Recognition

3.1.1 Introduction and Background

The selective recognition of anions by synthetic receptors constitutes an important element of supramolecular chemistry.[1] This is due to the fact that anions have widespread roles in the areas of medicine, catalysis, and environmental chemistry and are ubiquitous throughout biological systems.[2] For example, the polyanionic DNA, which carries the genetic information, is present in the nucleus of eukaryotic cells[3] and the majority of enzyme substrates and co-factors are anionic (i.e. the zinc containing carbonic anhydrase requires a metal ion-bound hydroxyl group to promote its activity).[4]

Despite the importance of anion recognition in biological systems, the majority of work with synthetic receptors has been concentrated on their behaviour in nonaqueous solvents. This is due to a number of reasons but primarily to the large free energies of hydration of anions, ΔG_{hyd}, (i.e. HCO_3^-, -335 kJ mol^{-1}; $H_2PO_4^-$, -465 kJ mol^{-1}; CO_3^{2-}, -1315 kJ mol^{-1}).[5] Thus, the design of suitable receptors for bioactive anionic species in physiological media, should take into account the need for a large electrostatic contribution to the binding, which is required to compensate for the endothermic desolvation of the anion. This can be achieved by using a positively charged receptor or a system that employs a combination of hydrogen bonds and electrostatic interactions.[6] Moreover, anions possess a wide range of geometries (spherical, linear, trigonal planar, tetrahedral, octahedral) and often exhibit pH-dependent speciation, becoming protonated at low pH and losing their charge. As a result, complementary of shape and size between the receptor and the anion is crucial in determining selectivity and the receptor must function within the pH window of the target anion.

The complexation of the anionic guest may arise through a variety of non-covalent interactions, such as electrostatic, hydrophobic, and hydrogen bonding interactions or *via* coordination to a metal ion, which may also be combined to produce highly

selective receptors.[2] For example, synthetic receptors for aqueous media, such as the cationic and neutral macrotricyclic quaternary ammonium hosts (Figure 3.1 a and b respectively), have been reported to form electrostatic based complexes with a variety of anions (i.e. halides), which are encapsulated within the macrotricycle.[7,8] Other reports of the binding interaction between a host and an anionic guest in aqueous solution, showed that the inclusion of a series of naphthalenesulfonates by β-cyclodextrins,[9] was primarily due to the hydrophobic effect, with the naphthalene residue displacing the water molecules from the internal cavity of the cyclodextrin. The negatively charged sulfonate group remained outside the cavity, in contact with the aqueous solvent, thereby apparently controlling the orientation of the naphthalene group within the cavity. In organic media, receptors containing the urea (Figure 3.1 c)[10] or thiourea groups, which are good hydrogen bond donors, showed effective bidentate chelation of Y-shaped anions such as carboxylate, through the formation of two hydrogen bonds. The key role played by hydrogen bonds in the host-guest interaction, is primarily due to directionality, which allows the design of receptors with specific shapes that are able to differentiate between anions with different geometries or hydrogen bonding requirements in non-polar solvents. The combination of electrostatic interactions with directional hydrogen bonds produces very effective receptors for anions as, for example, has been reported for several macrobicyclic ammonium cages (Figure 3.1 d), that coordinate to halide ions,[11] or for bicyclic guanidium based receptors[12] (Figure 3.1 e), which bind to carboxylate or phosphate. Electron deficient Lewis acidic centres are able to bind to anions by orbital overlap, which leads to a bonding interaction. This has resulted in the development of many new chelating and macrocyclic hosts for anions, containing atoms such as boron (Figure 3.1 f), and tin (Figure 3.1 g), which form complexes with chloride ions in acetonitrile solution. Lanthanide ions (i.e. Yb^{3+}, Eu^{3+}) are also effective Lewis acidic centres for anion binding, and complexes of them have been widely explored in the last twenty years, owing to their important spectral and magnetic properties.[13]

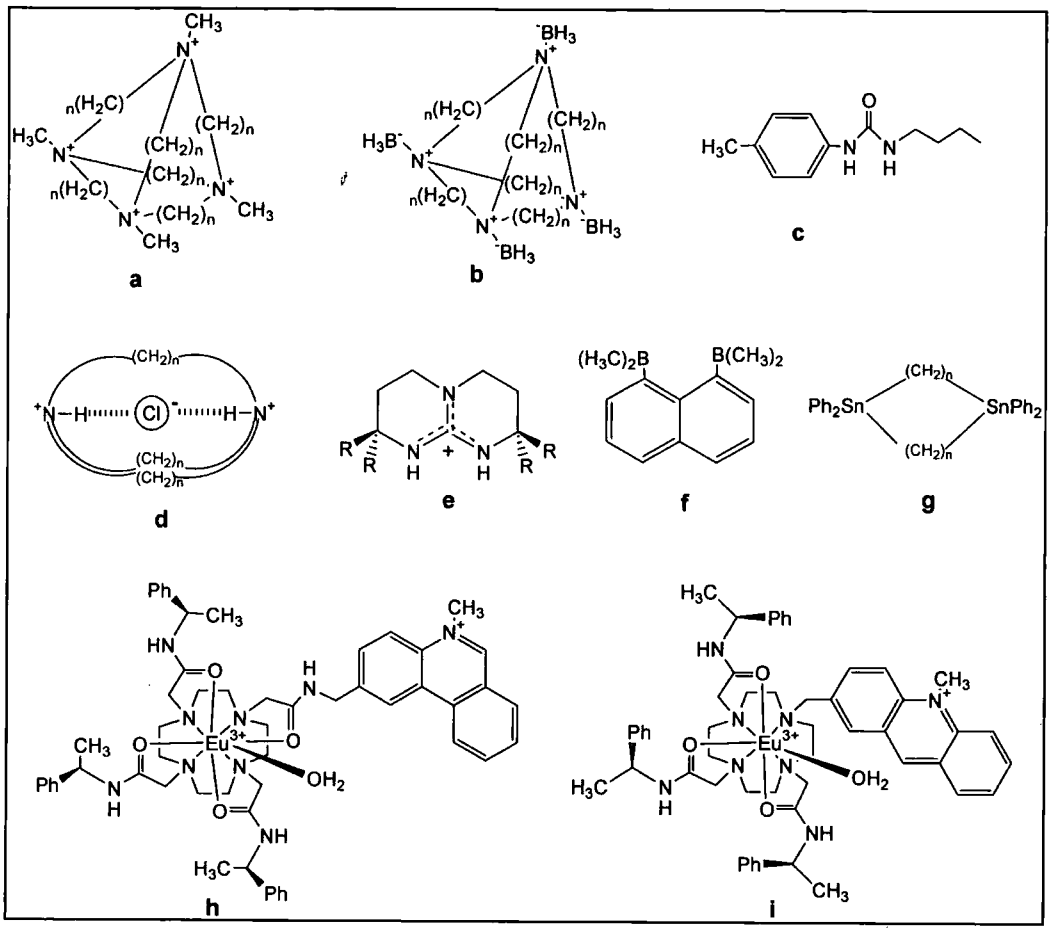

Figure 3.1 Examples of some anion receptors.

Any recognition process (i.e. the anion binding) requires a signal transduction which should correspond to the modulation of a measurable parameter. Magnetic resonance measurements, despite giving rise to significant structural information, can be rather insensitive, thus an increased interest has arisen towards the development of electrochemical and optical methods.[14] Electrochemical methods involving the measurement of a change in emf (potentiometry) or current (amperometry) upon anion binding, require careful calibration and possess slow response times. However, optical methods are fast and highly sensitive and have found widespread application in biological and clinical fields (1.4.5) for the detection and monitoring of a range of chemical species (i.e. cations or bioactive molecules). Examples of luminescent systems for signalling anion binding in aqueous media are the Tb^{3+} and Eu^{3+} cyclen-based complexes, bearing a pendent phenanthridinium or acridone moiety (Figure

3.1 h and i respectively). Such compounds have been reported to act as luminescent probes for halides,[15] and hydrogencarbonate[16] respectively. Chiroptical techniques may also be employed to monitor anion binding. For example, the observation of changes in the circular dichroism of lanthanide porphyrinates upon binding to neutral or zwitterionic guests (i.e. amino acids) have been reported.[17] Similarly anion binding to a series of chiral Eu^{3+} complexes has been effectively signalled by monitoring changes in the form and polarization of the circularly polarized luminescence.[18]

3.1.2 Signalling Reversible Anion Binding at Ln(III) Centres

The ability of the Ln^{3+} ions to exhibit high coordination numbers (8/9) allows much scope for the design of anion receptors wherein the affinity and selectivity may be modulated by suitable choice of the ligand and lanthanide ion. In the search for appropriate synthetic receptors for signalling anion binding in aqueous media, two classes of complexes of lanthanide ions have been defined. The first includes enantiopure, cationic, octa- or nonadentate macrocyclic cyclen based systems, bearing a pendent phenanthridinium group (Figure 3.1 h) for example, which have been shown to interact with oligonucleotides and DNA, with a selectivity depending on the complex helicity and the base-pair composition.[19] The second class is related to macrocyclic, chiral, heptadentate ligands (i.e. DO3Ph), which have been reported to form relatively stable, well-defined 1:1 ML complexes in aqueous solution with a variety of chelating (i.e. lactate, HCO_3^-) or monodentate (i.e. HPO_4^-) anions (Figure 3.2)[18,20] by displacement of the coordinated water molecules. The magnetic and optical properties exhibited by the Ln^{3+} ions allow structural information of the ML adducts to be gleaned and the anion binding may be effectively signalled by NMR (Yb^{3+}, Eu^{3+}), luminescence (Eu^{3+}, Tb^{3+}, Yb^{3+}) and chiroptical techniques (Yb^{3+}, Eu^{3+}).

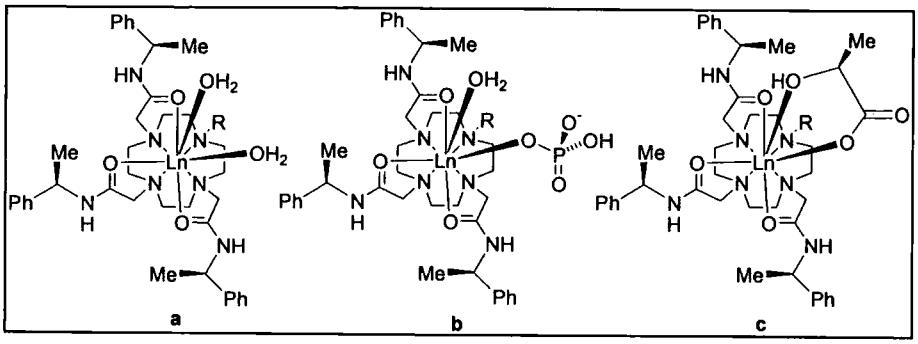

Figure 3.2 Chiral heptadentate Ln^{3+} complexes as diaqua species (a), phosphoadduct (b), and showing bidentate chelation of lactate (c).

Most of the studies performed on such systems have been focused on complexes of Yb^{3+} and Eu^{3+}. The choice of Yb^{3+} has been determined by its high charge density, which enhances the affinity towards anions, and also the angular and distance information provided by the LIS, which is dipolar in nature.[21,22] Furthermore, the analysis of the shift, which is determined to a considerable extent by the polarisability of the axial donor ligand, gives information on the nature of the complex-anion adduct in solution.[23,24] The chiral Yb^{3+} complexes are also amenable to study by circular dichroism spectroscopy, due to the magnetically-dipole allowed $^2F_{7/2} \rightarrow {}^2F_{5/2}$ transitions[25] (around 980 nm) which are very sensitive to the nature of the axial donor.[18,26]

The selection of the Eu^{3+} complexes for study has been dictated by the favourable spectroscopic characteristics of this lanthanide ion. In fact the emissive $^5D_0$ excited state for Eu^{3+} is non-degenerate, hence relatively simple emission spectra arise from the $^5D_0 \rightarrow {}^7F_j$ transitions.[27] Moreover, the magnetic dipole allowed $^5D_0 \rightarrow {}^7F_1$ transition, whose intensity is relatively independent of the Eu^{3+} coordination environment, shows a splitting of the components of its manifold which is sensitive to the local symmetry at the metal centre and, in axial symmetry, is directly proportional to the second order crystal field parameter, $\langle r^2 \rangle A_2^o$.[28,29] Finally, the electric dipole allowed $\Delta J = 2$ and $\Delta J = 4$ transitions are hypersensitive[30] and

perturbed significantly by variations in the polarisability of the ligand donors, and the ratio of the emission intensity for the $\Delta J = 2/\Delta J = 1$ spectral bands is a useful parameter to assess changes in the Eu^{3+} coordination environment.[31]

In Bleaney's theory of magnetic anisotropy[21] (2.3.1), the second order crystal field parameter $\langle r^2 \rangle A_2^0$ is predicted to determine the dipolar ^1H NMR shift of the paramagnetic Ln^{3+} complexes in solution (equation 3.1). Studies undertaken on a series of Yb^{3+} and Eu^{3+} eight- and nine-coordinate axially symmetric complexes based on cyclen (i.e. DOTA, DOTAMPh, Figure 2.9) showed that the second order crystal field coefficient $\langle r^2 \rangle A_2^0$, whose relative magnitude has been assessed by measuring the $\Delta J = 1$ splitting in the Eu^{3+} emission bands, not only determines the dipolar shift of such systems but also the sign and the magnitude of a major CD band in the near-IR-CD spectra of a series of enantiopure Yb^{3+} complexes.[26] Hence, the nature and the local symmetry of the Ln^{3+} coordination environment has been reported to determine the optical and NMR spectral properties of the paramagnetic Ln^{3+} complexes.[32]

$$\Delta_P = D\langle r^2 \rangle A_2^0 G = C_j \frac{\beta^2}{60k^2T^2} \cdot \frac{\langle r^2 \rangle A_2^0 (3\cos^2\theta - 1)}{r^3} \qquad \textbf{(3.1)}$$

3.2 Chiral Lanthanide(III) Complexes as Probes for Anions

The enantiopure, heptadentate Ln^{3+} complexes discussed in chapter 2 ($[Ln.Lc]^{3+}$, [Ln.Ld], $[Ln.Le]^{3+}$ and [Ln.Lf]) have been shown to bind effectively to lactate. With the aim of investigating the potential of such complexes to act as NMR, luminescent and CD probes for other bioactive species, the study of the reversible binding of common oxyanions in aqueous solution to the neutral and cationic leucine systems was undertaken.

3.2.1 Neutral Leucine Complexes

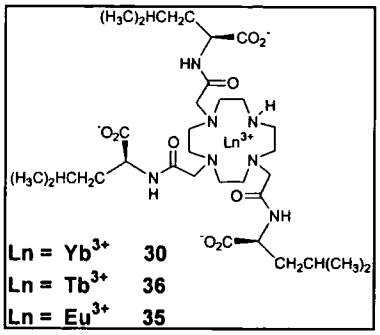

Figure 3.3 Structure of [Yb.Ld] **30**, [Tb.Ld] **36**, [Eu.Ld] **35**.

^1H NMR

The ^{1}H NMR spectra of a 10 mM solution of [Yb.Ld] **30** (Figure 3.3) were recorded in the presence of a ten-fold excess of a series of oxyanions ($4.5 < pD < 9$). The partial ^{1}H NMR spectra of the [Yb.Ld] adducts, in the high frequency region (Figure 3.4 and 3.5), illustrate the presence of only one species in solution, and the sensitivity of the overall paramagnetic shift to the nature of the added anion.

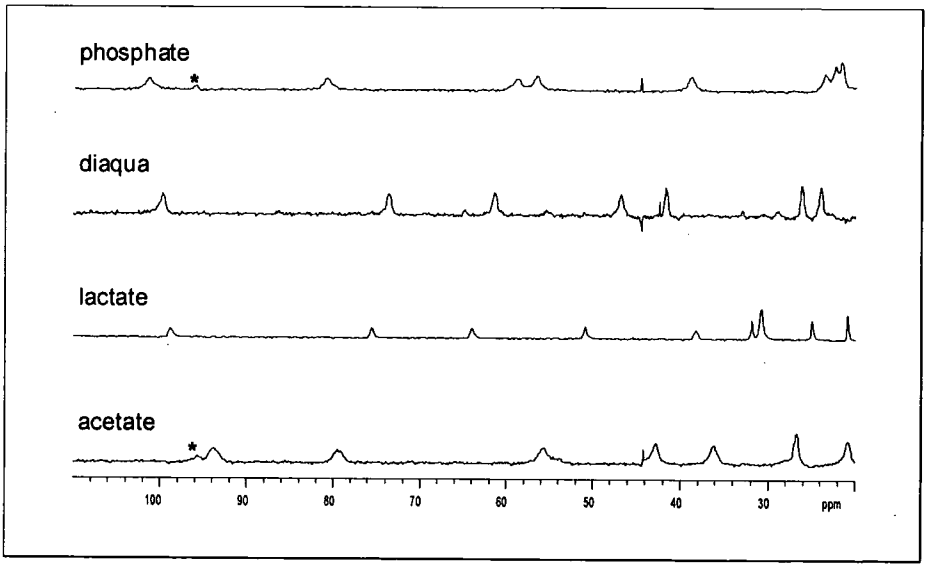

Figure 3.4 Partial ^{1}H NMR spectra for complexes of [Yb.Ld] **30** (10 mM) with the following added anions (ten-fold excess): HPO_4^- (pD 8.7); water (pD 4.4, spectrum of the 1 mM solution); lactate (pD 6.2); acetate (pD 6.6); (200 MHz, D_2O, 295 K). *Impurity of the tetraalkylated complex (< 5%).

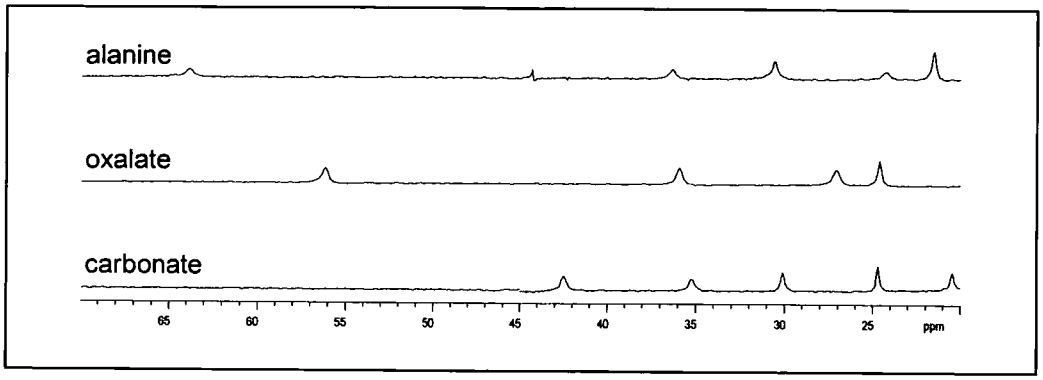

Figure 3.5 Partial ^{1}H NMR spectra for complexes of [Yb.Ld] **30** (10 mM) with the following added anions (ten-fold excess): alanine (pD 7.8); oxalate (pD 6.1); carbonate (pD 8.3); (200 MHz, D_2O, 295 K).

The values of the mean chemical shift of the four most shifted axial ring protons (H_{ax}) in each of the [Yb.Ld]-anion adducts, reveal a strong dependence on the nature of the donor atom located in the axial position (Table 3.1).

[Yb.Ld] + Anion	Axial donor	pD	Shift range (ppm)	Mean Shift δH_{ax}[a] (ppm)
S-OP-serine	H_2O	8.1	+110 → -83	82
phosphate	H_2O	8.8	+102 → -77	75
water	H_2O	4.4	+100 → -120	70
S-lactate	OH	6.2	+99 → -56	72
acetate	$CO^{\delta-}$	6.6	+93 → -94	68
citrate[b]	$CO^{\delta-}$	7.6	+89 → -100	64
S-serine	NH_2	7.8	+68 → -50	43
S-alanine	NH_2	7.8	+65 → -43	40
oxalate	CO^-	6.1	+56 → -31	36
carbonate	CO^-	8.3	+45 → -44	33

Table 3.1 Effect of the axial donor on the ^{1}H NMR spectral range observed for [Yb.Ld] **30** (200 MHz, D_2O, 295 K). [a]Mean chemical shift of the four most shifted axial protons of the 12N4 ring. [b]Minor species < 10%, due to the additional binding modes possible for the anion.

The more polarisable donors (i.e. carbonate > oxalate > alanine) give rise to the smallest shifts, whereas the hard uncharged axial donor oxygens in the lactate, aqua and hydrogen phosphate complexes give rise to the largest paramagnetic shifts. It is actually the polarisability of the axial donor which affects the second order crystal field coefficient $\langle r^2 \rangle A_2^0$ and hence determines the magnitude of the observed dipolar shift (equation 3.1).[21,26]

Recently, such correlations have been exploited to determine the binding modes of chiral heptadentate complexes (e.g. (RRR)-[Yb.DO3Ph]$^{2+}$, Figure 3.2 a) with a variety of anions, and the chelation modes reported were confirmed by X-ray crystallography and emission spectroscopy studies.[20] By adopting a similar correlation between the chemical shift and the polarisability of the axial donor, an interpretation of the ^{1}H NMR data of the [Yb.Ld]-anion adducts (Table 3.1), has been undertaken. For example, the observed chemical shift range of the acetate adduct (+93 → -94) is indicative of bidentate chelation through the C-terminal carboxylate oxygens, whereas the spectral range observed for alanine (+65 → -43) is consistent with a chelated structure involving the more polarisable amine (NH_2) in the axial position and the charged oxygen of the carboxylate equatorially disposed. This binding mode, favouring a 5-ring chelate, is consistent with the results of an extended study undertaken on each of the amino acid adducts with [Yb.DO3Ph]$^{3+}$.[33] The similar chemical shift values observed for the most shifted axial ring proton of the phosphate adduct compared to the diaqua complex (c.f. +102 vs +100 respectively), suggests that the phosphate is likely to bind in a monodentate manner, with the phosphate oxygen in the equatorial position, and the hard water oxygen donor binding axially. The spectral range of the phosphorylated amino acids (e.g. S-OP-serine: +110 → -83), at physiological pH, suggests that the ligation of the phosphate moiety in the equatorial position, is favoured over the amino acid chelation, which would give rise to a smaller shift range (c.f. S-serine: +68 → -50). Some of the structures of the anion adducts are depicted in Figure 3.6.

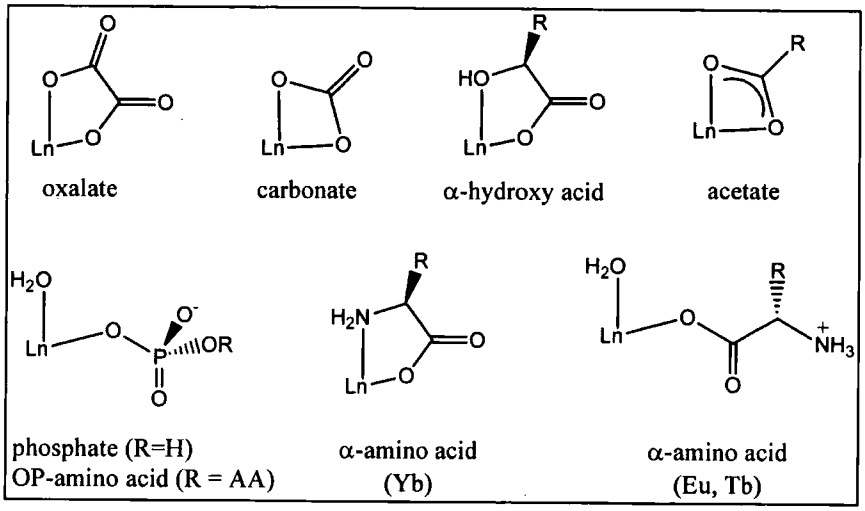

Figure 3.6 General structures of some of the anion adducts, established by ^{1}H NMR, emission spectroscopy and X-ray crystallography.[20,33]

Hydration States

With the aim of confirming the binding modes described above, the solution hydration states of [Tb.Ld] **36** and some of its anion adducts, were determined using the luminescence method[34] discussed in chapter 1 and 2 (1.4.4, 2.4.2). The results, reported in Table 3.2, showed that the [Tb.Ld] complex is coordinated to two water molecules (q = 2), which are replaced by the bidentate chelation of lactate (the partial q = 0.45 is due to the presence of the single O-H oscillator of lactate) (2.4.2).

[Tb.Ld] + Anion	pH	τ_{H2O} ms	τ_{D2O} ms	k_{H2O} $(ms)^{-1}$	k_{D2O} $(ms)^{-1}$	q
water	4.7	1.16	2.38	0.86	0.42	1.9
S-lactate	6.2	1.69	2.27	0.59	0.44	0.45
S-alanine	4.8	1.19	2.27	0.84	0.44	1.7
S-alanine	7.4	1.33	2.08	0.75	0.48	1.0

Table 3.2 Effect of a ten-fold excess of added anions on the lifetime and on the rate constant for depopulation of the excited state of [Tb.Ld] **36**, and derived hydration numbers, q, (λ_{ex} = 355 nm, 2.5 mM, 295 K).

The value of the hydration number of the adduct with S-alanine appeared to be pH dependent. At pH 7.4, the amino acid is in a zwitterionic form and is likely to bind to [Tb.Ld] in a monodentate manner (q = 1.0), by replacing the coordinated water molecule in the equatorial position with the charged oxygen of the carboxylate group (Figure 3.6). However, ^{1}H NMR studies suggested that the [Yb.Ld] complex binds to the amino acids in a bidentate manner, which is a consequence of the higher charge density of the Yb^{3+} ion, in comparison to Tb^{3+}, which results in a higher affinity towards the amino acids.[18] At pH 4.5, [Tb.Ld] did not bind to S-alanine (q = 1.7) due to protonation of both the carboxylate and the amino groups of the amino acid, giving rise to an overall positively charged alanine, which repels the tripositive core (Tb^{3+}). This is consistent with the ^{1}H NMR studies on [Yb.Ld] with amino acids, that showed only exchanged broadened spectra corresponding to the diaqua complex at pD< 6.

Emission Spectroscopy

With the aim of investigating the effect of added anions on the emission characteristics of [Eu.Ld] **35**, a ten-fold excess of a range of anions was added to a solution of the complex (2.5 mM, in 0.1 M MOPS buffer, pH 7.4) and the emission spectra were recorded (λ_{ex} = 397 nm, 295 K) (Figure 3.7).

Upon addition of all the anions, an increase in the intensity of emission was observed, consistent with the displacement of up to two bound water molecules. A relatively lower increase in the overall intensity was observed in the presence of the amino acids or phospho compounds, consistent with the replacement of only one of the two bound water molecules (monodentate ligation), compared to the emission spectra of [Eu.Ld] in the presence of the chelating anions (i.e. hydroxy acids, carbonate). Furthermore, changes in the splitting of the $\Delta J = 1$ manifold (sensitive to the local symmetry at the metal centre), in the fine structure of the hypersensitive $\Delta J = 4$ band and in the ratio of the $\Delta J = 2/ \Delta J = 1$ band intensity were observed (Figure 3.7). Similar emission spectra were recorded for [Eu.Ld] in the presence of the corresponding R-anions.

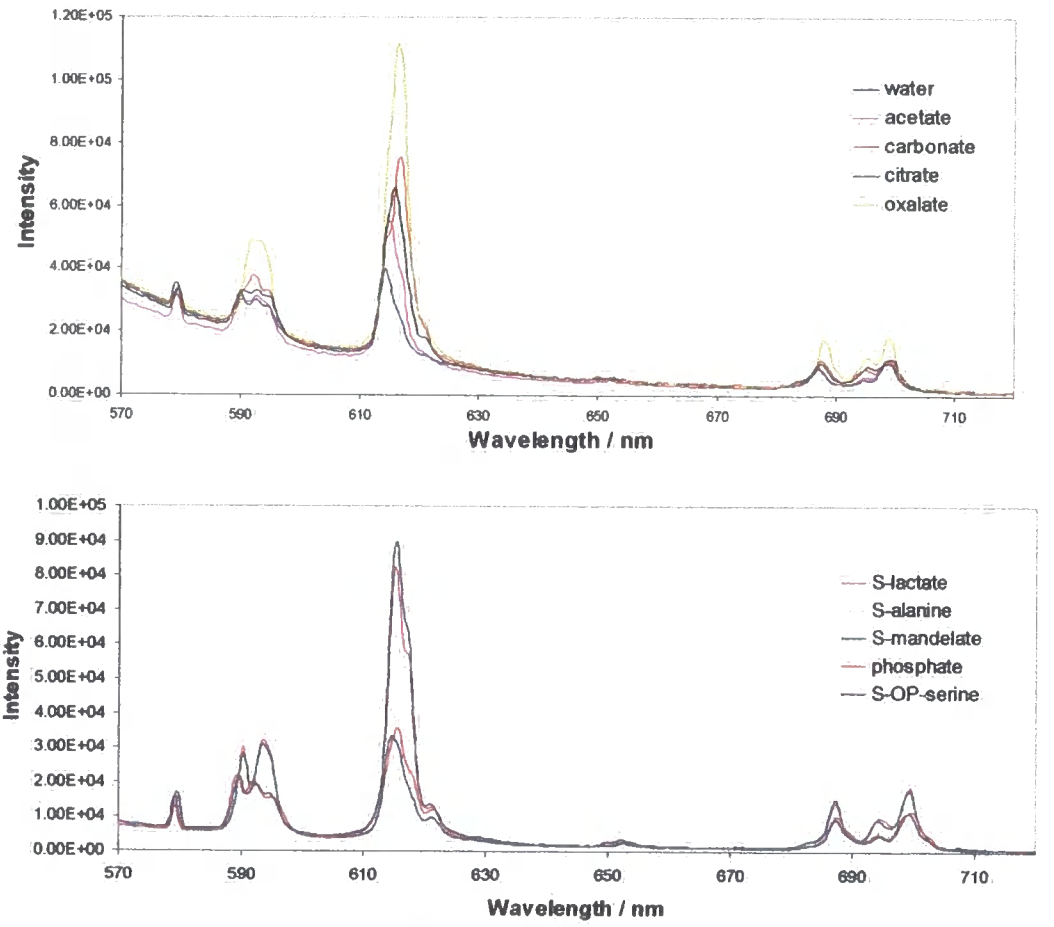

Figure 3.7 Variation in the emission spectrum of [Eu.Ld] **35** (2.5 mM, 0.1 M MOPS, pH 7.4, 295 K) following addition of a ten-fold excess of anions.

The $\Delta J = 1$ transition is relatively independent of the ligand environment whereas $\Delta J = 2$ is highly sensitive. To a first approximation, the $\Delta J = 2$ transition is dependent on the ligand dipolar polarisability.[26] Therefore, analysis of the integrated emission intensities for the $\Delta J = 2/\Delta J = 1$ spectral bands for the [Eu.Ld]-anion adducts, will provide a measure of the differences in the polarisability of the adducts. The more polarisable axial donors (smaller chemical shift) gave rise to the larger ratios (Table 3.3) and a linear correlation was observed between the measured chemical shift of the most shifted axial ring proton in the [Yb.Ld]-anion adducts with the $\Delta J = 2/\Delta J = 1$ band intensity ratios for the corresponding [Eu.Ld] analogues. Furthermore, the splitting of the $\Delta J = 1$ transition provides a direct measure of the second order crystal field parameter, and should also be highly dependent on the nature of the axial donor

(Table 3.3). The $\Delta J = 1$ band splitting was found to correlate well with the most shifted axial ring proton resonance (Figure 3.8) and the $\Delta J = 2/\Delta J = 1$ band intensity ratio. This indicates that the second order crystal field coefficient, $\langle r^2 \rangle A_2^o$, which determines the pseudocontact shift of the paramagnetic complexes (equation 3.1), is primarily affected by the axial ligand field in both the Yb^{3+} and Eu^{3+} complexes. Hence, the nature of the axial donor is effectively signalled through the emission characteristics: the more polarisable the donor, the greater the $\Delta J = 2/\Delta J = 1$ band intensity ratio and the greater the $\Delta J = 1$ splitting (cm^{-1}).

	[Yb.Ld]	[Eu.Ld]	[Eu.Ld]
+anion	**Most shifted δH_{ax} (ppm)**	**$\Delta J = 2/\Delta J = 1$**	**$\Delta J = 1$ splitting (3+2)/2-1 (10^4 cm^{-1})**
S-OP-serine	110	1.4	286
phosphate	102	1.5	222
water	100	1.5	286
S-lactate	99	2.2	267
acetate	93	2.3	308
oxalate	56	3.1	667
carbonate	45	3.1	800

Table 3.3 Effect of the axial donor polarisability on the optical and NMR spectral properties of [Yb.Ld] **30** and [Eu.Ld] **35**.

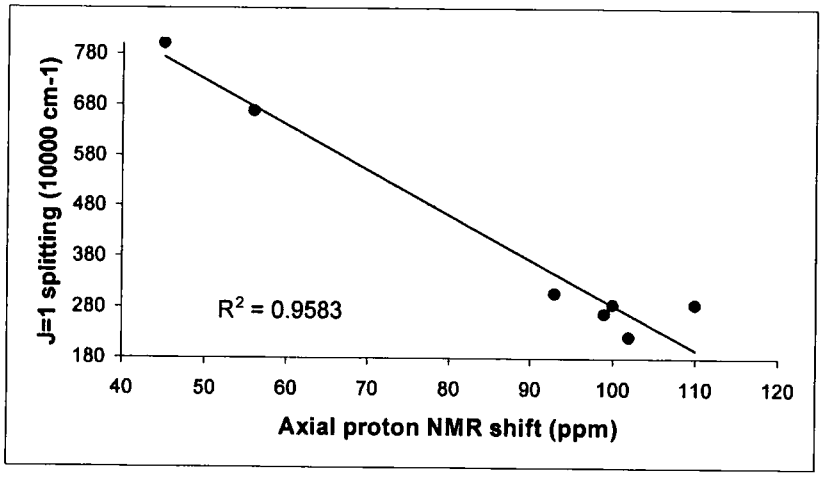

Figure 3.8 Correlation of the ^1H NMR shift of the most shifted axial ring proton resonance of the [Yb.Ld]-anion adducts (10 mM, D_2O, 200 MHz, 295 K), with the splitting of the $\Delta J = 1$ manifold in the emission spectra of [Eu.Ld] in the presence of the anions reported in Table 3.3 (2.5 mM, 0.1 M MOPS, pH 7.4, 295 K).

^{1}H NMR and Emission Spectra in a Competitive Anion Background

With the aim of investigating the relative affinity of the [Ln.Ld] complexes towards anions under physiological conditions, the emission and ^{1}H NMR investigations were undertaken in a simulated extracellular anionic environment (for 1 mM of complex: 30 mM total carbonate, 100 mM NaCl, 0.9 mM Na_2HPO_4, 2.3 mM lactate, and 0.13 mM citrate).[18] The emission spectra of [Eu.Ld] **35** (2.5 mM, H_2O) and the ^{1}H NMR spectra of [Yb.Ld] **30** (5 mM, D_2O) were recorded at different pH, in the stated anionic mixture, and the values of the integrated emission intensity for the $\Delta J = 2/\Delta J = 1$ spectral bands and the mean chemical shift of the four most shifted axial protons of the 12N4 ring are given in Table 3.4.

At pH 10, the appearance of the emission and the ^{1}H NMR spectra resembled that of the bound carbonate adduct (Table 3.4).

Anion		**[Yb.Ld] Mean Shift δH_{ax}[a] (ppm)**	**[Eu.Ld] $\Delta J = 2/\Delta J = 1$**	**Anion bound**
Carbonate		33	3.1	
Lactate		72	2.2	
Competing anion background	**pH 10**	33	3.9	carbonate
	pH 8.6	72 and 33 (2 species)	3.6	carbonate (**35**) carbonate+lactate (**30**)
	pH 7.4	72	2.9	carbonate (**35**) lactate (**30**)
	pH 5	72	2.0	lactate

Table 3.4 Results of the ^{1}H NMR and emission investigation of [Yb.Ld] **30** (5 mM, D_2O, 200 MHz, 295 K) and [Eu.Ld] **35** (2.5 mM, H_2O, 295 K, λ_{ex} 397 nm) respectively, in the presence of a competing anion background, at different pH. [a]Mean chemical shift of the four most shifted axial protons of the 12N4 ring.

At pH 8.6, the [Eu.Ld] band intensity ratio was indicative of carbonate binding, whereas [Yb.Ld] showed resonances corresponding to both carbonate and lactate-

bound adducts, probably due to the higher charge density of Yb^{3+}, which allows the lactate binding mode to compete. Lowering the pH reduced the effective concentration of first carbonate and then hydrogen carbonate, and the emission intensity ratio decreased from a value of 3.9 (pH 10) to a value of 2.9, at physiological pH, consistent with a mixture of the lactate and carbonate adducts. In the pH range 7.4-5.0, [Yb.Ld] appeared to be fully bound to lactate (mean shift δH_{ax} = 72 ppm) and no carbonate bound adduct was observed. The observed spectral emission profile (pH 5) resembled that in the presence of lactate alone with a decreased intensity ratio (2.0), consistent with the less polarisable lactate axial donor. At physiological pH, the [Yb.Ld] complex appears to bind selectively to lactate in the presence of a competing anion background, which augurs well for the development of such complexes as selective shift and relaxation agents for MRS, as discussed in Chapter 2.

Circular Dichroism

Circular dichroism associated with the metal centres of chiral Yb^{3+} complexes has been reported to be sensitive to changes in the first coordination sphere and is therefore potentially responsive to anion binding.[20,23] Yb^{3+} absorbs in the near-IR and exhibits bands centred around 980 nm due to the magnetically allowed $^2F_{7/2} \rightarrow {}^2F_{5/2}$ transitions. Spectra are usually complicated by the large number of sub-levels present, hence structure-spectral correlations have been limited. A ten-fold excess of a series of anions was added to a solution of [Yb.Ld] **30** (10 mM, in 0.1 M MOPS buffer, pH 7.4, 295 K) and the CD was measured. The CD spectra of the diastereomeric R and S anion adducts of [Yb.Ld] appeared the same.

The CD spectrum of the diaqua complex [Yb.Ld] exhibited three peaks at 966 nm, 978 nm and 989 nm respectively (Figure 3.9). Upon addition of a ten-fold excess of the anion, changes in the shape, wavelength and intensity of the peaks were observed. In particular, the peak at 966 nm was shifted to longer wavelength (~973 nm) and displayed a decrease in intensity, whilst the one at 989 nm shifted in a distinctive manner for each of the anionic adducts. In fact, the analysis of the CD data (Table 3.5) showed a distinct trend: by increasing the polarisability of the axial

donor (smaller shift in ^{1}H NMR), the wavelength of the CD band centred around 990 nm shifted to shorter wavelength. This apparent change must be related to the changes in the crystal field splittings, which reflect the permutation of the axial donor.

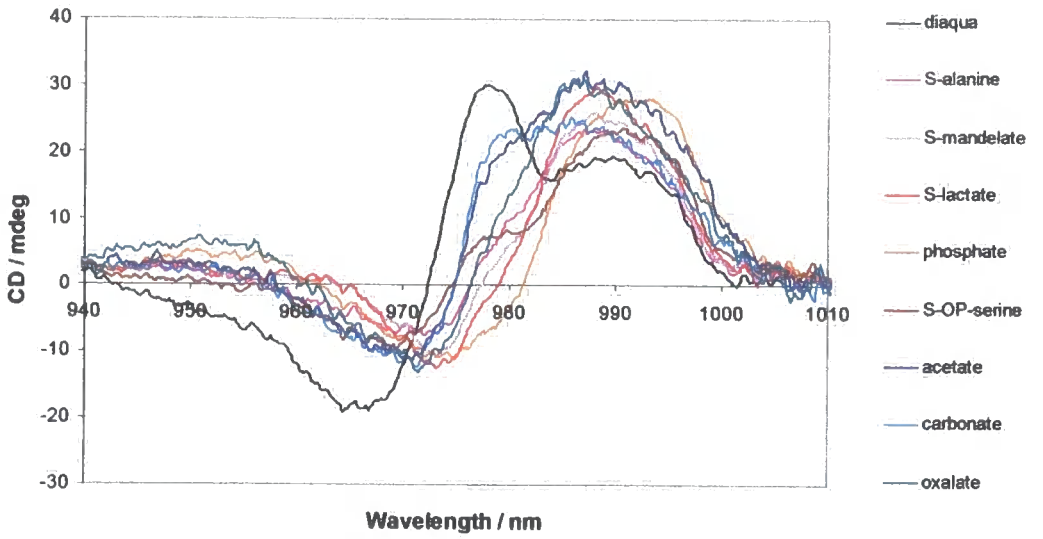

Figure 3.9 Near-IR CD spectra of [Yb.Ld] **30** and in the presence of a ten-fold excess of added anions (20 mM complex, 0.1 M MOPS, pH 7.4, 295 K).

+ Anion	[Yb.Ld] Most shifted δH_{ax} (ppm)	[Yb.Ld] CD wavelength (nm)
phosphate	102	992
S-OP-serine	110	988
water	100	989
S-lactate	99	987
acetate	93	986
S-alanine	65	986
oxalate	56	984
carbonate	45	982

Table 3.5 Effect of the axial donor polarisability on the ^{1}H NMR and CD spectral properties of the [Yb.Ld] **30** complexes.

The variation in the CD wavelength has been correlated to the variation in the axial ring proton shift. The correlation observed was not perfect ($R^2 = 0.7$), but the linear trend observed led to the conclusion that the same axial ligand effect is manifest in each parameter and is most probably associated with the second order crystal field coefficient, $\langle r^2 \rangle A_2^0$, which also determines the features of the NMR and Eu^{3+} optical spectra.

3.2.2 Cationic Leucine Complexes

Similar observations were recorded following the investigation of anion binding to the cationic $[Ln.Lc]^{3+}$ complexes depicted in Figure 3.10.

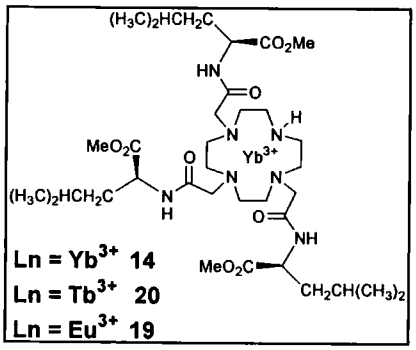

Figure 3.10 Structure of $[Yb.Lc]^{3+}$ **14**, $[Tb.Lc]^{3+}$ **20**, $[Eu.Lc]^{3+}$ **19**.

^{1}H NMR

The ^{1}H NMR spectra of a 10 mM solution of $[Yb.Lc]^{3+}$ **14** were recorded in the presence of a ten-fold excess of a series of oxyanions ($3.4 < pD < 9$). The values of the mean chemical shift of the four most shifted axial ring protons (H_{ax}), in each of the $[Yb.Lc]^{3+}$ adducts, revealed a strong dependence on the nature of the donor atom in the axial position, with the less polarisable donors (i.e. phosphate< lactate<carbonate) giving rise to the largest shifts (Table 3.6). Most of the adducts appeared as one species in solution.

Anion	Axial donor	pD	Shift range (ppm)	Mean Shift δH_{ax}[a] (ppm)
S-OP-serine*	H_2O	8.1	+113 → -79	82
phosphate	H_2O	9.1	+110 → -81	78
water	H_2O	3.4	+103 → -73	74
S-lactate	OH	4.9	+90 → -48	62
acetate	$CO^{\delta-}$	7.4	+81→ -93	60
citrate	$CO^{\delta-}$	8.1	+70 → -90	52
S-alanine	NH_2	7.8	+61→ -54 +63 minor species (M:m 2:1)	41
S-serine*	NH_2	7.8	+62→ -49	40
carbonate	CO-	8.5	+47 → -51	35
oxalate	CO^-	7.4	+43 → -34	29

Table 3.6 Effect of the axial donor on the ^1H NMR spectral range observed for $[Yb.Lc]^{3+}$ **14** (200 MHz, D_2O/CD_3OD, 295 K). [a]Mean chemical shift of the four most shifted axial protons of the 12N4 ring. *Mainly one species observed (6:1).

For the phosphate adduct, one species was initially observed in solution but, after some time, other small impurities became apparent in the ^1H NMR spectrum. These minor species were attributed to the partial hydrolysis of the pendent arms in the $[Yb.Lc]^{3+}$ adduct, which occurs under the basic conditions of the phosphate adduct. This observation was confirmed by the increase in the intensity of the integrals of the new resonances with time, and by the appearance of a peak for a hydrolysed adduct by ES^+ [983 (8%, $[M\text{-}H_2PO_4]^+$ one arm hydrolysed]. The lack of axial symmetry in $[Yb.Lc]^{3+}$ can result in two isomeric adducts for both the mono and di-hydrolysed products, depending on which arm the hydrolysis takes place. This is consistent with the several species observed in both the ^1H and ^{31}P NMR of the $[Yb.Lc]^{3+}$ in the presence of phosphate.

The ^1H NMR of the adduct with S-alanine revealed the presence of two species in solution in ratio 2:1. These can be due to constitutional isomers, associated with the amino acid mode of chelation, or to the diastereoisomers associated with the helicity of the arm rotation and the inversion of the ring (discussed in section 3.3.3).

Hydration States

The values of the estimated hydration states of $[Tb.Lc]^{3+}$ **20** (Table 3.7) showed that the complex is coordinated to two water molecules (q = 2), which are displaced by the chelation of lactate (q = 0.55 for the lactate adduct), as previously discussed (2.4.2).

$[Tb.Lc]^{3+}$ + Anion	pH	τ_{H2O} ms	τ_{D2O} ms	k_{H2O} $(ms)^{-1}$	k_{D2O} $(ms)^{-1}$	q
water	3	1.14	2.27	0.88	0.44	1.9
S-lactate	4.5	1.49	1.96	0.67	0.50	0.55
S-alanine	4.5	1.32	2.04	0.76	0.49	1.0

Table 3.7 Effect of a ten-fold added anions on the lifetime and on the rate constant for depopulation of the excited state of $[Tb.Lc]^{3+}$ **20**, and derived hydration numbers, q, (λ_{ex} = 355 nm, 2.5 mM, 295 K).

The hydration number of the adduct with S-alanine did not appear to be pH dependent in the range studied, as for [Tb.Ld] **36**. In fact, the monodentate ligation to the amino acid occurred even at acidic pH, consistent with the higher affinity of this cationic system for the anions.

Emission Spectroscopy and Circular Dichroism

Emission and circular dichroism investigation of the anion binding was undertaken for $[Eu.Lc]^{3+}$ **19** (2.5 mM, in 0.1 M MOPS buffer, pH 7.4, λ_{ex} 355 nm, 295 K) and $[Yb.Lc]^{3+}$ **14** (10 mM, in 0.1 M MOPS buffer, in H_2O and a minimum amount of CH_3OH, pH 7.4, 295 K) respectively. Analysis of the results (Table 3.8) led to similar conclusions to those discussed for the neutral [Ln.Ld] systems.

	$[Yb.Lc]^{3+}$	$[Yb.Lc]^{3+}$	$[Eu.Lc]^{3+}$	$[Eu.Lc]^{3+}$
+ Anion	**Most shifted δH_{ax} (ppm)**	**CD wavelength (nm)**	**$\Delta J = 2/\Delta J = 1$**	**$\Delta J = 1$ splitting (3+2)/2-1 (10^4 cm^{-1})**
S-OP-serine	113	991	1.6	308
phosphate	110	994	1.7	250
water	103	994	1.6	286
S-lactate	90	988	2.2	333
acetate	81	984	2.5	-
S-alanine	61	983	-	-
oxalate	43	984	3.2	667
carbonate	47	-	3.3	800

Table 3.8 Effect of the polarisability of the axial donor on the optical and NMR spectral properties of $[Yb.Lc]^{3+}$ **14** and $[Eu.Lc]^{3+}$ **19**.

The binding of $[Ln.Lc]^{3+}$ to anions with more polarisable axial donors (e.g. carbonate), resulted in larger values of both the $\Delta J = 2/\Delta J = 1$ band intensity ratio and the splitting of the $\Delta J = 1$ manifold, and smaller values of the paramagnetic NMR shift and the wavelength of the CD band centred around 990 nm. The changes in the emission, NMR and CD characteristics correlate well with each other (i.e. Figure 3.11) suggesting that the polarisability of the axial donor is associated with the same second-order crystal field parameter that determines both the optical and NMR features.

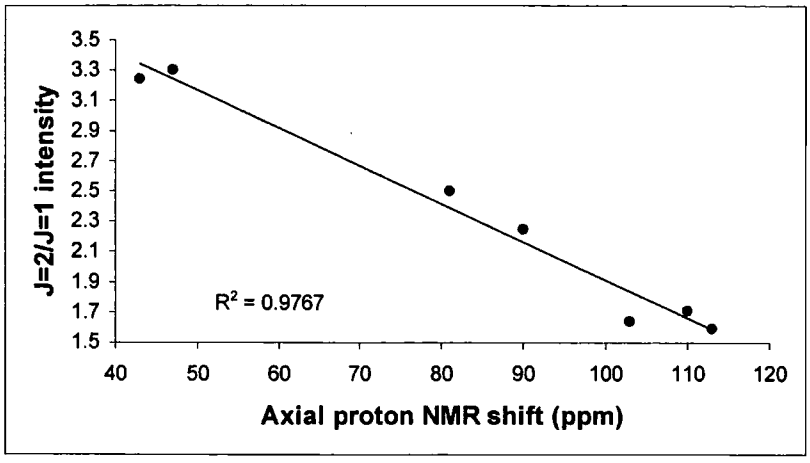

Figure 3.11 Correlation of the ^{1}H NMR shift of the most shifted axial ring proton resonance of the $[Yb.Lc]^{3+}$-anion adducts (10 mM, D_2O/CD_3OD, 200 MHz, 295 K), with the ΔJ =2 /ΔJ =1 band intensity ratio of $[Eu.Lc]^{3+}$ in the presence of added anions (2.5 mM, 0.1 M MOPS, pH 7.4, 295 K).

^{1}H NMR and Emission Spectra in a Competitive Anion Background

The emission and ^{1}H NMR investigation of $[Eu.Lc]^{3+}$ **19**, and $[Yb.Lc]^{3+}$**14**, undertaken in a simulated extracellular anionic environment (for 1 mM of complex: 30 mM total carbonate, 100 mM NaCl, 0.9 mM Na_2HPO_4, 2.3 mM lactate, and 0.13 mM citrate) at different pH, showed identical behaviour to the neutral analogues [Eu.Ld], and [Yb.Ld], previously discussed. The analysis of the shift and optical parameters of **19** and **14** in the stated anionic competitive media, showed that the Yb^{3+} complex (**14**) was carbonate-bound at basic pH and lactate-bound at both acidic and physiological pH (most shifted δH_{ax} = +46 and +90 ppm respectively). Similar considerations were made for the Eu^{3+} complex (**19**) although, at pH 7.4 the system was still carbonate-bound (ΔJ =2 /ΔJ =1 band intensity: 3.1).

3.2.3 N-Benzyl Leucine Complexes

The study of anion binding to the N-benzyl cationic and neutral leucine analogues, has been limited to the ^{1}H NMR investigation of $[Yb.Le]^{3+}$ **25** and [Yb.Lf] **41** (Figure 3.12). The ^{1}H NMR spectra of a 10 mM solution of $[Yb.Le]^{3+}$ **25** and [Yb.Lf] **41** were recorded in the presence of a ten-fold excess of a series of oxyanions.

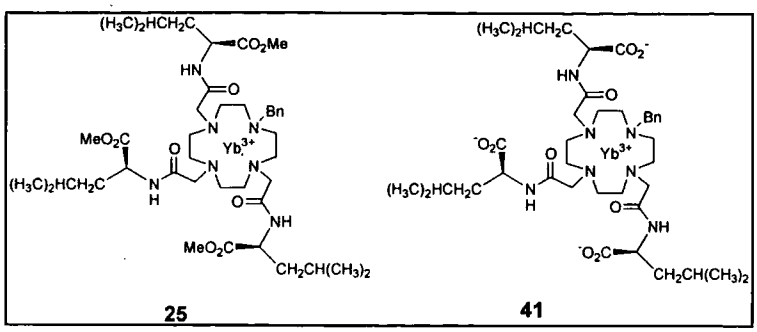

Figure 3.12 Structure of $[Yb.Le]^{3+}$ **25**, and [Yb.Lf] **41**

The binding of $[Yb.Le]^{3+}$ **25** to several anions was effectively signalled by ^1H NMR. For the chelating anions (citrate, lactate, acetate, serine, oxalate, carbonate) the spectral ranges observed were indicative of 9 coordinate SAP anion-adducts; the more polarisable axial donors giving rise to the smaller shifts (Table 3.9). In the parent $[Yb.Le]^{3+}$ complex, the hydrophobic and sterically demanding nature of the N-benzyl group favours an 8 coordinate SAP structure, with only one bound water molecule, as confirmed by independent hydration studies discussed in 2.4.2. The chemical shift range observed for the phosphate and S-OP-serine adducts (Table 3.9) was much smaller than that for the monoaqua system (107 vs 73 for diaqua and phosphate respectively), also consistent with the formation of an 8-coordinate adduct with mono-ligation through the phosphate donor. The 9 coordinate adduct is energetically favoured over a monodentate 8 coordinate system, with the chelating anions, due to the additional free energy in binding associated with the formation of a stable ring chelate.

$[Yb.Le]^{3+}$ + Anion	Axial donor	pD	Shift range (ppm)	Mean Shift δH_{ax}[a] (ppm)
water	OH_2[b]	4.4	+130→-82	107
citrate	OH	8.4	+135→-90 M +141→-88 m (M:m 2:1)	+90 M +89 m
S-lactate	OH	4.9	+129→-84	86
S-OP-serine	PO^{-}[b]	7.8	+114→-129 +minor AA bound	82
phosphate	PO^{-}[b]	9.3	+104→-105	73
acetate	$CO^{\delta-}$	7.6	+92→-56.3	72
S-serine	NH_2	8.0	+94→-84 M +90, 70, 62 m	61
oxalate	CO^{-}	7.4	+77→-73	49
carbonate	CO^{-}	8.5	+44→-75	38

Table 3.9 Effect of the axial donor on the ^1H NMR spectral range observed for $[Yb.Le]^{3+}$ **25** (200 MHz, D_2O/CD_3OD, 295 K). [a]Mean chemical shift of the four most shifted axial protons of the 12N4 ring. [b]The adducts are 8 coordinate and the donor is likely to occupy the equatorial position.

The ^1H NMR investigation (200 MHz, D_2O, 295 K) showed that the neutral [Yb.Lf] **41**, which is present as two species in solution (TSAP: SAP, 4:1), does not favour anion chelation and did not bind to phosphate, amino acids and phosphorylated amino acids, at any pH, despite a large excess of the anions being employed (> twenty-fold). Similarly, a large excess of lactate was required to achieve binding to the SAP form whereas traces of the unbound TSAP isomer were still apparent in the ^1H NMR spectrum. The binding to carbonate did occur but at pH ≥10 (mean shift δH_{ax} = 40 ppm). The dramatic decrease in the affinity towards the negatively charged compounds, is probably due to the synergic effect of the neutral charge of the system, combined with the steric encumbrance of the benzyl group and the presence of the major TSAP species in solution, which appears to disfavour anion binding. The TSAP is likely to be a structure with a lower coordination number so is less likely to expand its coordination.

3.2.4 Conclusions

The cationic and neutral leucine systems ($[Ln.Lc]^{3+}$ and [Ln.Ld]) have been shown to be powerful NMR, luminescent and chiroptical probes to signal the binding to anionic, bioactive species in aqueous media (neutral complexes). The nature of the axial donor determines the ligand field and affects, via the second order crystal field coefficient $\langle r^2 \rangle A_2^0$, the magnitude of the observed paramagnetic shift, the ratio of the $\Delta J = 2/\Delta J = 1$ band intensity, the splitting of the $\Delta J = 1$ manifold and the wavelength of the CD maxima centred around 990 nm.

The N-Bn cationic leucine system, $[Yb.Le]^{3+}$, appeared to be a useful NMR probe for anion binding, whereas [Yb.Lf], with its reduced charge density, was unable to bind to most of the anions.

3.3 Yb(III) Complexes as Potential Chiral Derivatising Agents

3.3.1 Introduction

The increased interest in enantioselective synthesis and development of single enantiomer pharmaceuticals has enhanced the need for appropriate methods for assigning the absolute configuration of chiral compounds and for the determination of enantiomeric excess.[35] Several techniques have been addressed to this purpose such as chiroptical and chromatographic methods, or X-ray crystallographic and circular dichroism analysis. However, the derivatisation of enantiomers with an enantiopure compound remains the most widely used NMR technique for the assessment of enantiomeric purity.[36] Chiral derivatising agents are optically pure compounds able to form diastereomeric complexes with enantiomers in slow exchange on the NMR timescale, and for which, the observed chemical shift non equivalence ($\Delta\Delta\delta$) is typically greater than for related complexes with a chiral shift reagent. Moreover, it is essential that no kinetic resolution occurs during the derivatisation process.

Most of the studies of chiral derivatising agents have been performed in organic media. Although several new water soluble chiral lanthanide shift reagents have been developed in recent years[37,38] (1.3.5), they exhibit very small ΔΔδ values. However, the use of novel, aqueous chiral lanthanide complexes (i.e. $[Ln.DO3Ph]^{3+}$ Figure 3.2 a) in determining the enantiomeric purity of chiral α-hydroxy acids, has been recently reported.[39] These water soluble complexes, upon addition of racemic lactate, showed not only the apparent absence of kinetic resolution in the formation of the diastereomeric R and S adducts, but also a large LIS (R-lactate δ_{CH3} = +30 ppm, S-lactate δ_{CH3} = +20 ppm, c.f. +1.3 ppm free form) and chemical shift non equivalence ($\Delta\Delta\delta_{CH3} \cong 10$ ppm), compared to the much smaller ΔΔδ values reported for shift reagents (≅ 1 ppm, and often < 0.1 ppm).[27]

3.3.2 ^{1}H NMR Studies of α-Hydroxy acids

In the search for shift and relaxation agents for lactate, the enantiopure heptadentate Yb^{3+} leucine complexes, $[Yb.Lc]^{3+}$ **14** and [Yb.Ld] **30**, were found to be unsuitable as they are in slow exchange on the NMR timescale (2.2.2). However, the large LIS experienced by the lactate-bound proton resonances, and the chemical shift non equivalence of the diastereomeric R and S lactate adducts ($\Delta\Delta\delta_{CH3} \cong 10$ ppm), along with the lack of enantioselectivity in the complex formation in the presence of racemic lactate (Table 3.10), augurs well for the development of these systems as chiral derivatising agents in NMR.

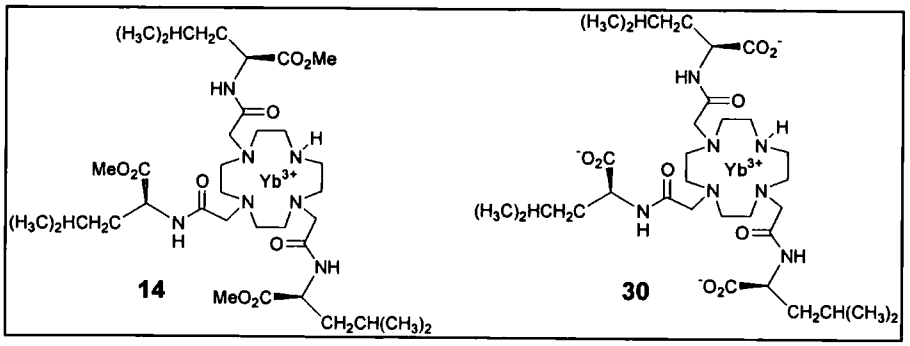

Complex	R-Lac δ_{CH3} (ppm)	S-Lac δ_{CH3} (ppm)	$\Delta\Delta\delta$
$[Yb.Lc]^{3+}$ **14**	+16	+25	9
[Yb.Ld] 30	+20	+30	10

Table 3.10 ^{1}H NMR investigation of $[Yb.Lc]^{3+}$ and [Yb.Ld] (10 mM) in the presence of racemic lactate (200 MHz, D_2O/CD_3OD for **14**, D_2O for **30**, 295K)

With the aim of assessing the potential use of $[Yb.Lc]^{3+}$ **14** and [Yb.Ld] **30** as chiral derivatising agents for chiral α-hydroxy acids, the ^{1}H NMR spectra of a solution of each of the complexes (10 mM, D_2O/CD_3OD for **14**, D_2O for **30**), in the presence of a varying concentration of R and S α-hydroxy acid (R to S ratio ranging from 1:4 to 4:1) were recorded.

Neutral Complex

Analysis of [Yb.Ld] **30** by ^{1}H NMR spectroscopy showed the presence of dimers (as discussed in 2.2.2) which, upon dilution, disappeared to give a single species, with chemical shifts indicative of a square antiprismatic (SAP) geometry (2.2.2). The eight distinct resonances shifted to higher frequency (+100 → +14 ppm) (Figure 3.13 a) were attributed to the four most shifted axial and equatorial protons of the ring.

Upon addition of 2 equivalents of the appropriate S α–hydroxy acid to [Yb.Ld] **30**, the ^{1}H NMR spectra exhibited a set of resonances for the α–hydroxy acid bound complex, which appeared as a single species in solution. On close inspection of the high frequency region of the bound adduct spectra, an additional resonance was apparent for each species, consistent with the shifted proton resonance of the CH at the α chiral centre. Indeed, additional shifted resonances could also be accounted for, attributed to the side chain of the hydroxy acids which is also held within the McConnell cone and hence experiences a large lanthanide induced shift.

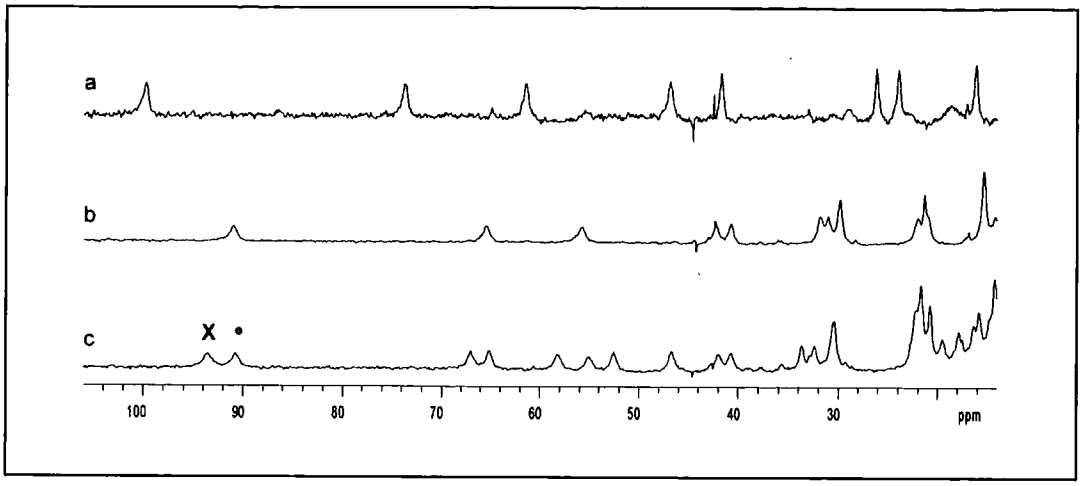

Figure 3.13 Partial ^{1}H NMR spectra of (a) [Yb.Ld] **30** (diaqua species), (b) in the presence of 2 equivalents of (S)-phenyl lactic acid and (c) 2 equivalents of racemic phenyl lactic acid, showing the most shifted axial ring proton of the S (•) and R (x) adducts (200 MHz, D_2O, 295 K).

For example, for the S-phenyl lactic adduct (Figure 3.13 b), additional resonances were observed, integrating to three protons, thus attributed to the hydroxy acid bound CH and side chain CH_2. The large dipolar shift experienced by the proton resonances in the α position, suggested that these anions bind in a bidentate manner with the hydroxyl group occupying the axial position and a carboxylate oxygen binding equatorially, as was observed for lactate (2.2.2). If a binding mode was adopted involving chelation through both of the carboxylate oxygens (c.f. acetate), the side chain resonances would not experience such a large induced shift.

Following the addition of 2 equivalents of racemic α–hydroxy acids to [Yb.Ld], a 1:1 ratio of the diastereomeric complexes was observed in the ^{1}H NMR spectrum for each of the adducts (e.g. phenyl lactate Figure 3.13 c). For the bound lactate adducts, the lactate methyl resonances are clearly resolved for the R and S diastereomers ($\Delta\Delta\delta \sim 10$ ppm) and experience large lanthanide induced shifts, resonating at +20 and +30 ppm, respectively (c.f. 1.3 ppm in free form). However, due to a lack of cross peaks being observed in the COSY analysis of the bound adducts, the α CH and the side chains for the other α-hydroxy derivatives could not be accurately

assigned. However, the magnitude of the shift difference ($\Delta\Delta\delta$) between the diastereomeric axial ring protons for the S- and R-bound adducts (Table 3.11) is of the order of 3-5 ppm. This in itself represents a great improvement over the much smaller values of chemical shift nonequivalence (~ 0.1 ppm) reported with aqueous lanthanide shift reagents currently in use.

Therefore, the apparent absence of kinetic resolution in the formation of the diastereomeric R and S adducts, and the large chemical shift non equivalence experienced by the resulting ternary complexes, enables [Yb.Ld] **30** to be considered as an effective aqueous chiral derivatising agent for α-hydroxy acids.

[Yb.Ld] + racemic Hydroxy acid	S:R	Most shifted S δH_{ax} (ppm)	Most shifted R δH_{ax} (ppm)	$\Delta\Delta\delta$ (ppm)	Structure
lactic	1:1	+99 δ_{CH3} +30	+97 δ_{CH3} +20	2 10	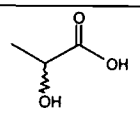
phenyllactic	1:1	+91	+94	3	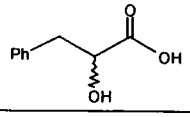
mandelic[a]	- 1:1	+96 +70	+94 +66	(2) 4	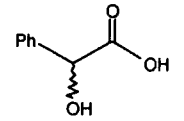
citramalic	1:1	+92	+97	5	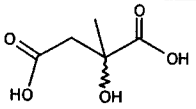
tartaric	1:1	+114	+109	5	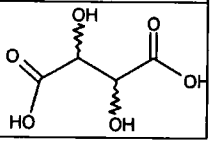

Table 3.11 ^{1}H NMR investigation of [Yb.Ld] **30** in the presence of racemic α-hydroxy acids (200 MHz, D_2O, 295 K). [a]As the resonance of the most shifted H_{ax} for the R and S diastereomers overlapped in the racemic mixture, they could not be used to assess the degree of enantioselectivity associated with the binding. Hence the enantioselectivity was determined using the subsequent most shifted resonance at 70 and 66 ppm for S and R respectively.

Cationic Complex

The ^{1}H NMR spectrum of $[Yb.Lc]^{3+}$ **14** showed the presence of a single isomer in solution, with chemical shifts indicative of a SAP geometry (2.2.2). In the high frequency region (+103 → +14 ppm) the eight observed resonances were attributed to the four most shifted axial and equatorial ring protons (Figure 3.14 a).

Upon addition of 2 equivalents of the appropriate S α–hydroxy acid to $[Yb.Lc]^{3+}$ **14**, a set of resonances attributed to the hydroxy acid bound complex was apparent, which appeared as a single species in solution (e.g. S-mandelic acid adduct, Figure 3.14 b).

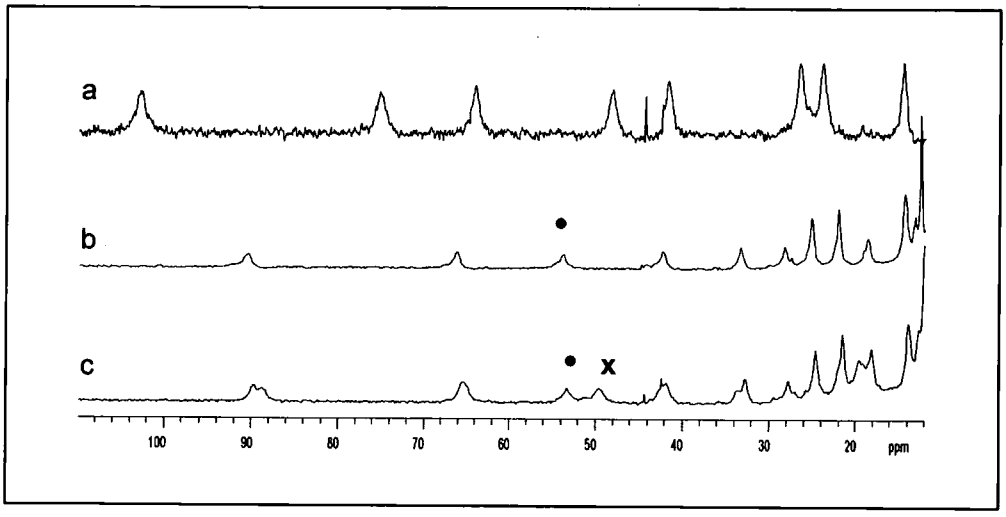

Figure 3.14 Partial ^{1}H NMR of (a) $[Yb.Lc]^{3+}$ **14** (diaqua species), (b) in the presence of 2 equivalents of (S)-mandelic acid and (c) 2 equivalents of racemic mandelic acid, showing the proton resonances of the S (•) and R (x) adducts, which were used to assess the degree of enantioselectivity in the binding (200 MHz, D_2O/CD_3OD, 295 K).

Following the addition of 2 equivalents of racemic α–hydroxy acid to $[Yb.Lc]^{3+}$, a 1:1 mixture of diastereomeric complexes was observed for the lactate and mandelic acid adducts only (Figure 3.14 c) ($\Delta\Delta\delta$ = 9 ppm and 3 ppm respectively (Table 3.12). The complex, **14**, showed a preferential binding for the S-phenyl lactic acid with

respect to the R form, whereas the overlapping diastereomeric peaks of the R and S citramalic and tartaric acid adducts, prevented assessment of the enantioselectivity.

$[Yb.Lc]^{3+}$ + racemic hydroxy acid	S:R	Most shifted S δH_{ax} (ppm)	Most shifted R δH_{ax} (ppm)	$\Delta\Delta\delta$ (ppm)
lactic	1:1	+90 δ_{CH3} +25	+87 δ_{CH3} +16	3 9
phenyllactic	1.5:1	+89	+94	5
mandelic[a]	1:1	+90 +53	+89 +50	- 3
citramalic	-	+92	+94	2
tartaric	-	+106	+106	-

Table 3.12 ^{1}H NMR investigation of $[Yb.Lc]^{3+}$ **14** in the presence of racemic α-hydroxy acids (200 MHz, D_2O/CD_3OD, 295 K). [a]The ratio between the R and S adduct has been determined on the second set of the shifts reported. The peaks at 90 ppm and 89 ppm appeared as a single broad peak in the racemic mixture adduct, thus they could not be used to assess the enantioselectivity associated with the binding.

The enantioselectivity in complex formation displayed by the cationic $[Yb.Lc]^{3+}$ complex coupled with the reduced water solubility renders it unsuitable for use as a chiral derivatising agent for α–hydroxy acids.

3.3.3 ^{1}H NMR Studies of α-Amino Acids

Introduction

Amino acids constitute the building blocks of several fundamental biomolecules, such as oligopeptides (e.g hormones, neurotransmitters), and proteins (e.g. enzymes, antibodies).[40] Therefore, the naturally occurring α–amino acids and their derivatives have become the important targets for molecular recognition by artificial host compounds.[41] Examples include some macrocyclic pseudopeptides, which have been reported to act as enantioselective carriers for racemic amino acid ester salts[42] or a zinc complex with an artificial porphyrin based receptor, which showed an effective recognition of various types of amino acid esters.[43] The zwitterionic nature of the amino acids, along with the functionality of their side chain, have led to the

development of receptors with multiple binding sites, capable of several host guest interactions (e.g. β–cyclodextrin derivatives bearing a benzo-crown ether)[44] or to compounds which interact with the carboxylate or the ammonium moieties of the amino acids.[45]

In recent years, there has been an increased interest towards the investigation of lanthanide coordination chemistry in the presence of the common amino acids. Ln^{3+} ions are hard acids which prefer to bind to hard bases in solution, thus negatively charged oxygen donors are preferred over neutral nitrogen donors. At physiological pH, the complexation is generally regarded to occur between the Ln^{3+} ion and the unprotonated oxygen of the zwitterionic form of the amino acid.[46] However, a limited number of studies also revealed that Ln^{3+} binding may occur through the side chain functionality, such as the hydroxyl group of serine.[47] The capability of the Ln^{3+} ion to coordinate to the unprotonated amine group of the amino acid had been the topic of controversy, due to the fact that by raising the pH to values at which this coordination can take place, lanthanide hydrolysis becomes highly competitive due to the small stability constants of the earlier systems studied.[48]

A recent elegant investigation has been undertaken on the binding of α-amino acids to a well-defined, relatively stable, heptadentate Yb^{3+}complex ($[Yb.DO3Ph]^{3+}$, Figure 3.15) in aqueous solution.[33] The analysis of the dipolar ^1H NMR paramagnetic shifts of the adducts suggested that the α-amino acids form a common chelated structure, adopting a 9 coordinate SAP geometry, with the amine N axially disposed and one carboxylate oxygen occupying the remaining equatorial site. Crystal structures of several of the chelated [Yb.DO3Ph]-amino acid adducts confirmed this binding mode (i.e.(RRR)-$[Yb.DO3Ph\text{-}S\text{-}alanine]^{2+}$).

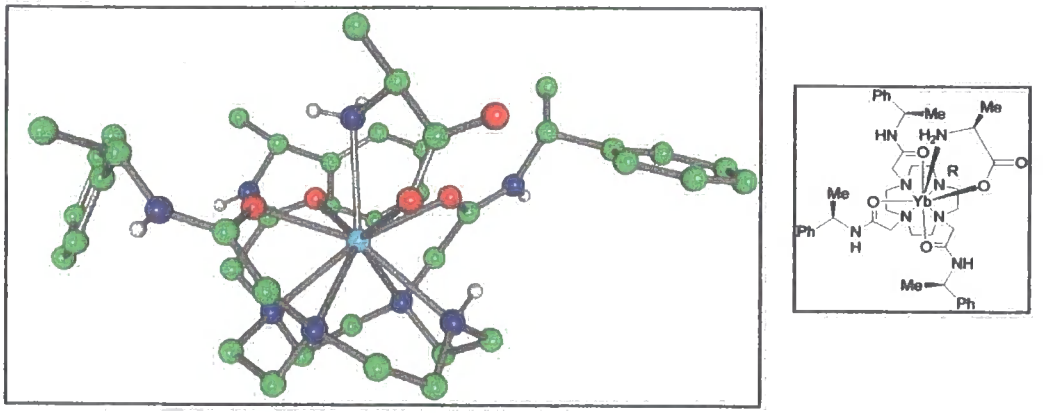

Figure 3.15 Side view representation of (RRR)-[Yb.DO3Ph-S-alanine]$^{2+}$ (SAP, Λ(δδδδ)) showing the amino acid NH occupying the axial position and a carboxylate O binding equatorially, completing the O_4 plane.

With the aim of assessing, primarily, the binding mode of selected natural α-amino acids to the cationic [Yb.Lc]$^{3+}$ **14** and neutral [Yb.Ld] **30** leucine systems and, secondly, the potential of these complexes to act as chiral derivatising agents for α-amino acids, the ^{1}H NMR spectra of a solution of each of the complexes (10 mM, D_2O/CD_3OD), in the presence of a 10 fold excess of S and racemic α-amino acids were recorded (200 MHz, 295 K). At pD < 6, the amino acids did not bind strongly and an exchange broadened spectrum corresponding to the diaqua complex was observed, thus the study was performed at physiological pH (pD ≅ 8).

Neutral Complex

Upon addition of a ten fold excess of the S-α-amino acids to (SSS)-[Yb.Ld] **30**, the observed chemical shift range appeared to be similar for each of the adducts (av. + 67→ - 50 ppm) (Table 3.13), consistent with a common binding mode, involving chelation with the more polarisable amine nitrogen in the axial position and one of the carboxylate oxygens binding equatorially, thus forming a favourable 5 membered chelate ring. Bidentate chelation through both of the carboxylate oxygens was ruled out as this would have given rise to a larger shift range, similar to that of acetate (+93→ -94 ppm) (Table 3.1). Furthermore, the observed chemical shift range shows

that chelation does not occur through side chain functionality, such as through the hydroxyl group in serine (Ser) or threonine (Thr) (c.f. lactate, +99 → -56 ppm) or the acidic side chain of glutamic acid (Glu) (c.f. acetate +93 → -94 ppm).

[Yb.Ld] + α-Amino acid	Shift Range (S-adduct) (ppm)	Most Shifted S δH_{ax} (ppm)	Most Shifted R δH_{ax} (ppm)	ΔΔδ	S:R	Side chain AA
Gly (achiral)	+63→ -47	+63	-		-	-H
Ala	+65→ -43	+65	+60	5	1:1	$-CH_3$
Ser	+68→ -50	+68	+59	8	1:2.2	$-CH_2OH$
Thr	+67→ -51	+67	+61	6	1:2	$-CHOHCH_3$
Met	+70→ -53	+70	+64	6	1:1.7	$-CH_2CH_2SCH_3$
Glu	+68→ -48	+68	+62	6	1:2.6	$-CH_2CH_2CO_2H$
Lys[a]	+66→ -47	+66 (57)[b]	+62	4	1:1	$-CH_2(CH_2)_3NH_2$
Phe	+72→ -62	+72	+68	4	1:2	$-CH_2Ph$

Table 3.13 Representative ^1H NMR data of [Yb.Ld] **30** (10 mM) in the presence of a ten-fold excess of added S-α-amino acids and racemic α-amino acids (200 MHz, D_2O/CD_3OD, 295 K, pD~8). [a]Mainly one species (minor species < 7%), [b] chemical shift of the most shifted axial proton ring in the minor species.

Most of the amino acid complexes studied appeared to exist as a single species in solution, whereas with the lysine adduct a trace of a minor isomer was also apparent (< 7 %). Upon amino acid chelation to (SSS)-[Yb.Ld], there are theoretically eight possible isomers in solution (Figure 3.16); the four of the isomers associated with the 12N4 ring conformation (δδδδ or λλλλ) and the helicity of the arm rotation (Δ or Λ), as discussed previously (2.2), and constitutional isomers, associated with the amino acid mode of chelation. In fact, for the NO chelate two different binding modes may occur, with the amine axially disposed (N_{ax}) and the carboxylate in the equatorial position or vice versa (O_{ax}) (Figure 3.17). Each of the 8 isomers are rended diastereomeric due to the remote chiral centre at the amide functionality.

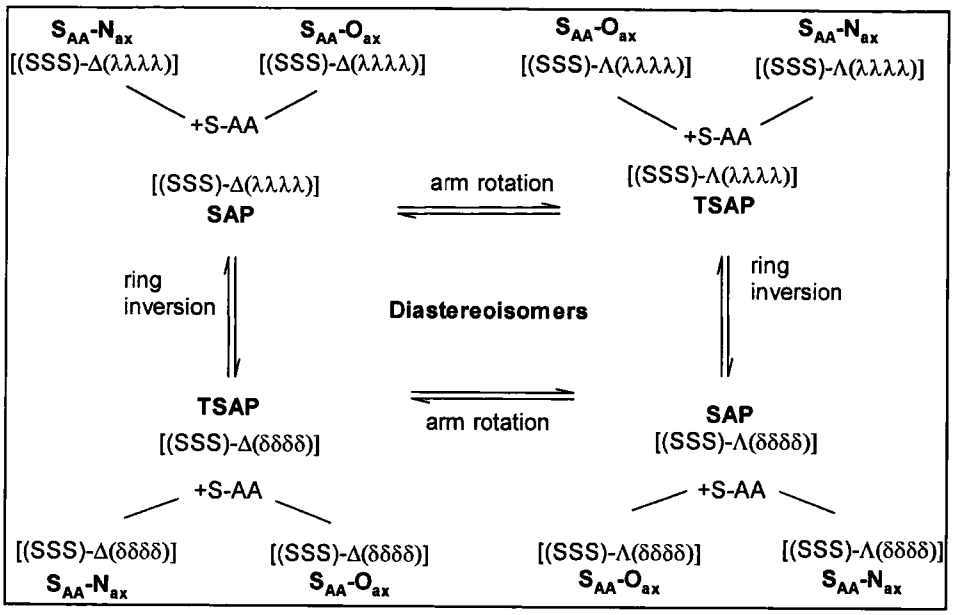

Figure 3.16 Schematic representation of the 8 possible diastereomers associated with (SSS)-[Yb.Ld] ternary amino acid complexes.

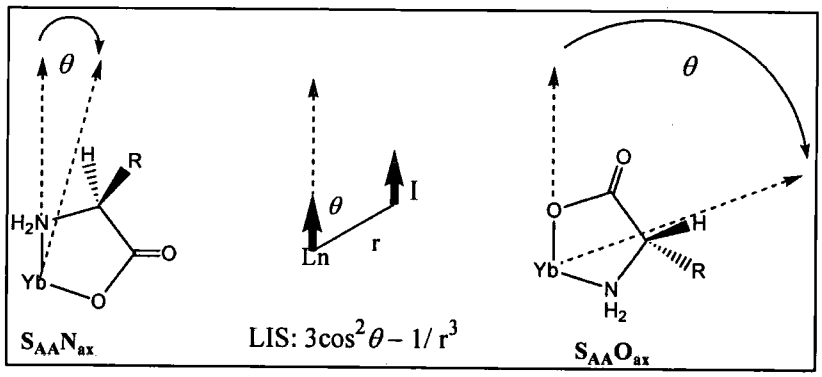

Figure 3.17 Possible modes of amino acid chelation to the Ln^{3+} complexes, showing the position of the H atom with respect to the principal magnetic axis.

Only in the conformation with the amine axially disposed ($S_{AA}N_{ax}$), should the resonance of the CH at the chiral centre of the amino acid experience a large induced shift, owing to its proximity to the principal magnetic axis of the Yb^{3+} ion ($(3\cos^2\theta - 1/r^3)$ dependence). On close analysis of each of the bound-adduct spectra, an

additional resonance, integrating to one proton, was apparent at a higher shifted frequency and was attributed to the amino acid CH. Hence, the bidentate chelation of the amino acid appeared to be identical in all of the adducts, with the carboxylate equatorially disposed and the amine occupying the axial position. The single species observed in solution in most of the (SSS)-[Yb.Ld]- α-amino acid adducts is likely to adopt the SAP geometry (Δλλλλ) which is consistent with the observed chemical shift range and the crystallographic data obtained for the analogous $[Yb.DO3Ph]^{3+}$-amino acid adducts.[33] The nature of the similarity of the observed chemical shift for the minor species that was apparent for lysine, suggests that a SAP geometry is adopted for both the isomers, which are likely to be stereoisomers (Δλλλλ and Λδδδδ) rather than constitutional isomers (N_{ax} vs O_{ax}).[33]

Following the addition of a ten-fold excess of a racemic mixture of α-amino acids to [Yb.Ld], preferential binding to the R-α-amino acids was observed in the presence of Ser, Met, Glu, and Phe (Table 3.13). This precludes the use of the complex as a broad spectrum chiral derivatising agent for direct NMR analysis of the enantiomeric purity of simple amino acids, despite the large values of the magnitude of the shift difference observed for the H_{ax} ring protons for diastereomeric R and S adducts ($\Delta\Delta\delta \sim 5$ ppm) (Table 3.13). However, no enantioselectivity in complex formation was observed with Ala (Figure 3.18 c) and Lys, which allows the use of [Yb.Ld] as an effective aqueous derivatising agent for these specific α-amino acids. Moreover, the ^1H NMR data (Table 3.13), showed that the resonance of the most shifted axial proton of the ring in each of the S-α-amino acid adducts resonates at a higher frequency than the most shifted axial proton in the R-diastereomer, hence [Yb.Ld] can be employed to determine the absolute configuration of α-amino acids of unknown chirality.

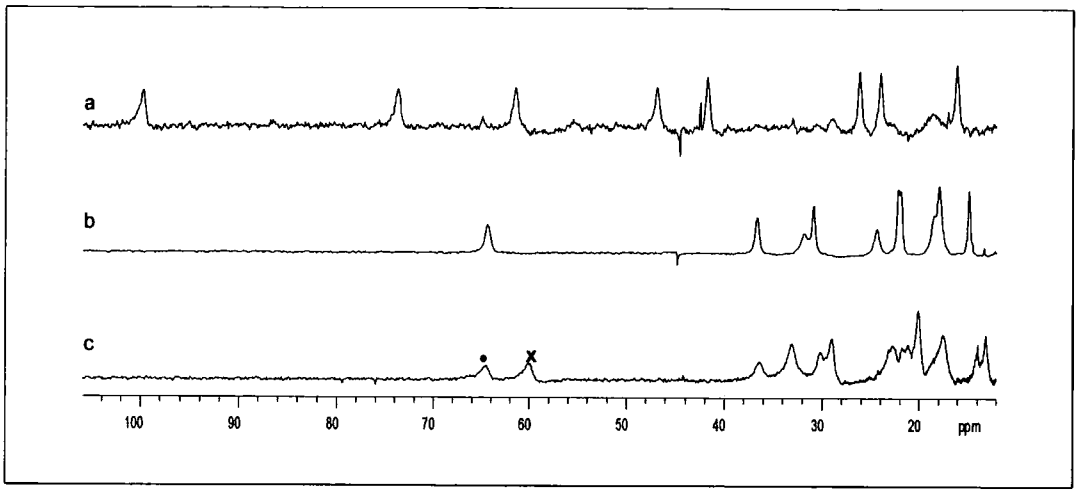

Figure 3.18 Partial ^{1}H NMR of (a) [Yb.Ld] **30** (diaqua species), (b) in the presence of 10 equivalents of (S)-alanine and (c) 10 equivalents of racemic alanine, showing the most shifted axial ring proton of the S (•) and R (x) adducts (200 MHz, D_2O/CD_3OD, 295 K, pD ~8).

Cationic Complex

The ^{1}H NMR data for each of the S-α-amino acids with (SSS)-$[Yb.Lc]^{3+}$ **14** (Table 3.14) led to similar conclusions to those discussed above for the neutral [Yb.Ld] analogue.

$[Yb.Lc]^{3+}$ + S–α-Aminoacid	No. of Species (ratio major:minor)	Shift Range major species (ppm)	Most Shifted δH_{ax} major isomer (ppm)	Most Shifted δH_{ax} minor species (ppm)
Gly (achiral)	2 (8:1)	+59→ -45	+59	+68
Ala	2 (3:1)	+61→ -54	+61	+63
Ser	2 (6:1)	+62→ -49	+62	+64
Thr	2 (13:1)	+63→ -50	+63	+60
Met	1	+62→ -53	+62	-
Glu	1	+61→ -53	+61	-
Lys[a]	2 (3:1)	+63→ -53	+63	+62
Phe	1	+72→ -45	+72	-

Table 3.14 Representative ^{1}H NMR data of $[Yb.Lc]^{3+}$ **14** (10 mM) in the presence of a ten-fold excess of added S-α-amino acids (200 MHz, D_2O/CD_3OD, 295 K, pD~8).

Out of the eight amino acids studied, only Met, Glu and Phe appeared as a single isomer in solution, whereas two species were observed for the remaining adducts. Again, the shift range exhibited by each of the adducts and isomers present in solution (when observed), is indicative of a SAP geometry and a bidentate chelation of the amino acids with the more polarisable amine in the axial position and one of the carboxylate oxygens binding equatorially. As an S configuration at the pendent arm δ to the chiral centre favours a ΔλλλΔ conformation, the major isomer is likely to be ΔλλλΔ-N_{ax} with the minor isomer adopting the SAP ΛδδδΔ-N_{ax} conformation.

Upon addition of a ten-fold excess of a racemic mixture of α-amino acids to $[Yb.Lc]^{3+}$, a large shift difference was observed for the H_{ax} ring protons for the diastereomeric S- and R-amino acid-$[Yb.Lc]^{3+}$ adducts (ΔΔδ between 5-10) (Table 3.15), compared to the much smaller values reported for aqueous Ln^{3+} shift reagents (~ 0.1 ppm).[27] However, the preferential binding to the R-α-amino acids, observed in the presence of Ser, Thr, Phe (Table 3.15), prevents the use of the complex as a broad spectrum chiral derivatising agent for direct NMR analysis of the enantiomeric purity of simple amino acids. No enantioselectivity in the complex formation was observed in the presence of Ala, Met (Figure 3.19), Glu, Lys but, due to the presence of two species in solution, analysis of the enantiomeric purity with $[Yb.Lc]^{3+}$ would therefore be more complicated.

$[Yb.Lc]^{3+}$ + α-Amino acid	No. of Species in R adduct (ratio major:minor)	Most Shifted R δH_{ax} (major) (ppm)	Most Shifted S δH_{ax} (major) (ppm)	ΔΔδ	S : R
Ala	2 (3:1)	+55	+61	6	1:1
Ser	1	+51	+62	11	1:2.2
Thr	2 (3:1)	+55	+62	7	1:2
Met	1	+57	+62	5	1:1
Glu	1	+56	+61	5	1:1
Lys[a]	2 (10:1)	+57	+63	6	1:1
Phe	1	+62	+72	10	1:2

Table 3.15 Representative ^1H NMR data of $[Yb.Lc]^{3+}$ **14** (10 mM) in the presence of a ten-fold excess of added racemic-α-amino acids (200 MHz, D_2O/CD_3OD, 295 K, pD~8).

As reported for [Yb.Ld], the resonance of the most shifted axial proton of the ring in each of the S-α-amino acid adducts resonates at a higher frequency than the most shifted axial proton in the R-diastereomer (Table 3.15), hence this cationic system can be employed to determine the absolute configuration of an α-amino acid.

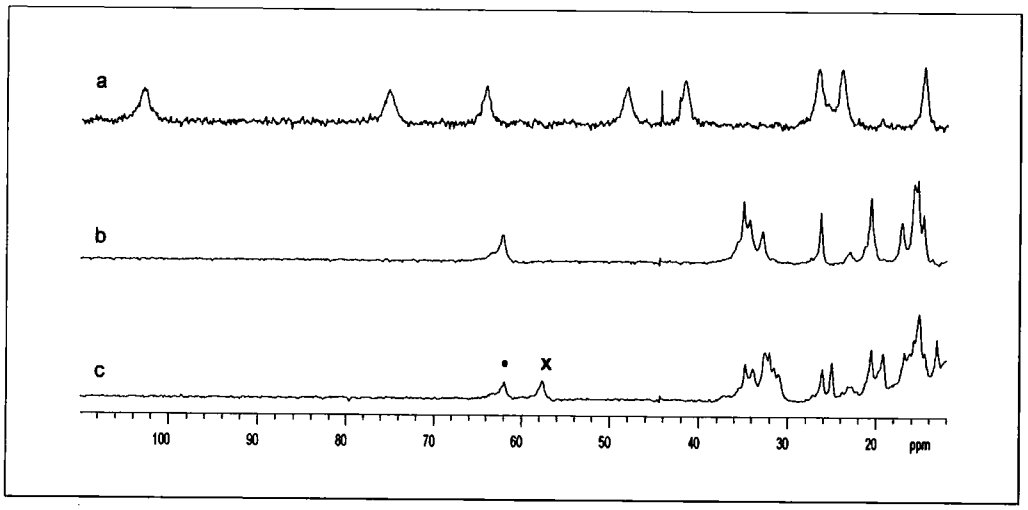

Figure 3.19 Partial ^{1}H NMR of (a) $[Yb.Lc]^{3+}$ **14** (diaqua species), (b) in the presence of 10 equivalents of (S)-methionine and (c) 10 equivalents of racemic methionine, showing the most shifted axial ring proton of the S (•) and R (x) adducts (200 MHz, D_2O/CD_3OD, 295 K, pD ~8).

3.4 NMR Studies of Phosphorylated Anions

Introduction

The oxyanions of pentavalent phosphorus probably constitute the most important class of anions in nature, owing to their pivotal roles in living systems.[49] Examples include the phosphorylated amines, such as phosphocholine (PC) and phosphoethanolamine (PE), which are membrane synthesis substrates, or AMP, ADP, ATP, DNA and RNA, which are involved in heredity, signal transduction, and energy storage processes.[50] Furthermore, phosphorylated sugars (e.g. glucose-6-P) are involved in fundamental cellular metabolic pathways (e.g. glycolysis), and proteins and peptides bearing phosphorylated amino acids, such as S-OP-serine, S-

OP-threonine and S-OP-tyrosine, control several cellular processes, including differentiation, development and proliferation.[51]

The quest for a selective recognition and sensing of phosphorylated species in cells, has led to the development of artificial receptors for aqueous solution. Examples include the optical sensors, such as the fluorescent chemosensors bearing two zinc ions coordinated to distinct dipicolylamine,[52] or the octadentate luminescent lanthanide (Eu^{3+}) complexes, bearing a pendent phenanthridinium[19] or acridone[53] chromophore. However, NMR probes, such as chiral heptadentate Ln^{3+} complexes (i.e. [Yb.DO3Ph]$^{3+}$ Figure 3.2 a)[20] have been reported to offer a convenient means of assessing the phosphorylated-anion binding, in particular to obtain structural information about the adducts.

Neutral Leucine Complex

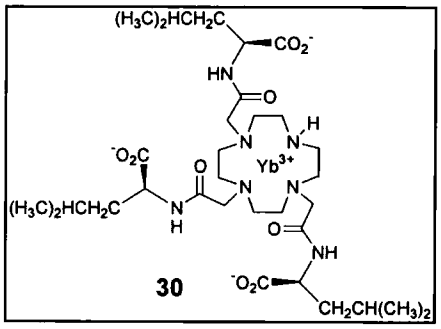

30

Figure 3.20 Structure of [Yb.Ld] **30**

With the aim of assessing the potential of the water soluble [Yb.Ld] **30** (Figure 3.20) complex as a NMR probe for phosphorylated bioactive species in aqueous solution, a ten-fold excess of selected phosphorylated anions was added to a 10 mM solution of the complex (D_2O, pD~8), and the ^1H and ^{31}P NMR spectra were recorded.

The ^1H NMR spectra of the adducts showed the presence of a single species in solution (SAP), with the exception of the glucose-6-P-complex, which exhibited a partial resolution of the most shifted axial proton resonances in the high frequency

region, probably related to the presence of glucopyranose/glucofuranose adducts or to the formation of α /β glucose epimers. Representative partial ^{1}H NMR spectra of some of the [Yb.Ld] adducts are depicted in Figure 3.21.

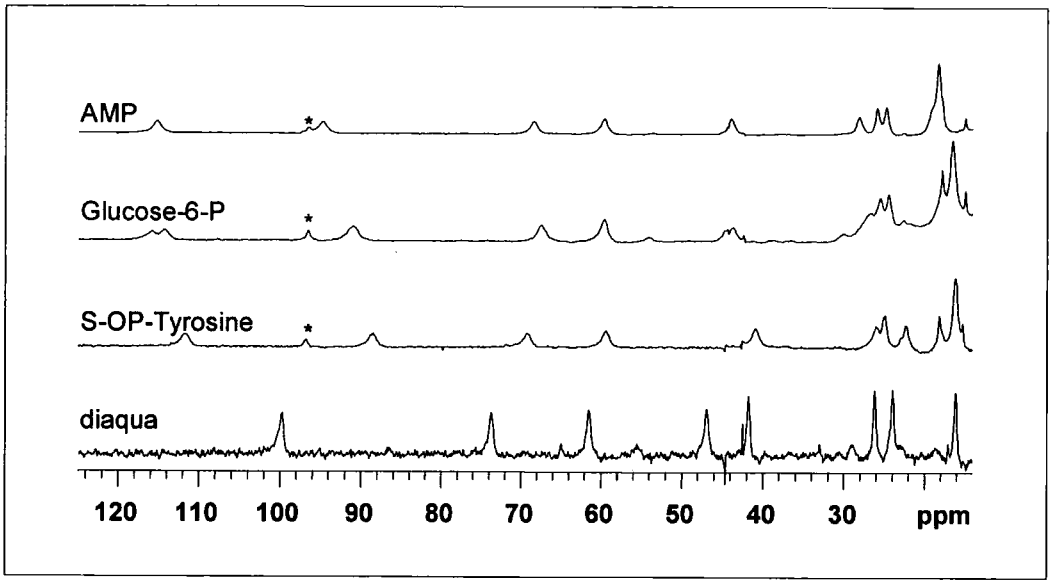

Figure 3.21 Partial ^{1}H NMR spectra for complexes of [Yb.Ld] **30** (10 mM) with the following added phosphorylated anions (ten-fold excess): AMP; glucose-6-P; S-OP-tyrosine; diaqua (200 MHz, D_2O, 295 K, pD 8). *Impurity of the tetraalkylated complex (< 5%).

The observed spectral range is similar for each of the phosphorylated adducts (Table 3.16), and is consistent with a common binding mode, involving mono-ligation of the phosphate moiety with displacement of the bound water molecule in the equatorial position.

[Yb.Ld] + anions	Axial donor	^{1}H NMR Shift range (ppm)	Mean Shift δH_{ax}[a] (ppm)	^{31}P $\Delta\Delta\delta$[c] (ppm)
PC	H_2O	+120→-86	91	68
PE	H_2O	+115→-85	86	60
AMP	H_2O	+115→-86	84	66
S-OP-threonine	H_2O	+114→-84	84	60
R-OP-serine	H_2O	+115→-85	84	57
Glucose-6-P[b]	H_2O	+116→-86 +114→-86	83	64 major 65 minor 2:1
S-OP-tyrosine	H_2O	+111→-82	83	51
S-OP-serine	H_2O	+110→-83	82	55
phosphate	H_2O	+102→ -77	75	37
diaqua	H_2O	+100→ -120	70	-
S-tyrosine	NH_2	+70→-63	44	-
S-threonine	NH_2	+67→-51	43	-
S-serine	NH_2	+68→ -50	43	-
R-serine	NH_2	+58→ -46	39	-

Table 3.16 Representative ^{1}H (200 MHz) and ^{31}P (500 MHz) NMR data for [Yb.Ld] **30** (10 mM) in the presence of a ten-fold excess of added phosphorylated anions (D_2O, 295 K, pD~8). [a]Mean chemical shift of the four most shifted axial protons of the 12N4 ring. [b]The splitting of this peak into two components may be related to isomeric saccharide complexes. [c]Absolute shift difference between the unbound and bound P species.

In the ternary adducts with the phosphorylated amino acids, there are two possible competing binding modes; chelation through the amino acid amine N and carboxylate O, forming a favourable 5-ring chelate or via monodentate coordination through the phosphate moiety. With the aim of understanding competition between the two binding modes, ^{1}H NMR spectra of [Yb.Ld] adducts with S-OP-tyrosine, S-OP-serine and S-OP-threonine have been recorded at different pH. At physiological pH the phosphorylated amino acid adducts existed as a single isomer in solution, with a large spectral range, indicative of chelation through the phosphate moiety. Upon raising the pH (10), S-OP-tyrosine appeared as a single species, with a narrow spectral range indicative of amino acid chelation, whereas the S-OP-serine and S-OP-threonine adducts exhibited two species, with shifts corresponding to the presence of both phospho mono-ligation, and amino acid chelation (3:1, respectively). At high pH, the amine group becomes deprotonated and thus the amino

acid chelation is favourable. At pH 5, only the diaqua complex spectra was observed, hence no binding was apparent, consistent with the general weaker affinity of the neutral system for anions, which has been observed also by the ^{31}P NMR investigation discussed in 2.2.3.

The potential of [Yb.Ld] as a chiral derivatising agent for chiral phosphorylated anions was assessed using O-P-serine. Although a large chemical shift non-equivalence for the R and S diastereomeric peaks was observed ($\Delta\Delta\delta = 4$ ppm), following the addition of the racemic phosphorylated amino acid, a preferential binding to the R-form (R:S 2:1) was apparent. Future studies may be addressed to the investigation of a wider range of chiral phosphorylated species.

Independent ^{1}H and ^{31}P NMR titrations showed that the phosphorylated adducts are in slow exchange on the NMR timescale with the diaqua precursor, as previously discussed for [Yb.Ld] in the presence of PC and PE (2.3.3), thus the system is unsuitable as a shift reagent for such anions. However, the ^{31}P NMR data showed that the bound anions did experience a huge lanthanide induced shift (Table 3.16), to regions in the spectrum where background signals would not interfere. Furthermore, a large difference in the magnitude of the observed ^{31}P chemical shifts is displayed by the various phosphorus adducts (e.g. $\Delta\Delta\delta$: 37 vs 68 ppm, for phosphate and PC adducts respectively). Therefore, each phosphorylated species can be distinguished by its unique chemical shift. Thus by observation of the ^{31}P shift of the bound [Yb.Ld] adducts, the nature of the phosphorylated species may be assessed. Future binding studies with [Yb.Ld] in the presence of a competitive phosphorylated anionic background, will be useful in assessing the potential and selectivity of this promising system as an aqueous NMR probe for phosphorylated species.

A luminescence investigation of the binding of the neutral Eu^{3+} analogue, [Eu.Ld] **35**, (2.5 mM, 0.1 M MOPS, pH 7.4, 295 K) to the phosphorylated species discussed above (10-fold excess) was also undertaken. However, as the actual coordination environment about the Eu^{3+} centre was the same for each adduct (i.e. H_2O axial,

phosphate donor equatorial), the emission characteristics were very similar for each of the phosphorylated adducts as expected. Similarly, near identical CD spectra were also recorded for each of the complexes (20 mM [Yb.Ld] + ten-fold excess added anion, 0.1 M MOPS, pH 7.4) indicative of the same local coordination environment about the Yb^{3+} ion. ^{31}P NMR studies are therefore the most effective method for signalling the binding of phosphorylated species.

Cationic Leucine Complex

A similar NMR investigation was carried out on the cationic $[Yb.Lc]^{3+}$ complex (10 mM, D_2O/CD_3OD, pD ~8) and results are given in Table 3.17. The chemical shifts observed for all the phosphorylated-$[Yb.Lc]^{3+}$ adducts, were consistent with a SAP conformation ($\Delta\lambda\lambda\lambda\lambda$) with monodentate ligation, via the phosphate moiety. For the phosphorylated amino acids, traces of a minor isomer (< 10%) were also apparent. The observed chemical shifts were consistent with phosphate binding rather than amino acid chelation (smaller shift range), hence the formation of the other diastereomeric SAP form ($\Lambda\delta\delta\delta\delta$) was proposed, as was adopted by the minor isomer of the amino acid chelates discussed above (3.3.3).

$[Yb.Lc]^{3+}$ + anions	Axial donor	Shift range (ppm)	Mean Shift δH_{ax}[a] (ppm)	Number of Species[b] (minor species δH_{ax}) (ppm)
S-OP-tyrosine	H_2O	+119→-78	90	2 (+100)
PC	H_2O	+120→-81	89	1
PE	H_2O	+119→-80	89	1
S-OP-threonine	H_2O	+118→-80	87	2 (+106)
R-OP-serine	H_2O	+113→-80	84	2 (+112)
S-OP-serine	H_2O	+113 →-79	82	2 (+110)
phosphate	H_2O	+110 →-81	78	2 (+108)
diaqua	H_2O	+103 → -73	74	1
S-tyrosine	NH_2	+64→ -60	42	2 (+66)
S-threonine	NH_2	+62→ -50	63	2 (+60)
S-serine	NH_2	+62→ -49	40	2 (+64)

Table 3.17 Representative ^1H NMR data of $[Yb.Lc]^{3+}$ **14** (10 mM) in the presence of a ten-fold excess of added phosphorylated anions (200 MHz, D_2O/CD_3OD, 295 K, pD~8). [a]Mean chemical shift of the four most shifted axial protons of the 12N4 ring. [b]Mainly one species was observed in solution, but small traces of a minor species were evident (< 10%).

3.5 Overall Conclusions

The enantiopure heptadentate lanthanide complexes, $[Ln.Lc]^{3+}$ and [Ln.Ld] have been shown to act as effective NMR, luminescent and chiroptical probes for the signalling of a variety of anions.The nature of the axial donor has been shown to play a prominent role in determining NMR, emission and CD spectral characteristics. Increasing the polarisability of the axial donor leads to a smaller NMR shift, a shorter wavelength of the CD band centres around 990 nm, a larger $\Delta J = 2/\Delta J = 1$ band intensity ratio and a larger $\Delta J = 1$ splitting (cm^{-1}).

The apparent absence of kinetic resolution in complex formation between the neutral [Yb.Ld] and racemic α-hydroxy acids augurs well for the development of such systems as aqueous chiral derivatising agents. Furthermore, the chemical shift non-equivalence ($\Delta\Delta\delta$~5 ppm) and large lanthanide induced shifts exhibited by this unique chiral derivatising agent can be compared to values reported in the literature for shift reagents which are generally < 0.1 ppm. Enantioselectivity in complex formation was observed with the neutral [Yb.Ld] system with some of the amino acids, hence it is unsuitable as a chiral derivatising agent for amino acids. However, the S-amino acid adducts always experienced a greater lanthanide induced shift compared to the R-adducts, therefore such complexes may be effectively used to determine the absolute configuration of α–amino acids in aqueous media. Furthermore, the neutral [Ln.Ld] complexes bind effectively to a variety of phosphorylated species via monodentate chelation through the phosphate moiety. The large ^{31}P lanthanide induced NMR shifts of the bound adducts are highly sensitive to the nature of the phosphorylated species, each adduct experiencing a unique lanthanide induced shift, therefore such systems may be used as effective aqueous probes for phosphorylated species.

References

1. Supramolecular Chemistry of Anions, Eds. A. Bianchi, K. Bowman-James, E. Garcia-Espana, Wiley-VCH, New York, 1997.
2. P. D. Beer, and P. A. Gale, *Angew. Chem. Int. Ed.*, 2001, **40**, 486
3. D. Voet, J. G. Voet, 'Biochemistry', Wiley, 1995, New York, Chapter 1.
4. D. Voet, J. G. Voet, 'Biochemistry', Wiley, 1995, New York, Chapter 14.
5. Y. Marcus, *J. Chem. Soc., Faraday Trans.*, 1991, **87**, 2995.
6. E. Graf, and J.M. Lehn, *Helv. Chim. Acta,* 1981, **64**, 1040.
7. F. P. Schmidtchen, *Chem. Ber.*, 1981, **114**, 597.
8. K. Worm, and F. P. Schmidtchen, *Angew. Chem., Int. Ed. Engl.*, 1995, **34**, 65.
9. Y. Inoue, T. Hakushi, Y. Liu, L. H. Tong, B. J. Shen, and D. S. Jin, *J. Am. Chem. Soc.*, 1993, **115**, 475.
10. T. R. Kelley, and M. H. Kim, *J. Am. Chem. Soc.*, 1994, **116**, 7072.
11. C. H. Park, and H. E. Simmons, *J. Am. Chem. Soc.*, 1968, **90**, 2431.
12. A. Echavarren, A. Galan, J. de Mendoza, A. Salmeron, and J.-M. Lehn, *J. Am. Chem. Soc.*, 1089, **111**, 4994.
13. D. Parker, *Chem. Soc. Rev.*, 2004, **33**, 156.
14. P. D. Beer, *Acc. Chem. Res.*, 1998, **31**,71.
15. D. Parker, K. Senanayake, and J. A. G. Williams, *J. Chem. Soc., Perkin Trans.*, 2, 1998, 2129.
16. Y. Bretonniere, M. J. Canñ, D. Parker, and R. Slater, *Org. Biomol. Chem.*, 2004, **2**, 1624.
17. H. Tsukube, S. Shinoda, and H. Tamiaki, *Coord. Chem. Rev.*, 2002, **226**, 227.
18. J. I. Bruce, R. S. Dickins, L. J.Govenlock, T. Gunnlaugsson, S. Lopinski, M. P. Lowe, D. Parker, R. D. Peacock, J. J. B. Perry, S. Aime, and M. Botta, *J. Am. Chem. Soc.*, 2000, **122**, 9674.
19. G. Bobba, R. S. Dickins, S. D. Kean, C. E. Mathieu, D. Parker, R. D. Peacock, G. Siligardi, M. J. Smith, J. A. G. Williams, and C. F. G. C. Geraldes, *J. Chem. Soc. Perkin Trans. 2,* 2001, 1729.
20. R. S. Dickins, S. Aime, A. S. Batsanov, A. Beeby, M. Botta, J. I. Bruce, J. A. K. Howard, C. S. Love, D. Parker, R. D. Peacock, and H. Puschmann, *J. Am. Chem. Soc.*, 2002, **124**, 12697.
21. B. J. Bleaney, *J. Magn. Reson.*, 1972, **8**, 91.
22. I. Bertini, and C. H. Luchinat, *Coord. Chem. Rev.*, 1996, **150**, 1.
23. L. Di Bari, G. Pintacuda, P. Salvadori, R. S. Dickins, and D. Parker, *J. Am. Chem. Soc.*, 2000, **122**, 9257.
24. J. I. Bruce, D. Parker, and D. J. Tozer, *Chem. Commun.*, 2001, 2250.
25. F. S. Richardson, *Inorg. Chem.*, 1980, **19**, 2806.
26. R. S. Dickins, D. Parker, J. I. Bruce, and D. J. Tozer, *Dalton Trans.*, 2003, 1264.
27. D. Parker, R. S. Dickins, H. Puschmann, C. Crossland, and J. A. K. Howard, *Chem. Rev.*, 2002, **102**, 1977.
28. B. R. McGarvey, *J. Magn. Reson.*, 1979, **33**, 445.
29. J. M. Ren, S. R. Zhang, A. D. Sherry, and C. F. G. C. Geraldes, *Inorg. Chim. Acta,* 2002, **339**, 273.
30. R. D. Peacock, *Struct. Bonding,* 1975, **22**, 83.

31. M. F. Reid, and F. S. Richardson, *J. Phys. Chem.*, 1984, **88**, 3579.
32. D. Parker, *Chem. Soc. Rev.*, 2004, **33**, 156.
33. R. S. Dickins, A. S. Batsanov, D. Parker, H. Puschman, S. Salamano, and J. A. K. Howard, *Dalton Trans.*, 2004, **1**, 70.
34. A. Beeby, I. M. Clarkson, R. S. Dickins, S. Faulkner, D. Parker, L. Royle, A. S. de Sousa, J. A. G. Williams, and M. Woods, *J. Chem. Soc., Perkin Trans. 2*, 1999, 493.
35. T. J. Wenzel, and J. D. Wilcox, *Chirality*, 2003, **15**, 256.
36. D. Parker, *Chem. Rev.*, 1991, **91**, 1441.
37. R. Hazama, K. Umakoshi, C. Kabuto, and Y. Sasaki, *Chem. Commun.*, 1996, 15.
38. M. Watanabe, T. Hasegawa, H. Miyake, and Y. Koijma, *Chem. Lett.*, 2001, 4.
39. R. S. Dickins, C. S. Love, and H. Puschmann, *Chem. Commun.*, 2001, **22**, 2308.
40. C. K. Mathews, and K. E. van Holde, 'Biochemistry', Benjamin/Cummings, Redwood City, 1990, Chapter 5.
41. H. Tamiaki, N. Matsumoto, S. Unno, S. Shinoda, and H. Tsukube, *Inorg. Chim. Acta*, 2000, **300**, 243.
42. H. Miyake, T. Yamashita, Y. Kojima, and H. Tsukube, *Tetrahedron. Lett.*, 1995, **36**, 7699.
43. Y. Kuruda, Y. Kato, T. Higashioji, J.Y. Hasegawa, S. Kawanami, M. Takahashi, N. Shiraishi, K. Tanabe, and H. Ogoshi, *J. Am. Chem. Soc.*, 1995, **117**, 10950.
44. I. Suzuki, K. Obata, J-I Anzai, H. Ikeda, and A. Ueno, *J. Chem. Soc., Perkin Trans. 2*, 2000, 1705.
45. H. Tsukube, H. Fukui, and S. Shinoda, *Tetrahedron Lett.*, 2001, **42**, 7583.
46. H. B. Silber, S. J. Parquette, 'Metal Ions in Biological Systems', Eds. A. Sigel, and H. Sigel, Marcel Dekker, New York, 2003, Chapter 3.
47. C. H. Evans, 'Biochemistry of the Lanthanides', Plenum Press, New York, 1990, Chapter 4.
48. G. A. Elgavish, and J. Reuben, *J. Magn. Reson.*, 1981, **42**, 242.
49. C. K. Mathews, and K. E. van Holde, 'Biochemistry', Benjamin/Cummings, Redwood City, 1990.
50. S-H. Li, W-T. Yuan, C-Q. Zhu, and J-G. Xu, *Anal. Biochem.*, 2004, **331**, 235.
51. J. A. Adam, *Chem. Rev.*, 2001, **101**, 2271.
52. A. Ojida, Y. Mito-oka, K. Sada, and I. Hamachi, *J. Am. Chem. Soc.*, 2004, **126**, 2454.
53. P. Atkinson, Y. Bretonniere, and D. Parker, *Chem. Commun.*, 2004, 438.

CHAPTER 4

Experimental

4.1 General Synthetic Procedures and Characterisation

4.1.1 Reaction Conditions

Reactions requiring anhydrous or inert conditions were carried out using Schlenk-line techniques under an atmosphere of dry argon. Anhydrous solvents, when required, were freshly distilled over the appropriate drying agent. Water was purified by the 'Purite$_{STILL}$ plus' system.

4.1.2 Purification Procedures

Thin-layer chromatography was carried out on neutral alumina plates (Merck Art 5550) or silica plates (Merck 5554) and visualised under UV (254 nm) or by staining with iodine. Preparative column chromatography was carried out using neutral alumina (Merck Aluminium Oxide 90, activity II-III, 70-230 mesh), pre-soaked in ethyl acetate, or silica (Merck Silica Gel 60, 230-400 mesh). Cationic exchange chromatography was performed using Dowex 50W strong ion exchange resin, which was pre-treated with hydrochloric acid (3 M).

4.1.3 Characterisation Techniques

Infra-Red spectra were recorded on a Perkin-Elmer 1600 FT-IR operating with GRAMS Analyst software. Oils were examined as thin films and solids incorporated into KBr discs as stated.

Melting points were recorded using a Köfler block and are uncorrected.

^{1}H, ^{13}C and ^{31}P NMR spectra were recorded on a Varian VXR console (^{1}H at 65.15 MHz), Varian Mercury 200 (^{1}H at 199.975 MHz, ^{13}C at 50.289 MHz, ^{31}P at 80.957 MHz), Varian Unity 300 (^{1}H at 299.908 MHz, ^{13}C at 75.412 MHz), Varian Mercury 400 (^{1}H at 399.968 MHz, ^{13}C at 100.572 MHz), or a Varian Inova 500 (^{1}H at 499.7 MHz, ^{13}C at 125.67 MHz, ^{31}P at 201.310 MHz) spectrometer. Two–dimensional and ^{1}H variable temperature spectra were carried out on a Varian Inova 500 spectrometer. Spectra were referenced internally relative to *tert*-butanol for paramagnetic

complexes or to the residual protio-solvent resonances which are reported relative to TMS. All chemical shifts are given in ppm and coupling constants are in Hz.

Electrospray mass spectra were recorded on a VG Platform II (Fisons instrument), operating in positive or negative ion mode as stated, with methanol as the carrier solvent. Accurate mass spectra were recorded at the EPSRC Mass Spectrometry Service at the University of Wales, Swansea.

4.2 General Luminescence Procedures

UV

Ultraviolet absorbance spectra were recorded on a Unicam UV2-100 spectrometer operating with Unicam Vision software. Samples were contained in quartz cuvettes with a path length of 1 cm. All spectra were run against a reference of pure solvent contained in a matched cell.

Excited State Lifetime

Lifetimes were measured on a Perkin-Elmer LS55 spectrofluorimeter using FL WinLab Software. Reported decay rates are the average of at least 3 separate measurements calculated by monitoring the emission intensity, at 545 nm for Tb^{3+}, after at least 20 different delay times, covering 2 or more lifetimes. The gate time was 0.1 ms and the excitation and emission slits were set to 15 nm bandpass. The phosphorescence decay curves were fitted by an equation of the form $I(t) = I(0)\exp(-t/\tau)$ using a curve fitting program, operating in Microsoft Excel, where I(0) is the initial intensity at $t = 0$ and I(t) is the intensity after time t and τ is the phosphorescence lifetime.

Emission

The emission spectra were recorded on an instrument S.A. Fluorolog 3, operating with DataMax software. Quartz fluorescence cuvettes of path length 1 cm were employed. The absorbance of each solution at the excitation wavelength was below

0.3 to avoid inner filter effects. Second order diffraction effects were obviated by using a 420 nm cut-off filter to remove the scattered light before it enters the emission monochromator. Eu^{3+} spectra were recorded between 570 nm and 730 nm, at 0.5 nm increments with 1 s integration time. Direct excitation at 397 nm was used for $[Eu.Lc]^{3+}$ **19** and [Eu.Ld] **35**, while sensitized emission at 254 nm was used for $[Eu.La]^{3+}$ **13**, [Eu.Lb] **29**, $[Eu.Le]^{3+}$ **26** and [Eu.Lf] **42**. Excitation and emission slits were 10 and 1 nm respectively.

4.3 Circular Dichroism

The NIR-CD spectra were recorded on a JASCO J-180 spectropolarimeter using a 150W air cooled xenon lamp, head-on photomultiplier tube and photoelastic modulator. Measurements were recorded in 1 cm quartz cuvettes at 25 °C. Spectra were recorded between 1050 to 920 nm using a continuous scanning method at 0.2 nm intervals with a speed of 20 nm min^{-1} and response time of 2 s. The band width was 2 nm, slit width 60 μm and 4 scans were taken per spectrum. A baseline spectrum of the solvent was taken in the same cuvette in the same orientation with respect to the light beam. This was subsequently subtracted from the spectra.

4.4 Synthetic Procedures and Characterisation for Chapter 2

Phenylalanine Systems

1. 2-Chloro-N-[(S)[1- ethoxycarbonyl-2-phenyl] ethyl] ethanamide

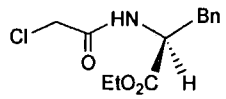

S-Phenylalaninethylester hydrochloride (3.00 g, 13.1 mmol) was dissolved in dry diethyl ether (100 ml) under argon and triethylamine (4.37 ml, 31.3 mmol) was added. The solution was cooled to –20 °C (acetone, CO_2 (s) bath) and

chloroacetylchloride (1.25 ml, 15.7 mmol) in dry diethyl ether (60 ml) was added dropwise, maintaining the temperature at –20 °C. The reaction mixture was allowed to warm to room temperature and stirred for 1 h. The resulting white precipitate was dissolved in water (60 ml) and the organic layer washed with hydrochloric acid (0.1 M, 80 ml), water (3 x 80 ml), dried (K_2CO_3) and the solvent was removed *in vacuo* to give a pale yellow solid. The product was recrystallised from ether adding hexane and was isolated as white needles (2.47 g, 70%), m.p. 38-40 °C; ν_{max} (solid)/cm^{-1} 3310 (NH), 1731 (COO), 1650 (CONH); ^1H NMR (200 MHz, $CDCl_3$) δ 7.30-7.10 (5H, m, Ar), 7.00 (1H, br s, NH), 4.84 (1H, m, CH), 4.17 (2H, q, ^3J = 7.2, CH_2O), 4.00 (2H, s, CH_2Cl), 3.14 (2H, d, ^3J = 5.8, CH_2Ph), 1.24 (3H, t, ^3J = 7, CH_3); ^{13}C NMR (50.29 MHz, $CDCl_3$) δ 171.2 (CO_2Et), 166.4 (CONH), 136.0 (ipso-Ar), 129.5 (m-Ar), 128.7 (o-Ar), 127.3 (p-Ar), 61.8 (OCH_2), 53.9 (CH), 42.6 (CH_2Cl), 37.8 (CH_2Ph), 14.2 (CH_3); m/z (ES^+) 292 (100%, MNa^+), 561 (90%, M_2Na^+), 270 (20%, MH^+) (Found: C, 57.7; H, 5.98; N, 5.12. $C_{13}H_{16}NO_3Cl$ requires C, 57.9; H, 5.98; N, 5.16%).

3. 1,4,7–Tris-[(S)-((1-ethoxycarbonyl-2-phenyl)ethyl)carbamoylmethyl]-1,4,7,10-tetraazacyclododecane

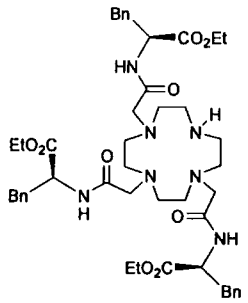

1,4,7,10-Tetraazacyclododecane (0.214 g, 1.24 mmol) was dissolved in ethanol (40 ml) and triethylamine (0.518 ml, 3.72 mmol) was added. Compound **1** (1.00 g, 3.72 mmol) in ethanol (20 ml) was added dropwise over 6 h to the stirred solution under an argon atmosphere, at room temperature. The reaction mixture was heated at 60 °C under argon and stirred overnight and then the temperature was increased to 90 °C and the mixture was stirred under argon for 5 days. The solvent was removed *in vacuo* and the reaction mixture was dissolved in dichloromethane (30 ml) and

washed quickly with purite water (3 x 30 ml) to remove traces of diamide. The organic phase was then washed exhaustively with purite water (7 x 30 ml) and the aqueous phase was concentrated to dryness to give the product as a white solid (0.443 g, 41%), m.p. 100-103 °C; ν_{max} (solid)/cm^{-1} 1736 (COO), 1659 (CONH); ^{1}H NMR (200 MHz, $CDCl_3$) δ 7.6 (2H, d, ^{3}J = 8, NHCO), 7.4 (1H, d, ^{3}J = 8, NHCO), 7.30-7.00 (15H, m, Ar), 4.63 (3H, m, CH), 4.03 (6H, m, OCH_2), 3.45-2.78 (29H, m, ring-CH_2, ring-NH, CH_2Ph, CH_2CO), 1.12 (9H, m, CH_3); ^{13}C NMR (62.9 MHz, $CDCl_3$) δ 172.0 (CO_2Et), 170.0 (CONH), 137.0 (ipso-Ar), 129.3 (m-Ar), 128.5 (o-Ar), 126.9 (p-Ar), 61.5 (OCH_2), 58.0-52.0 (ring-CH_2, CH, CH_2CO), 44.0 (ring-CH_2), 38.1 (CH_2Ph), 13.99 (CH_3); m/z (ES$^+$) 456 (100%, MCa $^{2+}$), 872 (5%, MH$^+$).
(See compound **10 (La)** for a better alternative route).

4. 8b-Methyl-decahydro-2a, 4a, 6a, 8a-tetraazacyclopent[*fg*] acenaphthylene

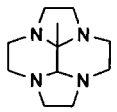

1,4,7,10-Tetraazacyclododecane (1 g, 5.80 mmol) was dissolved in purite water (20 ml) and acetonitrile (30 ml) with stirring and the solution was cooled to 4 °C (ice bath). A solution of pyruvic aldehyde (1.04 g, 5.80 mmol) in purite water was added dropwise and the reaction mixture was stirred at room temperature for 4 h. The solvent was then removed *in vacuo* and the residue was chromatographed over an alumina plug, eluting with dichloromethane. The product was isolated as an orange oil (0.89 g, 74%); ^{1}H NMR (300 MHz, $CDCl_3$) δ 2.75-2.40 (17H, m, ring-CH_2, CH), 0.89 (3H, s, CH_3); ^{13}C NMR (75.4 MHz, $CDCl_3$) δ 80.4 (C), 75.4 (CH), 46.6, 47.8, 49.9, 50.5 (ring-CH_2); m/z (ES$^+$) 231 (100%, MNa$^+$), 209 (70%, MH$^+$), 440 (40%, M_2Na^+).

5. 2a-Benzyl-8b-Methyl-decahydro-2a, 4a, 6a, 8a-tetraazacyclopent[*fg*] acenaphthylene

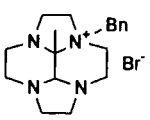

Compound **4** (0.89 g, 4.28 mmol) was dissolved in acetonitrile (10 ml) and benzylbromide (0.732 g, 4.28 mmol) was added. The mixture was stirred at room temperature for 24 h. The solvent was removed *in vacuo*, giving the product as a red solid (1.94 g, 92%); ^{1}H NMR (200 MHz, CD_3OD) δ 7.55 (5H, m, Ar), 3.71-3.12 (19H, br m, ring-CH_2, CH, CH_2Ph), 2.04 (3H, s, CH_3); ^{13}C NMR (50.29 MHz, CD_3OD) δ 132.2-126.7(Ar), 116.6 (CH_2Ph), 84.6 (C), 78.8 (CH), 48.1, 47.7, 47.3, 46.8, 46.4, 45.9, 45.6 (ring-CH_2), 19.3 (CH_3); m/z (ES^+) 299 (100%, M^+).

6. 1,4,7,10-Tetraazacyclododecane-molybdenum tricarbonyl[1]

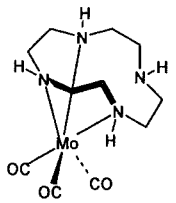

Dry dibutyl ether (50 ml) was added to 1,4,7,10-tetraazacyclododecane (1.5 g, 8.71 mmol) with stirring and the air in the reaction vessel was replaced with argon. Molybdenum hexacarbonyl (2.27 g, 8.71 mmol) was added and the reaction mixture was heated at reflux under argon for 2 h to give a bright yellow molybdenum tricarbonyl complex precipitate. The mixture was allowed to cool to room temperature and the yellow air sensitive product was filtered under argon and dried under vacuum (2.75 g, 90%).

7. 1-Benzyl-1,4,7,10-tetraazacyclododecane[1]

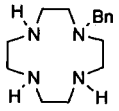

Benzylbromide (0.94 ml, 7.87 mmol) was added to compound **6** (2.75 g, 7.87 mmol) and fine mesh anhydrous potassium carbonate (1.52 g, 10.2 mmol) in degassed dry dimethylformamide (35 ml) and the reaction mixture was heated to 60 °C under an argon atmosphere for 2.5 h. The solvent was distilled off under vacuum and the

residue was taken up in a hydrochloric acid solution (1 M, 30 ml) and stirred under an air atmosphere for 18 h. The solid was removed by centrifugation and the aqueous supernatant was basified to pH 12 (NaOH pellets), washed with dichloromethane (3 x 30 ml) and the combined organic phases were dried (K_2CO_3). The solvent was removed under vacuum to give the product as a yellow green solid (0.87 g, 42%), m.p. 78-80 °C [Lit.[1] 78-79 °C]; ^{1}H NMR (200 MHz, $CDCl_3$) δ 7.34-7.18 (5H, m, Ar), 3.61 (2H, s, NCH_2Ph), 2.83-2.54 (19H, m, ring-CH_2, NH); [Lit.[1] (200 MHz, $CDCl_3$) δ 6.95 (5H, m, Ar), 3.25 (2H, s, NCH_2Ph), 2.10-2.50 (19H, m, ring-CH_2, NH)]; ^{13}C NMR (50.29 MHz, $CDCl_3$) δ 139.1, 128.9, 128.4, 127 (Ar), 59.3 (NCH_2Ph), 51.3, 47.2, 46.3, 45.1 (ring-CH_2); [Lit.[1] (50.29 MHz, $CDCl_3$) δ 139.1, 129.1, 128.5, 127.2 (Ar), 59.4 (NCH_2Ph), 51.5, 47.4, 46.6, 45.3 (ring-CH_2)]; m/z (ES^+) 285 (100%, MNa^+), 301 (80%, MK^+), 263 (30%, MH^+) (Found: MH^+, 263.2235. $C_{15}H_{27}N_4$ requires MH^+, 263.2236). [Lit.[1] Found: MH^+, 263.2194].

8. 1-Benzyl-4,7,10–Tris-[(S)-((1-ethoxycarbonyl-2-phenyl)ethyl) carbamoylmethyl]-1,4,7,10-tetraazacyclododecane

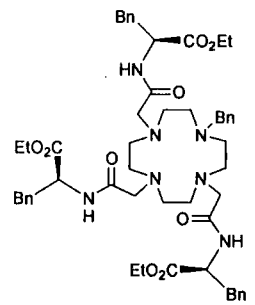

Compound **1** (2.68 g, 9.96 mmol) in dry N,N-dimethylformamide (5 ml) was added to a stirred solution of compound **7** (0.872 g, 3.32 mmol) and fine mesh anhydrous potassium carbonate (1.37 g, 9.96 mmol) in dry N,N-dimethylformamide (25 ml). The reaction mixture was heated at 60 °C under an argon atmosphere for 36 h. The solvent was distilled off under vacuum and the resulting brown oil was extracted into dichloromethane (40 ml), washed with purite water (3 x 40 ml), brine (40 ml), dried (K_2CO_3) and concentrated to dryness to give a yellow brown oil. The mixture was purified by alumina column chromatography (gradient elution from dichloromethane

to 0.5% methanol-dichloromethane) and the product was isolated as a pale yellow oil (1.54 g, 48 %); R_f (Al_2O_3; 10% CH_3OH-CH_2Cl_2; I_2 and u.v. detection) 0.5; ^1H NMR (200 MHz, $CDCl_3$) δ 7.8 (1H, br s, NHCO), 7.5 (2H, br s, NHCO), 7.3-7.0 (20H, m, Ar), 4.7 (3H, m, CH), 4.01 (6H, m, OCH_2), 3.8-2.2 (30H, m, ring-CH_2, CH_2CO, CH_2Ph, NCH_2Ph), 1.14 (9H, m, CH_3); ^{13}C NMR (50.29 MHz, $CDCl_3$) δ 171.8 (CO_2Et), 171 (CONH), 138.1 (ipso-Ar), 136.6 (ipso-Ar), 129.6, 129.3, 128.5, 127.1 (C-Ar*), 61.5 (OCH_2), 59.4-59.1 (br, NCH_2Ph, $N\underline{C}H_2CO$), 53.9- 52.0 (br, CH, ring-CH_2), 37.0 ($C\underline{C}H_2Ph$), 14.3 (CH_3); m/z (ES^+) 985 (100%, MNa^+), 963 (45%, MH^+), 501 (5%, MCa^{2+}).

*o, m, p-Ar resonances from the inequivalent aromatic rings appear to coincide.

10. 1,4,7–Tris-[(S)-((1-ethoxycarbonyl-2-phenyl)ethyl)carbamoylmethyl]-1,4,7,10-tetraazacyclododecane (La)

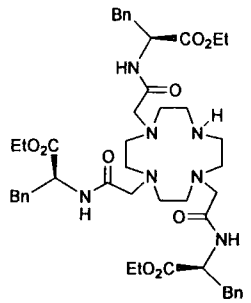

A hydrochloric acid solution (1 M, 1 ml) and a catalytic amount of palladium hydroxide on carbon were added to compound **8** (0.473 g, 0.49 mmol) in ethanol (25 ml) and the mixture was treated with hydrogen (45 psi) at room temperature for 48 h. The reaction mixture was filtered through celite and the solvent was removed under vacuum. The residue was taken into dichloromethane (30 ml) and washed with a solution of sodium bicarbonate (30 ml), brine (1 x 30 ml), dried (K_2CO_3) and concentrated to dryness to give the product as a pale yellow glassy solid (0.31 g, 71%), m.p. 84-88 °C; ν_{max} (solid)/cm^{-1} 1734 ($\underline{C}OO$), 1656 ($\underline{C}ONH$); ^1H NMR (200 MHz, $CDCl_3$) δ 7.6 (2H, d, ^3J = 8, NHCO), 7.4 (1H, d, ^3J = 8, NHCO), 7.30-7.00 (15H, m, Ar), 4.80 (3H, m, CH), 4.12 (6H, m, OCH_2), 3.45-2.20 (29H, m, ring-CH_2, ring-NH, CH_2Ph, CH_2CO), 1.12 (9H, m, CH_3); ^{13}C NMR (50.29 MHz, $CDCl_3$)

δ 172.1 (CO_2Et), 171.4 (CONH), 136.8 (ipso-Ar), 129.6 (m-Ar), 128.6 (o-Ar), 127 (p-Ar), 61.5 (OCH_2), 59.7 ($\underline{C}H_2CO$), 53.9-53.0 (ring-CH_2, CH), 47.3 (ring-CH_2), 37.8 (CH_2Ph), 14.3 (CH_3); m/z (ES^+) 456 (100%, MCa $^{2+}$) (A satisfactory accurate mass spectrum could not be obtained for this product).

12. $[Yb.La]^{3+}$

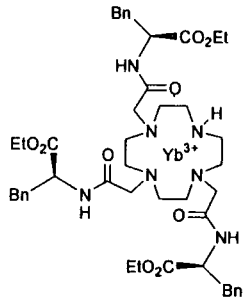

Ytterbium (III) triflate (0.099 g, 0.16 mmol) in dry acetonitrile (1 ml) was added to a solution of the ligand **10** (0.135 g, 0.16 mmol) in dry acetonitrile (4 ml) and the mixture was heated to reflux under argon overnight. The reaction solution was dropped onto stirring diethylether (50 ml) and the resulting white precipitate was collected by centrifugation and filtration. The solid was redissolved in the minimum amount of acetonitrile and the precipitation procedure repeated once more. A white solid resulted (0.134 g, 56%), m.p 142-144 °C; ν_{max} (solid)/cm^{-1} 1736 ($\underline{CO}O$), 1625 ($\underline{CO}NH$); ^1H NMR (200 MHz, CD_3OD) partial assignment δ major isomer 92.0 (1H, br s, ring-H_{ax}), 69.0 (1H, br s, ring-H_{ax}), 56.0 (1H, br s, ring-H_{ax}), 43.0 (1H, br s, ring-H_{ax}), 39.1 (1H, br s, ring-H_{eq}), 25.2 (1H, br s, ring-H_{eq}), 22.3 (1H, br s, ring-H_{eq}), 15.0 (1H, br s, ring-H_{eq}); δ minor isomer 96.0 (1H, br s, ring-H_{ax}), 67.0 (1H, br s, ring-H_{ax}), 59.0 (1H, br s, ring-H_{ax}), 43.0 (1H, br s, ring-H_{ax}), 41.0 (1H, br s, ring-H_{eq}), 27.0 (1H, br s, ring-H_{eq}), 23.0 (1H, br s, ring-H_{eq}), 19.0 (1H, br s, ring-H_{eq}); m/z (ES^+) 522 (100%, M^{2+}), 349 (5%, M^{3+}) (Found: M^{2+}, 522.2077. $C_{47}H_{64}N_7O_9Yb$ requires M^{2+}, 522.2077).

13. $[Eu.La]^{3+}$

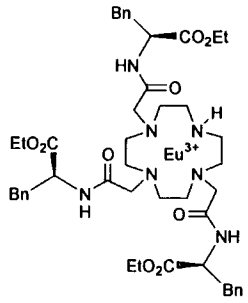

The title compound was prepared using a similar method to that for **12** using the ligand **10** (0.057 g, 0.065 mmol) in dry acetonitrile (2 ml) and europium (III) triflate (0.039 g, 0.065 mmol) in dry acetonitrile (3 ml) to yield a white solid (0.056 g, 59%), m.p. 146-148 °C ; ν_{max} (solid)/cm^{-1} 1734 (COO), 1619 (CONH); ^1H NMR (200 MHz, CD_3OD) partial assignment δ 24.1 (1H, br s, ring-H_{ax}), 14.0 (2H, br s, ring-H_{ax}), 12.3 (1H, br s, ring-H_{ax}), -5.20, -6.02, -9.34, -10.0, -12.4, -15.1, -20.0; m/z (ES^+) 512 (100%, M^{2+}), 587 (10%, $[M^{3+}+ (CF_3SO_3^-)]^{2+}$ (Found: M^{2+}, 511.6971. $C_{47}H_{64}N_7O_9Eu$ requires M^{2+}, 511.6989).

28. [Yb. Lb]

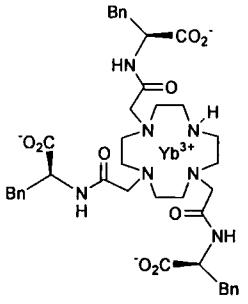

Compound **12** (0.100 g, 0.067 mmol) was dissolved in the minimum amount of methanol and treated with an aqueous sodium hydroxide solution (0.02 M, 13.4 ml). The solution was brought to pH 6, reduced to small volume and loaded onto a cationic exchange column (Dowex, 50 WH^+), eluting with water and then aqueous ammonia solution (6%). The ammonia layer was dried *in vacuo* giving the product as a yellow solid (0.035 g, 54%), m.p. > 250 °C; ν_{max} (solid)/cm^{-1} 1619 (br, CONH, COO); ^1H NMR (200 MHz, CD_3OD) partial assignment δ 90.0 (1H, br s, ring-H_{ax}), 64.0 (1H, br s, ring-H_{ax}), 52.0 (1H, br s, ring-H_{ax}), 27.0 (1H, br s, ring-H_{ax}), -22.9, -

25.1, -38.6, -46.7, -47.8, -49.9, -60.2, -82.3; m/z (ES^+) after addition of CF_3COOH: 959 (100%, MH^+) (Found: MH^+, 959.3137. $C_{41}H_{51}N_7O_9Yb$ requires MH^+ 951.3131).

29. [Eu.Lb]

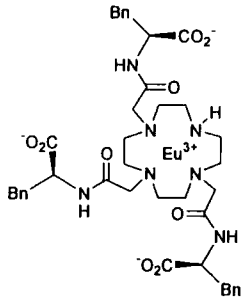

The title compound was prepared following a method similar for **28,** using compound **13** (0.150 g, 0.10 mmol), dissolved in the minimum amount of methanol and an aqueous sodium hydroxide solution (0.02 M, 20.4 ml). A yellow solid resulted (0.043 g, 45%), m.p. > 230 °C; ν_{max} (solid)/cm^{-1} 1612 (br, CONH, COO); ^1H NMR (200 MHz, CD_3OD) partial assignment not available, the spectrum showed broad signals between δ +30 and –20; m/z (ES^+) after addition of CF_3COOH: 938 (100%, MH^+) (Found: MH^+, 938.2962. $C_{41}H_{51}N_7O_9Eu$ requires MH^+ 938.2962).

Leucine Systems

2. 2-Chloro-N-[(S)[1-methoxycarbonyl-3-methyl] butyl] ethanamide

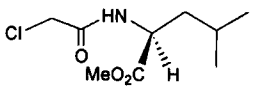

The title compound was prepared following a method similar to that for **1**, using S-leucinemethylester hydrochloride (3 g, 16.5 mmol) and triethylamine (5.52 ml, 39.6 mmol) in dry diethyl ether (100 ml) and reacting with a solution of chloroacetylchloride (1.58 ml, 19.8 mmol) in dry diethyl ether (60 ml). A brown oil resulted (3.21 g, 88%); ν_{max} (film)/cm^{-1} 3304 (NH), 1745 (COO), 1680 (CONH); ^1H NMR (200 MHz, $CDCl_3$) δ 6.90 (1H, br s, NH), 4.68-4.56 (1H, br m, CHNH), 4.04

(2H, s, $ClCH_2CO$), 3.72 (3H, s, OCH_3), 1.69-1.50 (3H, br m, $C\underline{H}_2C\underline{H}$), 0.92 (6H, d, ^3J = 5.8, CH_3); ^{13}C NMR (50.29 MHz, $CDCl_3$) δ 172.8 (CO_2Me), 166.6 (CONH), 52.2 (OCH_3), 51.0 (CHNH), 42.4 ($Cl\underline{C}H_2CO$), 40.7 ($\underline{C}H_2CH$), 24.7 ($CH_2\underline{C}H$), 22.7 (CH_3), 21.6 (CH_3); m/z (ES^+) 244 (100%, MNa^+) (Found: MNa^+, 244.0739. $C_9H_{16}NO_3NaCl$ requires MNa^+, 244.0716).

9. 1-Benzyl-4,7,10–tris-[(S)-((1-methoxycarbonyl-3-methyl)butyl) carbamoylmethyl]-1,4,7,10-tetraazacyclododecane (Le)

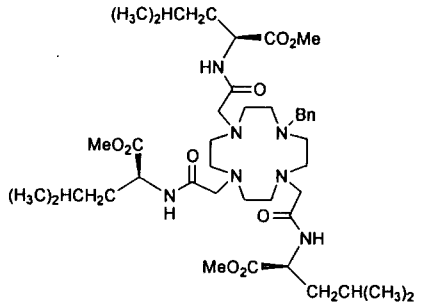

The title compound was prepared following a method similar to that for **8**, using compound **2** (1.33 g, 6.00 mmol) in dry N,N-dimethylformamide (5 ml) and reacting with a solution of compound **7** (0.526 g, 2.00 mmol) and fine mesh anhydrous potassium carbonate (0.830 g, 6.00 mmol) in dry N,N-dimethylformamide (25 ml). The product was obtained, after purification, as a brown oil (0.821 g, 50%); R_f (Al_2O_3; 10% CH_3OH-CH_2Cl_2; I_2 and u.v. detection) 0.38; ν_{max} (film)/cm^{-1} 1741 ($\underline{C}OO$), 1659 ($\underline{C}ONH$); ^1H NMR (200 MHz, $CDCl_3$) δ 8.0-7.8 (3H, br s, NHCO), 7.3-7.1 (5H, m, Ar), 4.5 (3H, m, $C\underline{H}NH$), 3.70-2.40 (33H, br m, ring-CH_2, CH_2CO, OCH_3, CH_2Ph), 1.58-1.40 (9H, br m, $C\underline{H}_2CH$, $CH_2C\underline{H}$), 0.87 (18H, m, CH_3); ^{13}C NMR (50.29 MHz, $CDCl_3$) δ 173.4 (CO_2Me), 173.2 (CO_2Me), 171.3 (CONH), 170.9 (CONH), 138.0 (ipso-Ar), 129.0, 128.5, 127.4 (C-Ar), 59.9-59.0 (br, NCH_2Ph, $N\underline{C}H_2CO$), 53.4-52.3 (br, ring-CH_2, OCH_3), 50.5 (CHNH), 41.3 ($\underline{C}H_2CH$), 25.1 ($CH_2\underline{C}H$), 23.0 (CH_3), 22.1 (CH_3); m/z (ES^+) 429 (100%, MCa^{2+}), 840 (30%, MNa^+) 440 (20%, MK^+Na^+) (Found: $(MHK)^{2+}$, 428.7514. $C_{42}H_{72}N_7O_9K$ requires $(MHK)^{2+}$, 428.7542).

11. 1,4,7–Tris-[(S)-((1-methoxycarbonyl-3-methyl)butyl) carbamoylmethyl]-1,4,7,10-tetraazacyclododecane (Lc)

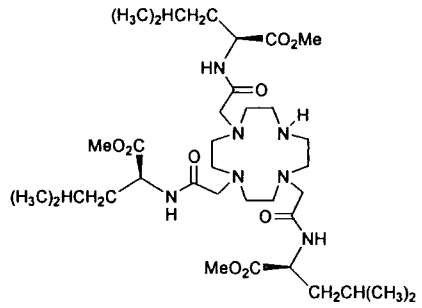

The title compound was prepared following a method similar to that for **10**, treating a solution of compound **9** (1.07 g, 1.31 mmol) in ethanol (45 ml) with hydrogen (45 psi), in the presence of a hydrochloric acid solution (1 M, 1 ml) and a catalytic amount of palladium hydroxide on carbon. The product was obtained as a yellow orange glassy solid (0.77 g, 81%), m.p. 120-122 °C; ν_{max} (solid)/cm^{-1} 1739 (COO), 1665 (CONH); ^{1}H NMR (200 MHz, $CDCl_3$) δ 8.0-7.84.(3H, br s, NHCO), 80-2.55 (35H, br m, ring-CH_2, CH_2CO, OCH_3, ring-NH, CHNH), 2.00-1.20 (9H, br m, CH_2CH, CH_2CH), 1.00-0.87 (18H, br, CH_3); ^{13}C NMR (50.29 MHz, $CDCl_3$) δ 173.8 (CO_2Me), 173.4 (CO_2Me), 171.6 (CONH), 171.5 (CONH), 59.6 (br, NCH_2CO), 53.8-52.3 (br, ring-CH_2, OCH_3), 50.7 (CHNH), 47 (ring-CH_2), 41.3 (CH_2CH), 25.1 (CH_2CH), 23.0 (CH_3), 21.1 (CH_3); m/z (ES$^+$) 384 (100%, MCa^{2+}), 728 (15%, MH^+) 766 (5%, MK^+) (Found: MH^+, 728.4878. $C_{35}H_{66}N_7O_9$ requires MH^+, 728.4922).

Cationic Complexes of Ligand Lc

14. [Yb.Lc]$^{3+}$

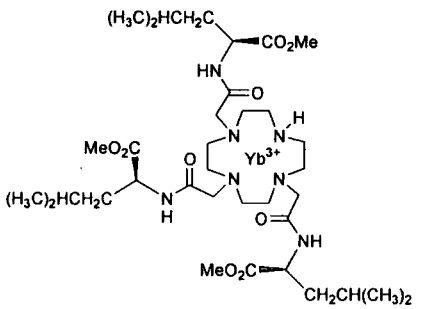

The title compound was prepared following a method similar for **12**, using ytterbium (III) triflate (0.44 g, 0.72 mmol) in dry acetonitrile (3 ml) and the ligand **11** (0.512 g, 0.72 mmol) in dry acetonitrile (4 ml). A yellow solid resulted (0.70 g, 75%), m.p. 142-144 °C; ν_{max} (solid)/cm^{-1} 1742 (COO), 1627 (CONH); ^{1}H NMR (200 MHz, CD_3OD) partial assignment δ 119.5 (1H, br s, ring-H_{ax}), 76.4 (1H, br s, ring-H_{ax}), 67.8 (1H, br, ring-H_{ax}), 53.9 (1H, br, ring-H_{ax}), 43.0 (1H, br s, ring-H_{eq}), 35.8 (1H, br s, ring-H_{eq}), 31.9 (1H, br s, ring-H_{eq}), 27.0 (1H, br, ring-H_{eq}), 12.1, -17.5, -19.1, -29.7, -33.8, -36.3, -41.1, -42.8, -48.5, -78.1, -91.0; m/z (ES$^+$) 450 (100%, M^{2+}) (Found: M^{2+}, 450.2109. $C_{35}H_{64}N_7O_9Yb$ requires M^{2+} 450.2077).

15. [Ce.Lc]$^{3+}$

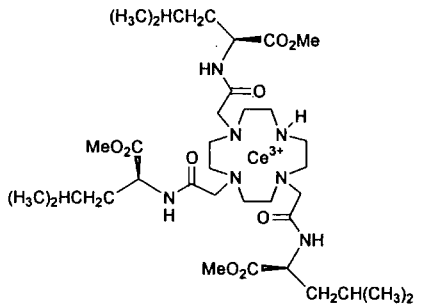

The title compound was prepared following a method similar for **12**, using cerium (III) triflate (0.056 g, 0.096 mmol) in dry acetonitrile (2 ml) and the ligand **11** (0.070 g, 0.096 mmol) in dry acetonitrile (2 ml). A yellow solid resulted (0.090 g, 71%), m.p. > 174 °C (dec.); ν_{max} (solid)/cm^{-1} 1742 (COO), 1627 (CONH); ^{1}H NMR (200 MHz, CD_3OD) partial assignment δ 15.0, 13.9, 10.4, 10.1, 8.14, 6.68, 6.1, -1.23, -3.92, -4.60, -8.12 (1H, br s, ring-H_{ax}), -12.1 (1H, br s, ring-H_{ax}); m/z (ES$^+$) 509 (100%, $[M^{3+} + (CF_3SO_3^-)]^{2+}$), 1164 (20%, $[M^{3+} + (CF_3SO_3^-)_2]^+$ (Found: M^{2+}, 433.1927. $C_{35}H_{64}N_7O_9Ce$ requires M^{2+} 433.1910).

16. $[Pr.Lc]^{3+}$

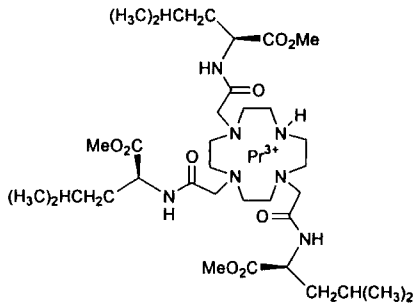

The title compound was prepared following a method similar for **12**, using praseodymium (III) triflate (0.283 g, 0.48 mmol) in dry acetonitrile (3 ml) and the ligand **11** (0.350 g, 0.48 mmol) in dry acetonitrile (3 ml). A yellow solid resulted (0.609 g, 96%), m.p. > 184 °C (dec.); ν_{max} (solid)/cm^{-1} 1742 (COO), 1627 (CONH); ^1H NMR (200 MHz, CD_3OD) partial assignment δ 25.1, 24.0, 20.71, 14.6, 11.8, 11.04, 8.94, 6.35, -2.0, -5.0, -7.2, -11.2, -13.8 (2H, br s, ring-H_{ax}), -17.1 (1H, br s, ring-H_{ax}), -29.9 (1H, br s, ring-H_{ax}); m/z (ES^+) 434 (100%, M^{2+}), 509 (40%, $[M^{3+} + (CF_3SO_3^-)]^{2+}$) (Found: $[M^{3+} + (CF_3SO_3^-)_2]^+$, 1166.3008. $C_{37}H_{65}N_7O_{15}F_6S_2Pr$ requires $[M^{3+} + (CF_3SO_3^-)_2]^+$ 1166.2961).

17. $[Nd.Lc]^{3+}$

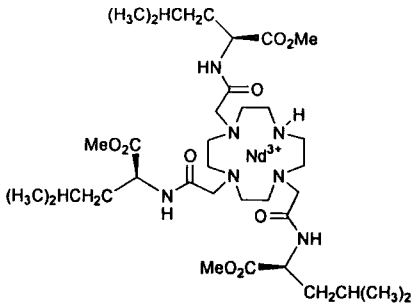

The title compound was prepared following a method similar for **12**, using neodymium (III) triflate (0.057 g, 0.096 mmol) in dry acetonitrile (2 ml) and the ligand **11** (0.070 g, 0.096 mmol) in dry acetonitrile (2 ml). A yellow solid resulted (0.093 g, 73%), m.p. > 180 °C (dec.); ν_{max} (solid)/cm^{-1} 1742 (COO), 1627 (CONH); ^1H NMR (200 MHz, CD_3OD) partial assignment δ 16.3, 15.3, 13.5, 10.2, 9.58, 9.03,

8.66, 5.96, -2.45, -6.03, -8.81, -16.3 (1H, br s, ring-H_{ax}); m/z (ES^+) 511 (100%, $[M^{3+} + (CF_3SO_3^-)]^{2+}$) (Found: M^{2+}, 434.1938. $C_{35}H_{64}N_7O_9Nd$ requires M^{2+} 434.1922).

18. $[Sm.Lc]^{3+}$

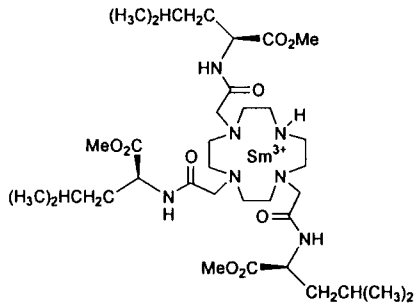

The title compound was prepared following a method similar for **12**, using samarium (III) triflate (0.074 g, 0.123 mmol) in dry acetonitrile (2 ml) and the ligand **11** (0.090 g, 0.123 mmol) in dry acetonitrile (2 ml). A yellow solid resulted (0.120 g, 73%), m.p. > 184 °C (dec.); ν_{max} (solid)/cm^{-1} 1742 (COO), 1627 (CONH); m/z (ES^+) 514 (100%, $[M^{3+} + (CF_3SO_3^-)]^{2+}$), 1176 (10%, $[M^{3+} + (CF_3SO_3^-)_2]^+$) (Found: M^{2+}, 439.2024. $C_{35}H_{64}N_7O_9Sm$ requires M^{2+} 439.1982).

19. $[Eu.Lc]^{3+}$

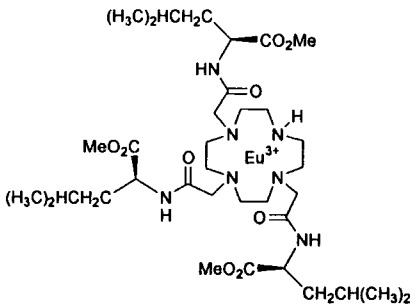

The title compound was prepared following a method similar for **12**, using europium (III) triflate (0.37 g, 0.62 mmol) in dry acetonitrile (3 ml) and the ligand **11** (0.450 g, 0.62 mmol) in dry acetonitrile (3 ml). A yellow solid resulted (0.713 g, 87%), m.p. > 178 °C (dec.); ν_{max} (solid)/cm^{-1} 1742 (COO), 1627 (CONH); ^1H NMR (200 MHz, CD_3OD) partial assignment δ 24.8 (1H, br s, ring-H_{ax}), 16.0 (1H, br s, ring-H_{ax}), 13.5 (1H, br s, ring-H_{ax}), 9.28 (1H, br s, ring-H_{eq}), -1.66, -4.83, -6.40, -7.33, -9.43, -11.6, -

13.6, -14.9, -19.0; m/z (ES^+) 440 (100%, M^{2+}), 514 (40%, $[M^{3+} + (CF_3SO_3^-)]^{2+}$) (Found: $[M^{3+} + (CF_3SO_3^-)_2]^+$, 1178.3163. $C_{37}H_{65}N_7O_{15}F_6S_2Eu$ requires $[M^{3+} + (CF_3SO_3^-)_2]^+$ 1178.3097).

20. $[Tb.Lc]^{3+}$

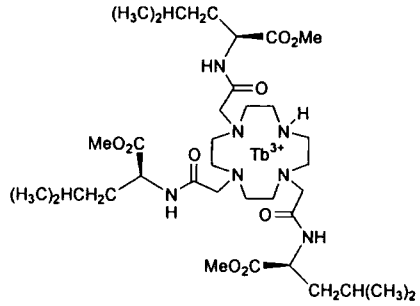

The title compound was prepared following a method similar for **12**, using terbium (III) triflate (0.075 g, 0.12 mmol) in dry acetonitrile (2 ml) and the ligand **11** (0.090 g, 0.12 mmol) in dry acetonitrile (2 ml). A yellow solid resulted (0.137 g, 83%), m.p. > 160 °C (dec.); ν_{max} (solid)/cm^{-1} 1742 (COO), 1627 (CONH); ^1H NMR (200 MHz, CD_3OD) partial assignment δ 81.3, -33.9, -55.6, -70.0, -85.2, -112.0, -126.4, -148.3, -166.9 (2H, br s, ring-H_{ax}), -234.8 (1H, br s, ring-H_{ax}), -319.7 (1H, br s, ring-H_{ax}); m/z (ES^+) 518 (100%, $[M^{3+} + (CF_3SO_3^-)]^{2+}$), 443 (60%, M^{2+}) (Found: M^{2+}, 442.7041. $C_{35}H_{64}N_7O_9Tb$ requires M^{2+} 442.7010).

21. $[Dy.Lc]^{3+}$

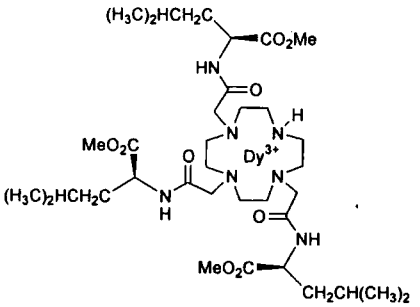

The title compound was prepared following a method similar for **12**, using dysprosium (III) triflate (0.075 g, 0.12 mmol) in dry acetonitrile (2 ml) and the ligand **11** (0.090 g, 0.12 mmol) in dry acetonitrile (2 ml). A yellow solid resulted (0.128 g,

77%), m.p. > 174 °C (dec.); ν_{max} (solid)/cm^{-1} 1742 (COO), 1627 (CONH); ^{1}H NMR (200 MHz, CD_3OD) partial assignment δ 300.0, 216.0, 191.4, 147.4, 133.6, 120.6, 91.5, 70.9, -62.3, -88.44, -113.3, -138.2, -158.4, -191.0 (1H, br s, ring-H_{ax}), -213.0 (1H, br s, ring-H_{ax}), -237.7 (1H, br s, ring-H_{ax}), -379.4 (1H, br s, ring-H_{ax}); m/z (ES$^+$) 444 (100%, M^{2+}), 520 (80%, $[M^{3+} + (CF_3SO_3^-)]^{2+}$), 1188 (5%, $[M^{3+} + (CF_3SO_3^-)_2]^{2+}$) (Found: M^{2+}, 445.2023. $C_{35}H_{64}N_7O_9Dy$ requires M^{2+} 445.2028).

22. $[Ho.Lc]^{3+}$

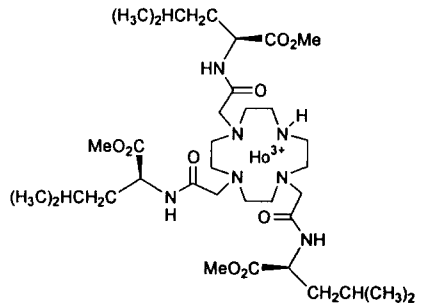

The title compound was prepared following a method similar for **12**, using holmium (III) triflate (0.29 g, 0.47 mmol) in dry acetonitrile (3 ml) and the ligand **11** (0.348 g, 0.47 mmol) in dry acetonitrile (3 ml). A yellow solid resulted (0.62 g, 97%), m.p. > 158 °C (dec.); ν_{max} (solid)/cm^{-1} 1742 (COO), 1627 (CONH); ^{1}H NMR (200 MHz, CD_3OD) partial assignment δ 191.3, 163.7, 110.8, 97.46, 81.0, 76.51, 74.0, 65.7, 61.0, 39.6, -14.8, -28.7, -59.10, -66.43, -79.81, -86.3 (1H, br s, ring-H_{ax}), -106.2 (1H, br s, ring-H_{ax}), -119.4 (1H, br s, ring-H_{ax}), -124.8 (1H, br s, ring-H_{ax}); m/z (ES$^+$) 446 (100%, M^{2+}) (Found: $[M^{3+} + (CF_3SO_3^-)_2]^+$, 1190.3165. $C_{37}H_{65}N_7O_{15}F_6S_2Ho$ requires $[M^{3+} + (CF_3SO_3^-)_2]^+$ 1190.3188).

23. $[Er.Lc]^{3+}$

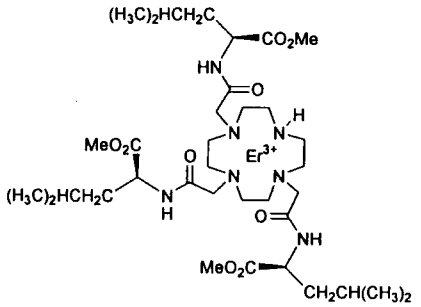

The title compound was prepared following a method similar for **12**, using erbium (III) triflate (0.076 g, 0.12 mmol) in dry acetonitrile (2 ml) and the ligand **11** (0.090 g, 0.12 mmol) in dry acetonitrile (2 ml). A yellow solid resulted (0.134 g, 81%), m.p. > 150 °C (dec.); ν_{max} (solid)/cm^{-1} 1742 (COO), 1627 (CONH); ^{1}H NMR (200 MHz, CD_3OD) partial assignment δ 117.6 (1H, br s, ring-H_{ax}), 78.1 (1H, br s, ring-H_{ax}), 54.2 (1H, br s, ring-H_{ax}), 50.8 (1H, br s, ring-H_{ax}), 30.2, 25.4, 20.6, -14.3, -17.9, -21.4, -28.4, -33.4, -41.9, -74.7; m/z (ES^+) 446 (100%, M^{2+}), 521 (80%, $[M^{3+} + (CF_3SO_3^-)]^{2+}$) (Found: M^{2+}, 446.2039. $C_{35}H_{64}N_7O_9Er$ requires M^{2+} 446.2034).

24. $[Tm.Lc]^{3+}$

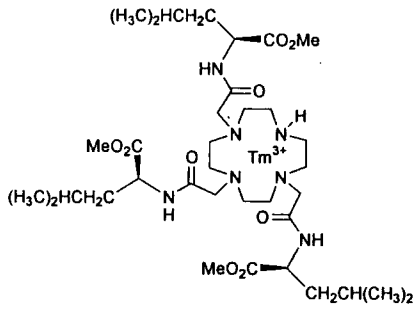

The title compound was prepared following a method similar for **12**, using thulium (III) triflate (0.076 g, 0.12 mmol) in dry acetonitrile (2 ml) and the ligand **11** (0.090 g, 0.12 mmol) in dry acetonitrile (2 ml). A yellow solid resulted (0.130 g, 78%), m.p. > 164 °C (dec.); ν_{max} (solid)/cm^{-1} 1742 (COO), 1627 (CONH); ^{1}H NMR (200 MHz, CD_3OD) partial assignment δ 293.0 (1H, br s, ring-H_{ax}), 261.9 (1H, br s, ring-H_{ax}), 228.0 (1H, br s, ring-H_{ax}), 179. (1H, br s, ring-H_{ax}), 136.5, 111.7, 70.7, 64.7, 30.6, -37.2, -44.1, -58.1, -77.3, -88.3, -96.8, -108.6, -130.7, -139.7, -175.2, -253.6; m/z (ES^+) 447 (100%, M^{2+}), 523 (15%, $[M^{3+} + (CF_3SO_3^-)]^{2+}$) (Found: M^{2+}, 447.7052. $C_{35}H_{64}N_7O_9Tm$ requires M^{2+} 447.7054).

Neutral Complexes of Ligand Ld

30. [Yb.Ld]

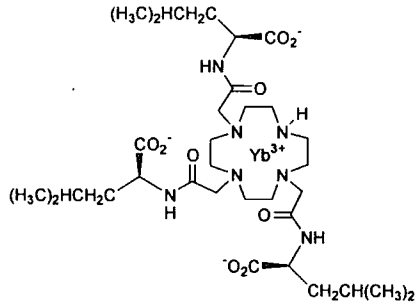

The title compound was prepared following a method similar to that for **28**, using compound **14** (0.25 g, 0.18 mmol), dissolved in the minimum amount of methanol and an aqueous sodium hydroxide solution (0.02 M, 37 ml). A yellow solid resulted (0.080 g, 50%), m.p. > 250 °C; ν_{max} (solid)/cm^{-1} 1625 (br, CONH, COO); ^{1}H NMR (200 MHz, CD_3OD) partial assignment δ 105.6 (1H, br s, ring-H_{ax}), 99.1 (1H, br s, ring-H_{ax}), 79.0 (1H, br s, ring-H_{ax}), 75.0 (1H, br s, ring-H_{ax}), 43.4 (1H, br s, ring-H_{eq}), 27.0 (3H, br s, ring-H_{eq}), 21.7, 18.7, 10.4, 8.15, -17.0, -22.8, -24.3, -33.0, -36.3, -46.7, -51.9, -54.3, -58.5, -61.7, -121.3; m/z (ES^+) after addition of CF_3COOH: 429 (100%, $[M + 2H^+]^{2+}$) (Found: MH^+, 857.3681. $C_{32}H_{57}N_7O_9Yb$ requires MH^+ 857.3607).

31. [Ce.Ld]

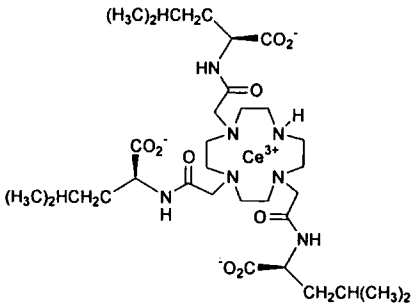

The title compound was prepared following a method similar to that for **28**, using compound **15** (0.090 g, 0.068 mmol), dissolved in the minimum amount of methanol and an aqueous sodium hydroxide solution (0.02 M, 13.5 ml). A yellow solid

resulted (0.032 g, 57%), m.p. > 250 °C; ν_{max} (solid)/cm^{-1} 1625 (br, CONH, COO); ^{1}H NMR (200 MHz, CD_3OD) partial assignment δ 19.4, 18.2, 17.1, 15.9, 13.3, 9.62, 8.89, 7.23, 6.59, -1.2, -1.80, -2.2, -2.73, -3.32, -9.96 (1H, br s, ring-H_{ax}), -10.94 (1H, br s, ring-H_{ax}), -15.0 (2H, br s, ring-H_{ax}); m/z (ES^+) after addition of CF_3COOH: 412 (100%, $[M + 2H^+]^{2+}$) (Found: MH^+, 823.3288 $C_{32}H_{57}N_7O_9Ce$ requires MH^+ 823.3272).

32. [Pr.Ld]

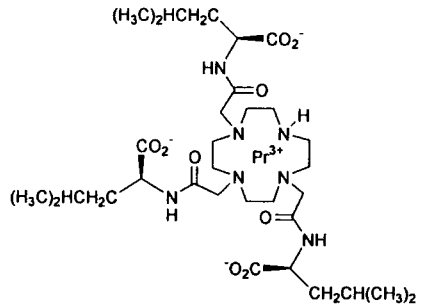

The title compound was prepared following a method similar to that for **29**, using compound **16** (0.400 g, 0.30 mmol), dissolved in the minimum amount of methanol and an aqueous sodium hydroxide solution (0.02 M, 76 ml). A yellow solid resulted (0.150 g, 60%), m.p. > 250 °C; ν_{max} (solid)/cm^{-1} 1625 (br, CONH, COO); ^{1}H NMR (200 MHz, CD_3OD) partial assignment δ 34.2, 32.2, 31.8, 27.0, 26.42, 21.3, 20.86, 15.82, 14.2, 13.0, 12.65, 10.9, -7.62, -23.4 (1H, br s, ring-H_{ax}), -24.0 (1H, br s, ring-H_{ax}), -27.1 (1H, br s, ring-H_{ax}), -33.1 (1H, br s, ring-H_{ax}); m/z (ES^+) after addition of CF_3COOH: 413 (100%, $[M + 2H^+]^{2+}$) (Found: MH^+, 824.3298 $C_{32}H_{57}N_7O_9Pr$ requires MH^+ 824.3294).

33. [Nd.Ld]

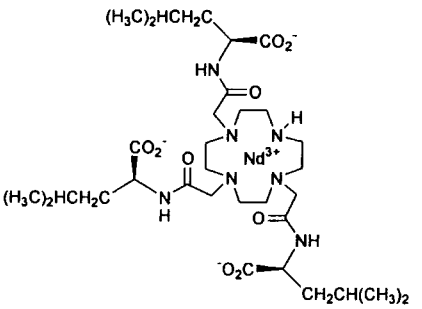

The title compound was prepared following a method similar to that for **28**, using **17** (0.090 g, 0.068 mmol), dissolved in the minimum amount of methanol, and an aqueous sodium hydroxide solution (0.02 M, 13.5 ml). A yellow solid resulted (0.025 g, 45%), m.p. > 260 °C; ν_{max} (solid)/cm^{-1} 1625 (br, CONH, COO); ^{1}H NMR (200 MHz, CD_3OD) partial assignment δ 17.5, 16.1, 11.8, 10.2, 9.77, 7.77, 7.20, 6.54, 9.91, 5.67, -11.2 (1H, br s, ring-H_{ax}), -12.0 (1H, br s, ring-H_{ax}), -15.78 (1H, br s, ring-H_{ax}), -16.7 (1H, br s, ring-H_{ax}); m/z (ES$^+$) after addition of CF_3COOH: 413 (100%, [M + 2H$^+$]$^{2+}$) (Found: MH$^+$, 825.3299 $C_{32}H_{57}N_7O_9Nd$ requires MH$^+$ 825.3289).

34. [Sm.Ld]

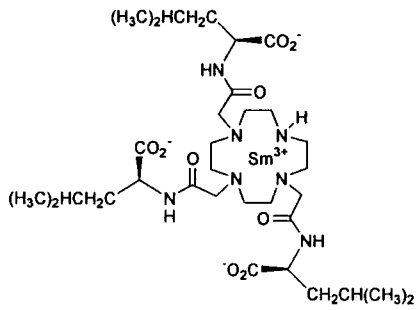

The title compound was prepared following a method similar to that for **28**, using compound **18** (0.090 g, 0.067 mmol), dissolved in the minimum amount of methanol and an aqueous sodium hydroxide solution (0.02 M, 13.6 ml). A yellow solid resulted (0.028 g, 50%), m.p. > 250 °C; ν_{max} (solid)/cm^{-1} 1625 (br, CONH, COO); m/z (ES$^+$) after addition of CF_3COOH: 418 (100%, [M + 2H$^+$]$^{2+}$) (Found: MH$^+$, 835.3412 $C_{32}H_{57}N_7O_9Sm$ requires MH$^+$ 835.3410).

35. [Eu.Ld]

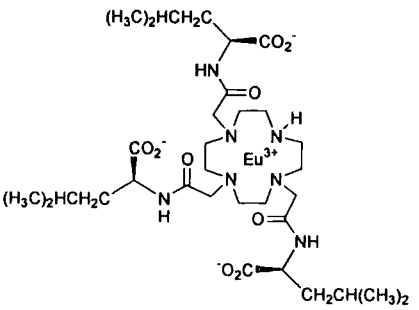

The title compound was prepared following a method similar to that for **28**, using compound **19** (0.500 g, 0.37 mmol), dissolved in the minimum amount of methanol and an aqueous sodium hydroxide solution (0.02 M, 75 ml). A yellow solid resulted (0.028 g, 50%), m.p. > 250 °C; ν_{max} (solid)/cm^{-1} 1625 (br, CONH, COO); ^{1}H NMR (200 MHz, CD_3OD) partial assignment δ 25.7 (1H, br s, ring-H_{ax}), 23.4 (1H, br s, ring-H_{ax}), 18.0 (1H, br s, ring-H_{ax}), 17.6 (1H, br s, ring-H_{ax}), 11.03, -1.12, -2.34, -2.78, -3.32, -5.13, -5.37, -6.89, -7.28, -8.84, -9.33, -11.1, -12.8, -14.6, -15.43; m/z (ES^+) after addition of CF_3COOH: 418 (100%, $[M + 2H^+]^{2+}$) (Found: MH^+, 836.3474 $C_{32}H_{57}N_7O_9Eu$ requires MH^+ 836.3430).

36. [Tb.Ld]

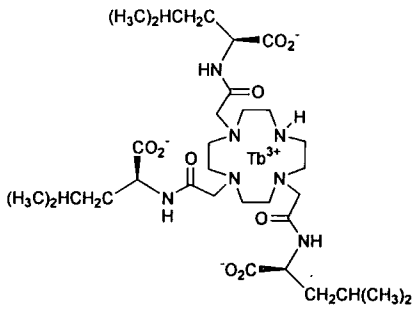

The title compound was prepared following a method similar to that for **28**, using compound **20** (0.090 g, 0.067 mmol), dissolved in the minimum amount of methanol and an aqueous sodium hydroxide solution (0.02 M, 13.5 ml). A yellow solid resulted (0.030 g, 53%), m.p. > 260 °C; ν_{max} (solid)/cm^{-1} 1625 (br, CONH, COO); ^{1}H NMR (200 MHz, CD_3OD) partial assignment δ 250.0, 232.0, 151.7, 141.1, 127.2, 69.8, 62.7, 49.4, 36.9, 31.4, 25.3, -16.4, -44.5, -53.7, -58.4, -89.2, -95.3, -128.6, -148.3 (1H, br s, ring-H_{ax}), -212.4 (1H, br s, ring-H_{ax}), -241.0 (1H, br s, ring-H_{ax}), -333.2 (1H, br s, ring-H_{ax}); m/z (ES^+) after addition of CF_3COOH: 422 (100%, $[M + 2H^+]^{2+}$) (Found: MH^+, 842.3519 $C_{32}H_{57}N_7O_9Tb$ requires MH^+ 842.3471).

37. [Dy.Ld]

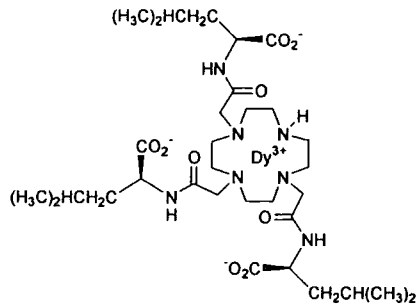

The title compound was prepared following a method similar to that for **28**, using compound **21** (0.090 g, 0.067 mmol), dissolved in the minimum amount of methanol and an aqueous sodium hydroxide solution (0.02 M, 13.5 ml). A yellow solid resulted (0.033 g, 58%), m.p. > 260 °C; ν_{max} (solid)/cm^{-1} 1625 (br, CONH, COO); ^{1}H NMR (200 MHz, CD_3OD) partial assignment δ 250.0, 246.0, 187.0, 100.8, 88.0, 73.4, 68.4, 43.8, 36.2, 28.2, -23.82, -49.54, -131.0, -151.9, -270.0 (2H, br s, ring-H_{ax}), -309.2 (1H, br s, ring-H_{ax}), -380.5 (1H, br s, ring-H_{ax}); m/z (ES^+) after addition of CF_3COOH: 424 (100%, $[M + 2H^+]^{2+}$) (Found: MH^+, 847.3553 $C_{32}H_{57}N_7O_9Dy$ requires MH^+ 847.3510).

38. [Ho.Ld]

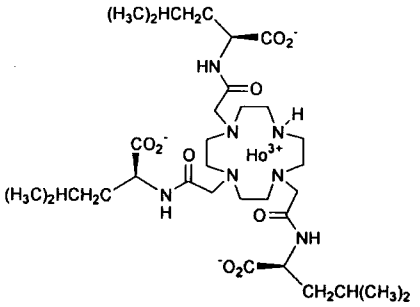

The title compound was prepared following a method similar to that for **28**, using compound **22** (0.40 g, 0.30 mmol), dissolved in the minimum amount of methanol and an aqueous sodium hydroxide solution (0.02 M, 74 ml). A yellow solid resulted (0.100 g, 40%), m.p. > 250 °C; ν_{max} (solid)/cm^{-1} 1625 (br, CONH, COO); ^{1}H NMR (200 MHz, CD_3OD) partial assignment δ 142.4, 134.3, 88.3, 70.8, 44.5, 41.44, 38.2, 35.3, 30.0, -40.8, -49.8, -58.6, -78.2, -123.4 (1H, br s, ring-H_{ax}), -142.7 (1H, br s, ring-H_{ax}), -183.1 (1H, br s, ring-H_{ax}), -194.6 (1H, br s, ring-H_{ax}); m/z (ES^+) after

addition of CF_3COOH: 425 (100%, $[M + 2H^+]^{2+}$) (Found: MH^+, 848.3534 $C_{32}H_{57}N_7O_9Ho$ requires MH^+ 848.3521).

39. [Er.Ld]

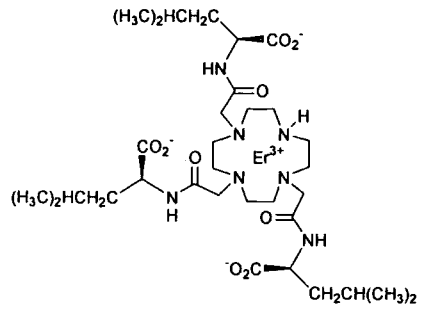

The title compound was prepared following a method similar to that for **28,** using compound **23** (0.090 g, 0.067 mmol), dissolved in the minimum amount of methanol and an aqueous sodium hydroxide solution (0.02 M, 13.5 ml). A yellow solid resulted (0.030 g, 53%), m.p. > 250 °C; ν_{max} (solid)/cm^{-1} 1625 (br, CONH, COO); ^1H NMR (200 MHz, CD_3OD) partial assignment δ 122.8 (1H, br s, ring-H_{ax}), 106.3 (1H, br s, ring-H_{ax}), 66.86 (2H, br s, ring-H_{ax}), 52.2, 37.5, 31.7, 24.0, 19.4, 17.2, 14.2, -14.8, -27.7, -31.3, -32.8, -39.6, -45.6, -49.5, -56.2, -64.9; m/z (ES^+) after addition of CF_3COOH: 425 (100%, $[M + 2H^+]^{2+}$) (Found: MH^+, 849.3578 $C_{32}H_{57}N_7O_9Er$ requires MH^+ 849.3521).

40. [Tm.Ld]

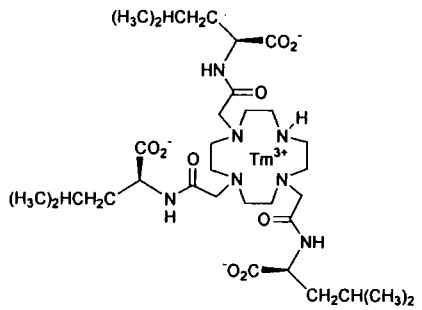

The title compound was prepared following a method similar to that for **28**, using compound **24** (0.090 g, 0.067 mmol), dissolved in the minimum amount of methanol and an aqueous sodium hydroxide solution (0.02 M, 13.4 ml). A yellow solid

resulted (0.025 g, 44%), m.p. > 250 °C; ν_{max} (solid)/cm^{-1} 1625 (br, CONH, COO); ^{1}H NMR (200 MHz, CD_3OD) partial assignment δ 289.7 (2H, br s, ring-H_{ax}), 199.0 (1H, br s, ring-H_{ax}), 191.0 (1H, br s, ring-H_{ax}), 121.0, 78.2, 69.9, 56.9, 27.8, -35.5, -57.6, -65.5, -84.3, -94.7, -146.3, -164.3, -175.9, -182.5, -389; m/z (ES^+) after addition of CF_3COOH: 427 (100%, $[M + 2H^+]^{2+}$) (Found: MH^+, 852.3556 $C_{32}H_{57}N_7O_9Tm$ requires MH^+ 852.3560).

Cationic N-Bn Complexes of Ligand Le

25. $[Yb.Le]^{3+}$

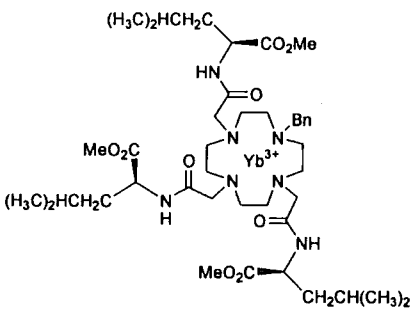

The title compound was prepared following a method similar for **12**, using ytterbium (III) triflate (0.099 g, 0.16 mmol) in dry acetonitrile (1 ml) and the ligand **9** (0.131 g, 0.16 mmol) in dry acetonitrile (4 ml). A yellow solid resulted (0.200 g, 87%), m.p. > 140 °C (dec.); ν_{max} (solid)/cm^{-1} 1740 (COO), 1622 (CONH); ^{1}H NMR (200 MHz, CD_3OD) partial assignment δ 140.0 (1H, br s, ring-H_{ax}), 134.0 (2H, br s, ring-H_{ax}), 112.3 (1H, br s, ring-H_{ax}), 34.8 (2H, br s, ring-H_{eq}), 29.0 (1H, br s, ring-H_{eq}), 24.65 (1H, br s, ring-H_{eq}), 23.8, 19.0, -9.63, -10.5, -15.7, -16.9, -28.9, -51.1, -60.5, -66.3, -69.1, -75.4, -79.6, -86.1, -89.69; m/z (ES^+) 495 (100%, M^{2+}) (Found: M^{2+}, 495.2322. $C_{42}H_{70}N_7O_9Yb$ requires M^{2+}, 495.2312).

26. $[Eu.Le]^{3+}$

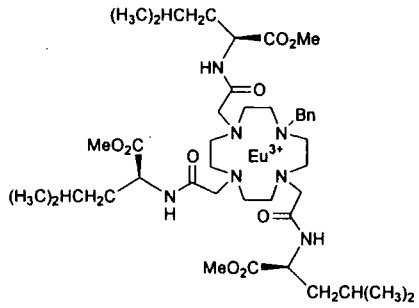

The title compound was prepared following a method similar to that for **12**, using europium (III) triflate (0.088 g, 0.147 mmol) in dry acetonitrile (3 ml) and the ligand **9** (0.120 g, 0.147 mmol) in dry acetonitrile (3 ml). A yellow solid resulted (0.181 g, 87%), m.p. > 150 °C (dec.); ν_{max} (solid)/cm^{-1} 1740 (COO), 1622 (CONH); ^1H NMR (200 MHz, CD_3OD) partial assignment δ 21.5 (1H, br s, ring-H_{ax}), 20.4 (1H, br s, ring-H_{ax}), 17.8 (1H, br s, ring-H_{ax}), 16.9 (1H, br s, ring-H_{eq}), 12.0, 8.20, 7.60, -4.85, -5.50, -7.20, -8.50, -8.90, -9.50, -9.80, -10.8, -11.2, -12.0, -18.5; m/z (ES^+) 484 (100%, M^{2+}), 1119 (30%, $[M^{2+} + (CF_3SO_3^-)]^+$) (Found: M^{2+}, 484.7217. $C_{42}H_{70}N_7O_9Eu$ requires M^{2+}, 484.7218).

27. $[Tb.Le]^{3+}$

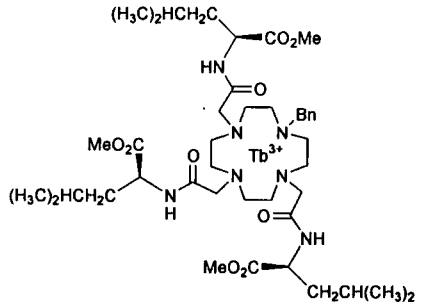

The title compound was prepared following a method similar to that for **12**, using terbium (III) triflate (0.037 g, 0.061 mmol) in dry acetonitrile (3 ml) and the ligand **9** (0.050 g, 0.061 mmol) in dry acetonitrile (3 ml). A yellow solid resulted (0.060 g, 70%), m.p. > 168 °C (dec.); ν_{max} (solid)/cm^{-1} 1740 (COO), 1622 (CONH); ^1H NMR (200 MHz, CD_3OD) partial assignment δ 380.0, 360.0, 300, 260.0, 200.0, 180.0, 140.0, -80.0, -110.0, -170.0, -160.0, -220.0, -250.0 (1H, br s, ring-H_{eq}), -266.0

(1H, br s, ring-H_{eq}), -320.0 (1H, br s, ring-H_{eq}), -330.0 (1H, br s, ring-H_{eq}); m/z (ES^+) 487 (100%, M^{2+}), 563 (20%, $[M^{3+} + (CF_3SO_3^-)]^{2+}$), 1275 (5%, $[M^{3+} + (CF_3SO_3^-)_2]^+$) (Found: M^{2+}, 487.7239. $C_{42}H_{70}N_7O_9Tb$ requires M^{2+}, 487.7239).

Neutral N-Bn Complexes of Ligand Lf

41. [Yb.Lf]

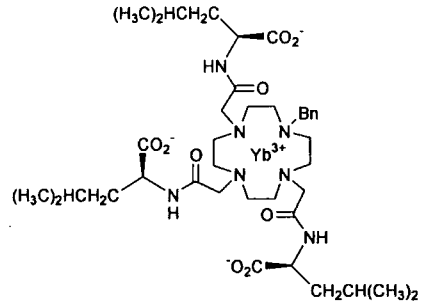

The title compound was prepared following a method similar to that for **28**, using compound **25** (0.100 g, 0.069 mmol), dissolved in the minimum amount of methanol and an aqueous sodium hydroxide solution (0.02 M, 13.9 ml). A yellow solid resulted (0.035g, 40%), m.p. > 250 °C; ν_{max} (solid)/cm^{-1} 1623 (br, CONH, COO); ^1H NMR (200 MHz, CD_3OD) partial assignment δ major isomer 107.1 (1H, br s, ring-H_{ax}), 102.7 (1H, br s, ring-H_{ax}), 83.2 (1H, br s, ring-H_{ax}), 61.74 (1H, br s, ring-H_{ax}), 59.3, 51.0, 42.0, 38.6, 37.0, 34.0, 28.3, 19.1, 17.1, -10.89, -12.06, -24.67, -28.95, -30.0, -43.0, -44.19, -46.3, -47.3, -55.8, -66.6, -72.1, -83.2, -98.6, -102.0, -105.3, -131.4; δ minor isomer 71.0 (1H, br s, ring-H_{ax}), 35.68 (1H, br s, ring-H_{ax}), 20.32 (1H, br s, ring-H_{ax}), 14.80 (1H, br s, ring-H_{ax}), -4.86, -6.58; m/z (ES^+) after addition of CF_3COOH: 474 (100%, $[M + 2H^+]^{2+}$) (Found: MH^+, 947.4077. $C_{39}H_{63}N_7O_9Yb$ requires MH^+ 947.4077).

42. [Eu.Lf]

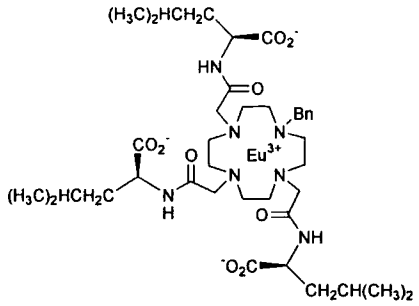

The title compound was prepared following a method similar to that for **28,** using compound **26** (0.080 g, 0.056 mmol), dissolved in the minimum amount of methanol and an aqueous sodium hydroxide solution (0.02 M, 11.3 ml). A yellow solid resulted (0.024 g, 46%), m.p. > 250 °C; ν_{max} (solid)/cm^{-1} 1623 (br, CONH, COO); ^{1}H NMR (200 MHz, CD_3OD) partial assignment δ 21.27 (1H, br s, ring-H_{ax}), 11.67 (3H, br s, ring-H_{ax}), 9.03, 8.4, 6.06, -6.5, -9.33, -11.0, -13.63, -17.8, -18.25, -19.03; m/z (ES^+) after addition of CF_3COOH: 463 (100%, $[M + 2H^+]^{2+}$) (Found: MH^+, 926.3899. $C_{39}H_{63}N_7O_9Eu$ requires MH^+ 926.3894).

43. [Tb.Lf]

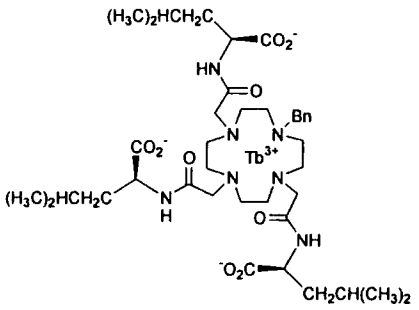

The title compound was prepared following a method similar to that for **28,** using compound **27** (0.040 g, 0.028 mmol), dissolved in the minimum amount of methanol and an aqueous sodium hydroxide solution (0.02 M, 5.6 ml). A yellow solid resulted (0.010 g, 38%), m.p. > 250 °C; ν_{max} (solid)/cm^{-1} 1623 (br, CONH, COO); ^{1}H NMR (200 MHz, CD_3OD) partial assignment δ 574.0, 404.3, 257.6, 235.5, 168.0, 131.4, -139.2, -157.9, -176.4, -185.9, -195.8, -214.7, -228.6, -250.6, -278.8, -291.6, -

369.3 (1H, br s, ring-H_{ax}); m/z (ES^+) after addition of CF_3COOH: 466 (100%, $[M + 2H^+]^{2+}$) (Found: MH^+, 932.3937. $C_{39}H_{63}N_7O_9Tb$ requires MH^+ 932.3935).

Aziridine Systems

44. (2S, 3R)-2-Amino-3-hydroxy butyric acid methyl ester

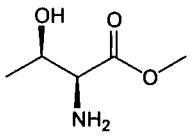

(2S, 3R)-Threonine (1.06 g, 8.89 mmol) was dissolved in methanol (8 ml) and thionyl chloride (1.29 ml, 17.8 mmol) was added. The reaction mixture was refluxed for 2 h under argon and the solvent was removed under vacuum giving the product as a white oil (1.18 g, 100%); ν_{max} (film)/cm^{-1} 1739 (COO); ^1H NMR (200 MHz, D_2O) δ 4.3 (1H, m, CHOH), 3.95 (1H, d, $^3J = 4$, $CHNH_2$), 3.70 (3H, s, OCH_3), 1.18 (3H, d, $^3J = 6.8$, CH_3CH); ^{13}C NMR (50.29 MHz, D_2O) δ 169.3 ($COOCH_3$), 65.61 (CHOH), 58.82 ($CHNH_2$), 54.37 (OCH_3), 19.62 (CH_3CH); m/z (ES^+) 134 (100%, MH^+), 267 (40%, M_2H^+).

46. (2S, 3R)-3-Hydroxy-2-(toluene-4-sulfonylamino)-butyric acid methyl ester

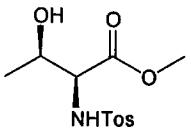

Triethylamine (2.21 ml, 15.9 mmol) was added to a solution of compound **44** (0.70 g, 5.29 mmol) and p-tosylchloride (1.00 g, 5.29 mmol) in acetonitrile (5 ml) and the reaction mixture was stirred at room temperature for 12 h. The resulting white precipitate was removed by centrifugation and the supernatant was dried under vacuum. The residue was taken into dichloromethane (40 ml), washed with hydrochloric acid (0.1 M, 40 ml), water (40 ml), dried (K_2CO_3) and the solvent was removed *in vacuo* to give the product as a brown oil (1.2 g, 73%); ν_{max} (film)/cm^{-1}

1649 (COO); ^{1}H NMR (200 MHz, $CDCl_3$) δ 7.67 (2H, d, ^{3}J = 8, o-Ar), 7.17 (2H, d, ^{3}J = 8, m-Ar), 4.45 (1H, br, NH), 4.1 (1H, m, CHOH), 3.63 (1H, d, ^{3}J = 4.2, CHNH), 3.48 (3H, s, OCH_3), 2.37 (3H, s, CH_3-Ar), 1.12 (3H, d, ^{3}J = 6, CH_3CH); ^{13}C NMR (50.29 MHz, $CDCl_3$): δ 172.1 (CO_2CH_3), 143.2 (p-Ar), 137.9 (ipso-Ar), 129.6 (m-Ar), 127.3 (o-Ar), 68.3 (CHOH), 63.0 ($CHCOOCH_3$), 52.3 (OCH_3), 21.6 (CH_3-Ar), 20.1 (CH_3CH); m/z (ES^+) 310 (100%, MNa^+)

48. (2S, 3S)-3-Methyl-1-(toluene-4-sulfonyl)-aziridine-2-carboxylic acid methyl ester

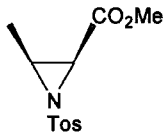

Diethylazodicarboxylate (1.16 ml, 7.40 mmol) was added dropwise over a period of 30 minutes to a cooled (0 °C), stirring mixture of compound **46** (1.42 g, 4.93 mmol) and triphenylphosphine (1.94 g, 7.40 mmol) in tetrahydrofuran (5 ml). The reaction mixture was stirred for 15 h at room temperature under argon. The solvent was removed and the crude product was purified by flash chromatography on silica gel (hexane/ethylacetate, 2/1) to yield **48** as a white solid (0.594 g, 45%); R_f (silica; hexane/ethylacetate 2/1, I_2 and u.v. detection) 0.25; ν_{max} (solid)/cm^{-1} 1743 (COO); ^{1}H NMR (200 MHz, $CDCl_3$) δ 7.81 (2H, d, ^{3}J = 8.2, o-Ar), 7.32 (2H, d, ^{3}J = 8.4, m-Ar), 3.70 (3H, s, OCH_3), 3.35 (1H, d, ^{3}J = 7, $CHCOOCH_3$), 3.07 (1H, m, $CHCH_3$), 2.41 (3H, s, CH_3-Ar), 1.28 (3H, d, ^{3}J = 5.6, CH_3CH); ^{13}C NMR (50.29 MHz, $CDCl_3$) δ 166.4 (CO_2CH_3), 145.2 (p-Ar), 134.9 (ipso-Ar), 130.0 (m-Ar), 128.2 (o-Ar), 52.7 (OCH_3), 41.37 ($CHCOOCH_3$), 40.28 ($CHCH_3$), 21.8 (CH_3-Ar), 12.4 (CH_3CH); m/z (ES^+) 292 (100%, MNa^+), 270 (15%, MH^+) (Found: MNa^+, 292.0632. $C_{12}H_{15}NO_4NaS$ requires MNa^+ 292.0619).

45. (2S, 3R)-2-Amino-3-hydroxy butyric acid isopropyl ester

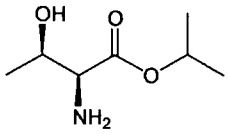

The title compound was prepared following a method similar to that for **44,** using (2S, 3R)-threonine (2.00 g, 16.79 mmol) in isopropanol (8 ml) and reacting with thionyl chloride (2.44 ml, 38.58 mmol). A brown oil resulted (2.71 g, 100%); ν_{max} (film)/cm^{-1} 1728 (COO); ^{1}H NMR (500 MHz, D_2O) δ 4.86 (1H, m, CH(CH$_3$)$_2$), 4.20 (1H, m, CHOH), 3.82 (1H, d, ^{3}J = 4, CHNH$_2$), 1.15 (3H, d, ^{3}J = 6.85, CH$_3$CHOH), 1.11 (6H, d, ^{3}J = 6, CH(CH$_3$)$_2$); ^{13}C NMR (125.7 MHz, D_2O) δ 168 (COO), 72.0 (OCH(CH$_3$)$_2$), 66.20 (CHOH), 59.10 (CHNH$_2$), 22.30 (CH(CH$_3$)$_2$). 19.8 (CH$_3$CHOH), 22.30 (CH(CH$_3$)$_2$). m/z (ES$^+$) 162 (100%, MH$^+$), 323 (70%, M$_2$H$^+$).

47. (2S, 3R)-3-Hydroxy-2-(toluene-4-sulfonylamino)-butyric acid isopropyl ester

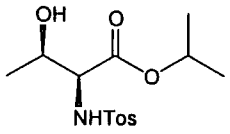

The title compound was prepared following a method similar to that for **46,** using triethylamine (3.58 ml, 26.7 mmol), compound **45** (1.38 g, 8.56 mmol) and p-tosylchloride (1.63 g, 8.56 mmol) in dry acetonitrile (40 ml). An orange solid resulted (1.64 g, 61 %), m.p. 118-124 °C; ν_{max} (solid)/cm^{-1} 1730 (COO); ^{1}H NMR (500 MHz, $CDCl_3$) δ 7.1 (2H, d, ^{3}J = 8.5, o-Ar), 7.6 (2H, d, ^{3}J = 8, m-Ar), 4.85 (1H, br s, NH), 4.75 (1H, m, CH(CH$_3$)$_2$), 4.05 (1H, m, CHOH), 3.65 (1H, d, ^{3}J = 3.5 CHNH), 2.3 (3H, s, CH$_3$-Ar), 1.16 (3H, d, ^{3}J = 6, CH$_3$CHOH), 1.02 (3H, d, ^{3}J = 6, CH$_3$CH), 0.95 (3H, d, ^{3}J = 6, CH$_3$CH); ^{13}C NMR (125.7 MHz, $CDCl_3$) δ 171 (CO$_2$), 143.2 (p-Ar), 138 (ipso-Ar), 130 (m-Ar), 127 (o-Ar), 70.1 (CH(CH$_3$)$_2$), 68.2 (CHOH), 62.3 (CHNH), 21.7 (CH$_3$-Ar), 21.6 ((CH$_3$)$_2$CH), 20.2 (CH$_3$CHOH); m/z (ES$^+$) 354 (100%, MK$^+$), 338 (90%, MNa$^+$).

49. (2S, 3S)-3-Methyl-1-(toluene-4-sulfonyl)-aziridine-2-carboxylic acid isopropyl ester

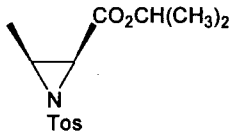

The title compound was prepared following a method similar for **48,** reacting diethylazodicarboxylate (0.36 ml, 2.31 mmol) with compound **47** (0.485 g, 1.54 mmol) and triphenylphosphine (0.605 g, 2.31 mmol) in tetrahydrofuran (8 ml). A white solid resulted (0.280 g, 61 %), m.p. 96-98 °C; R_f (silica; hexane/ethylacetate 2/1, I_2 and u.v. detection) 0.45; ν_{max} (solid)/cm^{-1} 1743 (COO); ^{1}H NMR (400 MHz, $CDCl_3$) δ 7.78 (2H, d, ^{3}J = 8.4, o-Ar), 7.29 (2H, d, ^{3}J = 8.8, m-Ar), 4.97 (1H, septet, ^{3}J = 6, CH(CH_3)$_2$), 3.26 (1H, d, ^{3}J = 7.6, CHCOO), 3.02 (1H, m, CH_3CHN-Tos), 2.37 (3H, s, CH_3-Ar), 1.37 (3H, d, ^{3}J = 4.8, CH_3CHN-Tos), 1.16 (3H, d, ^{3}J = 6.4, CH_3CHCH_3), 1.15 (3H, d, ^{3}J = 6.4, CH_3CHCH_3); ^{13}C NMR (100.6 MHz, $CDCl_3$) δ 165 (CO_2), 145 (p-Ar), 134 (ipso-Ar), 130 (m-Ar), 128.2 (o-Ar), 69.79 (CH(CH_3)$_2$) 41.73 (CHCOO), 40.18 (CH_3CHN-Tos), 21.9 (CH_3)$_2$CH), 21.8 (CH_3Ar), 12.3 (CH_3CHN-Tos); m/z (ES$^+$) 320 (100%, MNa$^+$), (Found: MNa$^+$, 320.0919. $C_{14}H_{19}NO_4NaS$ requires MNa$^+$ 320.0932).

4.5 Experimental Details for Chapters 2 and 3

4.5.1 Solution ^{1}H and ^{31}P NMR Studies

Lactate

The following procedure was adopted to investigate the effect of added lactate (R or S) on the NMR spectrum of the Ln^{3+} complexes. 0.01 ml aliquots of a solution of the appropriate sodium lactate salt (in D_2O, 175 mM, complex to lactate ratio ranging from 4:1 to 1:2) were added successively to a solution of the complex (0.70 ml, 10 mM) and the ^{1}H spectrum was run for each increment. The following solvents systems were used: [Yb.La]$^{3+}$ **12** (0.25 ml CD_3OD, 0.45 ml D_2O); [Yb.Lb] **28** (0.30

ml CD_3OD and 0.4 ml D_2O); $[Ln.Lc]^{3+}$ (**14-20**), $[Yb.Le]^{3+}$ **25** (0.20 ml CD_3OD, 0.50 ml D_2O); [Ln.Ld] (**30-40**), [Yb.Lf] **41**(0.70 ml D_2O).

The following procedure was adopted to investigate the effect of added Ln^{3+} complex on the NMR spectrum of S-lactate. 0.01 ml aliquots of a solution of the appropriate $[Ln.Lc]^{3+}$ and [Ln.Ld] complex (7.0 mM, MeOD) was added to a solution of S-lactate (0.70 ml, 10 mM) and the ^1H spectrum was run.

α-Hydroxy Acids

The following procedure was used to investigate the potential of the Yb^{3+} complexes to act as chiral derivatising agents for α-hydroxy acids. ^1H NMR spectra of a solution of the complex (0.70 ml, 10 mM), containing 2 equivalents of S-α-hydroxy acid (0.02 ml, 710 mM), were run after successive addition of the corresponding R-α-hydroxy acid solution (710 mM, R to S ratio ranging from 1:4 to 4:1). The following solvent systems were used: $[Yb.Lc]^{3+}$ **14** (0.20 ml CD_3OD, 0.50 ml D_2O); [Yb.Ld] **30** (0.70 ml D_2O).

Amino Acids

The following procedures were adopted to investigate the effect of adding 10 equivalents of amino acids to a solution of the complexes (0.70 ml, 10 mM). The following solvent system was used: $[Yb.Lc]^{3+}$ **14**, [Yb.Ld] **30** (0.20 ml CD_3OD, 0.50 ml D_2O). The pD was adjusted to 8 by the addition of NaOD solution.

Procedure 1: (S-Ala, R-Ala, S-Ser, R-Ser, S-Thr, R-Thr, Gly, S-Lys, R-Lys). The amino acid was added as a solid, a few crystals at a time and dissolution was aided by heating.

Procedure 2: (S-Glu, R-Glu, S-Met, R-Met, S-Phe, R-Phe). The amino acid was dissolved in D_2O (0.50 ml) and 1 drop of NaOD solution and the complex in CD_3OD (0.20 ml) was added.

Anions and Phosphorylated Compounds

The following procedure was adopted to investigate the effect of added anions and phospho compounds (pD 8, by the addition of NaOD solution), on the NMR spectra of the Yb^{3+} complexes. The appropriate anion (10 equivalents) was added, as a solid, to a solution of the complex (0.70 ml, 10 mM) and the ^{1}H and ^{31}P NMR spectra were run. The following solvent systems were used: $[Yb.Lc]^{3+}$ **14**, $[Yb.Le]^{3+}$ **25** (0.20 ml CD_3OD and 0.50 ml D_2O); [Yb.Ld] **30**, [Yb.Lf] **41** (D_2O).

Phosphoethanolamine and Phosphocholine

The following procedure was adopted to investigate the effect of added phosphor-compound on the NMR spectra of Ln^{3+} complexes. 0.02 ml aliquots of a solution of PE or PC (in D_2O, 175 mM) were added to a solution of the complex (0.70 ml, 10 mM) and the ^{1}H and ^{31}P spectra were run. The following solvent systems were used: $[Pr.Lc]^{3+}$ **16**, $[Eu.Lc]^{3+}$ **19**, $[Ho.Lc]^{3+}$ **22**, $[Yb.Lc]^{3+}$ **14** (0.2 ml CD_3OD and 0.5 ml D_2O); [Pr.Ld] **32**, [Eu.Ld] **35**, [Ho.Ld] **38**, [Yb.Ld] **30** (D_2O).

Competitive Anion Background

The following procedure was adopted to investigate the effect of pH on the competitive binding of anions to the Yb^{3+} complexes. Solutions of the complexes (0.70 ml, 5 mM), containing 150 mM $NaHCO_3$, 500 mM NaCl, 4.5 mM Na_2HPO_4, 0.65 mM citrate and 11.5 mM lactate, were prepared and investigated by ^{1}H NMR at different pH (10, 8.6, 7.4, and 5). The following solvent systems were used: $[Yb.Lc]^{3+}$ **14**, $[Yb.Le]^{3+}$ **25** (0.2 ml CD_3OD and 0.5 ml D_2O); [Yb.Ld] **30**, [Yb.Lf] **41** (D_2O).

4.5.2 Lifetime and Emission Investigation

Effect of Added Anions on Lifetime

The following procedure was adopted for the investigation of the effect of added anions on the excited state lifetimes of Tb^{3+} complexes. An excess of the anion (10 equivalents) was added, as a solid, to a solution of the complex (0.50 ml, 2.5 mM for direct excitation; 0.25 mM for indirect excitation, H_2O) and the lifetime was measured (for $[Tb.Lc]^{3+}$ **20**, $[Tb.Le]^{3+}$ **27** a small amount of CH_3OH was required to

complete dissolution). For direct excitation: λ_{ex} = 355, λ_{em} = 545, slit $width_{ex}$ and slit $width_{em}$ = 15 nm, t_g = 0.1 ms, t_d = 0.1-4 ms; for indirect excitation: λ_{ex} = 254, λ_{em} = 545, slit $width_{ex}$ and slit $width_{em}$ = 15 nm, t_g = 0.1 ms, t_d = 0.1-5 ms.

Effect of Added Anions on Emission Spectra

The following procedure was adopted for the investigation of the effect of added anions on the emission spectra of Eu^{3+} complexes. An excess of the anion (10 equivalents) was added, as a solid, to a solution of the complexes (0.50 ml, 2.5 mM for direct excitation; 0.25 mM for indirect excitation) prepared in a MOPS (0.1 M, pH 7.4) buffer. The emission spectra were then recorded.

Emission Spectra in a Competitive Anion Background

The following procedure was adopted to investigate the emission spectra of Eu^{3+} complexes as a function of pH, in a solution containing a competitive anion background. Complex solutions (0.50 ml, 2.5 mM, in H_2O) containing 75 mM $NaHCO_3$, 250 mM NaCl, 2.25 mM Na_2HPO_4, 0.325 mM citrate, 5.75 mM S-lactate were prepared and their emission spectra were run at different pH (10, 8.6, 7.4, and 5).

Binding Affinity for S-Lactate

The following procedure was adopted to determine the binding constant of the Eu^{3+} complexes with S-lactate. To a solution of $[Eu.Lc]^{3+}$ **19** or [Eu.Ld] **35** (2.5 ml, 1 mM, in 0.1 M MOPS buffer at pH 7.4) was successively added a freshly prepared solution of S-lactate (0.001 ml, 0.083 M, in 0.1 M MOPS, complex to lactate ratio ranging from 1:0 to 1:4) and the variation of the Eu^{3+} emission intensity (614 nm) was recorded as a function of added lactate. The same procedure was adopted for $[Eu.Le]^{3+}$ **26** and [Eu.Lf] **42** (2.5 ml, 0.25 mM, in 0.1 M MOPS buffer at pH 7.4), using a 0.02 M solution of S-lactate. Data analysis was performed using an iterative least-squares fitting procedure, assuming a 1:1 binding stoichiometry, operating in Microsoft Excel.[2] For the binding of a given anion A^- to the lanthanide complex, [LnL], the following equilibrium was assumed:

$$[LnL]^{n+} + [A]^{m-} \underset{}{\overset{K}{\rightleftharpoons}} [LnLA]^{(n-m)+}$$

The following equation was minimized in terms of K, where A_i is the total anion concentration and Ln_i is the complex concentration (spreadsheet of the binding data in Appendix 2):

$$2[Ln_i]\,(I_{obs}-I_{init})/(I_{final}-I_{init}) = [Ln_i] - [A_i] + 1/K - (\{[Ln_i] + [A_i] + 1/K\}^2 - 4[Ln_i]\,[A_i])^{1/2}$$

4.5.3 CD Investigation

Effect of Added Anions on CD

The following procedure was adopted for the investigation of the effect of added anions on the CD of the Yb^{3+} complexes. An excess of the anion (10 eq) was added as a solid to a solution of $[Yb.Lc]^{3+}$ **14** (0.50 ml, containing 0.10 ml CH_3OH, 10 mM) or of [Yb.Ld] **30** (0.50 ml, 20 mM) prepared in a MOPS (0.1 M, pH 7.4) buffer and the CD was measured.

References

1. K. P. Pulukkodi, T. J. Norman, D. Parker, L. Royle, and C. J. Broan, *J. Chem. Soc., Perkin Trans.* 2, 1993, 605.
2. J. I. Bruce, R. S. Dickins, L. J. Govenlock, T. Gunnlaugsson, S. Lopinski, M. P. Lowe, D. Parker, R. D. Peacock, J. J. B. Perry, S. Aime, and M. Botta, *J. Am. Chem. Soc.*, 2000, **122**, 9674.

Appendix 1: Synthetic Attempt of the +2 System

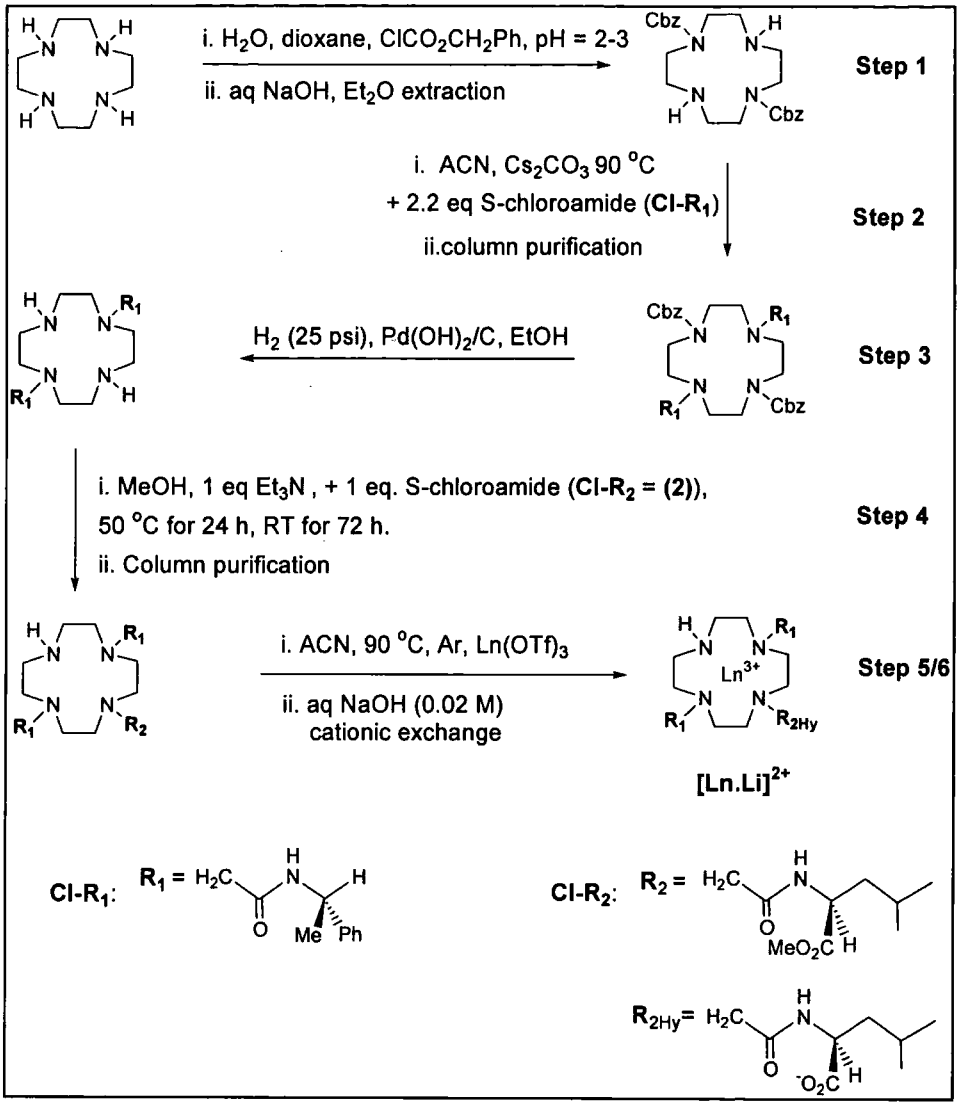

Synthesis of the S-Chloroamides

The S-Chloroamide, **Cl-R_1**, is a literature compound (Ref. 8, Chapter 2), whereas the synthesis of the chloroamide **Cl-R_2** has been reported in Chapter 4 (compound **2**).

Step 1

1,7-Bis(benzyloxycarbonyl)-1,4,7,10-tetraazacyclododecane

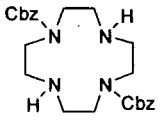

The synthesis and characterization of the above compound has been reported in literature (Ref. 23, Chapter 2).

Step 2

1,7-Bis(benzyloxycarbonyl)-4,10-bis-[(S)-1-(1-phenyl)ethylcarbamoyl methyl]-1,4,7,10-tetraazacyclododecane

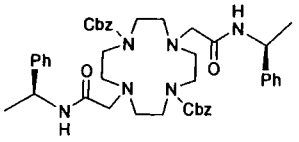

The S-chloroamide, **Cl-R_I**, (1.00 g, 5.00 mmol) was added to a stirred solution of 1,7-Bis(benzyloxycarbonyl)-1,4,7,10-tetraazacyclododecane (1.00 g, 2.27 mmol) and Cs_2CO_3 (1.63 g, 5.00 mmol) in dry acetonitrile (30 ml). The reaction mixture was refluxed under an argon atmosphere for 48 h. The solvent was removed under vacuum and the residue was taken into dichloromethane (40 ml), washed with purite water (3 x 40 ml), brine (40 ml), dried (K_2CO_3) and concentrated to dryness to give a yellow oil. The mixture was purified by alumina column chromatography (gradient elution from dichloromethane to 2% methanol-dichloromethane) and the product was isolated as a pale yellow oil (1.3 g, 75 %); R_f (Al_2O_3; 2.5% CH_3OH-CH_2Cl_2; I_2 and u.v. detection) 0.3; ^{1}H NMR (300 MHz, $CDCl_3$) δ 7.70 (2H, br, NH), 7.33-7.19 (20H, m, Ar), 5.14 (2H, m, CH), 4.96 (4H, s, CH_2Ph), 3.60-2.60 (20H, br, ring-CH_2, NCH_2CO), 1.45 (6H, br s, CH_3); ^{13}C NMR (75.4 MHz, $CDCl_3$) δ 170.4 (CONH), 157 (NCO_2), 144.0 (ipso-Ar), 136.7 (ipso-Ar, Cbz), 128.9, 128.5, 128.4, 127.4, 126.6, 126.4 (Ar), 67.5 (OCH_2), 59.2 ($N\underline{C}H_2CO$), 56-54 (ring-CH_2), 48.8 (CHN), 47.5 (br, ring-CH_2), 22.0 (CH_3); m/z (ES^+) 763 (100%, MH^+), 785 (20%, MNa^+).

Step 3

1,7-Bis[(S)-1-(1-phenyl)ethylcarbamoylmethyl]-1,4,7,10-tetraazacyclo dodecane

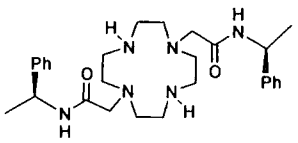

A catalytic amount of palladium hydroxide on carbon was added to 1,7-bis(benzyloxycarbonyl)-4,10-bis-[(S)-1-(1-phenyl)ethylcarbamoylmethyl]-1,4,7,10-tetraazacyclododecane (1.00 g, 1.30 mmol) in ethanol (30 ml) and the mixture was treated with hydrogen (25 psi) at room temperature for 48 h. The reaction mixture was filtered through celite and the solvent was removed under vacuum, yielding the product as a solid (0.60 g, 92%); ^{1}H NMR (200 MHz, $CDCl_3$) δ 8.00 (2H, br s, NHCO), 7.25-7.15 (10H, m, Ar), 5.00 (2H, m, CH), 3.50-2.40 (22H, br m, ring-CH_2, ring-NH, NCH_2CO), 1.40 (6H, br s, CH_3); ^{13}C NMR (50.29 MHz, $CDCl_3$) δ 170.6 (CONH), 143.6 (ipso-Ar), 128.6, 127.2, 126.4 (Ar), 57.2 ($N\underline{C}H_2CO$), 51.3 (br, ring-CH_2), 49.4 (CHN), 44.6 (br, ring-CH_2), 22.3 (CH_3); m/z (ES^+) 496 (100%, MH^+), 267 (60%, MCa^{2+}).

Step 4

1,7-Bis[(S)-1-(1-phenyl)ethylcarbamoylmethyl]-4-[(S)-((1-methoxy carbonyl-3-methyl)butyl)carbamoylmethyl]-1,4,7,10-tetraazacyclo dodecane

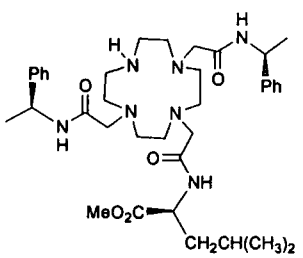

The S-chloroamide, Cl-R_2 (**2**) (0.179 g, 0.80 mmol) was added to a solution of 1,7-bis[(S)-1-(1-phenyl)ethylcarbamoylmethyl]-1,4,7,10-tetraazacyclododecane (0.40 g, 0.80 mmol) and dry triethylamine (0.112 ml, 0.80 mmol) in dry methanol (20 ml).

After stirring the reaction mixture at 50 ^{0}C for 24 h and at RT for 72 h, under an argon atmosphere, the solvent was removed under vacuum. The residue was taken into dichloromethane (40 ml), washed with purite water (3 x 40 ml), brine (40 ml), dried (K_2CO_3) and concentrated to dryness to give a brown oil. Attempted purification by column chromatography (Al_2O_3, gradient elution from dichloromethane to 0.5% methanol-dichloromethane) was unsuccessful. [A mixture of the required product and the tetraalkylated analogue was observed].

Appendix 2: Spreadsheet of the Binding Data

(i.e. $[Eu.Lc]^{3+}$ with lactate; isotherm in Fig. 2.39, Chapter 2)

Fit:minimised Σ(Icalcd-I)²/I½ by varying K, I initial, I final, least square

		Σ(Icalcd-I)²/I½	**χ²(I,Icalcd)**	
		36202.14	4.04689E-37	
[Lactate] mM	**Intensity at 614.5 nm**	**Calculated Intensity**	**(Icalcd-I)²/I½**	**(Icalcd-I)/I½**	
0.00	16203.09	1.73E+04	9452.44	8.617325	8.617325
0.07	18481.02	1.86E+04	119.51	0.937613	0.937613
0.13	19712.56	1.97E+04	3.94	-0.167454	0.167454
0.20	20180.14	2.06E+04	1220.01	2.930564	2.930564
0.27	21096.71	2.14E+04	511.07	1.875809	1.875809
0.33	21472.06	2.20E+04	2163.49	3.842456	3.842456
0.40	22509.72	2.26E+04	73.82	0.701427	0.701427
0.47	22054.72	2.31E+04	7704.73	7.202833	7.202833
0.53	23131.97	2.36E+04	1293.44	2.916213	2.916213
0.60	23359.55	2.40E+04	2500.53	4.044827	4.044827
0.67	24311.98	2.43E+04	4.57	0.171208	0.171208
0.73	24850.34	2.47E+04	219.52	-1.180065	1.180065
0.80	25138.02	2.50E+04	200.75	-1.125234	1.125234
0.87	25060.72	2.52E+04	178.08	1.060615	1.060615
0.93	25463.90	2.55E+04	0.73	0.067680	0.067680
1.00	26113.54	2.57E+04	1054.98	-2.555087	2.555087
1.13	26527.99	2.61E+04	1117.78	-2.619701	2.619701
1.27	27056.86	2.64E+04	2271.06	-3.715738	3.715738
1.40	27030.49	2.67E+04	496.49	-1.737772	1.737772
1.53	27257.02	2.70E+04	378.50	-1.514136	1.514136
1.67	27421.64	2.72E+04	201.76	-1.103816	1.103816
2.00	28351.77	2.77E+04	2403.86	-3.778415	3.778415
2.33	28149.67	2.81E+04	24.91	-0.385282	0.385282
2.67	28913.20	2.84E+04	1673.35	-3.137034	3.137034
3.00	28834.52	2.86E+04	269.99	-1.260933	1.260933
3.33	28515.96	2.88E+04	549.37	1.803691	1.803691
3.67	28756.65	2.90E+04	320.11	1.373925	1.373925
4.00	28755.10	2.91E+04	848.34	2.236688	2.236688

I initial	1.73E+04	
I final	31000	
[complex]	1.00E-03	
K (mM-1)	1.59E+00	
K(M-1)	1.59E+03	
logK	3.20E+00	

Appendix 3: Courses, Lectures and Conferences Attended

First Year Courses Attended

Practical Spectroscopy

Paramagnetic NMR

Bioinorganic Chemistry

Combinatorial Chemistry

Lectures Attended

The following were attended, organised by the Department of Chemistry (January 2002-July 2004).

2002

January 22 Dr Ian Fallis, University of Cardiff
Size is Everything

January 30 Dr Peter Hore, PCL, University of Oxford
Chemistry in a spin: effects of magnetic fields on chemical reactions

February 13 Dr Helen Aspinall, Department of Chemistry, University of Liverpool
Defining effective chiral binding sites at lanthanides - enantioselective reagents and catalysts

February 19 Ezat Khosdel, Unilever
Industrial aspects of research

February 26 Dr Mike Griffin, Forensic Science Service, Metropolitan Police
Smack, Crack, Speed and Weed: A forensic chemists tale

March 12 Professor David Williams, Cardiff
Beer and Health: 7000 years of history

May 8	Professor Paul Madden, PCL, University of Oxford Covalent Effects in "Ionic" Systems
October 2	Professor Gideon Davies, Department of Chemistry, University of York Structural Enzymology of Glycosyl Transfer: How Enzymes Make and Degrade Polysaccharides
October 15	Professor Mike Zaworotko from the University of South Florida Supramolecular Synthesis of Functional Molecules & Materials
October 23	Professor Marcetta Darensbourg, Department of Chemistry, Texas A&M University Functioning Catalysts Inspired by Active Sites in Bio-Organometallic Chemistry: The Hydrogenases
October 30	Professor Tim Bugg, Department of Chemistry, Warwick University Enzymes in Aromatic Degredation
November 12	Dr Dave Alker, Pfizer The Discovery of a New Medicine
November 20	Dr Mike George, School of Chemistry, University of Nottingham Time Resolved IR Spectroscopy: From Organometallic Nobel Gas Compounds to IR Probes of DNA
November 27	Professor Marc Lemaire, University Claude Bernard Lyon 1 Organic Synthesis and Heterogenous Asymmetric Catalysis

2003

January 15 Professor Pat Bailey, Department of Chemistry, UMIST
Planned and unplanned routes to bio-active target molecules

January 22 Dr David Procter, Department of Chemistry, University of Glasgow
New Strategies and Methods for Organic Synthesis

February 12 Professor Paul Raithby, Department of Chemistry, University of Bath
Adventures in Organometallic Polymer Chemistry

February 19 Professor Tony Ryan, Department of Chemistry, University. of Sheffield
Introducing Soft Nanotechnology

March 4 Professor Richard Taylor, University of York
Adventures in Natural Product Synthesis

March 12 Professor David Lilley, School of Life Sciences, University of Dundee
Structure, folding and catalytic activity in RNA molecules

March 19 Professor Kevin Shakesheff, The Pharmacy School, University of Nottingham
Polymer materials in tissue engineering

October 21 Dr Roger Newton, Maybridge plc
The Pharmaceutical Industry - Does it have a Future?

November 18 Professor David Fenton, University of Sheffield
Urease - A Muse for the Coordination Chemist

December 3 Dr Malcom Levitt, School of Chemistry, Southampton University
Customising selection rules in solid-state NMR and the determination of biomolecular structures

2004

January 21 Professor Mark Bradley, School of Chemistry, University of Southampton
Arrays and Combinatorial Chemistry

January 28 Dr Lesley Yellowlees, Department of Chemistry, Edinburgh University
Electrochemical and spectroelectrochemical studies of transition metal complexes

February 2 Dr Andrew Burgess, ICI
Human Skin - Barrier Function and Material Properties (Kindly Sponsored by NEPA)

February 11 Professor D Parker FRS, Department of Chemistry, University of Durham
Chiral Lanthanide Complexes: Structure, dynamics and function

February 17 Professor A P De Silva, Queens University of Belfast
Designer Molecules for Photonic Signalling

February 18 Professor J Waltho, Molecular Biology and Biotechnology, University of Sheffield
Protein folding and misfolding from an NMR perspective

February 25 Professor Robin Clark - RSC Liversidge Lecture
Raman Microscopy: a Powerful Technique in Inorganic Chemistry and for Surface, Nanoparticulate and Pigment Studies

March 9 Professor Hugh Pennington, University of Aberdeen
Smallpox, Anthrax and Syphilis - Weapons Of Mass Destruction

March 16 Dr Chris Clarke, Unilever
The Science of Ice Cream

March 24 Dr D.N. Woolfson, Department of Biochemistry, University of Sussex
Bottom-up assembly of peptide-based supramolecular and nanoscale Structures

July 2 Professor Sir Harry Kroto, Nobel Laureate in Chemistry (1996)
2010: a NanoSpace Odyssey

Conferences Attended

2002 RSC UK Macrocyclic and Supramolecular Chemistry Group*
York (UK), (18/19 December)

2003 Perkin Division North East Annual Meeting**
Newcastle (UK) (June)

2004 RSC UK Macrocycles and Supramolecular Chemistry Meeting*
Sheffield (UK), (8/9 January)

2004 13th International Symposium on Supramolecular Chemistry*
Notre Dame (USA), (25-30 July)

2004 RSC Organic Chemistry Symposium*
Huddersfield (UK), (20 September)

*indicates poster presentation

** 1st prize for poster presentation

Courses Attended

2002 'Two half-day induction sessions on Teaching and Demonstrating'
Durham (UK) (October)

2003 'Research Councils Graduate School and CRAC insight into management'
West Sussex (UK) (May)